OPTIMAL CONTROL OF AN INTERNAL COMBUSTION ENGINE AND TRANSMISSION SYSTEM

by

SQUADRON LEADER DONALD McLEAN, R.A.F.

A Doctoral Thesis

Submitted in partial fulfilment of the requirements

for the award of

Doctor of Philosophy of the Loughborough University of Technology

April 1973

Supervisor : G.K. CREIGHTON, Ph.D.

Department of Electronic

and

Electrical Engineering

PREFACE

This thesis is a report of research carried out part-time at the Department of Electronic and Electrical Engineering of the University of Technology, Loughborough, and at the Royal Air Force College, Cranwell from September 1968 to August 1972.

It is believed to represent the first attempt to apply the methods of optimal control theory to the problem of controlling an internal combustion engine with an associated transmission system. The major part of the thesis is the independent work of the author : the work of others has been indicated at the appropriate points in the text.

The author acknowledges with gratitude the assistance of a number of people during the period of this work. In particular he wishes to express his gratitude to Dr. G.K. Creighton for supervising the research; to Professor J.E. Griffiths for his encouragement, to Commander L.J. Stacey, R.N., and to Wg.Cdr. B. Dickinson, RAF(Ret'd) for their support and supervision at RAF Cranwell. Special thanks are due to Air Commodore C.E.P. Suttle, RAF, of the RAF Education Branch for support and encouragement. Finally, thanks are due to Mr. N. Slater, Chief Technician of the Department at Loughborough, for his patient instruction in the rudiments of building practice, elementary plumbing and fundamental concreting.

SUMMARY

The control of an internal-combustion engine such that it will produce its required output, with a minimum consumption of fuel, even in the presence of random load disturbances, has become a necessary requirement for future prime-mover and vehicular applications. This thesis is concerned with an attempt to produce a practical scheme to meet that requirement from a study of several methods of achieving optimal engine regulation and a method of obtaining optimal start-up.

An attempt was made first to identify the response of the engine-transmission-load combination with a mathematical model obtained by the use of computers. The servo-mechanism associated with the throttle was identified also, and then a complete state-variable description of the system was obtained. Next an automatic gear-changing scheme was designed and implemented. With the availability of this practical system an optimal control function was generated then to implement optimal start-up. The optimal function was calculated by solving the associated multi-point boundary value problem by means of technique of quasilinearisation. To subject the system to random loads an artificial road was simulated, and a scheme was devised to vary the dynamometer loading in response to this 'road' signal.

The remainder of the thesis is concerned with a study of several different methods of obtaining optimal or sub-optimal

schemes of regulation and with comparisons of experimental results and the results from associated theoretical computer studies.

Many suggestions for further investigations are contained in the final chapter.

CONTENTS

LIST OF FIGURES

APPENDICES

CHAPTER ONE - INTRODUCTION

In the discipline of control engineering a besetting problem of current concern is the growing separation between practice and theory. The substantial growth in the body of theory, known generically as modern control theory, has occurred over a relatively short period, and the number of applications of this theory reported in the technical literature over the same period is confined principally to the aerospace or to the process industries.

At the same time there is a common awareness of the overwhelming need to conserve the known energy resources of the earth in the face of increasing rates of depletion. Since much of the control theory developed so recently is concerned wholly with the determination of control schemes which will either minimize energy use or alternatively will maximize the return from that use, it was considered worthwhile to attempt to use this new theory to solve a problem concerned with energy expenditure. In so doing some of the difficulties of applying the theory would be considered, and it was hoped that some solutions would be obtained which would contribute partially to a reduction of the gap.

It was decided therefore to design, to build, and to apply an optimal controller to an internal combustion engine and its associated transmission system so that the system would use as little fuel as possible to perform some defined task.

An engine and gearbox, surplus to the requirements of the Department, were available for the experiment. The coupling used between the engine and the transmission system was a fluid flywheel, a hydrokinetic drive which is characterized by having no torque multiplication (GILES [1963] and ANSDALE [1964]). This fact suggested the possibility of designing an automatic gear-changing scheme and finding an optimal start-up procedure that would drive the load up to its desired speed; here an optimal regulator would become effective to hold the engine at this speed even in the presence of disturbances. In this way it was hoped that fuel expenditure would be at least less than for manual control of the same task.

The work reported hereafter was carried out independently by the author in an attempt to solve the problem. It is believed to be the first attempt to control an internal-combustion engine together with its associated transmission system using the methods associated with modern control theory. The attempt inevitably has involved considerable use of computers : both analogue and digital.

In chapter 2 an account is given of the work undertaken to establish several mathematical models from measured experimental data. Because of the nature of the load which had to be used, the system was non-linear. A non-linear model suitable for use with the optimal regulation study was devised, as well as a more detailed model associated with the performance of the system during gear changes.

For comparison, and for subsequent ease of synthesis, an

optimal linear model was also established.

Chapter 3 is concerned with detailing the design and implementation of the automatic gear-changing scheme used in this research.

To subject the engine-transmission system to the same kind of random disturbances to which it may be subjected if installed in some industrial or vehicular application, a simple simulated road was manufactured. The signal derived from this device controlled the engine loading. A description of the device, together with the details of the statistical properties of the road, is given in chapter 4 which also contains a brief account of the ON/OFF servomechanism used to control the load.

In chapter 5 the problem of providing optimal start-up is considered. Because of the non-linear model, which it is necessary to use when gear changing is required, a solution to the problem had to be determined iteratively on a digital computer using the method of quasilinearisation. An account of the program development, its characteristics and its limitations is given together with the results obtained from an analogue computer simulation study. A practical start-up generator for fixed time-interval changes is also described and some experimental results are given.

The problems of engine regulation are described in chapter 6. Several different methods of obtaining numerical solutions are considered and a comparison of their relative effectiveness is made. Computer study results are presented before the results of practical experimental runs are shown and discussed. In an effort to account for known defects in the linear system model, alternative control schemes are considered

in chapter 7. These schemes were supposed to provide minimal sensitivity i.e. the regulation would be optimal and little affected by a slightly inaccurate model. To simplify the computation involved a model-following scheme was also considered and the results of the study are presented and compared with earlier results.

In chapter 8 further regulation schemes are presented which took into specific account the non-linear nature of the system. The computational aspects of these schemes are presented together with the resulting experimental data obtained from subsequent investigations.

Many proposals for further investigations, both theoretical and practical, are contained in the final chapter in which the results of the work are reconsidered and compared.

CHAPTER TWO - MATHEMATICAL MODELS OF THE ENGINE, TRANSMISSION SYSTEM AND LOAD

2.1. The Engine and its Load

The internal combustion engine used as the driving member of the plant to be controlled was a 6-cylinder, o.h.v. Daimler engine of 2433 c.c. capacity. Associated with this engine was a 4-speed* Daimler/Wilson pre-selector gearbox with the ratios listed in table 2.1

GEAR	1	2	3	4
RATIO	3.84:1	2.21:1	1.47:1	1:1

Table 2.1 - Gear Ratios

To absorb the energy delivered by the engine via the transmission system a dynamometer was used : the arrangement is shown as a schematic diagram in figure 2.1

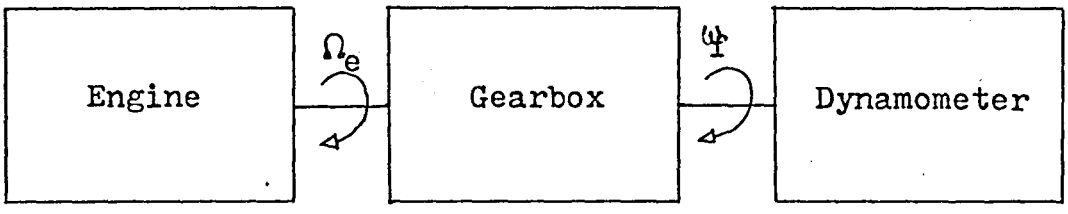

Ω_e = engine shaft speed (rad/s)

ω_f = output shaft speed (rad/s)

Figure 2.1 - Gearbox, Dynamometer Schematic

* A reverse gear is also provided but was not used in this study.

The maximum quoted* power available from the engine at 4400 rev/min was 74.57 kW. However the maximum quoted* torque was developed at 2500 rev/min and equalled 176 Nm. If the gearbox was to be fully employed in any control scheme, the maximum torque which the dynamometer would be required to match would be approximately 700 Nm at a shaft speed of 650 rev/min, when 1st gear had been selected. Such a figure is beyond the range of the usual type of engine dynamometer available. In addition, the location of the engine at its particular site inhibited the employment of dynamometer types other than a fan because of the limited water and electrical supply facilities at that site. The dynamometer selected for use in this research was therefore a fan type and the energy delivered from the engine system was dissipated in the surrounding air; this choice of dynamometer met the physical requirements of the site. However, if 1st gear were selected, control action to regulate the speed was not required because only an insignificant speed change could be produced by this dynamometer load when it was driven at a nominal speed of 650 rev/min. Consequently it was necessary to restrict the selection of gears to 2nd, 3rd or 4th.

The standard engine ignition system was used with engine timing controlled by a conventional diaphragm advance-retard control mechanism. Engine cooling was effected by controlling

---

*These figures were obtained from the Engine Specifications contained in the Owner's Manual for the Daimler Conquest saloon (1952) from which the engine and gearbox were obtained.

water flow through the engine block. A continuous flow was maintained with the heated water being discharged to an external drain. The sensitivity of the performance of any internal combustion engine to changes in operating temperature is well known (RICARDO [1953]), but because it was the intention to provide a control system resulting in optimal, or near optimal, performance even with widely varying engine parameters, and because it was possible to control manually the excursions of temperature to within a range of $\pm 15^{\circ}F$, the water-flow was controlled by a manually-operated valve. Although the dynamics of this manual control system were not considered in subsequent analysis it was assumed that changes in performance due to this effect would be of less significance than larger changes due to variations in the load (see section 2.3).

Engine and output shaft (dynamometer) speeds were measured by means of tachometers for static performance checks. When recordings were taken the speeds were taken as the output voltages from two d.c. tachogenerators driven directly from the engine rig. The sensitivity of both tachogenerators was 20 v/1000 rev/min but the drive for the dynamometer-associated tachogenerator was obtained from a pick-off point that was geared down by 6:1 so that the effective sensitivity of the output shaft tachogenerator was 20 v/6000 rev/min. The output signals from both tachogenerators were contaminated heavily with noise which arose from two principal causes :

(i) the ripple voltage associated with the commutator of any d.c. tachogenerator

(ii) an oscillation due to mechanical resonance of the experimental rig.

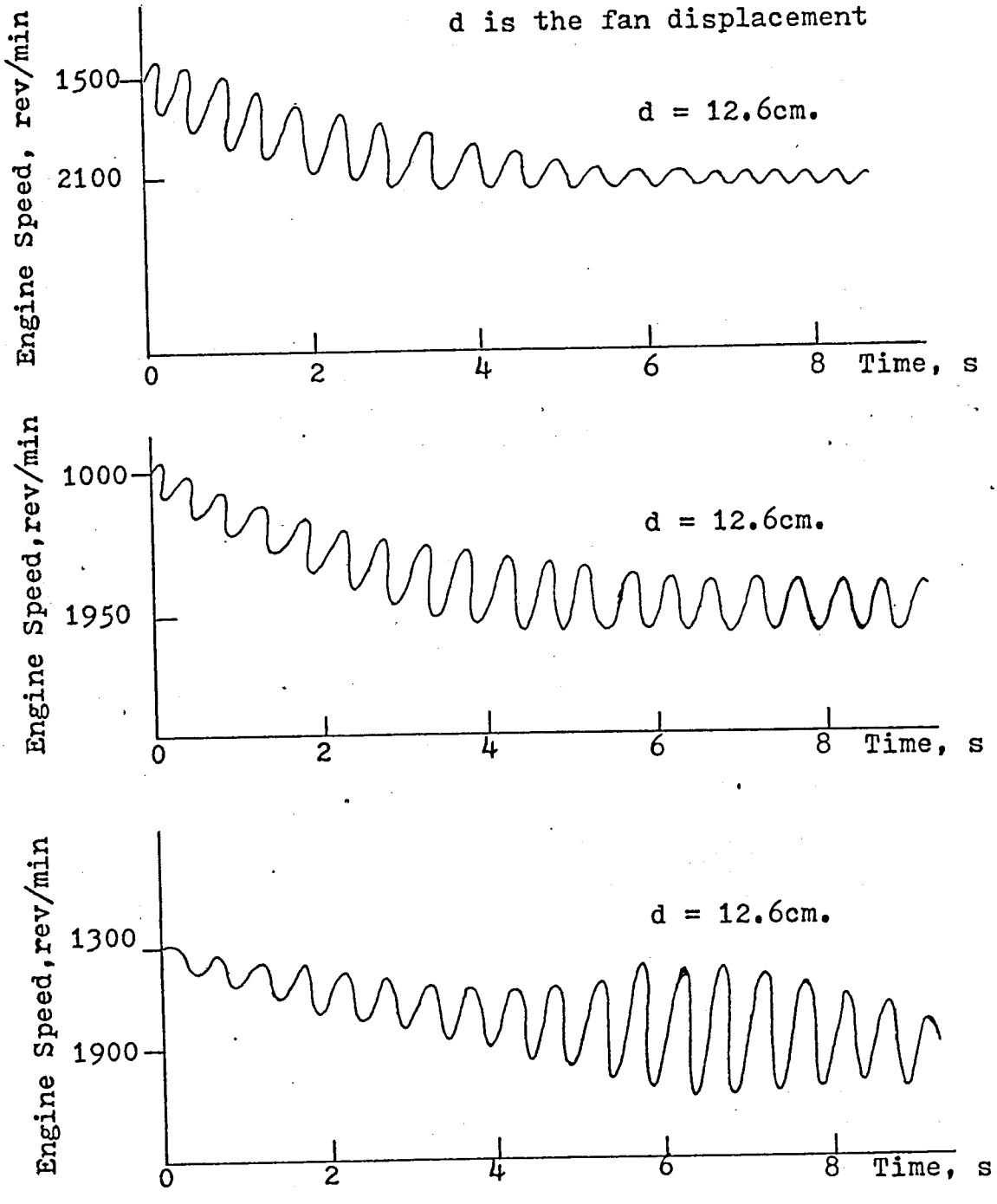

Figure 2.2 - Tachogenerator Speed Curves

The second component was the most significant and occurred because of the mounting arrangement for the engine and gearbox. To reduce engine vibration to manageable levels rubber mounts were used to attach the engine and gearbox to the engine bed. That the oscillations superimposed on the output from the tachogenerator were due to this mounting arrangement may be inferred from observing that in the responses shown as figure 2.2 the amplitude of the superimposed oscillation changed with engine speed which is a measure of the forcing frequency. It was decided therefore to use a simple 1st order filter network with a time constant short enough to ensure that the dynamics associated with the filters would not jeopardise later regulation schemes, but with a time constant of sufficient duration to provide adequate attenuation of the noise components. The simple filter used for each signal is shown in figure 2.3.

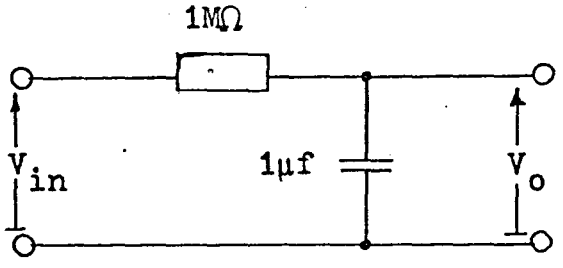

Figure 2.3 - Tachogenerator Filter

Graphs of engine power and torque vs. engine speed are shown in figure 2.4. From that figure it can be seen that the engine delivered greater power at the highest water temperature for the same engine speed. It will be noted also that the engine did not develop the quoted maximum power : from figure 2.14a it can be determined by extrapolation that there was no value of fan displacement for which the engine could deliver 74.6 kW at a speed of 4400 rev/min.

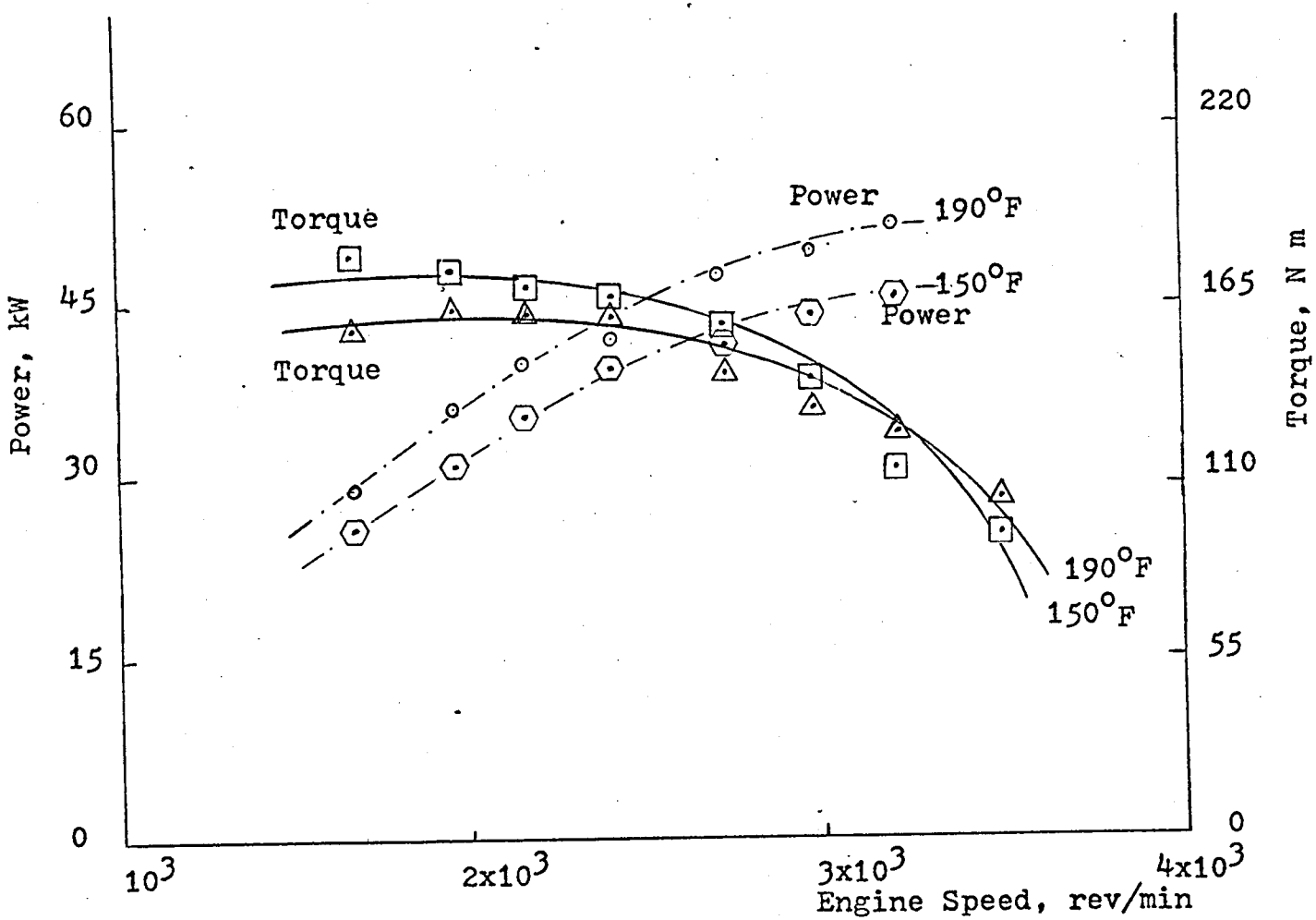

Figure 2.4 - Engine Power and Torque/Speed Curves

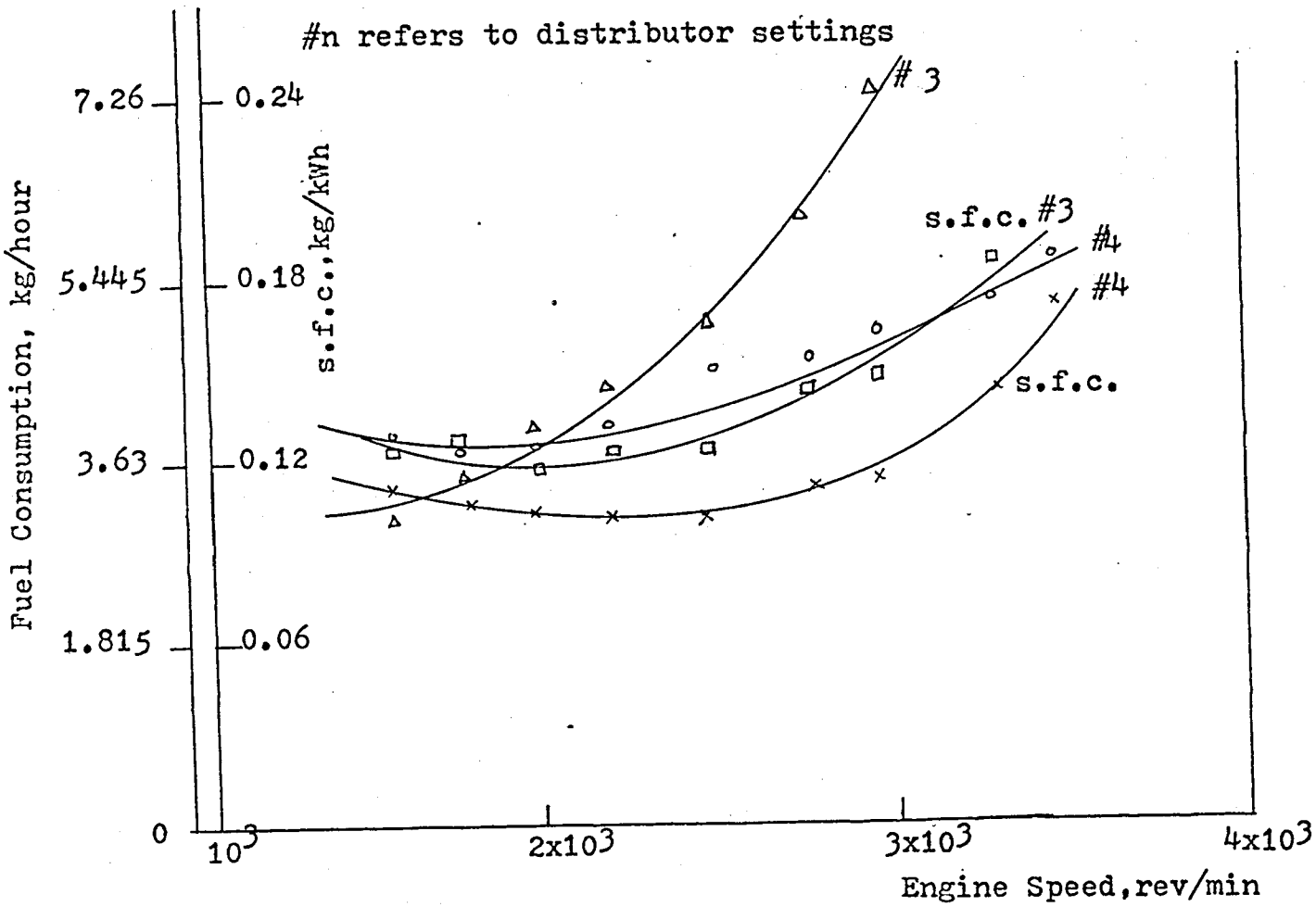

Figure 2.5 - Fuel Consumption Curves

The maximum torque, developed at a speed of 2000 rev/min, is not defined sharply. The torque did remain above the value of 90% of maximum, however, up to an engine speed of 2600 rev/min. From studies of performance curves published for other engines* it is reasonable to expect that the engine torque would have fallen off below 2000 rev/min and would have fallen to about 90% of the maximum value at approximately 1500 rev/min. It was taken that the torque would remain approximately constant over the range of 1000 rev/min when the engine was running at an equilibrium speed of 2000 rev/min. The significance of this assumption is emphasised by figure 2.5 which represents graphs of ordinary and specific fuel consumption. From that figure it is evident that the consumption of fuel increased with engine speed. The specific fuel consumption (s.f.c.) however was almost constant and at a minimum, for the quoted distributor setting, over a symmetrical range of 1000 rev/min centred on a speed of 2000 rev/min. By retarding the ignition of the spark a higher fuel consumption resulted and a sharper s.f.c. curve was obtained. This latter curve is characterised by a more clearly defined minimum at a speed of 2100 rev/min. All subsequent measurements and experiments were conducted with distributor setting 4 (34^{o} B.T.D.C.).

In all the experimental work the engine speed was set by adusting the throttle opening via a d.c. servomechanism, a schematic representation of which is presented in figure 2.6. Because of the electrical characteristics of the available servomotor, a thermionic valve amplifier was used. Some

---

*and from similar experimental runs carried out at R.A.F. Cranwell on a 4-cylinder, o.h.v. Vauxhall Viva engine of capacity 1000 c.c.

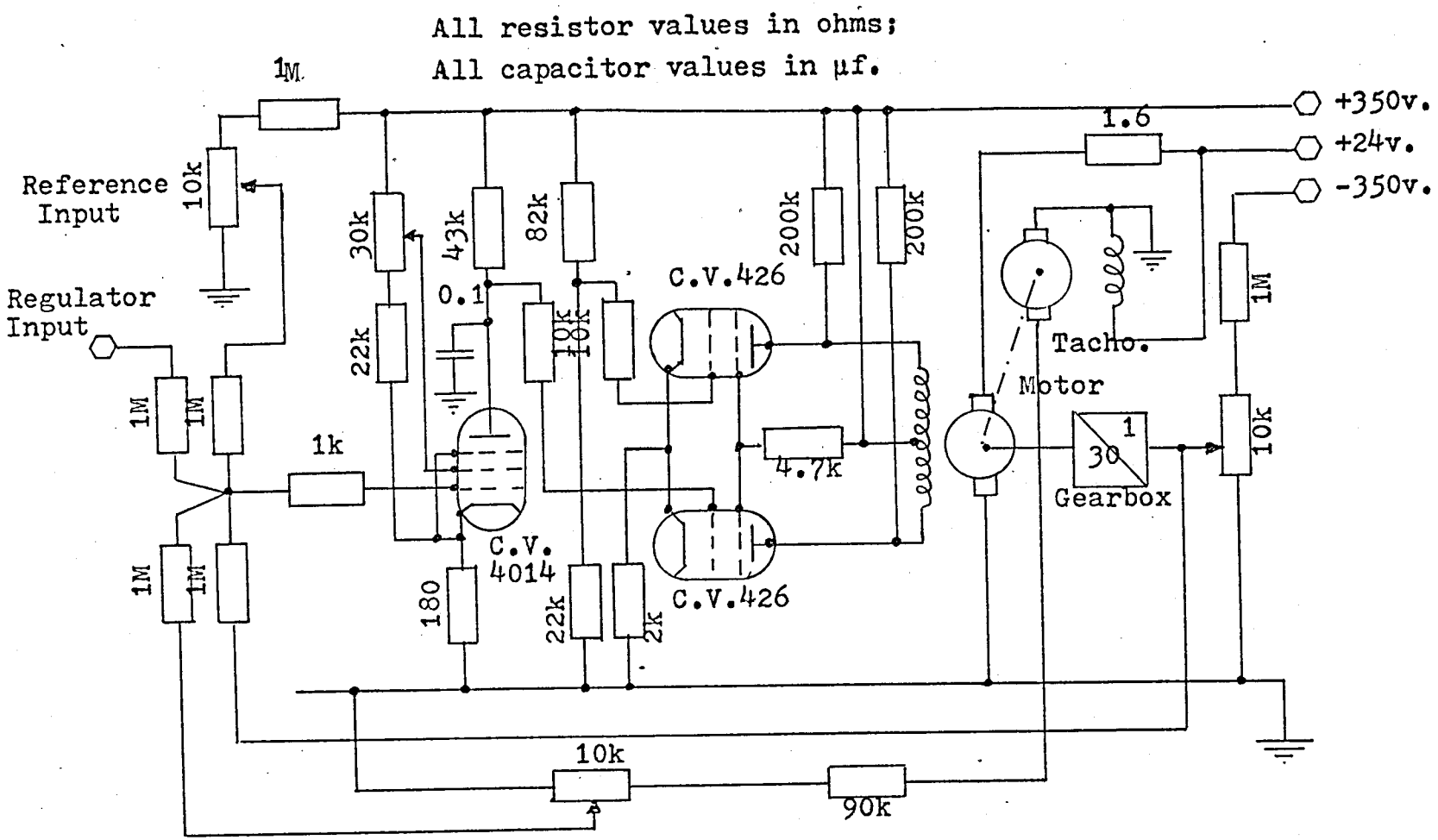

Figure 2.6 - Schematic Diagram of Throttle Servomechanism

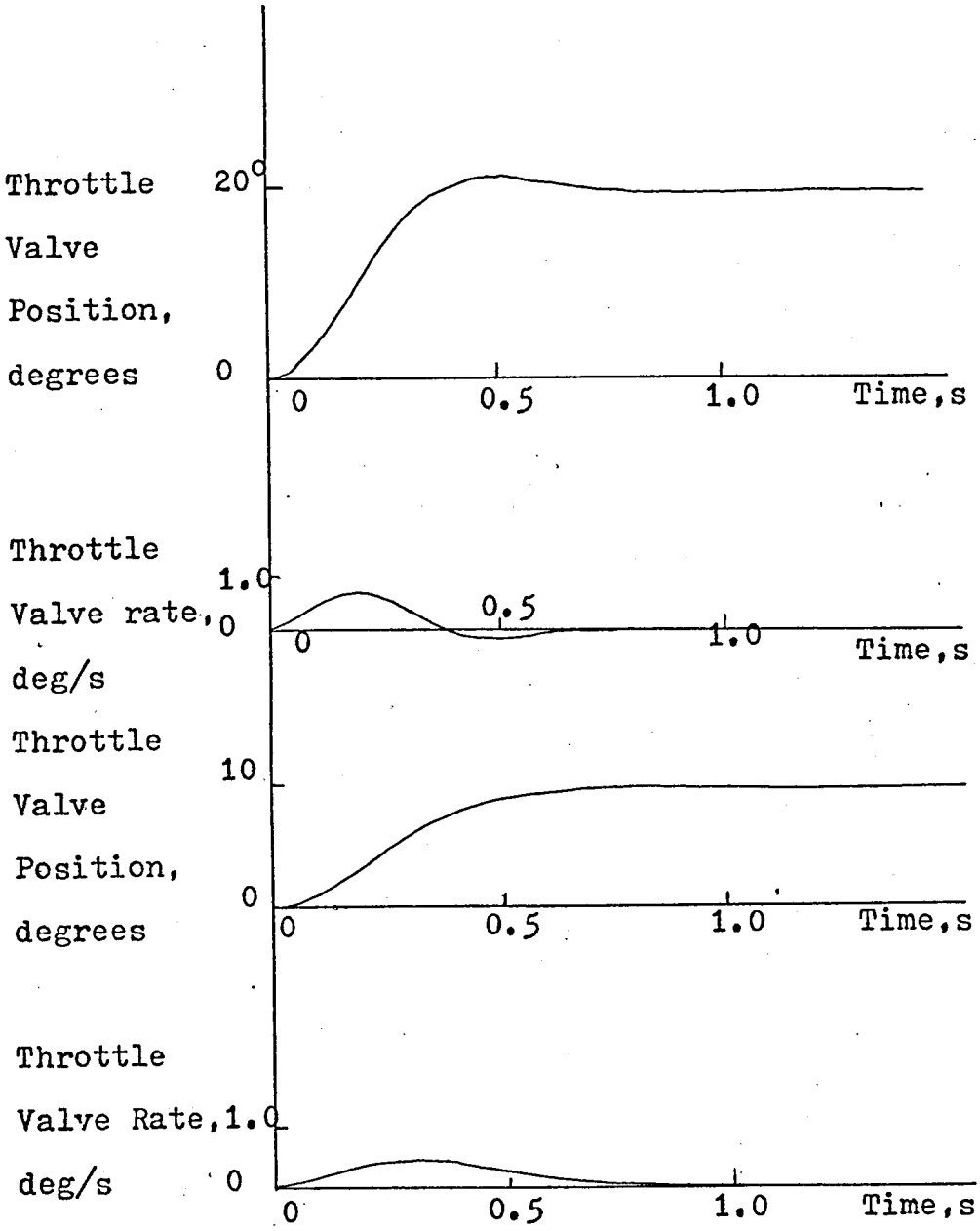

Figure 2.7 - Throttle Valve Response

d represents fan displacement

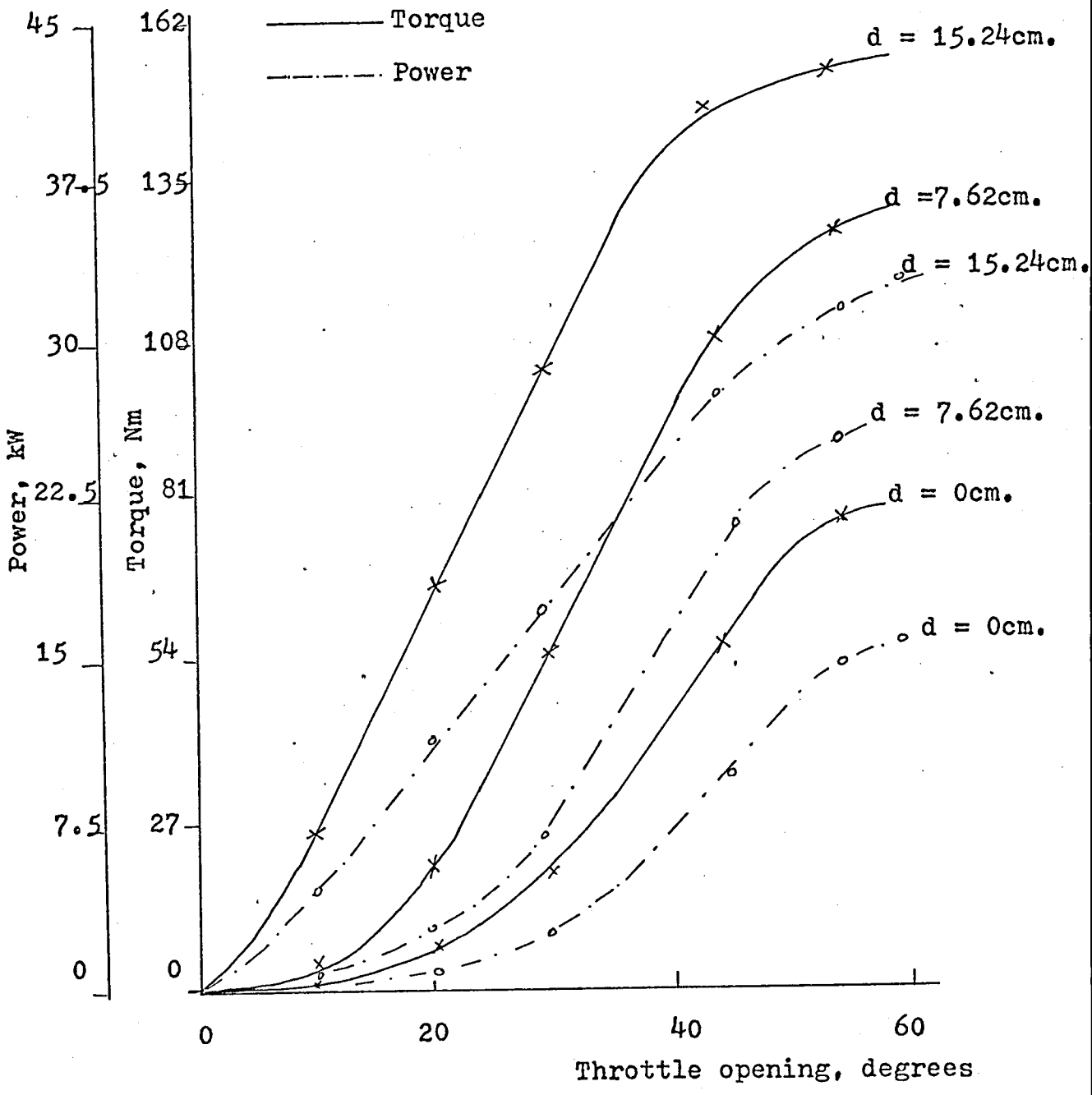

Figure 2.8 - Power and Torque vs. Throttle Angle

typical responses of the throttle valve to demands for new speeds are shown in figure 2.7. From data obtained from these curves the servomechanism was described by a linear differential equation :

$$\ddot{\theta}+a\dot{\theta}+b\theta = cV_{in} \qquad (2.1)$$

where a, b, and c are constants.

θ is the throttle valve opening, in radians, and V_{in} represents the command voltage, in volts. The description by (2.1) ignores some small, but observable, non-linearities in the response of the servomechanism. From the data obtained from figure 2.7 the servomechanism was identified* and the following values were assigned to the constant coefficients :

$$a = 16$$
$$b = 130 \qquad (2.2)$$
$$c = 43.3$$

Letting $x_2 = \theta$ (2.3)

and $x_3 = \frac{d\theta}{dt} = \dot{\theta}$

then (2.1) may be re-expressed, using (2.2) and (2.3), as :

$$\dot{x}_2 = x_3 \qquad (2.4)$$
$$\dot{x}_3 = -130x_2-16x_3+43.3V_{in}$$

A simulation of the throttle servomechanism is shown in figure 2.10. (For an explanation of the symbols used in that diagram see Appendix A.2). Note the use of the variable diode function generator (v.d.f.g.) to simulate the measured characteristics of the engine throttle system, shown in figures 2.8 and 2.9. In the simulation the torque characteristic

---

*The method by which the engine was identified is discussed later in this section.

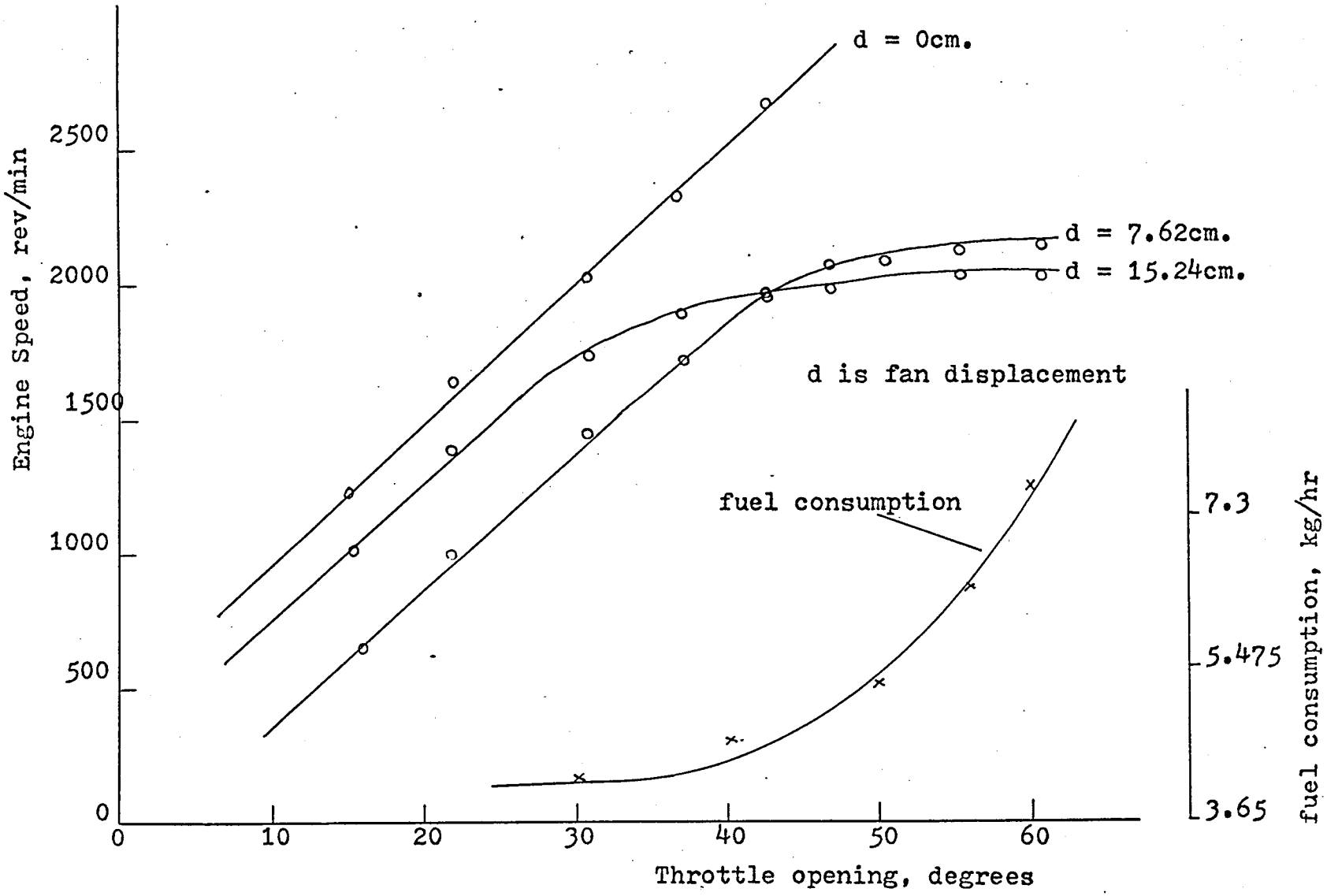

Figure 2.9 - Engine Speed/Throttle Angle

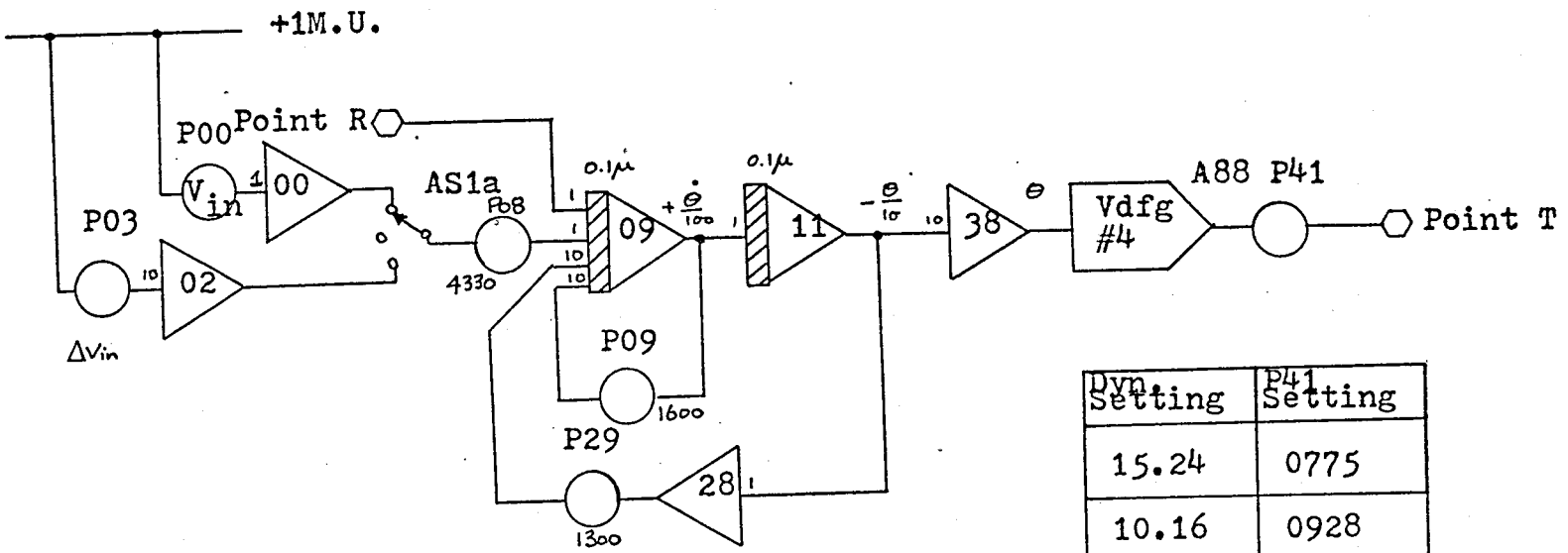

Dyn Setting	P41 Setting
15.24	0775
10.16	0928
07.62	1000
05.08	1072
02.54	1146
00.00	1225

V_{in} sensitivity: 1v. = 3.3° throttle opening

Figure 2.10 - Simulation Diagram of Throttle Servomechanism

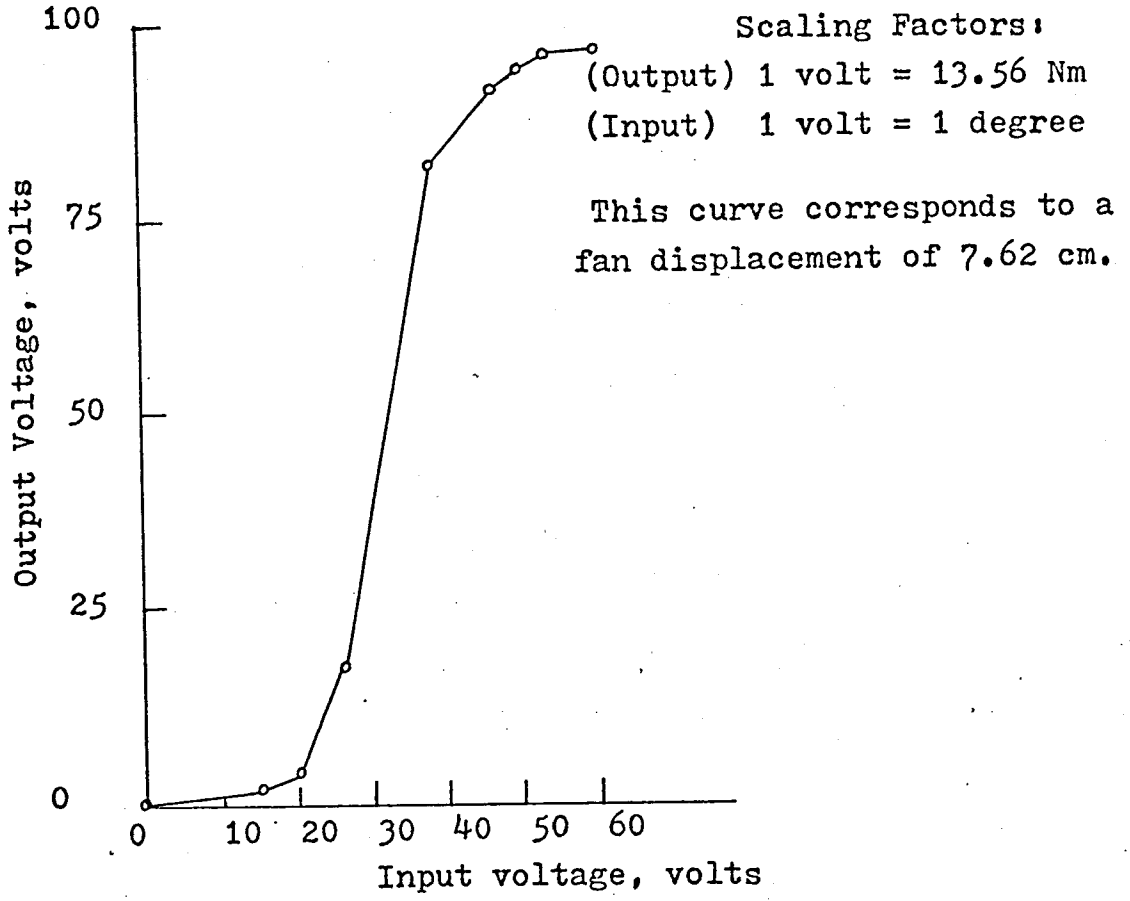

Figure 2.11 - Simulated Torque Characteristic

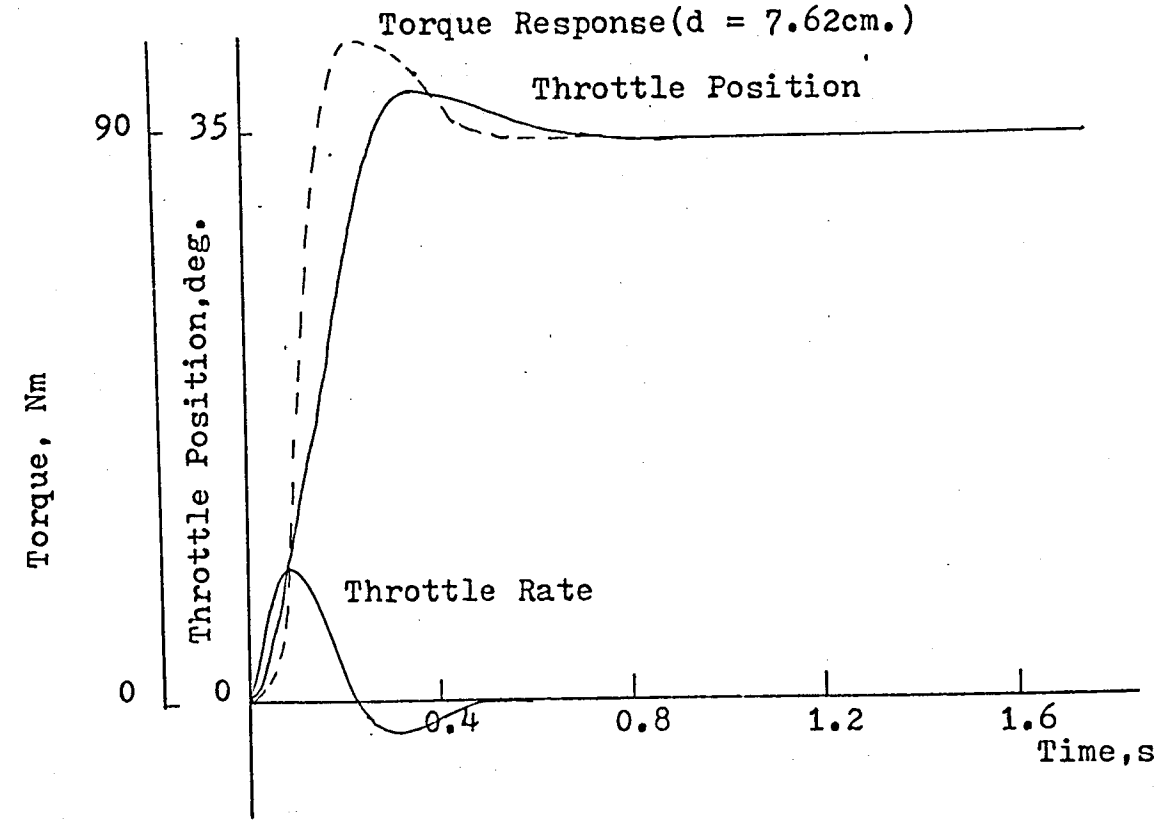

Figure 2.12 - Simulated Servomechanism Response

was placed ahead of the engine for convenience. The actual simulated torque characteristic output from the v.d.f.g. is shown in figure 2.11 which should be compared to figure 2.8. Potentiometer P41was adjusted to scale the torque characteristics for different dynamometer settings. The appropriate settings are shown in the small table inset in figure 2.10. The simulated servo response is shown in figure 2.12, Note that the inclusion of the static torque characteristic had a destabilising effect; this can be confirmed from observing that the overshoot of the simulated response was greater than the overshoot exhibited by the throttle servomechanism.

To identify the response of the engine and the throttle servomechanism under load*, sets of experimental data were obtained and were used as the inputs for the digital computer program BEARDM20. (See Appendix A.3). The program was used to identify any system which can be described by the vector differential equation :

$$\dot{\underline{x}} = A\underline{x} + Bu \qquad (2.5)$$

In this research, the state vector $\underline{x}$ was of dimension 3 and comprised the following elements :

x_1 the engine speed (rad./s)

x_2 the throttle position (rad)

x_3 the rate of change of throttle position (rad/s)

The input to the throttle servomechanism, in volts, was taken to be u. The program is based upon the work of YORE and TAKAHASHI (1967). It was written to produce the elements of

---

*4th gear was selected. Hence engine and output shaft speeds were identical in the steady state.

the coefficient matrix A. An extension of the program to provide an estimate of the driving matrix B can be done only in very special and limited cases. In this study it was not possible to estimate the matrix by use of the program because B was a rectangular matrix and an inversion of the matrix was required within the body of the program to effect this particular identification.* The program may be used for this purpose if u(t) was always a well-defined input, such as a step function, for then the state equation could be augmented by including the input as an additional state variable, x_4. For this research work an alternative method of assessing a value for B was chosen : u(t) was known to be a step function and the matrix B was known to be of the form $[0 \quad 0 \quad b_3]'$. It was easy therefore to identify b_3 and hence the matrix, B, from steady-state measurements.

Provided that the state vector $\underline{x}$ was measurable, free from noise, and was not constant over any small interval of time it was possible sometimes to identify the matrix, A, by use of the program. The matrix, A, produced by the computer, was obtained from successive iteration of the equation :

$$A_c^{k+1} = A_c^k + DA^k \qquad (2.6)$$

The integer k denotes the appropriate iteration. A_c^{k+1} was the estimated coefficient matrix at iteration k+1, whereas A_c^k was the coefficient matrix evaluated previously at the k^{th} iteration.

---

*Later work involved such inversion and a brief summary of matrix formulae associated with this is given in Appendix A.5.3. However unique matching was not possible. Therefore as stated in the text an alternative scheme was used here.

$(DA)^k$ was a special matrix denoting the normalised estimation error and was obtained from a sequence of error vectors formed thus :

$$\underline{e}^k(j) = \underline{x}(j) - \underline{x}_c^k(j) \qquad (2.7)$$

$$j = 1,2,3.....$$

$\underline{x}(j)$ was the state vector, measured from the recorded responses at some instant of time, j, and then used as the input to the program as the j^{th} set of data. $\underline{x}_c^k(j)$ was the computer-estimated vector for the same instant, j, on the k^{th} iteration.

A square matrix, E, was formed then by using the error vectors, $\underline{e}^k(j)$, as its columns :

$$E^k = [\underline{e}^k(j), \underline{e}^k(j+1), \underline{e}^k(j+2)] \qquad (2.8)$$

Another square matrix, X_{orig}, was formed by reading in as columns of the matrix the vectors $\underline{x}(j)$ thus :

$$X_{orig} = [\underline{x}(j), \underline{x}(j+1), \underline{x}(j+2)] \qquad (2.9)$$

The matrix, X_{orig}, was composed of data from actual measurements; it did not change therefore from iteration to iteration. The matrix, E^k, however, was calculated by the computer and did change from iteration to iteration until eventually it was zero, or until an estimate of sufficient accuracy had been achieved. The normalised error matrix DA^k could then be obtained. It was defined as :

$$DA^k = T^{-1}E^k [X_{orig}]^{-1} \qquad (2.10)$$

where T was the constant interval of time between measurements and was a scalar.

Provided that the state variables changed between intervals, the elements of X_{orig} were different and it was non-singular. (2.5) was re-expressed as

$$A_c^{k+1} = A_c^1 + \sum_{i=1}^{k} DA^i \qquad (2.11)$$

in which A_c^1 was an initial matrix the elements of which were assigned by the program user as an initial guess. The vectors $\underline{x}_c(j)$ were obtained from a sub-routine which solved the equation :

$$\dot{\underline{x}}_c^k = A_c^k \underline{x}_c + Bu \qquad (2.12)$$

BELLMAN [1960] has shown that the solution of (2.12) is given by :

$$\underline{x}_c^k(t) = \exp(A_c^k(t-t_o))\underline{x}_c(t_o) + \int_{t_o}^{t} \exp(A_c^k(t-\tau))Bu(\tau)d\tau \qquad (2.13)$$

The sub-routine evaluated the quantities

$$\exp(A_c^k(t-t_o)) \text{ and } \int_{t_o}^{t} \exp(A_c^k(t-\tau)Bd\tau$$

The iterations in the program were terminated when

$$\left\| E^k \right\| < \epsilon \qquad (2.14)$$

where ϵ was a small positive number assigned by the user as an acceptable degree of accuracy. In this research a value of 0.001 was used.

The vector norm used in this work was the Euclidean norm. The corresponding matrix norm was :

$$[\lambda_{max}(E^{'k}{}_{E}{}^{k})]^{\frac{1}{2}}$$

In use it was found that the program had several limitations which are indicated below :

(a) Sensitivity to Choice of T

T had to be small enough to satisfy the requirements of the sampling theorem due to SHANNON [1948]. Failure to meet these requirements meant that the program would not converge. To ensure convergence Yore and Takahashi proposed the use of the criterion

$$\left|a_{i_{max}j_{max}}\right| \times T \quad < \quad \frac{\log_e 2}{n} \qquad (2.15)$$

The integer, n, represented the order of the system and $a_{i_{max}j_{max}}$ is the value of the largest element of the matrix, A, which has yet to be identified. The practical solution to the problem of choosing T was empirical. An initial guess was made; if convergence was achieved T was increased and another run was made. If convergence was obtained again the procedure was repeated until a minimum successful value of T was found. If, at the first guess, convergence was not achieved T was reduced. Only a few runs were needed to obtain

a satisfactory choice of T. However, every alteration of T requires a new set of data from the recordings at every changed value.

(b) Vectors x(j) Must Differ

Identification of the autonomous linear systems with large rates of changes proved to be very easy when the program was being validated. Slow or small changes in system response resulted in unsatisfactory solutions and frequently poor convergence. This characteristic can affect the estimated matrix, A_c, obtained for the same equation but for different sets of data derived from the same response. For example, the matrix, A_c, evaluated upon the basis of the vector set, say,

$$X_{orig} = [\underline{x}(18T), \underline{x}(19T), \underline{x}(20T)] \qquad (2.16)$$

could bear little resemblance to the matrix evaluated for the earlier vector set

$$X_{orig} = [\underline{x}(0), \underline{x}(T), \underline{x}(2T)] \qquad (2.17)$$

This phenomenon resulted because the later data set was measured when the rates of change in the system responses were nearly zero i.e. the system was almost at its steady-state.

(c) Noise

The presence of noise on the recorded response can affect seriously the convergence of the program because all the input data have been perturbed randomly and there is no correlation with future values. Provision was made in the program to prevent the excessive computing times associated with convergence failure.

(d) Non-linearities in the System

It was claimed by Yore and Takahashi that the method would work for a limited class of non-linearities; that class allows the identification only of a linear equation for small excursions about some operating point. Such a limited

All responses filtered

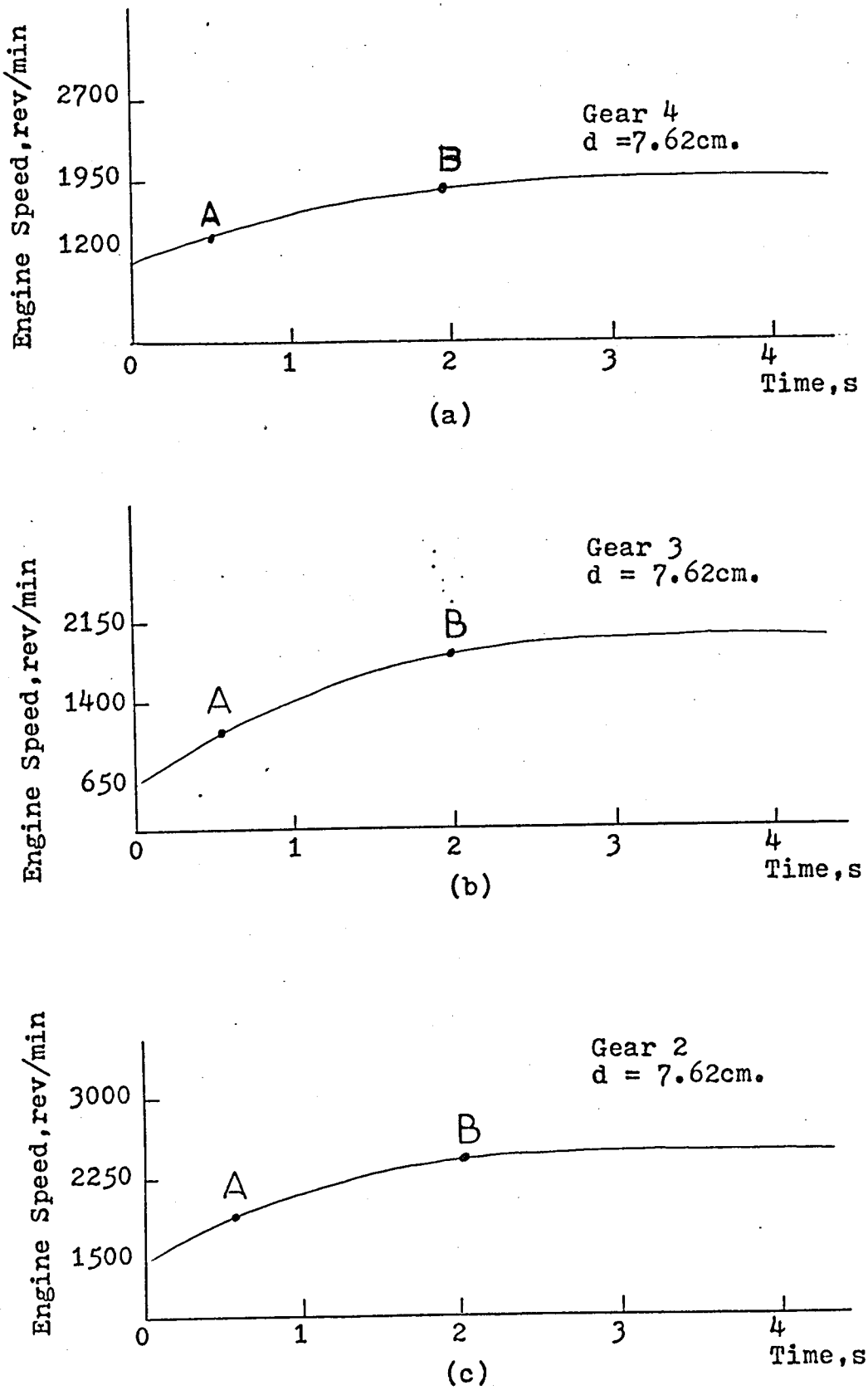

Figure 2.13 - Typical Engine Response to Throttle Demand

description was inappropriate when the data sets for the full combination were used with the program. Convergence was infrequent; on the occasions when convergence did occur it was found that the estimated matrix, A_c, was unrealistic, because it was determined that it had positive eigenvalues although the experimental data had been taken from bounded, and hence stable* output responses. To check the validity of the A_c matrices produced from the program two methods were used :

(i) the eigenvalues were evaluated and checked for sign

(ii) the matrix, A_c, was input to a program BEARDM34 (see Appendix A.3) and the response $\underline{x}_c(t)$ was evaluated. This was compared to the original responses, and if too great a discrepancy was evident an incorrect matrix, A_c, had been obtained.

By this technique the matrix, A, describing the servo-mechanism was obtained and thence the values of a and b quoted in (2.2). The coefficient, c, was evaluated from steady-state considerations. The A matrices for the entire engine arrangement were totally unsatisfactory and closer examination of the response showed that they exhibited non-linear behaviour. (See section AB of figure 2.13). The responses were not from very nearly linear systems as had been supposed initially. Therefore the responses were atypical of other transient responses published for other

---

*The assumption of stability from observing a bounded response is possible only because the technique of the program is based upon linear systems theory.

engines. (See for example MONK and COMFORT (1971)). Attention was directed therefore to the dynamics associated with the dynamometer since other published responses were obtained from engines using dynamometers different from the fan type used in this work.

2.2 The Dynamometer

The power absorbed by the fan dynamometer used in this research was a function of shaft speed cubed. Calibration curves for the dynamometer are shown in figure 2.14. Figure 2.15 is derived from figure 2.14. A graph, derived from figure 2.14, showing the relationship between torque and fan displacement for constant shaft speeds is given in figure 2.15b. From this graph it was inferred that if the control scheme could maintain the engine speed approximately constant the load torque on the engine could be taken as a linear function of fan displacement over the range 2.5 cm.-10 cm. approximately.

It was decided to study the dynamometer dynamics by means of analogue simulation. To check the resulting mathematical model in the steady-state the results of the simulation which is shown in figure 2.16 were compared with those values obtained from figure 2.15b. In the simulation amplitude scaling was employed :

$$1 \text{ volt} = 30.4 \text{ rev/min} \qquad (2.18)$$

which implied that

$$1 \text{ volt} = 13.56 \text{ Nm} \qquad (2.19)$$

The quality of the simulation may be assessed from the torque vs speed curves : compare figures 2.14b and 2.17.

The acceleration equation describing the dynamometer dynamics was determined to be :

$$\dot{\omega}_f = -3.33k\omega_f^2 + 3.33u \qquad (2.20)$$

in which k is a coefficient. It is a function of fan displacement; ω_f is the shaft speed in rad/s and u is the torque in Nm.

From comparison of the responses obtained from the engine and load system with the responses obtained from the simulation for the fan setting range from 2.5 cm. to 10 cm. it was observed that they were very similar. By inference it was concluded that for some conditions* of system operation the dynamic response of the engine was determined entirely by the characteristic of the dynamometer. When this is the condition the engine may then be regarded, for analytical purposes, as a simple device which converts fuel flow into torque, with a characteristic corresponding to figure 2.18, in a negligible time compared to the response time of the engine-dynamometer combination.

For some part of the research, therefore, (2.20) was regarded as the equation describing the dynamics of the complete engine-load system. But for the attempt to secure optimal engine regulation a linear model was needed, because its availability permitted significant simplification of the associated analysis, and of the resulting synthesis of the controller. A possible method of obtaining this model was to expand the non-linear term in (2.20) by means of a Taylor series, and by then considering only the linear terms in that expansion. By assuming an incremental change of speed, $\Delta\omega_f$, about some equilibrium

---

*These conditions pertain when the engine is operating with fourth gear and the torque load is an approximately linear function of engine speed.

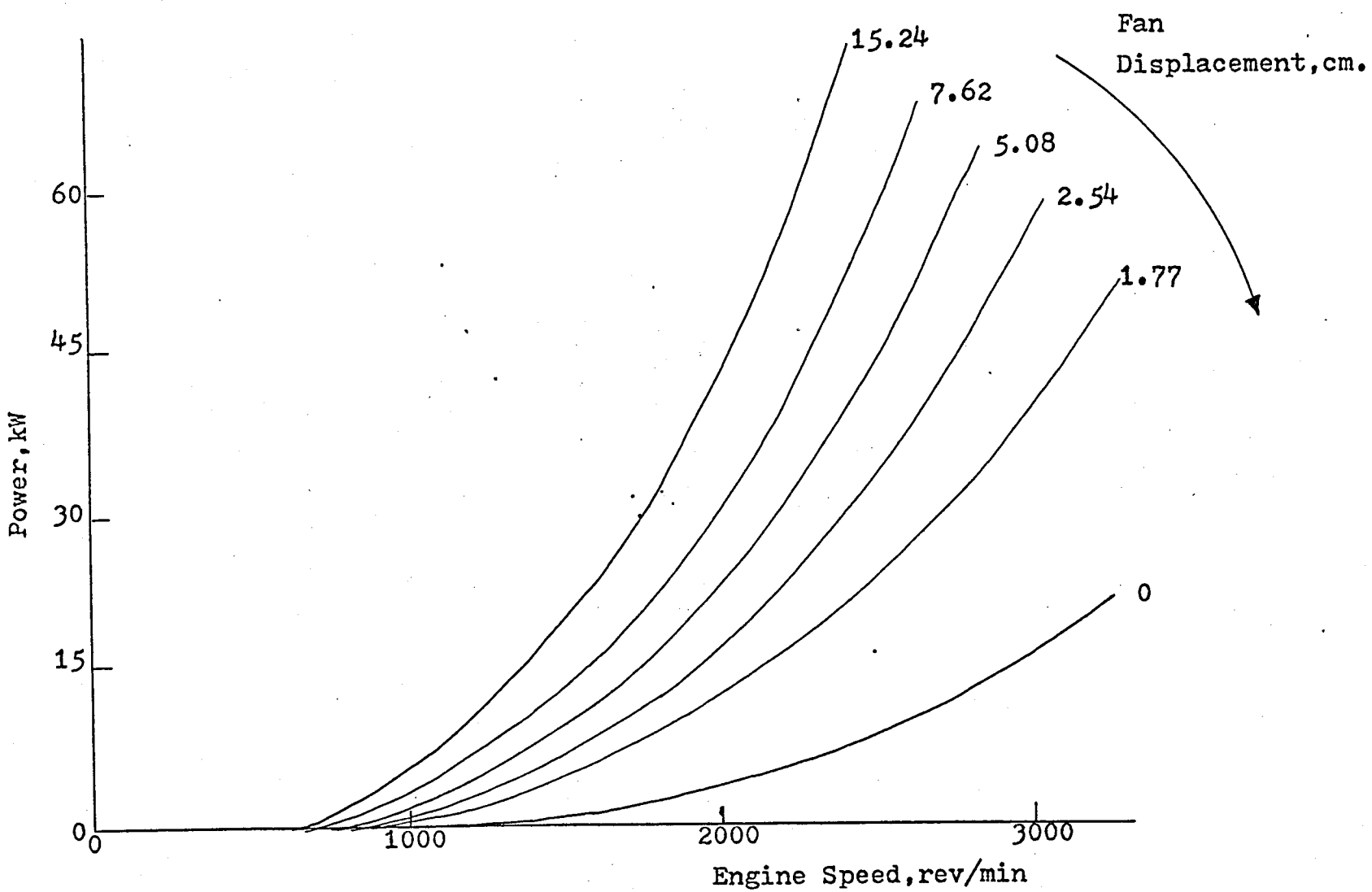

Figure 2.14a - Dynamometer Calibration Curve

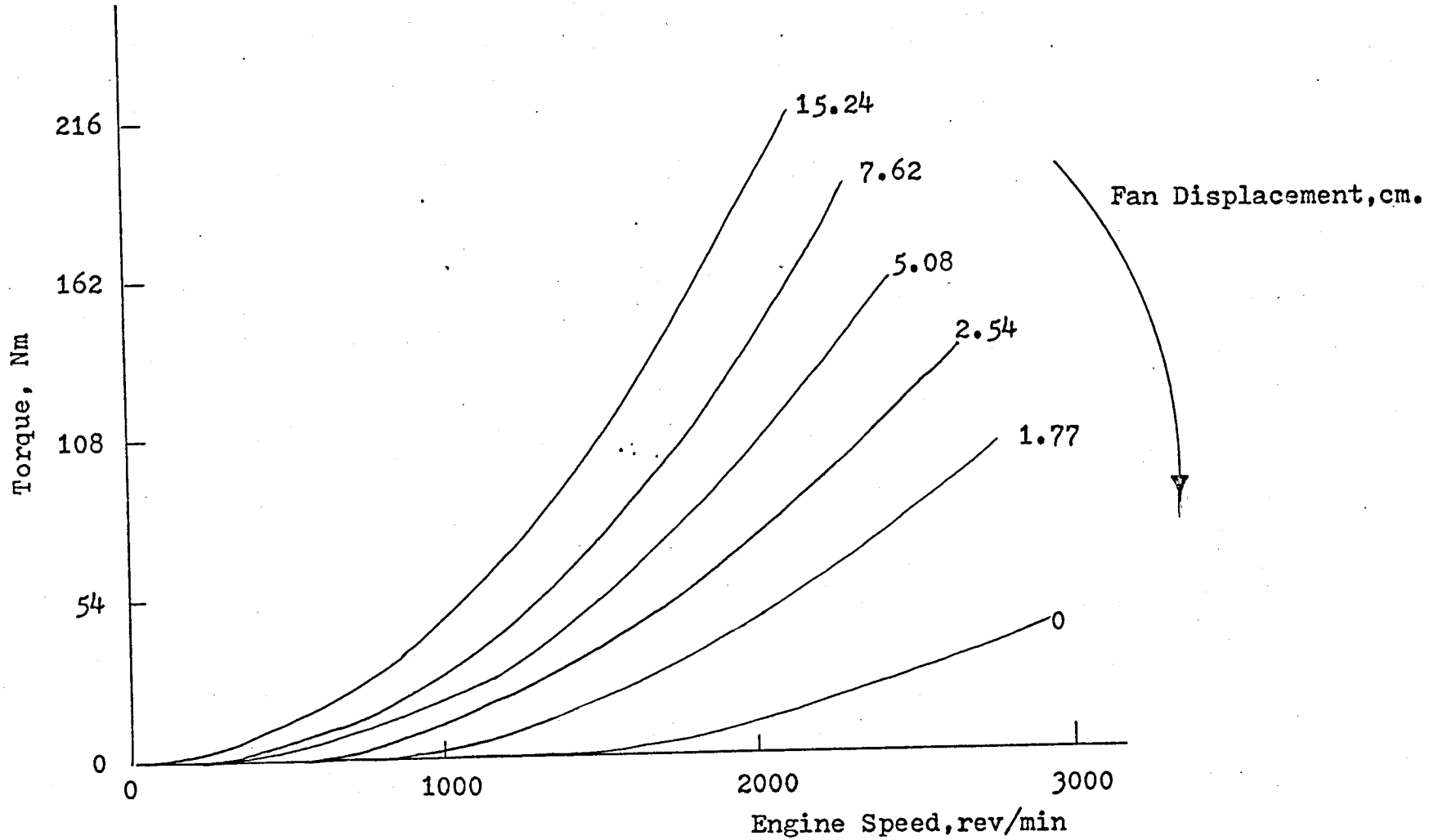

Figure 2.14b - Dynamometer Calibration Curve

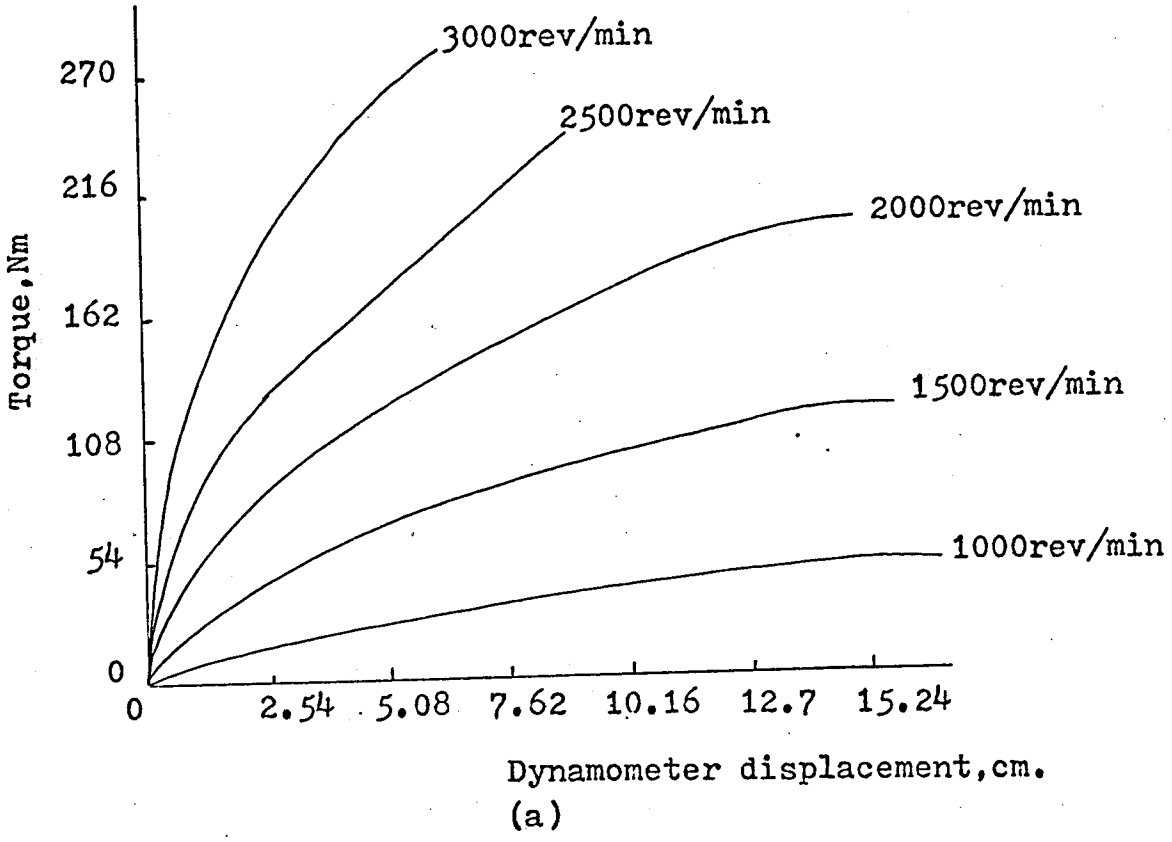

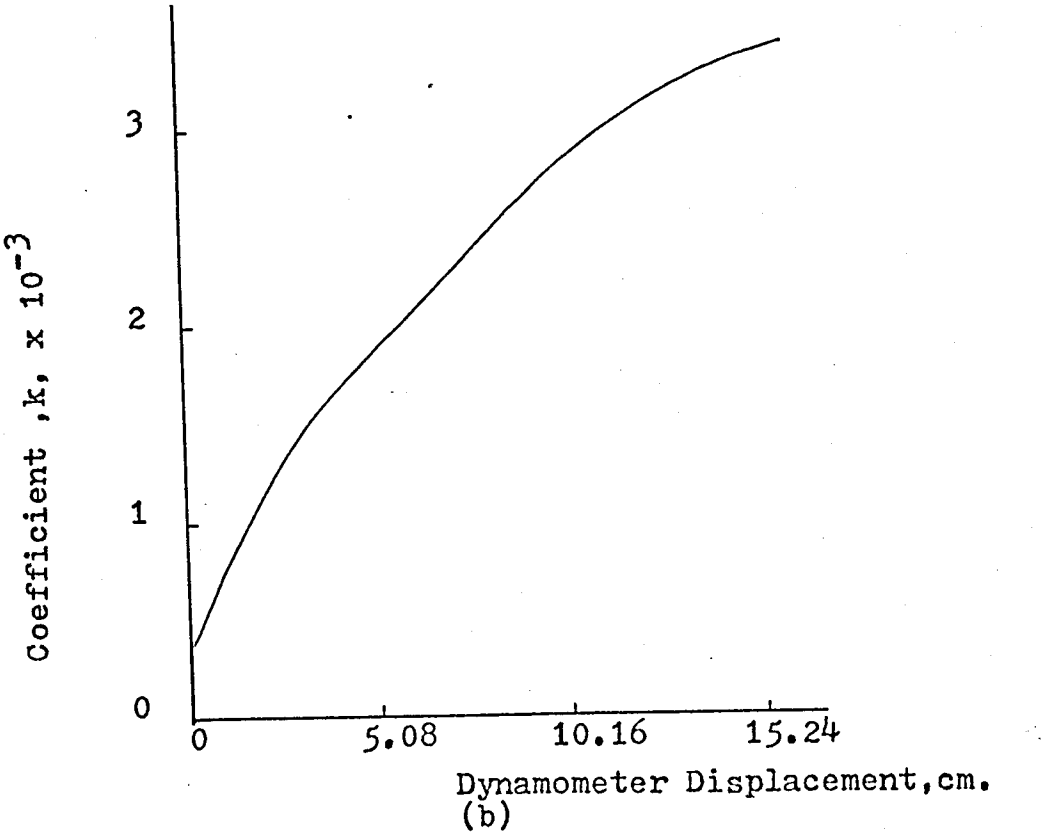

Figure 2.15 - Dynamometer Calibration Curves

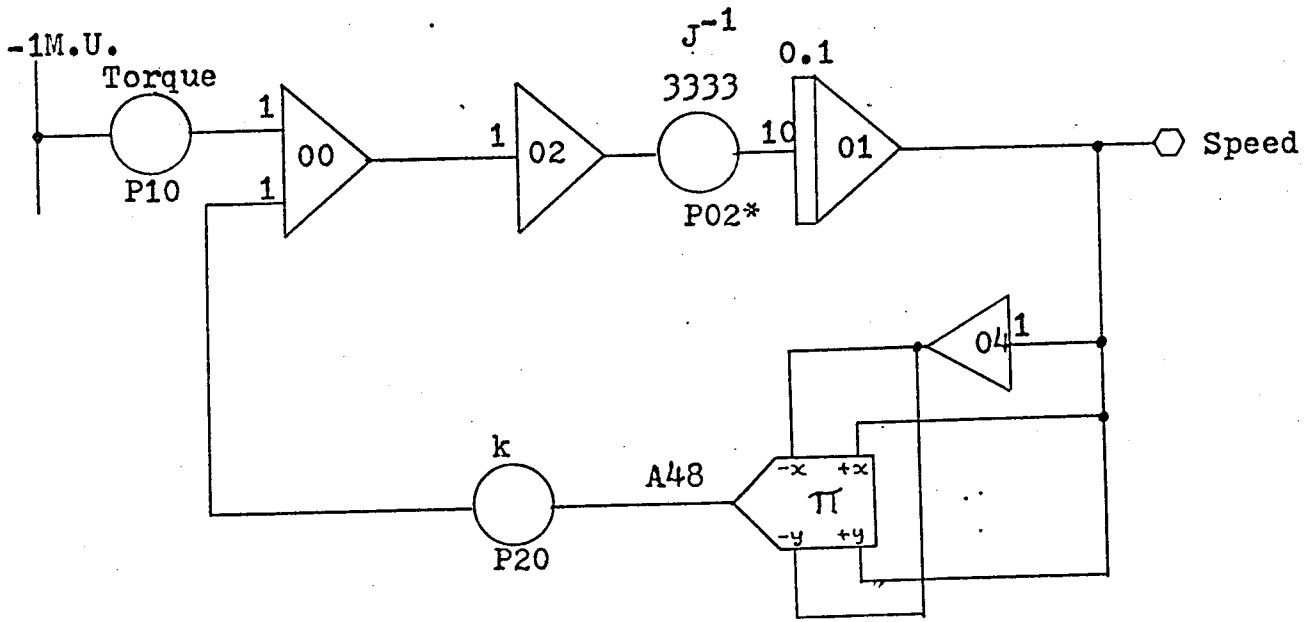

* P02 is adjusted to match measured response time.

Figure 2.16 - Simulation of the Dynamometer

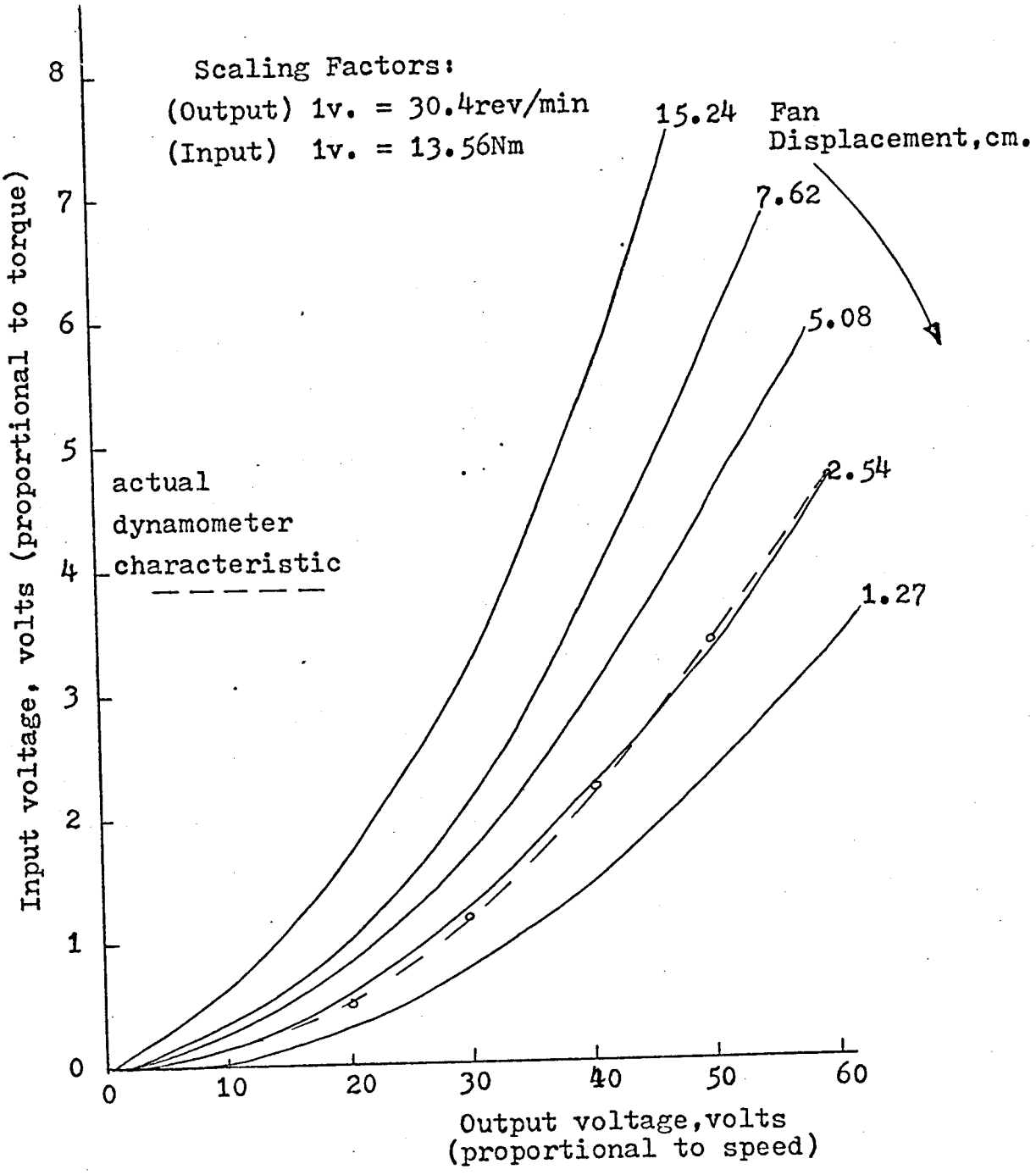

Figure 2.17 - Torque/Speed Curves from Simulation

value, Ω, the incremental variation of (2.20) could be given as :

$$\frac{d(\Delta\omega_f)}{dt} + 6.66k\Omega\Delta\omega_f = 333\Delta u \qquad (2.21)$$

where Δu is the incremental change in torque needed to produce the speed increment $\Delta\omega_f$. For a step increment in Δu the resulting variation in speed was given by :

$$\Delta\omega_f(t) = \frac{\Delta u}{2k\Omega}(1-\exp(-6.66k\Omega t)) \qquad (2.22)$$

To describe completely the engine response to changes of torque would require an entire family of these linear equations corresponding to every possible steady speed, Ω.* From this basic consideration it was evident that a linear model could be obtained but that it would be subjected to some constraints upon its validity. Since such a model could be obtained it was logical to attempt to establish the optimum linear model.

2.3 Optimal Linearisation

The method of optimal linearisation selected was to match (2.20) with the linear model equation (2.24) i.e.

given

$$\dot{\omega}_f = -c\omega_f^2 + b_1 u \qquad (2.23)$$

and assuming

$$\dot{\omega}_f = -\lambda\omega_f + b_2 u \qquad (2.24)$$

choose λ in some optimal way yet to be described. The gain of the linear system, b_2, had to be adjusted also to ensure that the steady-state speeds of the linear model and the dynamometer were identical for the same value of input, u. BLACQUIERE [1962] proposed that in such an approach λ should be chosen to minimise the integral of error-squared,

---

*This technique has been applied to a boiler problem by BANHAM and SMITH [1966]. The boiler used a fan as a forced air blower.

where the error, ϵ, was defined as :

$$\epsilon(\lambda,t) = -\lambda\omega_f(t) + c\omega_f^2(t) + (b_2-b_1)u(t) \qquad (2.25)$$

An alternative optimal model was available if the Ritz method, detailed in CUNNINGHAM (1959), was employed. In that method the criterion which had to be minimised was :

$$J = \int_o^\infty \epsilon(t)\phi(t)dt \qquad (2.26)$$

where $\phi(t)$ was a function of time associated with the model and where $\epsilon(t)$ was the residual which resulted from substituting an assumed solution in the original non-linear equation and which, in general, it did not satisfy.

2.3.1 The Integral of Error-Squared Method

The squared error was obtained from (2.25)

$$\epsilon^2(\lambda,t) = \lambda^2\omega_f^2(t) - 2c\lambda\omega_f^3(t) + c^2\omega_f^4(t) + (b_2-b_1)^2u^2(t) \qquad (2.27)$$

The condition for optimality was that

$$\frac{\partial}{\partial\lambda}\int_o^\infty \epsilon^2(t)dt = 0 \qquad (2.28)$$

Hence,

$$2\lambda^o\bar{\omega}_f^2(t) - 2c\bar{\omega}_f^3(t) = 0 \qquad (2.29)$$

where

$$\bar{\omega}_f^2(t) = \int_o^\infty \omega_f^2(t)dt \qquad (2.30)$$

and where

$$\bar{\omega}_f^3(t) = \int_o^\infty \omega_f^3(t)dt \qquad (2.31)$$

From (2.29) it followed that

$$\lambda^o = c\bar{\omega}_f^3(t)/\bar{\omega}_f^2(t) \qquad (2.32)$$

The evaluation of λ^o required the evaluation of the integrals defined in (2.30) and (2.31). Such an evaluation would require a solution for $\omega_f(t)$. For constant input, u(t),

the solution of (2.23) was found as follows :

$$\dot{\omega}_f = -c\left(\omega_f^2 - \frac{b_1 u}{c}\right) \qquad (2.33)$$

thence

$$\int_o^{\omega_f} \frac{d\lambda}{(\lambda^2 - \frac{b_1 u}{c})} = -c\int_o^t d\mu \qquad (2.34)$$

where λ, and μ are dummy variables.

The solution of (2.34) is given by :-

$$\frac{\sqrt{c}}{2\sqrt{b_1 u}} \times \log_e \left\{ \frac{\left(\omega_f\sqrt{\frac{b_1 u}{c}} - \frac{b_1 u}{c}\right)}{\left(-\omega_f\sqrt{\frac{b_1 u}{c}} - \frac{b_1 u}{c}\right)} \right\} = -ct \qquad (2.35)$$

From (2.35) it can be derived that

$$\tanh^{-1}\left\{ \frac{\omega_f\sqrt{\frac{b_1 u}{c}}}{\frac{-b_1 u}{c}} \right\} = -\sqrt{b_1 u c}\, t \qquad (2.36)$$

Then,

$$-\omega_f\sqrt{\frac{c}{b_1 u}} = -\tanh\left(\sqrt{b_1 u c}\, t\right) \qquad (2.37)$$

and thus :

$$\omega_f = \sqrt{\frac{b_1 u}{c}}\ \tanh\left(\sqrt{b_1 u c}\, t\right) \qquad (2.38)^*$$

---

*When the forcing function is absent from (2.23) the solution is given by :- $\omega_f(t) = \dfrac{\omega_f(0)}{\omega_f(0)ct+1}$ (2.38a)

Physically $\omega_f(0)$ cannot be negative; however, in a computer simulation, if $\omega_f(0)$ is negative, theresponse of the simulation will be unbounded at $t = \dfrac{\omega_f(0)}{c}$

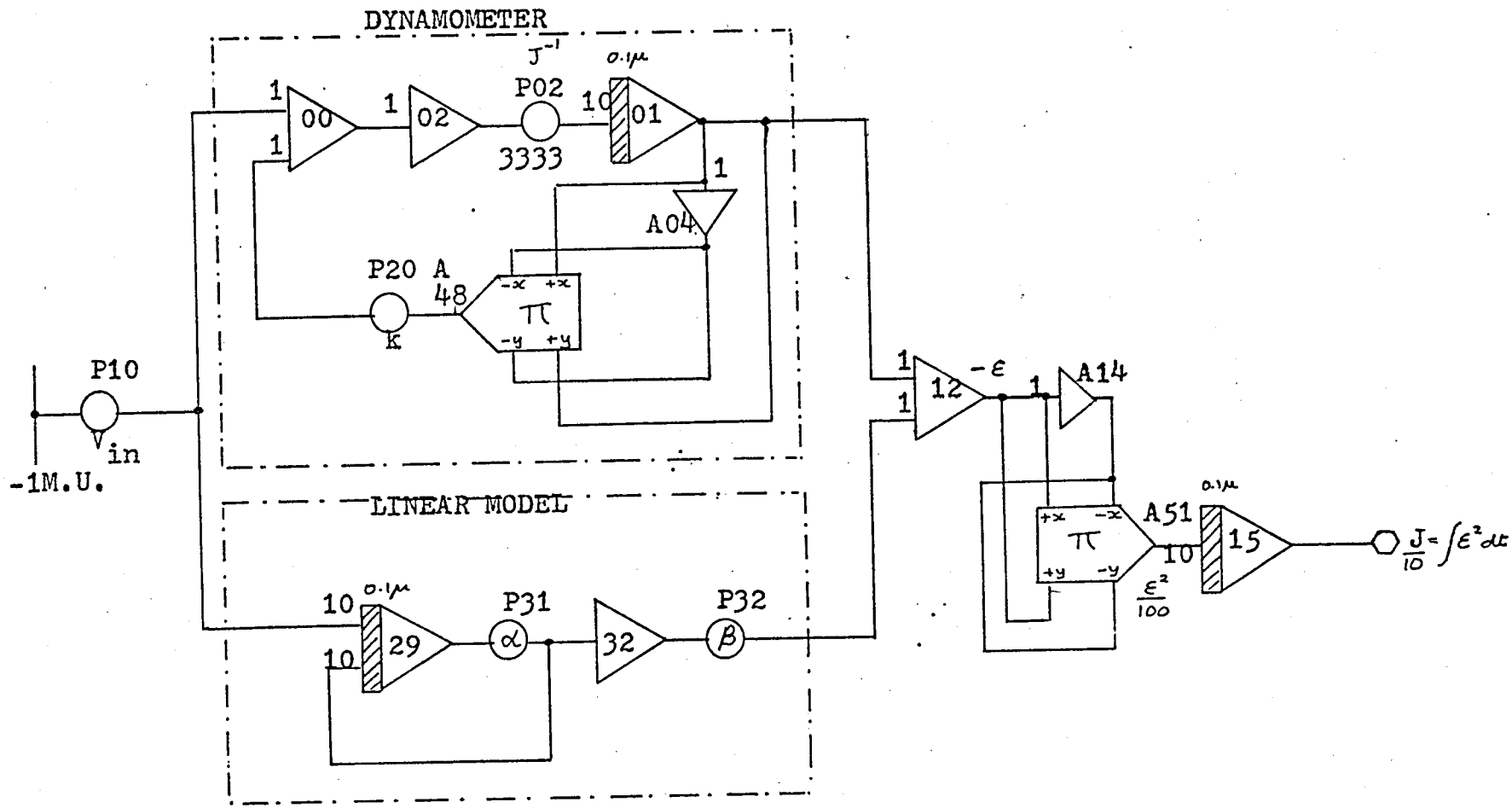

Figure 2.18 - Linear Modelling Technique

Attempts to solve (2.32) by substitution of (2.38) in the integrals (2.30) and (2.31) lead to analytical difficulties. The problem was circumvented by using an analogue computer to simulate both (2.23) and (2.24). The outputs of these simulations were subtracted, the remaining difference was squared in an accurate multiplier and its output was integrated over a period of time of sufficient length to approximate to the upper limit of the integral of the performance criterion. The integrator output was reduced to a minimum by adjustment of the parameter, λ, in the linear model. Before the adjustment of λ for optimality a preliminary run was made to adjust the gain of the linear model simulation to reduce the error, $\epsilon(\infty)$, to zero. The diagram of the analogue computer simulation is shown in figure 2.18 and the results obtained are quoted in table 2.2. The overall accuracy of the computer used* was 0.1%. The tests which provided the results of table 2.2 were completed immediately following acceptance trials for the computer. Part of the acceptance was a stringent test of machine and component accuracy to ensure that the computer performance was better than the specified overall accuracy of 0.1% .

---

*The analogue computer was a REDIFON-ASTRODATA Ci - 175, with a 100 volts machine unit and a maximum iteration frequency of 1kHz.

Serial Number	Dynamometer Displacement	Potentiometer Settings				A01 and A32	A15
		P10	P20	P31	P32		
01	15.24	1148	3333	1034	5144	5880	0010
02	"	0600	"	0677	7079	4251	0074
03	"	0100	"	0258	1729△	1736	0000
04	10.16	1200	2888	0960	5374	6456	0130
05	"	0600	"	0657	7608	4565	0070
06	"	0100	"	0241	1853△	1877	0004
07	7.62	1000	2388	0794	6475	6483	0755
08	"	0600	"	0600	8356	5029	0105
09	"	0100	"	0226	2039△	2064	0003
10	5.08	0600	1845	0532	9510	5712	0167
11	"	0100	"	0197	2332△	2335	0003
12	2.54	0615	1350	5293°	1096△	6761	0031
13	"	0100	"	1942°	2716△	2736	0023
14	1.77	0500	0925	3488°	1640△	6593	0415
15	"	0100	"	1576°	3281△	3303	0288
16	0	0200	0360	1517°	3525△	7896	1384
17	"	0100	"	0980°	5251△	5286	0908

° Indicates that gain of A29 was reduced to unity.

△ Indicates that gain of A32 was increased to X10.

P02 set at 3333 throughout experiment.

Table 2.2

Serial No	Input Torque N-m	Steady Output Speed (rev/min)	λ^o (sec^{-1})	b_2 ($kg^{-1} m^{-2}$)
01	156	1765	1.034	5.13
02	82.5	1292	0.667	4.72
03	13.56	526	0.258	4.45
04	164	1960	0.960	5.16
05	82.5	1390	0.657	5.06
06	13.56	570	0.241	4.5
07	164	1965	0.794	5.15
08	82.5	1530	0.60	5.0
09	13.56	628	0.226	4.6
10	82.5	1740	0.532	5.05
11	13.56	710	0.197	4.6
12	82.5	2060	0.529	5.8
13	13.56	830	0.194	5.12
14	54	2000	0.349	5.69
15	13.56	1040	0.158	5.15
16	30.4	2400	0.152	5.32
17	13.56	1610	0.098	5.15

$$\dot{\omega}_f = -\lambda^o \omega + b_2 u$$

Table 2.3

Whe A15 is recorded in table 2.2 as reading 0031 (serial no. 12) it means that the voltage recorded across the output terminals of the amplifier (A15) on a digital voltmeter on its 100-volts range was 00.31 volt, or 310 mv. The column headed A15 in table 2.2 represents the minimum value of I.S.E. If λ is optimal I.S.E., and consequently the output of A15, should be zero. From inspection it is apparent that for all fan displacements greater than 1.77 cm. the linear models obtained were optimal. For example, at maximum level of torque input, at a fan displacement of 7.5 cm. the value of I.S.E. represents over the interval of measurement, an error* of 0.2% approximately. The interval of measurement was taken to be 120 seconds; in every case the transient responses of the simulations had long ceased to be significant before the upper limit of the 120 second period was reached.

In table 2.3 the values of λ^{o} and b_2 are given to correspond to the data presented in table 2.2 These results are summarised in graphical form in figures 2.19 and 2.20 where some additional results were used to complete the graphs. The time constants and the gains of the linear models are seen to depend upon the load and equilibrium speed. If these varied with time then the linear model would have to be regarded as time-varying. Because the intention was to change the load dynamically the non-linear system could then be represented by a linear time-varying equation. The suggestion that this kind of linear representation of non-linear systems would result was made first, as far as can be determined by this author, by PEARSON (1962).

---

*This was an average error figure.

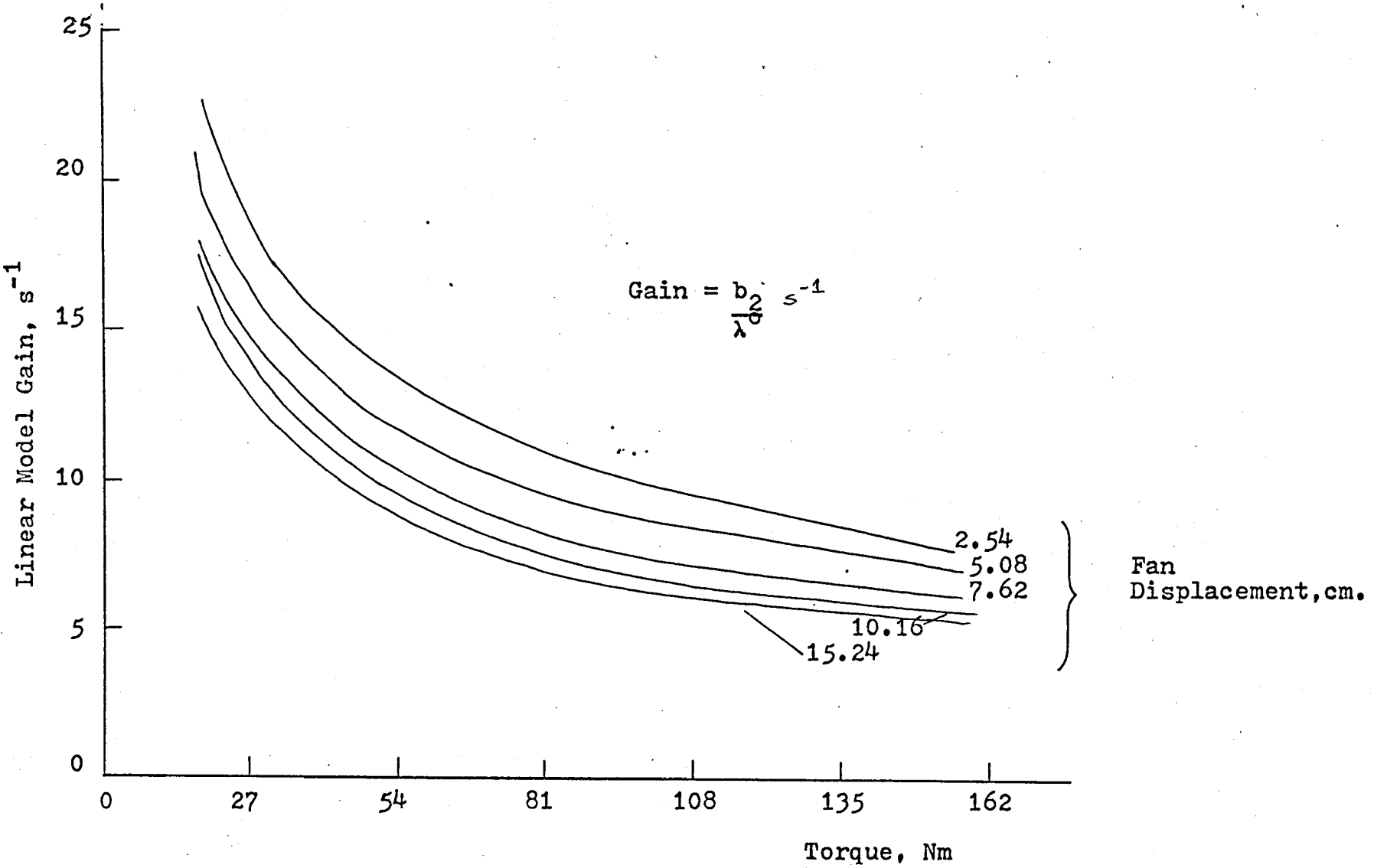

Figure 2.19 - Variation of Model Gain with Torque

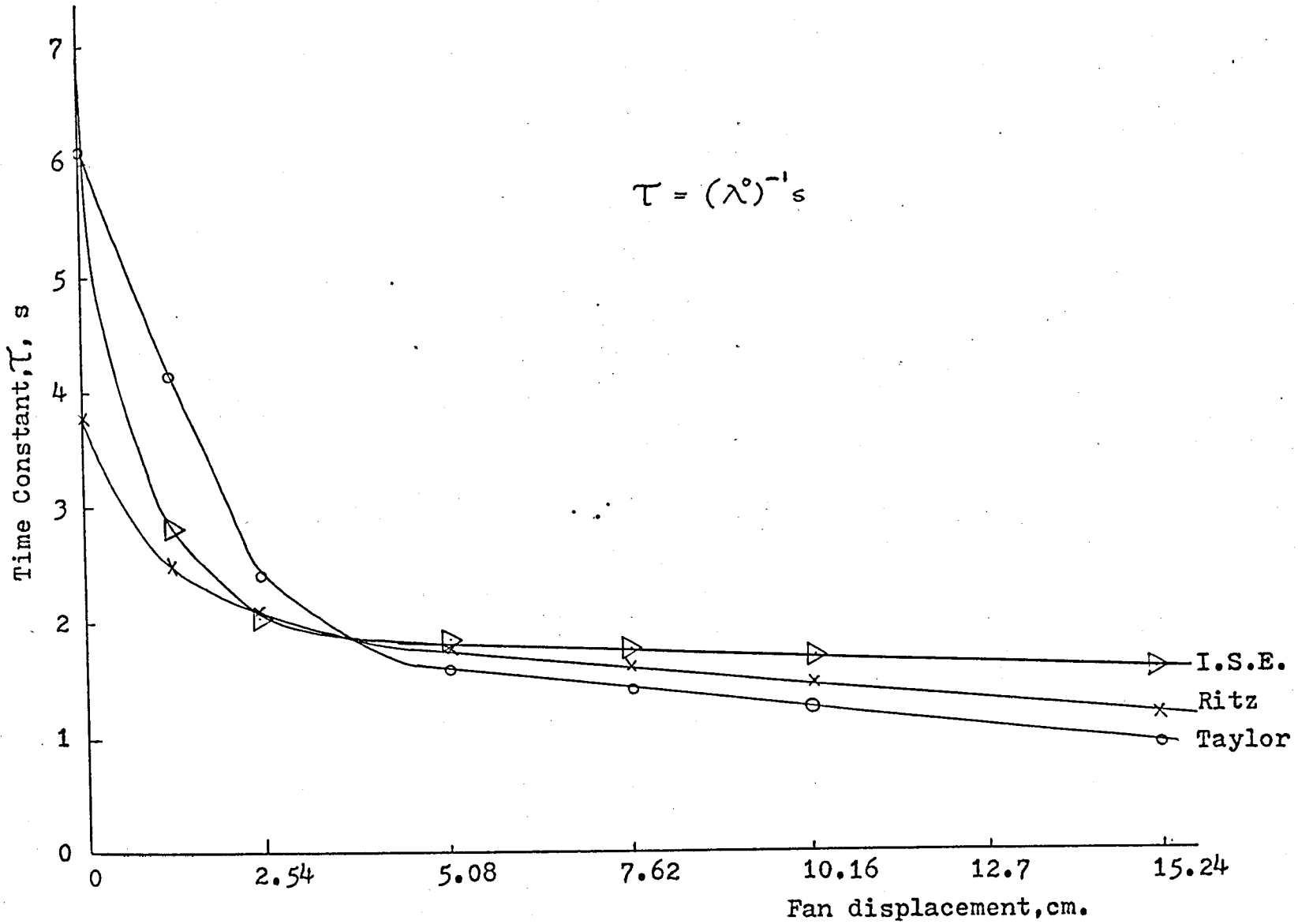

Figure 2.20 - Variation of Linear Model Time Constant with Fan Displacement

2.3.2 Ritz Method

In this approach the assumed solution for (2.23) was :

$$\omega_f(t) = \hat{\omega}_f(1 - \exp(-\lambda t)) \qquad (2.39)$$

where

$$\hat{\omega}_f = \left\{(b_1 u/c)\right\}^{1/2} \qquad (2.40)$$

The residual was given then by :

$$\epsilon(t) = (\lambda\hat{\omega}_f - 2b_1 u)(\exp(-\lambda t) + (b_1 u)\exp(-2\lambda t) \qquad (2.41)$$

From (2.39) the function, $\varphi(t)$, associated with the assumed model was :

$$\varphi(t) = (1-\exp(-\lambda t)) \qquad (2.42)$$

In this method also λ was chosen to minimise the performance index i.e.

$$\frac{\partial}{\partial\lambda}\int_0^\infty (1-\exp(-\lambda t))\left\{(\lambda\hat{\omega}_f - 2b_1 u)\exp(-\lambda t) + (b_1 u)\exp(-2\lambda t)\right\}dt = 0 \qquad (2.43)$$

From (2.43)

$$\frac{5b_1 u}{6\lambda^o} = \hat{\omega}_f/2 \qquad (2.44)$$

from which, using the substitution for $\hat{\omega}_f$ defined in (2.40)

$$\lambda^o = \frac{5(cb_1 u)^{\frac{1}{2}}}{3} \qquad (2.45)$$

Substitution of (2.45) in (2.39) gave the optimal linear equation

$$\omega_f(t) = \hat{\omega}_f\left\{1 - \exp\left(-\frac{5}{3}(cb_1 u)^{1/2} t\right)\right\} \qquad (2.46)$$

In figure 2.20 for I.S.E., Ritz, and the Taylor models* the variation of $(\lambda^o)^{-1}$ with fan displacement are shown together for the purpose of comparison. In figure 2.21 for a fan

---

*The Taylor model was obtained from the engine responses by treating them as truly exponential curves, which they were not, and by determining the settling time (to within 1% of final value). This provided more easily a linear model which was much cruder than the I.S.E. or the Ritz.

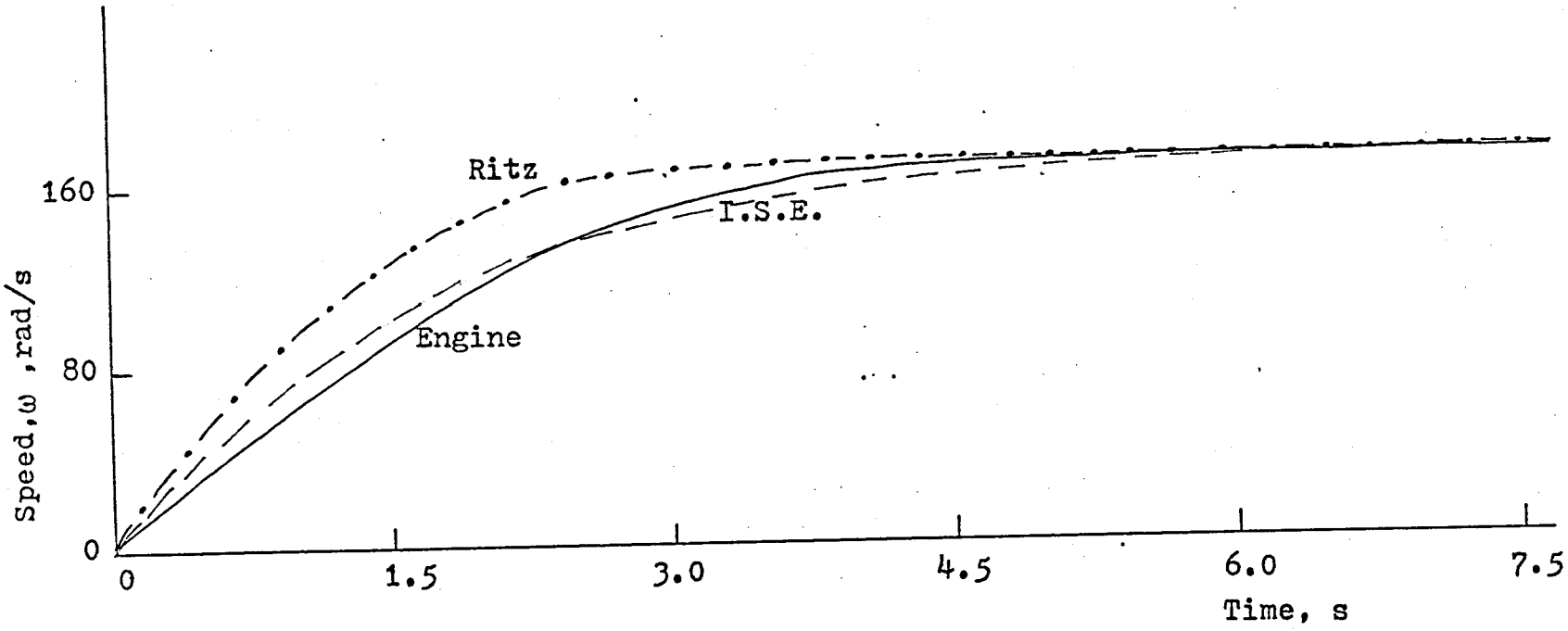

Figure 2.21 - Response of Engine and Models to Sudden Change of Torque

displacement of 7.6 cm. the recording of filtered engine speed and the responses recorded from the suitably scaled simulated I.S.E. and Ritz models are shown for comparison.

From figure 2.21 it was decided that, provided that changes of torque were not too large, the linear model for the engine combination was acceptable for later use in this research. For small changes of torque, of say 15 Nm. over a large range of equilibrium speeds the choice of

$$b_2 = 5.0 \ kg^{-1} \ m^{-2} \qquad (2.47)$$

was obtained from table 2.3 However the changes in λ^o and b_2 which occurred due to alteration of speed and/or load condition meant that special care had to be addressed to the problem of devising regulation control laws. From figure 2.21 it is plain that, for most operating conditions, a reasonable choice for λ^o was

$$\lambda^o = 1.0 \qquad (2.48)$$

Therefore, the model equation, which the engine system will be controlled to provide throughout subsequent regulation tests, was taken to be :

$$\dot{\omega}_f = -\omega_f + 5.0u \qquad (2.49)$$

2.4 Gear Changing

2.4.1 Effects of Gear Ratios on System Equation

Up to this point the identification of the engine system dynamics had depended upon data derived from experimental records acquired from engine runs for which fourth gear was selected. To examine how the describing equations would be altered if an alternative gear was selected required an extension of the analysis. The extension was based upon the schematic diagram of figure 2.22 in which the symbols have the following meanings :

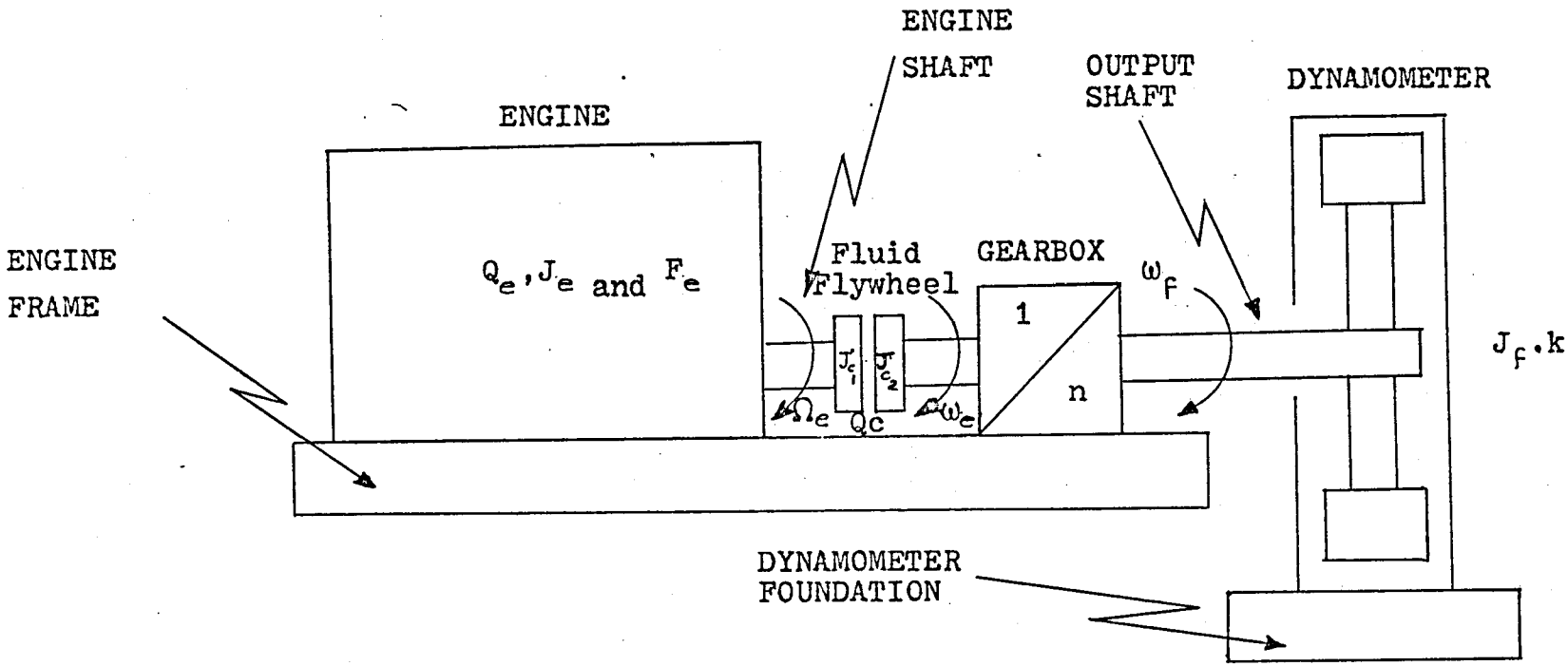

Figure 2.22 - Schematic Diagram of Engine and Transmission System

n is the appropriate gear ratio

Q_e is torque developed by the engine (Nm)

Q_c is slip torque of fluid flywheel (Nm)

Q_f is load torque applied by fan (Nm)

J_e is inertia of engine (kg m^2)

J_f is inertia of fan (kg m^2)

J_{c_1}, J_{c_2} are inertias of fluid flywheel coupling (kg m^2)

k is damping coefficient of fan

Ω_e is speed of engine (rad/s)

ω_f is dynamometer shaft speed (rad/s)

F_e is engine friction (Nm s)

The specific value of k depended upon the displacement of the fan, as before; the engine friction was assumed to be due wholly to viscous friction. The engine static friction was negligible. From figure 2.22 then

$$J_e \frac{d^2\theta_e}{dt^2} + F_e \frac{d\theta_e}{dt} + Q_c = Q_e \qquad (2.50)$$

in which

$$Q_c = \frac{Q_f}{n} \qquad (2.51)$$

and θ_e is the angular displacement of the engine shaft.*

But
$$\theta_f = \theta_e/n \qquad (2.52)$$

and
$$Q_f = J_f \frac{d^2\theta_f}{dt^2} + \frac{k(d\theta_f)^2}{dt} \qquad (2.53)$$

From these equations (2.50) was re-expressed as :

$$J_e \frac{d^2\theta_e}{dt^2} + F_e \frac{d\theta_e}{dt} + \frac{J_f}{n^2} \frac{d^2\theta_e}{dt^2} + \frac{k}{n}\left(\frac{d\theta_f}{dt}\right)^2 = Q_e \qquad (2.54)$$

---

*θ_f is the angular displacement of the fan.

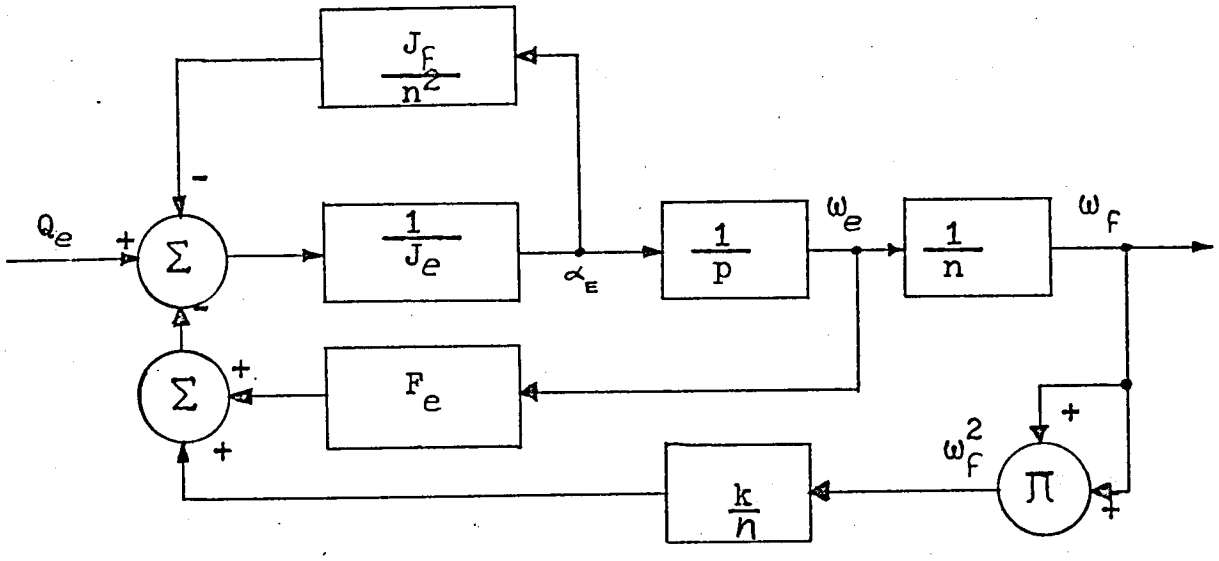

Figure 2.23 - Block Diagram of Engine, Load and Gearbox

In the figure

$$\alpha_e = \frac{d^2\theta_e}{dt^2} \qquad (2.55)$$

$$\omega_e = \frac{d\theta_e}{dt} \qquad (2.56)$$

$$\omega_f = \frac{d\theta_f}{dt} \qquad (2.57)$$

The symbol p has its usual meaning in a control engineering context: it represents the Heaviside operator, i.e.

$$p = \frac{d}{dt} \qquad (2.58)$$

Substitution of (2.52) in (2.54) provided

$$\left\{J_e + \frac{J_f}{n^2}\right\} \frac{d^2\theta_e}{dt^2} + \frac{F_e d\theta_e}{dt} + \frac{k}{n^3}\left(\frac{d\theta_e}{dt}\right)^2 = Q_e \qquad (2.59)$$

If J_e and F_e were negligible (or could be assumed to be so) (2.59) reduced to

$$\dot{\omega}_f = -\frac{k}{J_f}\omega_f^2 + \frac{n}{J_f}Q_e \qquad (2.60)$$

$$\dot{\omega}_f = -c\omega_f^2 + b_1'u \qquad (2.61)$$

From a comparison of (2.61) with (2.23) it was evident that

$$b_1' = nb_1 \qquad (2.62)$$

The inverse time constant, λ, of the quasi-linear equation can be derived from (2.61), and the work of section 2.3 ,and was

$$\lambda_j^o = \sqrt{n_j}\lambda_4 \qquad (2.63)$$

where j = 4,3, or 2.

The values of j depended upon the gear selected; for example if 4th gear was used then j would equal 4. The ratio appropriate to whichever gear was selected was n_j; the values of n_j were obtained from table 2.1. From (2.63) and (2.45)

$$\lambda_j^o = \frac{5(cb_1un_j)^{1/2}}{3} \qquad (2.64)$$

where j and n_j had the same meanings as before.

2.4.2 Dynamic Response to a Gearchange

In figure 2.24 the responses were obtained from the engine rig with fixed throttle setting and fixed fan displacement. From inspection of these recordings two features were noted :

(i) some responses exhibit overshoots whilst others for exactly the same conditions except the direction of the gearchange, failed to exhibit such overshoots.

(ii) the period of the oscillation associated with the overshoot exceeded the duration of the response

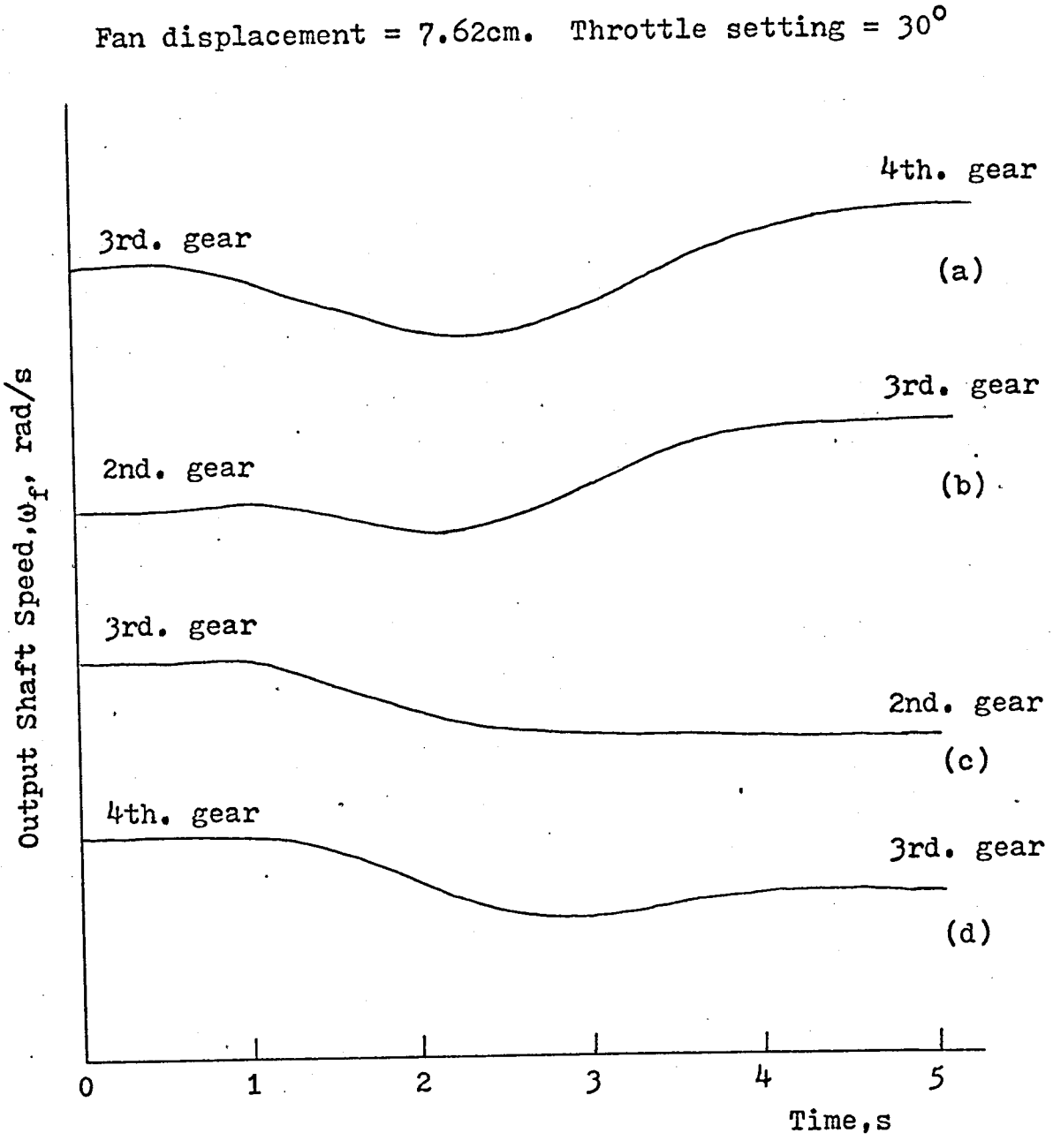

Figure 2.24 - Gearchange Responses

from the old to the new equilibrium speed, (see figure 2.24c for example).

Any overshoot must occur because there is some form of energy exchange within the system. Consequently the order of the system must increase from one. This increase in system order could be accounted for only by the action of the fluid flywheel used with the gearbox. The existence, or lack, of overshoot for some up/down* gearshifts in figure 2.24 was because of the non-linear nature of the load-transmission system : the nature of the response depended upon the equilibrium speed. The overshoots cannot be accounted for by the use of linear system theory to characterise the system behaviour because the measured duration of the overshoots was much greater than half the total response time and that phenomenon cannot occur in any linear system.

As a consequence of these observations the model of the gearchanging system already developed was modified further to include the dynamics associated with the fluid flywheel. From figure 2.25.

$$Q_e = (J_{c_1} + J_e)\dot{\Omega}_e + F_e\Omega_e + Q_c \qquad (2.65)$$

where

$$Q_c = \gamma(\Omega_e - \omega_e) \qquad (2.66)$$

is the coupling coefficient in Nm s.

$$\omega_e = n\omega_f \qquad (2.67)$$

$$Q_c = \gamma(\Omega_e - n\omega_f) \qquad (2.68)$$

---

*Direction of change is implied in the statement UP/DOWN. It means changing from higher numbered gear to lower numbered gear, e.g. 4 to 3, or 3 to 2. DOWN/UP means shifting up a gear.

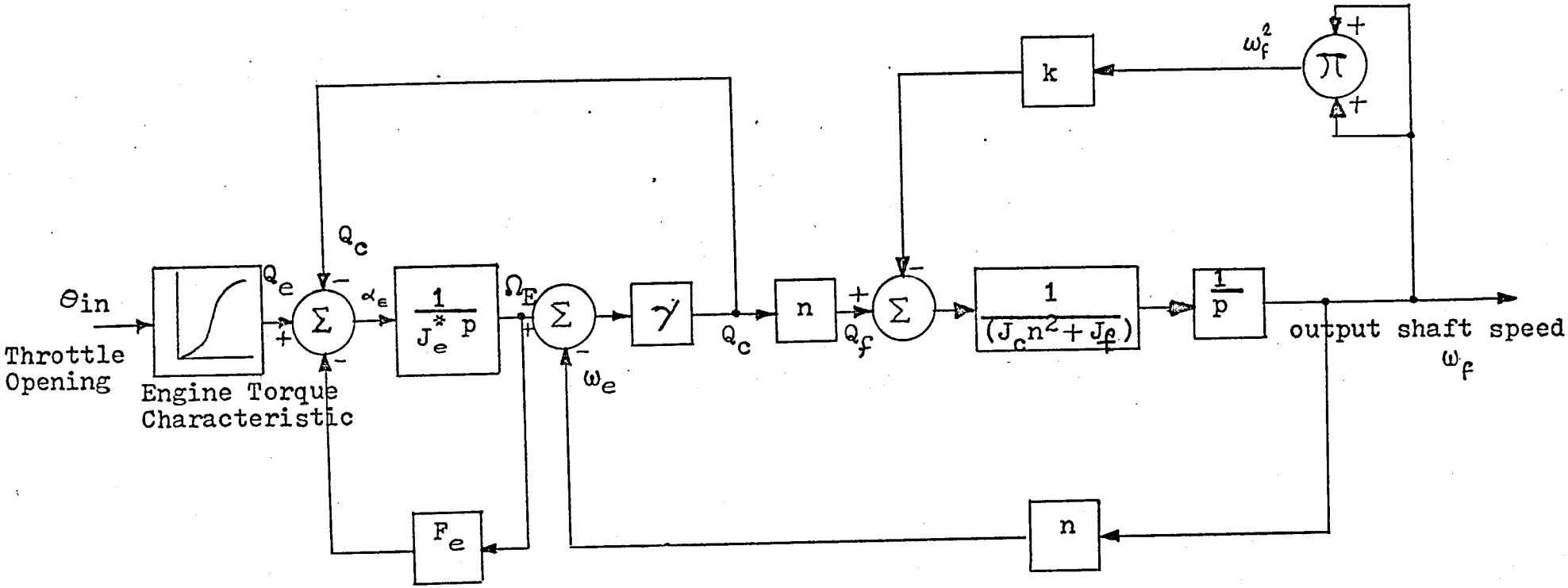

Figure 2.25 - Block Diagram of Engine, Transmission and Load

and

$$Q_e = (J_{c_1} + J_e)\dot{\Omega}_e + (F_e + \gamma)\Omega_e - n\gamma\omega_f \tag{2.69}$$

but

$$nQ_c = J_{c_2}n^2\dot{\omega}_f + J_f\dot{\omega}_f + k\omega_f^2 \tag{2.70}$$

i.e.

$$n\gamma(\Omega_e - n\omega_f) = J_{c_2}n^2\dot{\omega}_f + J_f\dot{\omega}_f + k\omega_f^2 \tag{2.71}$$

Therefore

$$\dot{\Omega}e = \frac{-(F_e + \gamma)\Omega_e}{(J_{c_1} + J_e)} + \frac{n\gamma\omega_f}{(J_{c_1} + J_e)(J_{c_1} + J_e)} + \frac{Q_e}{} \tag{2.72}$$

$$\dot{\omega}_f = \frac{-k}{(J_{c_2}n^2 + J_f)}\omega_f^2 - \frac{n^2\gamma}{(J_{c_2}n^2 + J_f)}\omega_f + \frac{n\gamma_{c_2}}{(J_{c_2}n^2 + J_f)}\Omega_e \tag{2.73}$$

i.e. $$\underline{v} = \underline{f}(\underline{v}, Q_e) \tag{2.74}$$

where

$$\underline{v} = \begin{bmatrix} \Omega_e \\ \omega_f \end{bmatrix} \tag{2.75}$$

A block diagram representation of (2.72) and (2.73) is given in figure 2.25.

2.4.3 Qualitative Account of Gearshift Overshoot

In this section a qualitative description of how the overshoot occurred on a gearshift is presented. The account developed an approach contained in EVERSHED (1966) for an application involving a dry friction clutch and an electric motor driving a linear load.

Considered first was the effect upon the speed of the fan of a sudden application of engine torque via the fluid coupling.

$$nQ_c = J_{c_2} n^2 \dot{\omega}_f + J_f \dot{\omega}_f + k\omega_f^2 \qquad (2.70)$$

i.e.

$$\dot{\omega}_f = \frac{-k}{(J_{c_2} n^2 + J_f)} \omega_f^2 + \frac{n}{(J_{c_2} n^2 + J_f)} Q_c \qquad (2.76)$$

The solution of this differential equation was found, from (2.38), to be :

$$\omega_f(t) = \sqrt{\frac{nQ_c}{k}} \tanh \left\{ \frac{\sqrt{nkQ_c}}{(J_{c_2} n^2 + J_f)} t \right\} \qquad (2.77)$$

The applied torque, Q_c, is assumed to be constant. Suppose that just prior to applying this fan torque the engine had been running at some equilibrium speed

$$\Omega_e = \frac{Q_e}{F_e} \qquad (2.78)$$

With this sudden torque the engine would be loaded and its speed would fall. The kinetic energy associated with the inertia of the engine could be transferred partially to the dynamometer during this short period of acceleration. When the fluid flywheel stopped "slipping" the engine could return to steady-state speed. The engine speed was changed, therefore, by a component of speed, due to Q_c, given by (2.77). Figure 2.26 shows how the engine speed varies with this application of load torque. During this interval of slipping the engine speed increased towards a new steady value. The dashed line in figure 2.26 shows a fan acceleration characteristic, modified as appropriate by n_j. From the graph it is seen that at some time, t_s, the engine and fan speeds were identical again. At this time the "slipping" had stopped

and Q_c was zero. In figure 2.25 the negative feedback path, corresponding to the signal, Q_c, was open-circuited. The engine and fan followed the same acceleration curve to the new equilibrium speed.

2.4.5 Simulation of the Engine, Transmission, and Load System

Figure 2.25 was the basis of the analogue simulation shown in figure 2.27. The arrangements for displaying and recording the outputs of the simulation are shown in figure 2.27 also, together with the analogue portion of the automatic gear-changing scheme. The associated logic diagram is given in figure 2.27b. A simplification of this logic arrangement would be possible on a machine in which more than eight digital-to-analogue (D/A) switches were provided. The logic inverters, N24, N25 and N26, shown in figure 2.27b, would be required no longer. These inverters were used to control the logic which determined the integrator mode : the integrators (A43, A45, A47) were patched as logic-controlled summers (see Appendix A1) in lieu of D/A switches. The potentiometer settings, and their corresponding function representations, have been set down in table 2.4. An explanation of the analogue switch functions is furnished in table 2.5.

The simulation was used to determine the engine and transmission system parameters by matching simulated and experimental responses. The static engine torque characteristic has been moved ahead of the engine simulation to become the block following the servomechanism : this was done for computational convenience and has been discussed earlier in section 2.1. From figure 2.8 it is seen that there was a substantially

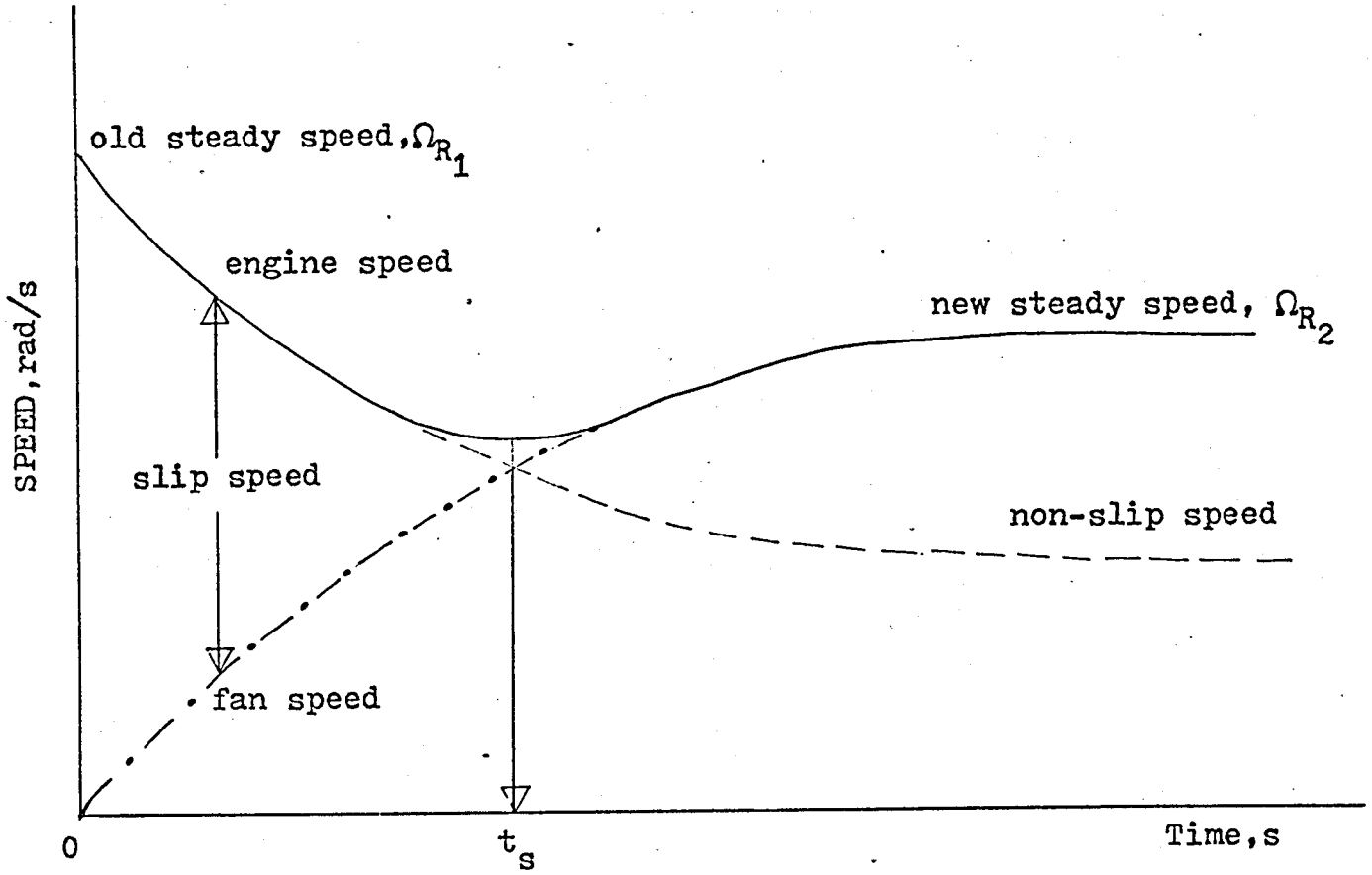

Figure 2.26 - Variation of Engine Speed with Gear Actuation

Figure 2.27a - Analogue Simulation Diagram

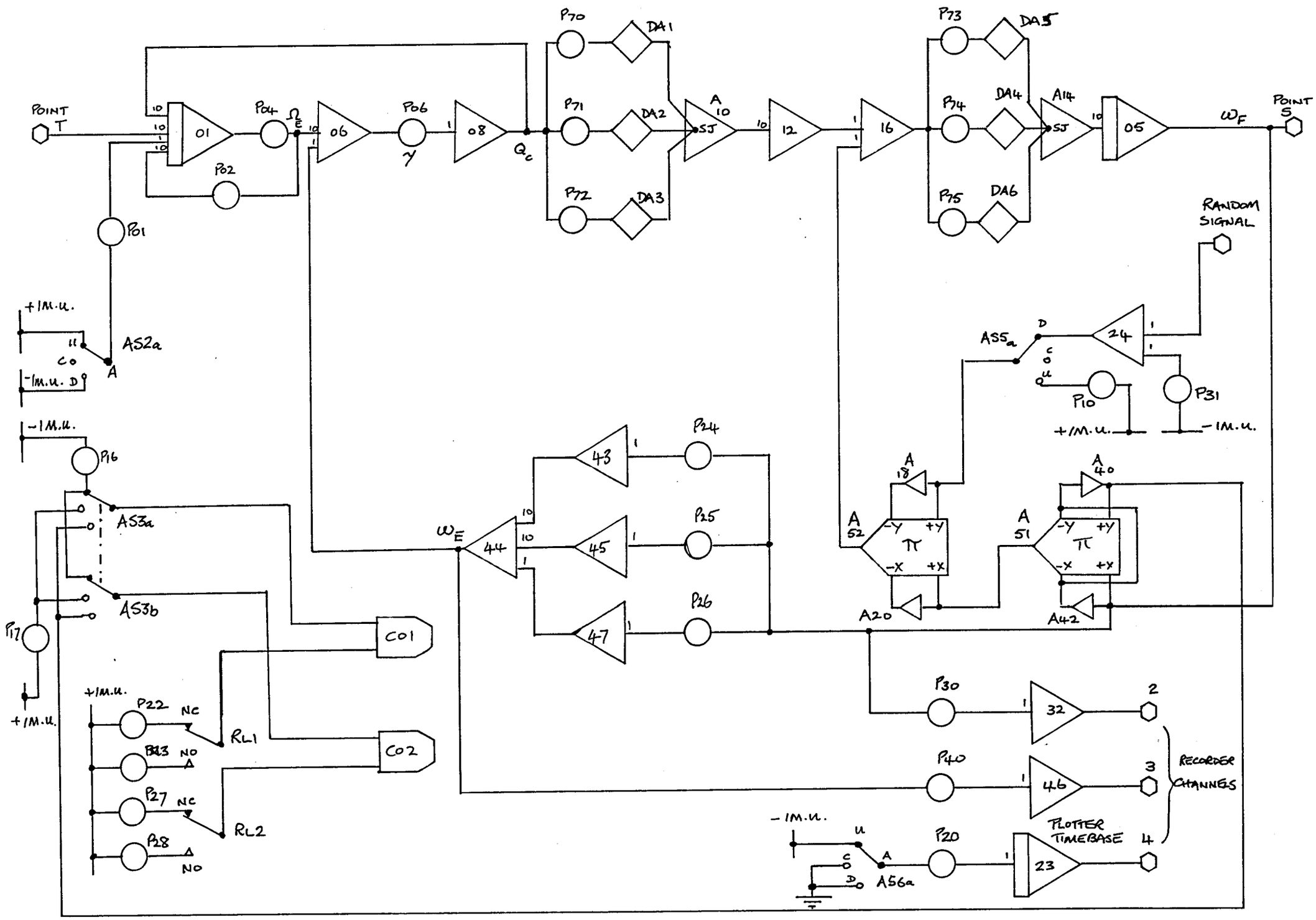

Figure 2.27a — Analogue Simulation of Engine, Transmission and Load

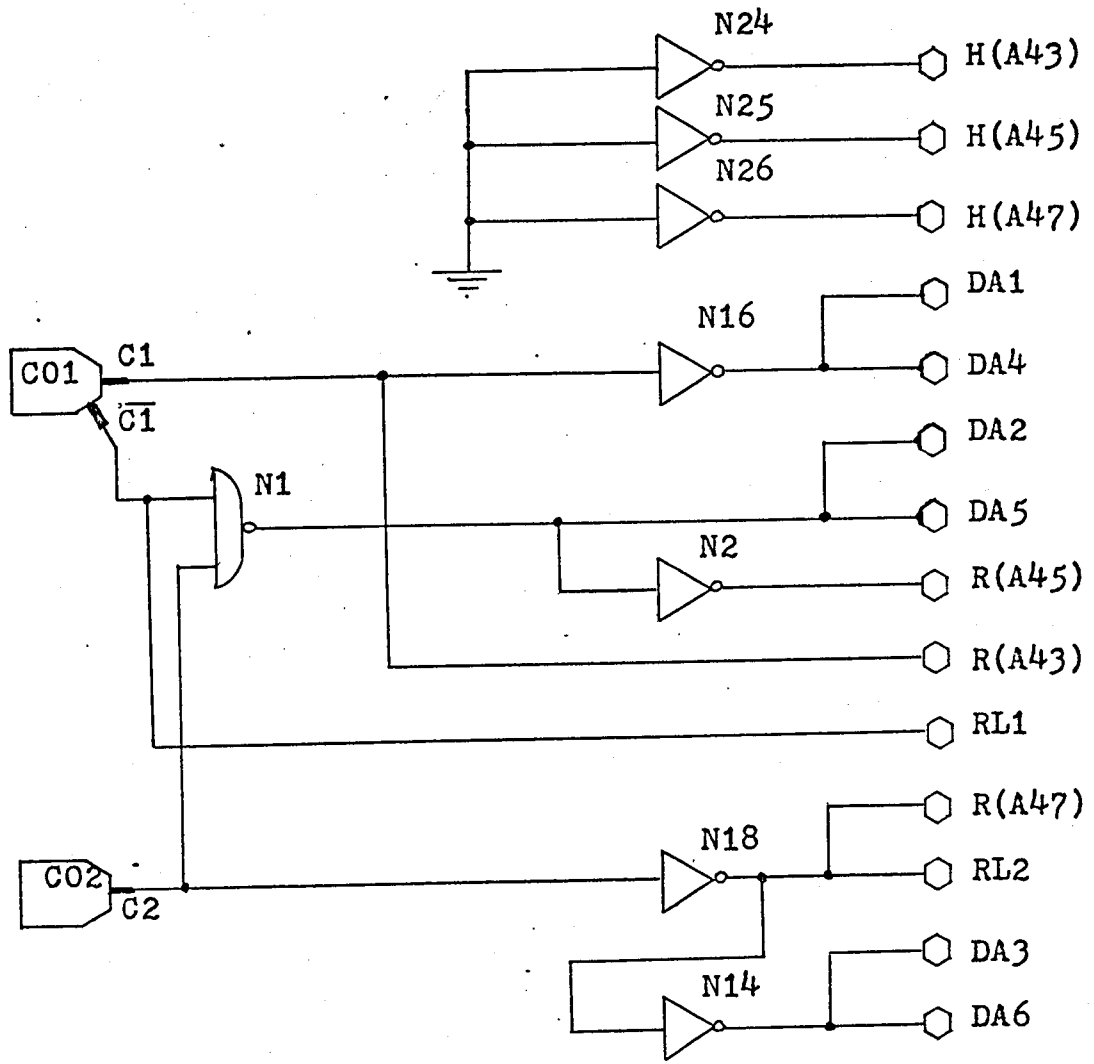

Figure 2.27b - Logic Diagram for Control of Analogue Simulation of Figure 2.27a

SYSTEM FUNCTION	POTENTIOMETER	
	ADDRESS	SETTING
O.L. DEMAND TORQUE, Q_o	P00	1200
TORQUE DISTURBANCE, Q_u	P01	0600
ENGINE FRICTION, F_e	P02	1567
C.L. DEMAND TORQUE, Q_c	P03	1200
(ENGINE & FLYWHEEL INERTIA)$^{-1}$	P04	1894
FLYWHEEL COUPLING COEFFICIENT	P06	4730
THROTTLE SERVO GAIN (OPEN-LOOP)	P08	4330
THROTTLE SERVO PARAMETER	P09	1600
DYNAMOMETER COEFFICIENT	P10	3333,2888,2385
(depends on fan setting)		1845,1350,0925
THROTTLE SERVO GAIN (C.L.)	P12	4330
MANUAL GEARSHIFT (3/4)	P16	3300
INPUT PLOTTER TIME-BASE	P20	0100
NO 2 GEAR SELECTION VALUE(DOWN)	P22	2600
NO 3 GEAR SELECTION VALUE(UP)	P23	2700
2ND GEAR RATIO	P24	2210
3RD GEAR RATIO	P25	1470
4TH GEAR RATIO	P26	9999
NO 3 GEAR SELECTION VALUE(DOWN)	P27	4300
NO 4 GEAR SELECTION VALUE(UP)	P28	4400

Table 2.4 : POTENTIOMETER SETTINGS FOR ANALOGUE COMPUTER SIMULATION OF ENGINE, FLUID FLYWHEEL, GEARBOX AND DYNAMOMETER (refers to figure 2.27a)

SYSTEM FUNCTION	POTENTIOMETER	
	ADDRESS	SETTING
THROTTLE SERVO PARAMETER	P29	1300
CONTROLLER GAIN, d_1	P30	see Chap 6
DYNAMOMETER COEFFICIENT	P31	same as P10
CONTROLLER GAIN, d_2	P32	see Chap 6
CONTROLLER GAIN, d_3	P33	see Chap 6
SCALING FACTOR (U.V. RECORDER)	P40	9999
STATIC TORQUE GAIN	P41	see Chap 6
2ND GEAR RATIO	P70	2210
3RD GEAR RATIO	P71	1470
4TH GEAR RATIO	P72	1000
$(Jc_2n_1^2 + J_f)^{-1}$	P73	1275
$(Jc_2n_2^2 + J_f)^{-1}$	P74	1980
$(Jc_2n_3^2 + J_f)^{-1}$	P75	2500

Table 2.4 : (continued from Page 61)

ADDRESS	SWITCH POSITION	FUNCTION
AS1	U	OPEN LOOP - COMMAND INPUT
	C	---
	D	CLOSED LOOP COMMAND INPUT
AS2	U	FIXED TORQUE DISTURBANCE (+)
	C	---
	D	FIXED TORQUE DISTURBANCE (-)
AS3	U	GEAR 3 SELECTED
	C	GEAR 4 "
	D	AUTOMATIC GEARCHANGE
AS4	U	X-Y PLOTTER DISPLAY
	C	---
	D	C.R.O. DISPLAY
AS5	U	FAN ADJUSTMENT - MANUAL
	C	---
	D	RANDOM INPUT FAN ADJUSTMENT
AS6	U	X-TIME BASE FOR PLOTTER
	C	NO TIME BASE
	D	" " "

TABLE 2.5 - SWITCH LEGEND FOR SIMULATION DIAGRAM

linear regime and in that regime torque was related to throttle opening by (2.79) viz.

$$Q_e = K_e\theta \qquad (2.79)$$

Some typical responses from the simulation are shown in figure 2.28. Note that the inclusion of the fluid flywheel dynamics in the simulation has resulted in the characteristic overshoot on UP/DOWN shifts. On curve (a) the overshoot is very slight because the equilibrium speed (corresponding to that torque input) has been reached almost exactly at the time of the gearshift. For curve (b) with less available torque, note that in 4^{th} gear a lower final steady speed was achieved. Selection of third gear provided the necessary increased torque to raise the final steady-state speed. In this situation when the load and the available torque were within a particular range of values there was likely to be some difficulty with any automatic gear-changing scheme. (See chapter 3, section 1).

2.5 Mathematical Model of Engine, Transmission, and Load

The values of the parameters of the engine and transmission system obtained from the simulation are listed in table 2.5 below.

K_e	=	80 Nm/rad
F_e	=	0.0213 Nm s
$(J_e + J_{c_1})$	=	0.715 kg m^2
J_{c_2}	=	0.1108 kg m^2
J_f	=	0.4122 kg m^2
γ	=	0.6413 Nm s

Table 2.5 - Estimated Parameters of Engine System

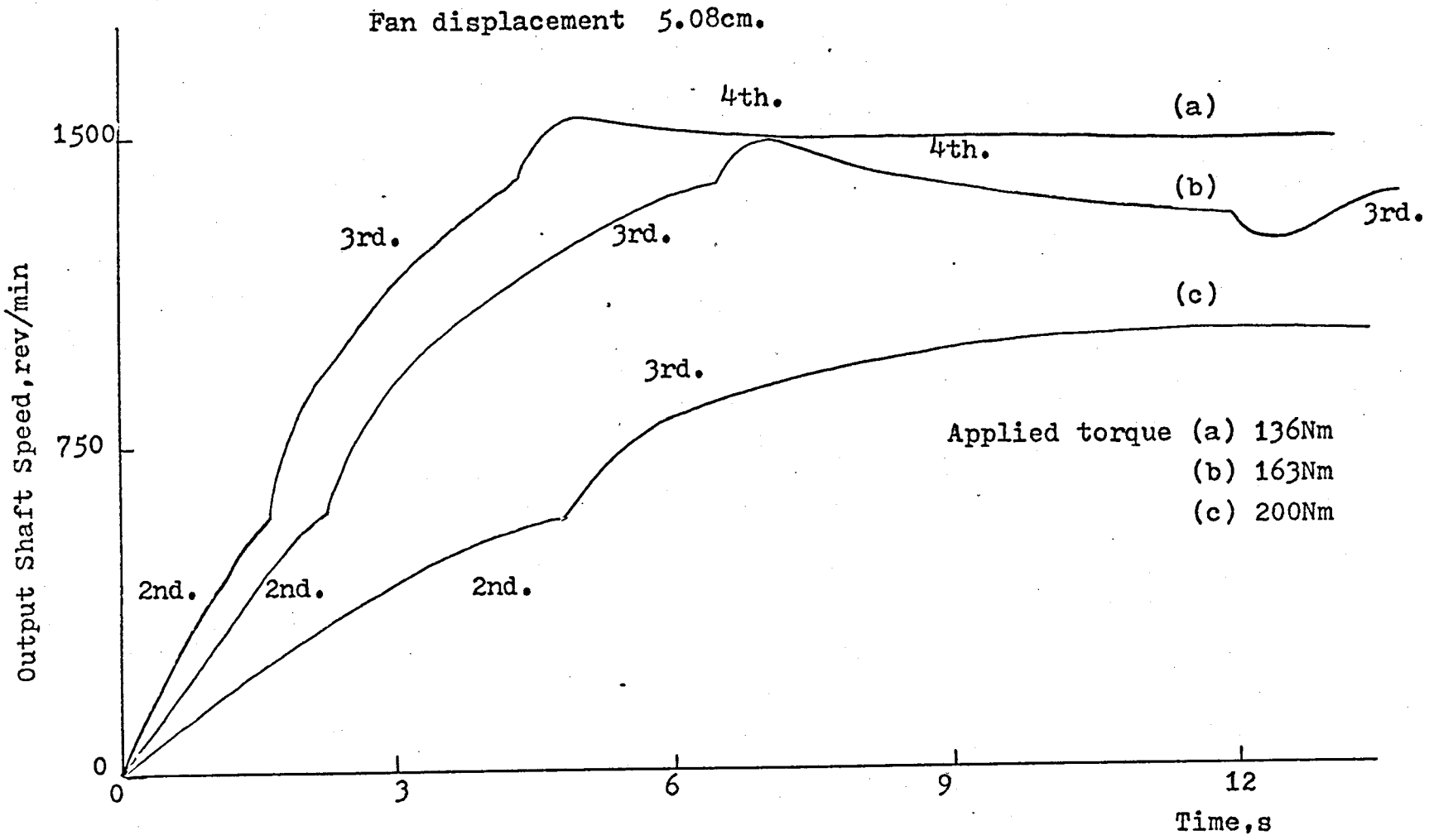

Figure 2.28 - Typical Simulated Gearchange Responses

The model of the engine, transmission and load system was obtained from (2.72) and (2.73) and table 2.5. It is given by :

$$\dot{v}_1 = -0.925v_1 + av_2 + 1.894u \qquad (2.80)$$

$$\dot{v}_2 = dv_1 - cv_2 - kbv_2^2 \qquad (2.81)$$

where, as before,

$$\begin{aligned} v_1 &= \Omega_e \\ v_2 &= \omega_f \\ u &= Q_e \end{aligned} \qquad (2.82)$$

The value of the coefficients a,b,c and d depended upon the gear selected. The values corresponding to particular gears are listed in table 2.6

Gear	a	b	c	d
2	1.98	1.275	2.94	1.33
3	1.315	1.98	2.02	1.372
4	0.894	2.5	1.165	1.165

Table 2.6 - Coefficients Used in Mathematical Model

The value of k, the damping coefficient of the dynamometer, is taken from figure 2.15.

The mathematical model of (2.80) and (2.81) is used in connection with the study of optimal start-up of the engine presented in chapter 5.

To provide a pseudo-linear model of the system for use with the regulation studies presented in chapter 6 the equations (2.49), (2.78), and (2.4) were combined to form (2.5) in which the coefficient matrix A was defined as :

$$A = \begin{bmatrix} -1.0 & 400 & 0 \\ 0 & 0 & 1 \\ 0 & -130 & -16 \end{bmatrix} \qquad (2.83)$$

And driving matrix, B, was defined as

$$B = \begin{bmatrix} 0 & 0 & 43.3 \end{bmatrix}' \qquad (2.84)^*$$

The state vector, $\underline{x}$, and the control input, u, were defined in (2.5).

In the study of the regulation properties of the plant a non-linear model was used also; it was found from (2.78), (2.4) and (2.20). It was

$$\begin{aligned} \dot{x}_1 &= -3.33kx_1^2 + 267x_2 \\ \dot{x}_2 &= x_3 \\ \dot{x}_3 &= -130x_2 - 16x_3 + 43.3V_{in} \end{aligned} \qquad (2.85)$$

The x_i in (2.85) were the components of the state vector defined for (2.5).

---

*The system is controllable : the matrix, H, had rank 3.

That is,

$$H = (B \vdots AB \vdots A^2B) = \begin{bmatrix} 0 & 0 & 17320 \\ 0 & 43.3 & -6928 \\ 43.3 & -692.8 & 5455.8 \end{bmatrix} \rightarrow \text{rank } 3$$

CHAPTER 3 - A SYSTEM FOR CHANGING GEAR

3.1 Introduction

In the preceding chapter the effect of gearchanging upon the dynamic response of the system was considered. In this present chapter the physical procedure by which gearchanging was effected is described. A specially devised scheme for automatic gearchanging is presented together with an account of its performance.

Much of the detail in this chapter relates to the "hardware" implementation of the scheme devised : by the nature of experimental work the actual implementation could be improved greatly now and the inter-unit wiring could be much simplified by using compatible logic and electronic circuits.*

Where sub-systems have been introduced solely to assist the engineering implementation, but which, in principle, are not required ,will be pointed out in the text at the appropriate point; the reason for the inclusion of the element will be given also.

3.2 Gearchanging Logic Schemes

It was explained in section 2.1 why first gear could not be used : the gears employed were 2nd, 3rd, and 4th. Physically gears are changed on a Daimler/Wilson gearbox by

*By using in the experimental rig elements and components which were available immediately (for convenience and cheapness) a large number of different power supplies were needed. Compatible elements would reduce this number to one or two.

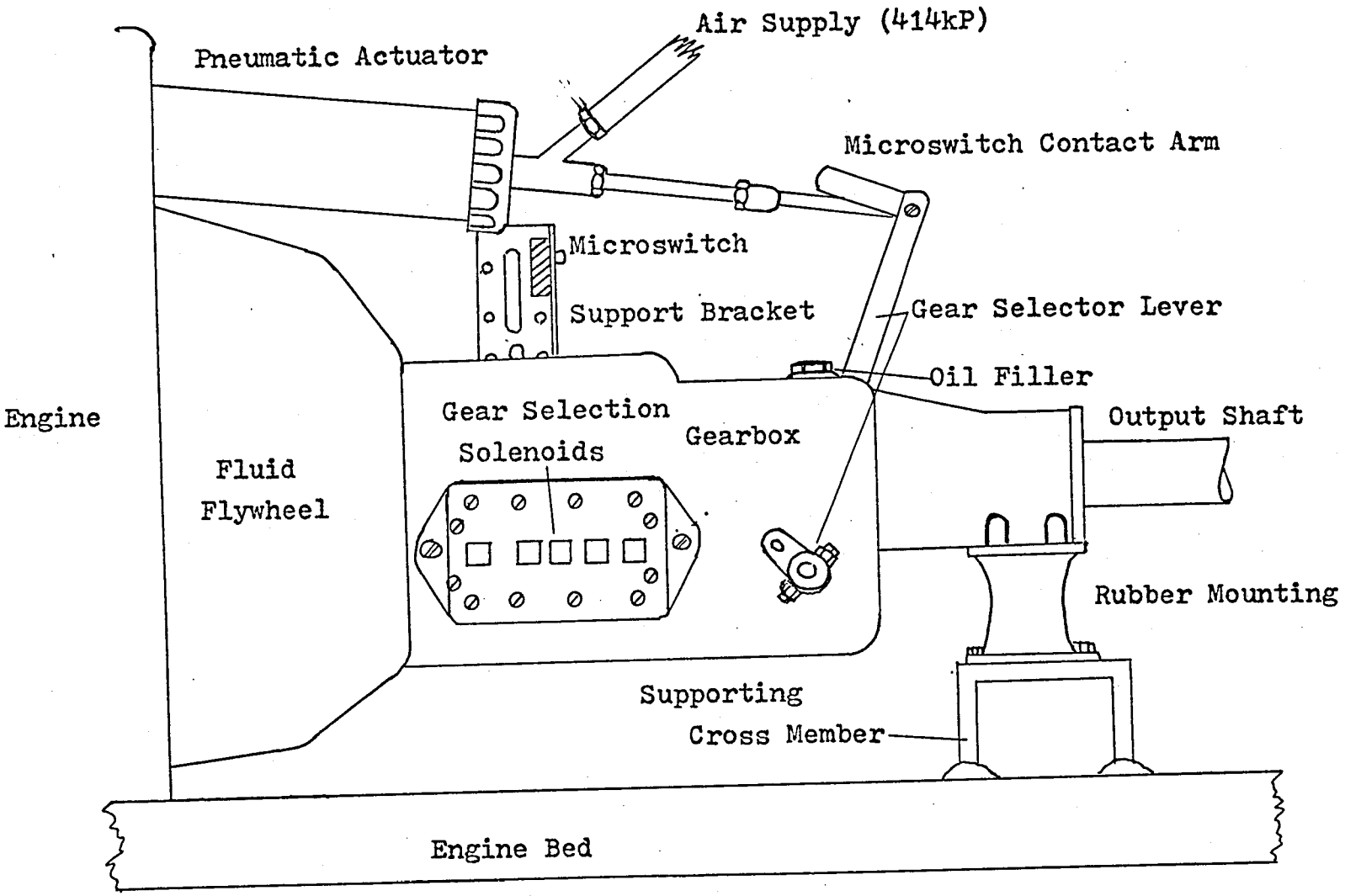

Figure 3.1 - Automatic Gearbox Assembly

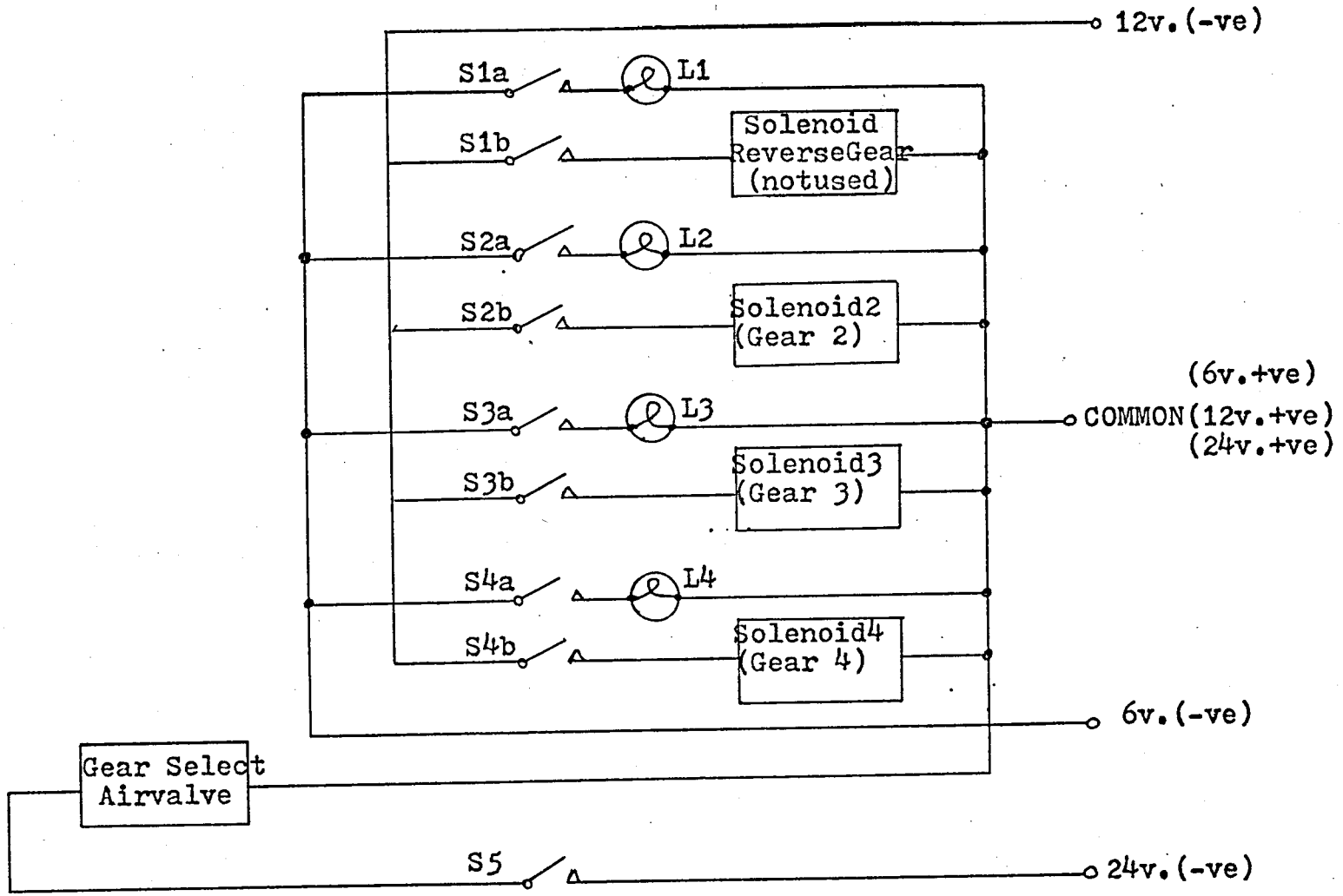

Figure 3.2 - Circuit Diagram of Manual Gearchange Scheme

pre-selecting the gear required and then, when the change is required, by depressing the gear-selector lever. (See figure 3.1). The engine torque is transmitted to the gearbox through the fluid flywheel. In this research the gears were selected by selecting a solenoid which actuated the toggle arm in the gearbox to pre-select the required gear. By switching a solenoid-operated air valve a pneumatic, linear actuator moved the gear-selector lever and the gear change was effected. A circuit diagram of the manual gearchange scheme is given in figure 3.2. The time for a gear to be changed from the instant of switching the solenoid of the air valve to selection of new gear is 1.2 seconds, approximately. The response of engine speed during such a change was discussed and modelled in chapter 2. The modelling was based upon a com puter simulation and the logic scheme to change gears automatically was developed on the analogue computer. The logic diagram is shown in figure 3.3. From figure 2.4 it was noted that the engine delivered its maximum torque at a speed of 2000 rev/min. This speed also corresponded to minimum specific fuel consumption. (See figure 2.5). Consequently the gearchange programme was designed such that at some starting time, say t_o, gear 2 was selected* and the engine was accelerated from its idling speed of about 400 rev/min. At the first reference speed, ω_{f23}, the first change of gear (from 2nd to 3rd) occurred. The second change (from 3rd to 4th) occurred at the second reference speed, ω_{f34}. These reference speeds were chosen such that the engine speed was 2000 rev/min when the change was started. These speeds were therefore :

$$\omega_{f23} = 95 \text{ rad/s} \qquad (3.1)$$

$$\omega_{f34} = 145 \text{ rad/s} \qquad (3.2)$$

---

*This assumption pre-supposed that the progression through the gears (2-3-4) would be the sequence for the optimal solution.

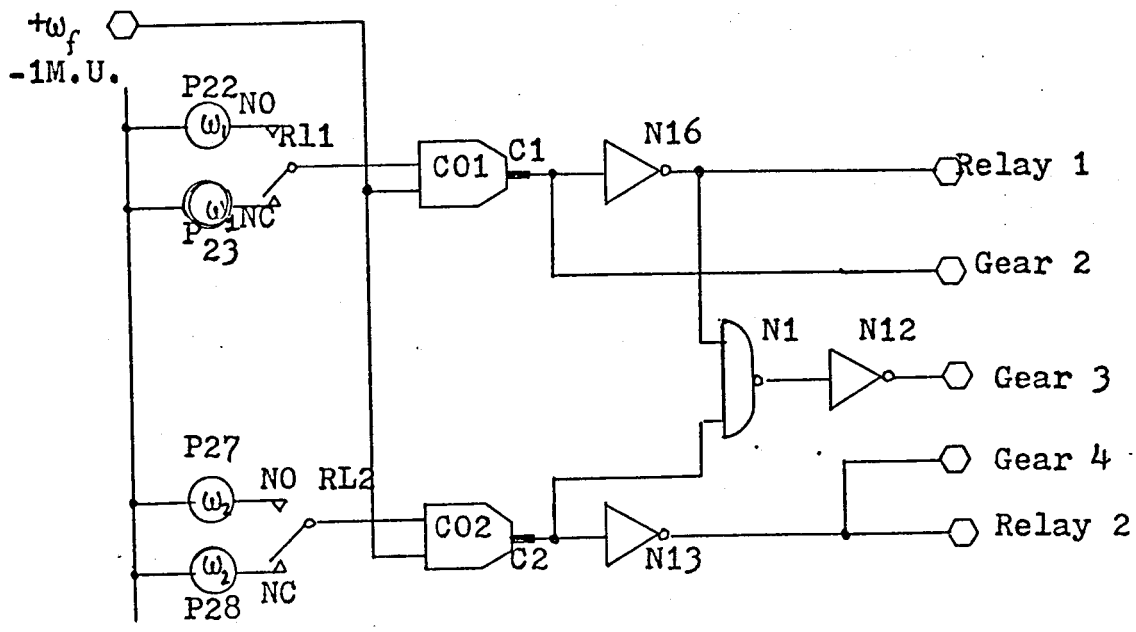

Figure 3.3 - Gear-changing Logic System

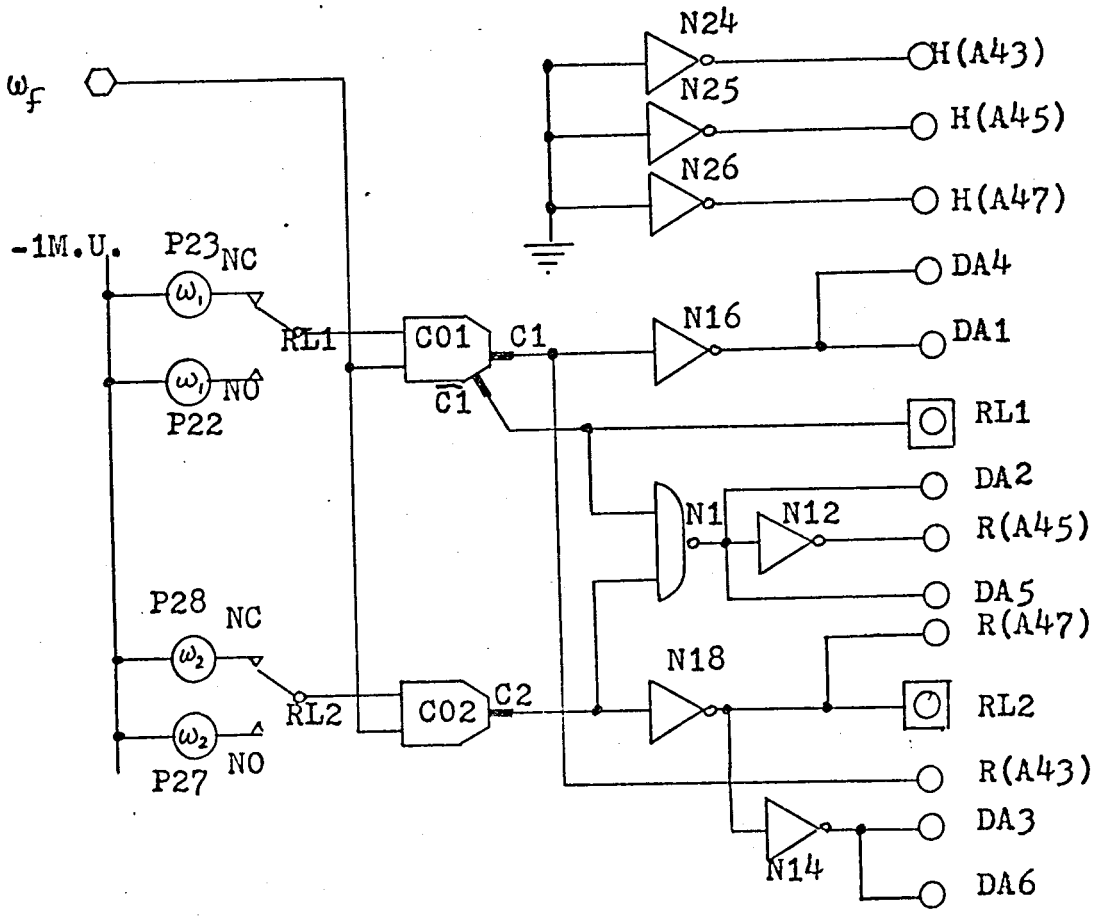

Figure 3.5 - C_i - 175 Gear-changing Logic Diagram

From the account of the automatic gearchange system given later in this chapter it may be seen that in any automatic system the UP and DOWN changes would be initiated at slightly different values of ω_{f23} and ω_{f34}.

When the dynamometer shaft speed was greater than the reference speed, ω_1, (set on P22 of figure 3.3) the comparator, C_1, changed state. Gear 2 had been selected previously (by virtue of the initial logic states) and now, because of the comparator switch action, gear 3 was selected until the dynamometer speed exceeded ω_2 at which point comparator, C_2, changed state and gear 4 was selected. With this scheme included in the engine simulation then on gearchange, for certain load conditions, the feedback loop opened and the upper gear was selected again. Because of the load the engine speed fell again, and consequently the dynamometer speed fell until it again reached the reference speed and the lower gear was selected. This sequence was repeated and an oscillation was set up. Figure 3.4 illustrates this phenomenon (see curves 4 and 5). Such hunting is a feature of all automatic transmissions and a recognised and conventional cure is to provide the means whereby UP changes are effected at slightly higher reference speeds than DOWN changes. By introducing this threshold into the switching the hunting was limited. However, if the changeover limit was kept narrow, as it had to be if the automatic transmission was to be efficient, hunting could still occur under extreme conditions of load. In commercial

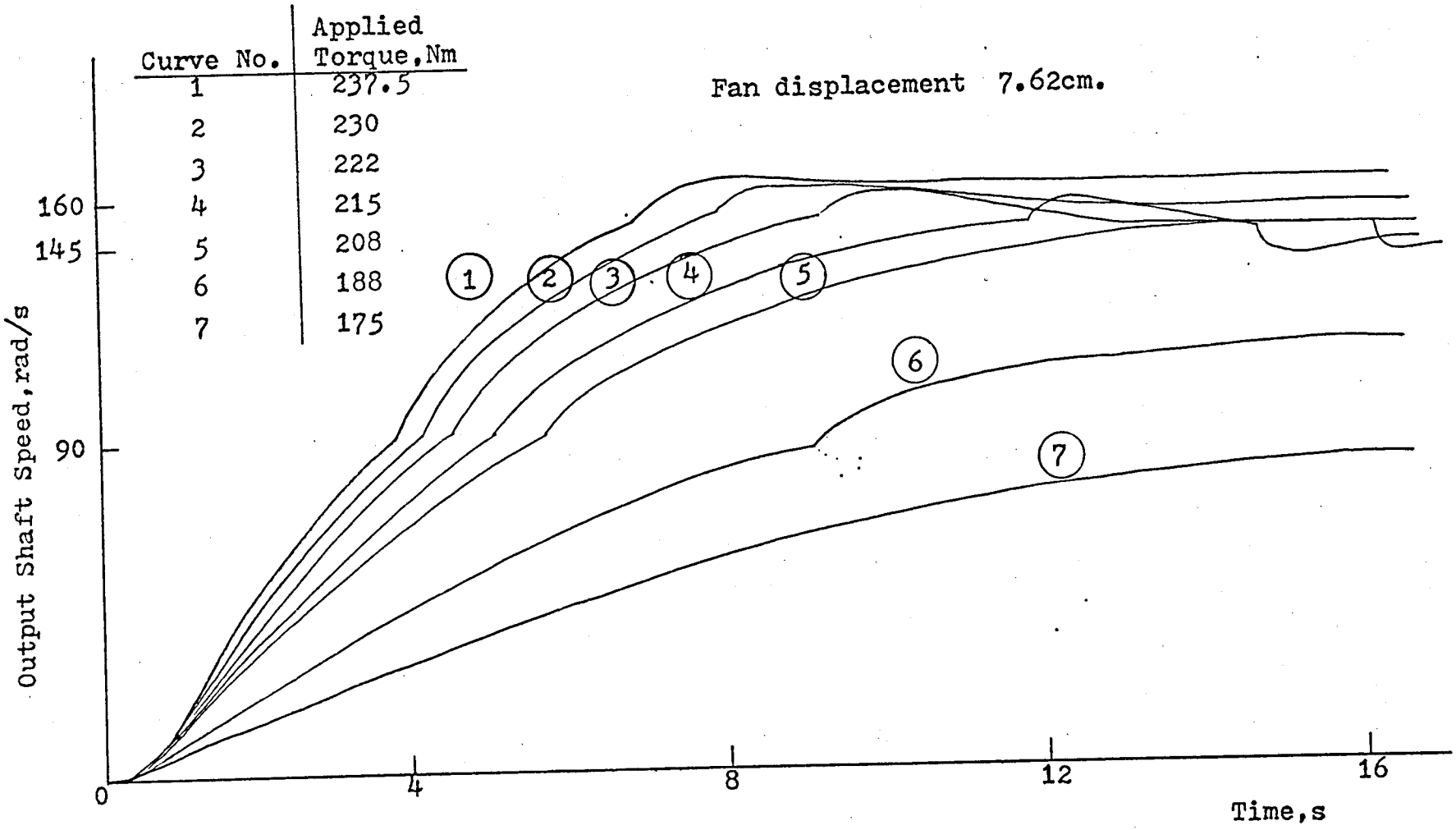

Figure 3.4 - Hunting during Gearchanges

automatic transmissions the solution is to provide LOCK, or manual override, facilities by means of which the operator may hold a lower gear until the desired engine speed has been achieved, or the load condition has improved. In figure 3.4 it can be seen that the hunting occurs only for a very restricted load and final speed combination. In the computer simulation, figure 2.27a, it was possible to select either 3rd or 4th gear manually by means of the analogue switch AS3. (See table 2.5). In the automatic gearchange scheme used, as soon as the change had been effected, the reference speed was altered to a slightly lower value. To alter the reference speed two relays and additional potentiometers were used. (See figure 3.3). The truth table corresponding to the arrangement of figure 3.3 is given in table 3.1.

Speed Condition	C	$\bar{C}_1$	C_2	$\bar{C}_2$	N_{12}
$(\omega_f + \omega_1) > 0$	1	0	1	0	0
$(\omega_f + \omega_1) < 0$	0	1	1	0	1
$(\omega_f + \omega_2) < 0$	0	1	0	1	0

$\omega_1 < \omega_2$

Table 3.1 - Truth Table for Gear Logic

In figure 3.5 the additions necessary to effect gearchanges on the engine simulation are shown. The component addresses refer to the engine simulation shown in figure 2.27. In figure 3.3 the gearchange scheme simply actuated the gear; in the engine system itself the logic signal, at the gear terminal (n), actuated a solenoid. Another signal had to be generated from the logic to actuate the linear pneumatic actuator to move the gear selector lever on the gearbox. (See figure 3.1).

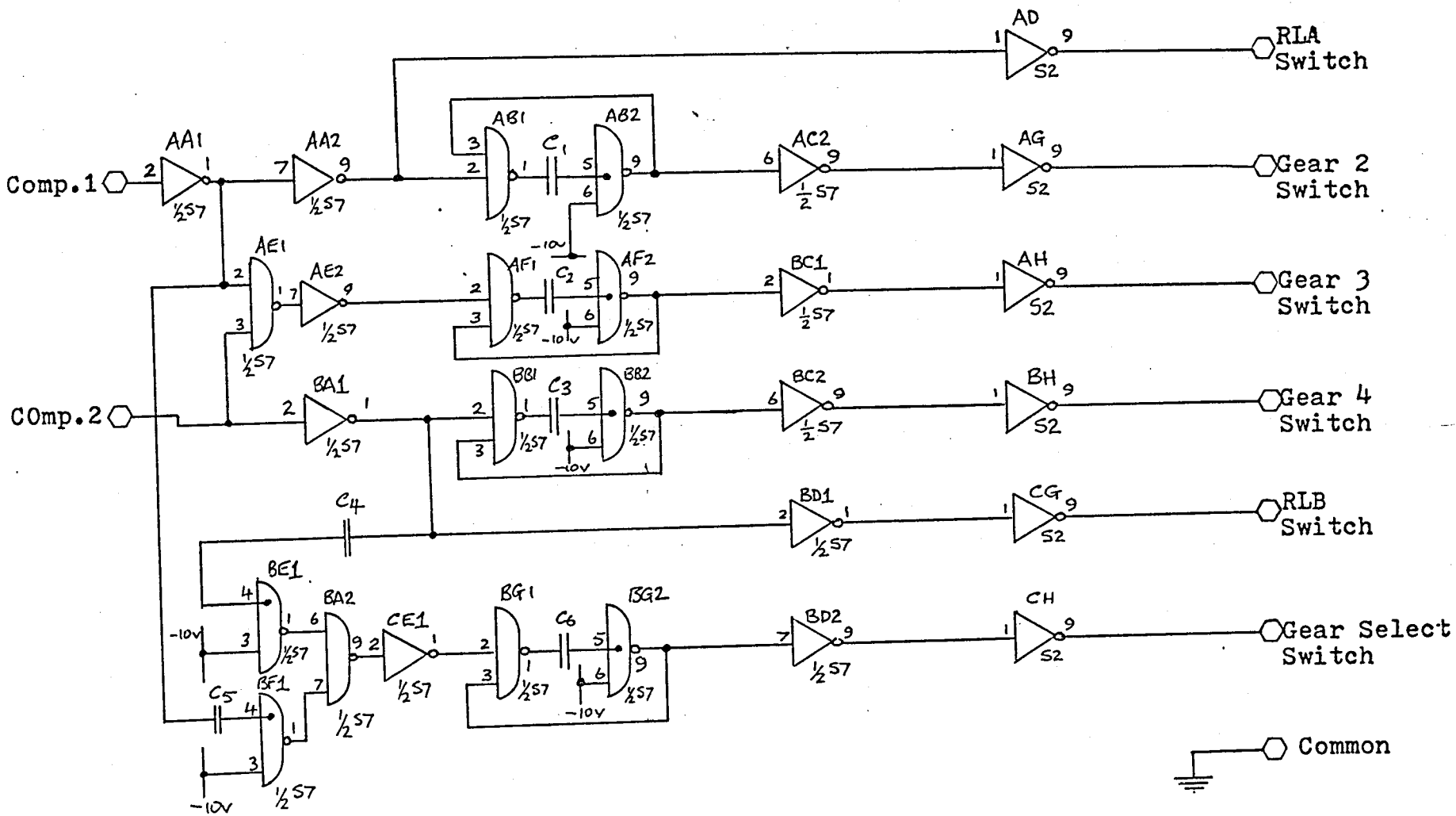

Figure 3. 6 - Initial Gear-changing Logic Scheme

3.3 Practical Gearchange Unit

The logic for gear selection was based firmly upon figure 3.3. Certain practical considerations however dictated the final implementation of the design. First, the actuation for the gear selector lever was ON/OFF - controlled by a solenoid air valve which worked from a 24v. d.c. supply and had a resistance of 16Ω. The air pressure required for the pneumatic system was 414 kilopascals. The solenoids which actuated the gear toggle arm required a 12v. d.c. supply and had resistance of 6Ω. The air valve and the solenoids were not continuously rated at the required respective standing currents of 1.5 and 2A. Consequently the logic unit had to provide a logic sequence viz. gear preselected by a solenoid, pneumatic actuator switched on, gear-selector lever moved, gearchange effected, actuator switched off and returned to neutral position, gear pre-selector solenoid switched off. With this sequence the duty cycle of the electrical components was restricted sufficiently to permit their use in this application. The logic elements, however, could not provide sufficient power to drive either the air valve or the solenoids. A solid-state driving unit had to be provided therefore. Because the logic (defined in Appendix A2) was negative true, and because the electrical system of the engine was positive earth it was convenient to use npn transistors to drive the solenoids and air valve. The logic scheme devised initially used MINILOG elements (produced by Elliot Ltd.) : the arrangement is shown in figure 3.6. The inputs to this unit were acquired from the comparators and the outputs were used as the inputs to the drive unit (not shown). The logic signals in the

four channels viz. 2,3,4 and SELECT were processed into long pulses by the appropriate delay units. To ensure that the gear selector would be actuated only on a change of comparator state i.e. only when a gearchange is necessary, the logic signals for the SELECT channel were differentiated and hence the actuator would switch off after a delay determined by C_6 (see figure 3.6). The delay had to be sufficient for the actuator to travel its full length and select the gear. 1 second was chosen as the delay. The scheme worked in laboratory tests but proved to be totally unreliable in service because of the second-hand nature of the elements* Further experimental use of this unit was abandoned because of the detrimental effects of abusive gearchanges which resulted with component failure and malfunction. An alternative gear switching unit was designed using System 11 logic elements (Texas Instruments). These units were positive true logic devices which required a different supply voltage from the MINILOG elements. The same drive unit was employed with the new switching unit. However the logic signals for the input to the drive unit were incorrect in polarity and level. A logic conversion unit had to be designed and constructed therefore. The overall gearchanging arrangements are shown in schematic form in figure 3.7. Each block in that figure has a unit annotation and a corresponding figure reference. A description of each block of figure 3.7 follows.

---

*These units were available at R.A.F. CRANWELL but they had been used in some other apparatus previously.

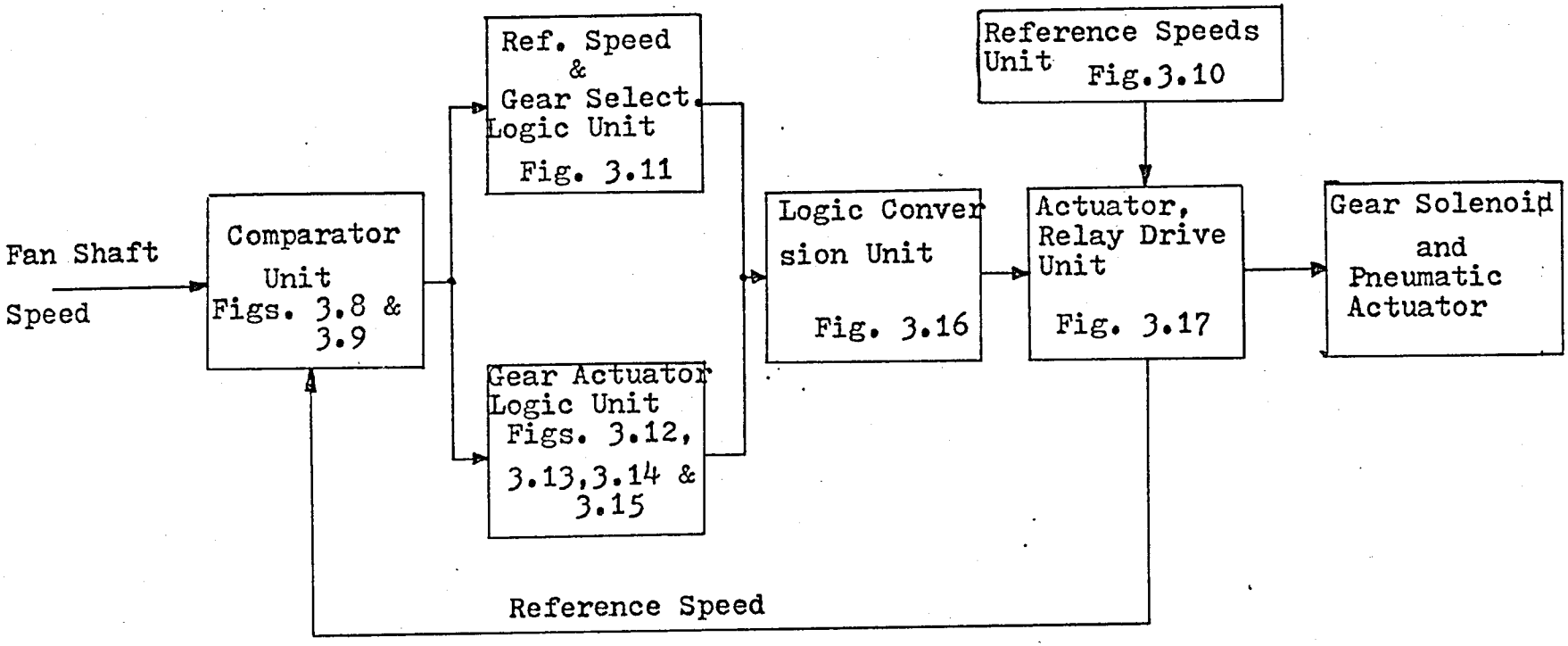

Figure 3.7 - Automatic Gear System

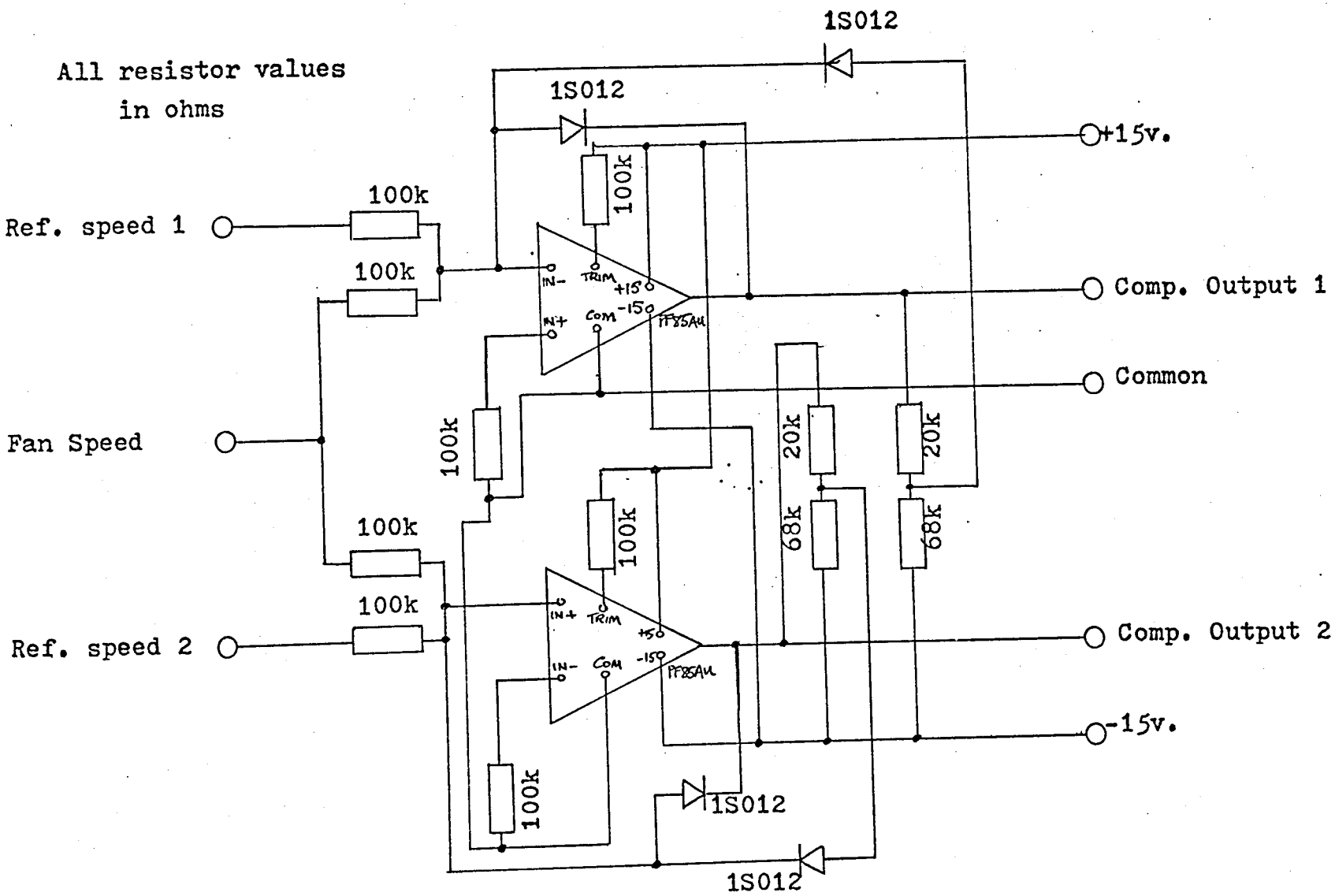

Figure 3.8 - Circuit Diagram of the Comparator Unit

3.3.1 Comparator Unit

These units were designed to produce the following logic conditions :

Analogue Input Condition	Output Logic
$(\omega_f + \omega_1) < 0$	1
$(\omega_f + \omega_1) > 0$	0

Logic 1 = +4v. Logic 0 = 0v.

Table 3.2 - Comparator Logic Definition

The circuit used is shown in figure 3.8. Commercial operational amplifiers were used; the amplifiers chosen were the low cost, low performance types PF85AU*. It was found on test that the loading of these amplifiers by the logic elements which they had to drive was too great. Buffer amplifiers had to be devised therefore and were interposed between the operational amplifiers and the inputs of the associated logic elements. The circuit diagram is shown in figure 3.9. The output voltage levels available from either comparator of figure 3.8 were 0v. and -4v; the buffer amplifier (figure 3.9 below) was an inverter so that at its output the desired logic levels were obtained.

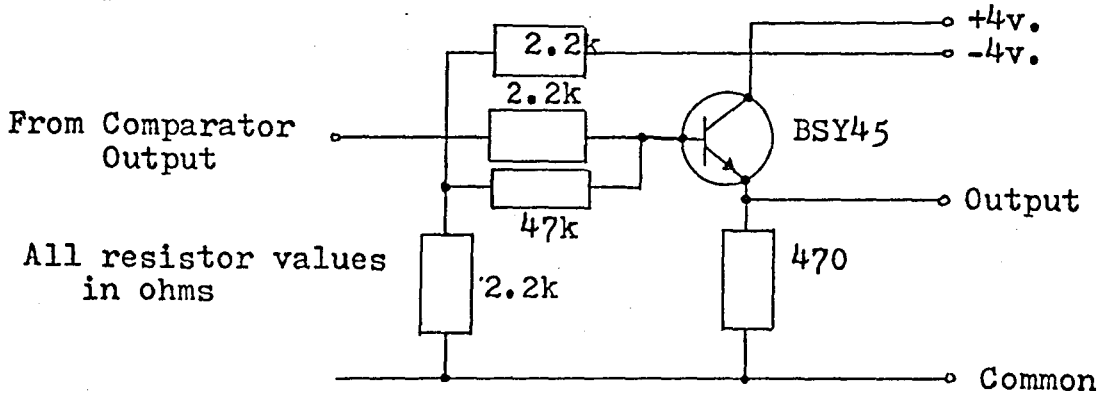

Figure 3.9 - Comparator Buffer Amplifier

*Manufactured by Philbrick Ltd.

N.B. Ov. was not quite obtained for logic 0. When the buffer amplifiers were connected to the logic elements the voltages measured at the output terminals of the buffer amplifiers for logic 0 were below the maximum voltage level defined for this logic state for these elements.

3.3.2 Reference Speed Units

Reference speeds were derived as voltages on the potentiometers used in this unit. (See figure 3.10). The relays which selected the reference voltages were housed in the actuator unit for convenience. These voltages were connected from the actuator unit to the inputs of the comparators.

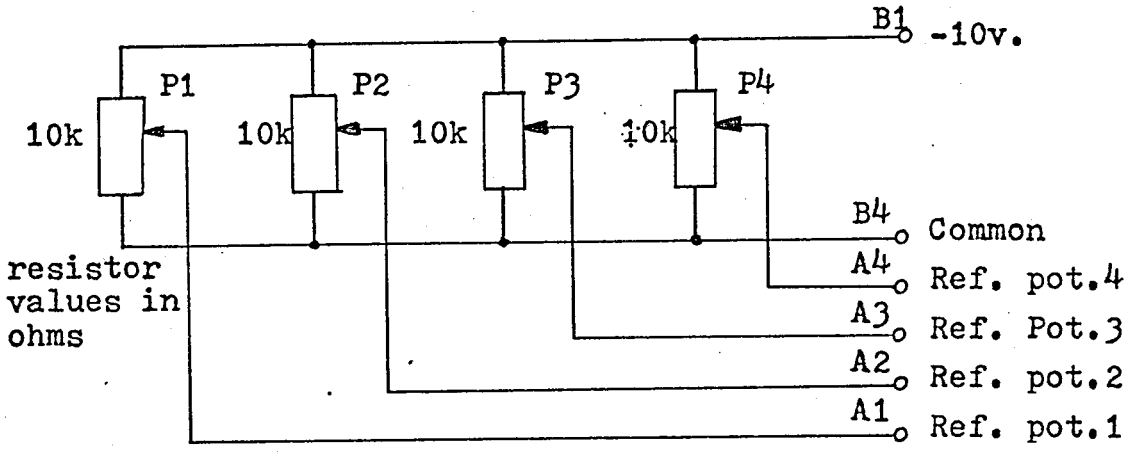

Figure 3.10 - Reference Speed Unit

Reference voltage settings* were derived as follows :-

Design speed for 2/3 gearshift = 905 rev/min (3.3)

Design speed for 3/4 gearshift = 1365 rev/min (3.4)

The sensitivity of the output shaft tachogenerator was given in chapter 2 as 3.33v./1000 rev/min. The maximum reference voltage available from the reference speed unit was -10 volts. Hence the reference voltage for shift 2/3 ⟶ 3.02 volts.

for shift 3/4 ⟶ 4.55 volts.

---

* Earlier these settings were quoted in rad/s, but they are given here in rev/min for analytical convenience.

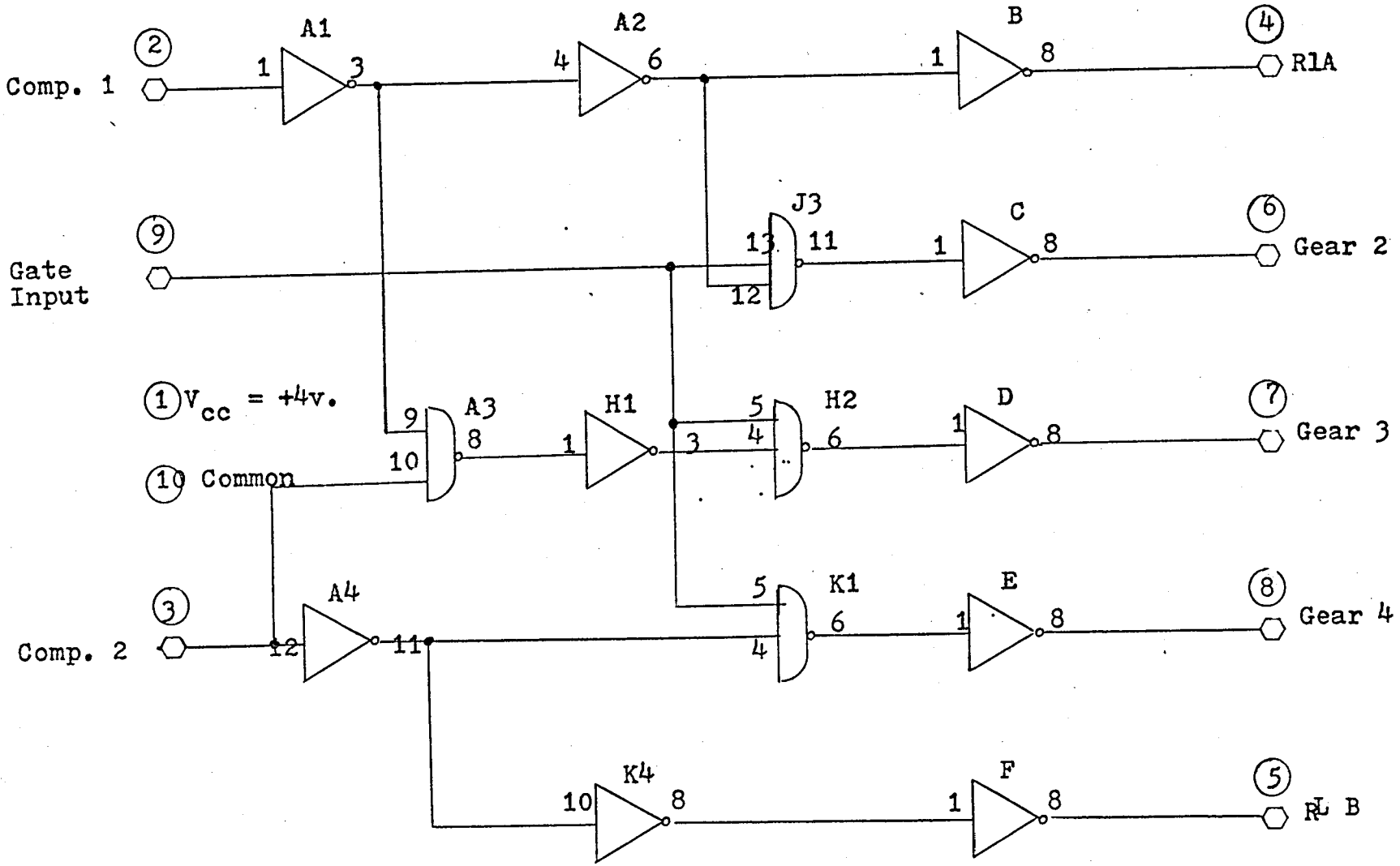

Figure 3.11 - Gear Logic Unit

The appropriate potentiometer settings were therefore as given in table 3.3 :

Potentiometer Address	P_1	P_2	P_3	P_4
Setting	2900	3020	4430	4550
Shift Direction	Down	Up	Down	Up

Table 3.3 - Reference Potentiometer Settings

3.3.3 Reference Speed and Gear Solenoid Selection Unit

The logic signals required to drive the relays which select the correct reference speed and also to drive the appropriate gear-selector solenoid were generated in this unit the logic diagram for which is given in figure 3.11. Encircled numbers in this diagram refer to terminal pins. For clarity the function associated with each pin is annotated nearby. Logic inputs to the unit are shown coming from the left of the diagram; logic outputs are at the right. Element addresses refer to individual components e.g. A4 refers to INVERTER No.4 in QUAD INVERTER element A. Again for clarity the pin numbers associated with the elements are shown. The truth table for this unit is shown in table 3.4.

Inputs		Relays		Gears*		
1	2	A	B	2	3	4
1	1	0	0	1	0	0
0	1	1	0	0	1	0
0	0	1	1	0	0	1

*In any gear logic 1 will persist only for as long as the gate input signal is logic 1 also.

Table 3.4 - Truth Table for Gear Selection Unit

The gate input was received from a microswitch actuated by the gear-selector lever. (See figure 3.1).

3.3.4 Gear Actuation Logic Unit

The logic signal, which controls the air valve, and hence the gear-selector lever via the pneumatic actuator, was generated in this unit the diagram for which is shown as figure 3.12. Where two inverters appear in this figure in cascade indicates that there was a need to buffer one logic unit from some critical loading condition. The pulse steering unit, shown in detail in figure 3.13, ensured that a pulse of the correct polarity arrived at the input of the monostable circuit of figure 3.14 every time a comparator changed state.

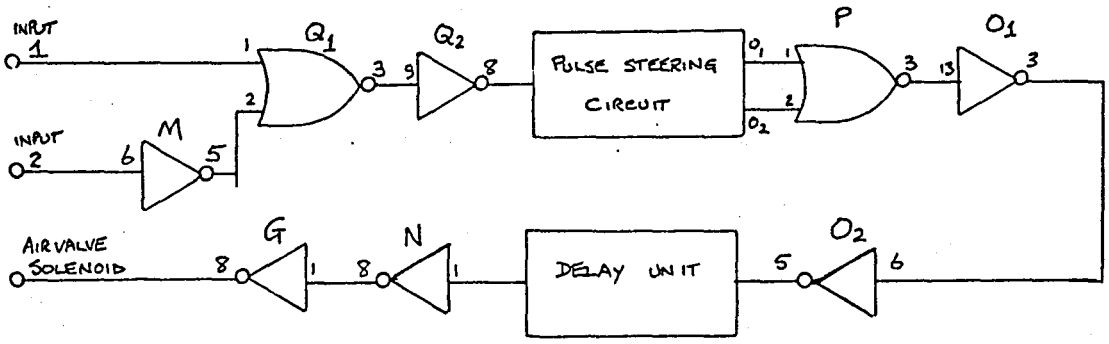

Figure 3.12 - Gear Actuation Logic Unit

The delay of the monostable was variable and an external control (10kΩ variable resistor) was provided to change the value of the period of the delay to allow the actuator to deploy fully. The input stages* to figure 3.12, which are shown separately in figure 3.15, define the output, Q_2, as shown in table 3.5.

---

*A NOR gate was used in this circuit. The element used was a Motorola MC 724P which required a supply voltage of 3.6v.

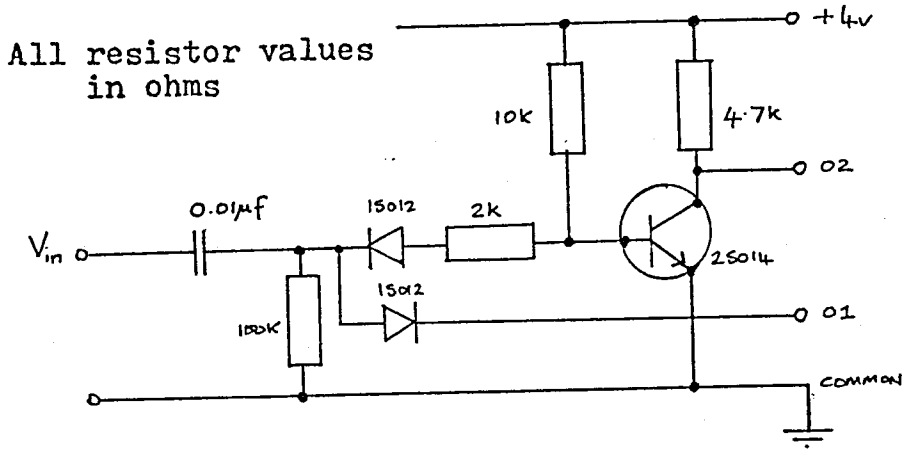

Figure 3.13 - Pulse Steering Circuit

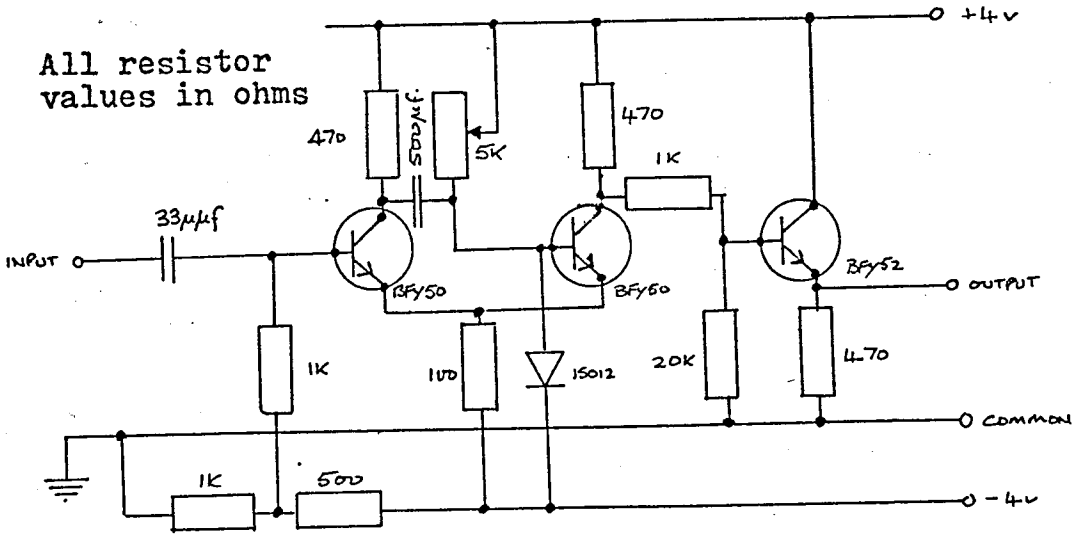

Figure 3.14 - Delay Circuit

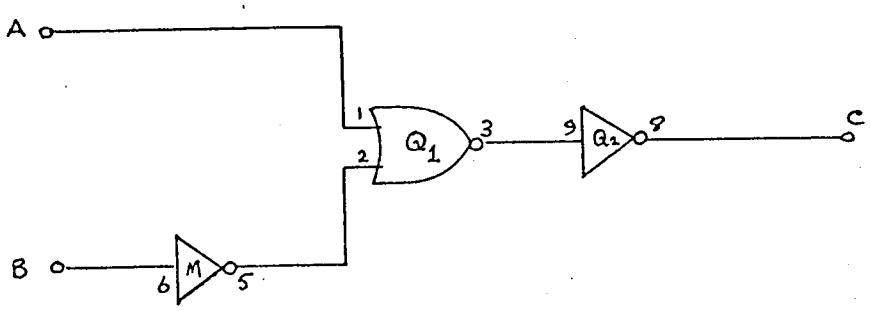

Figure 3.15 - Input Circuit

All transistors type NKT 124.

All resistor values in ohms.

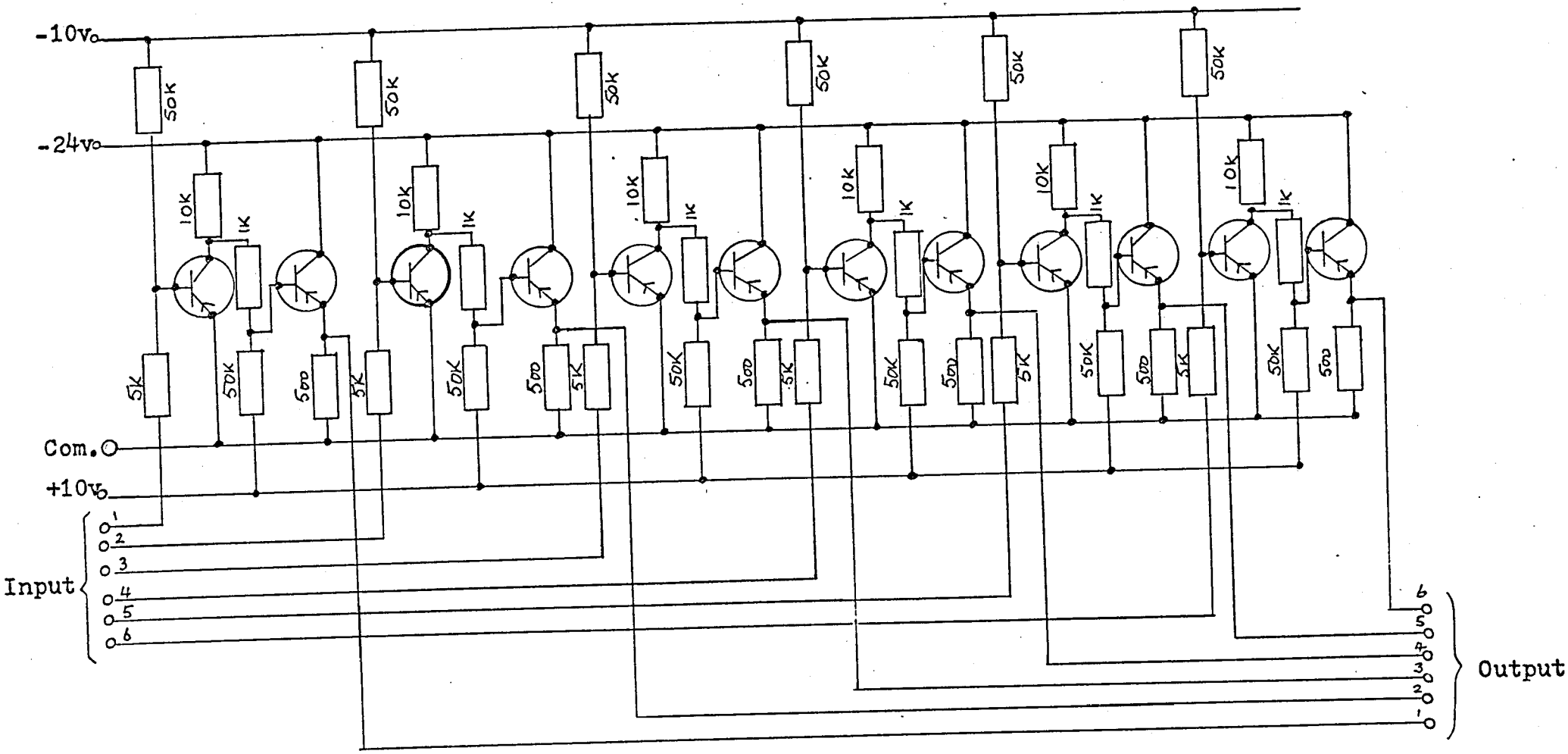

Figure 3.16 - Logic Conversion Circuit

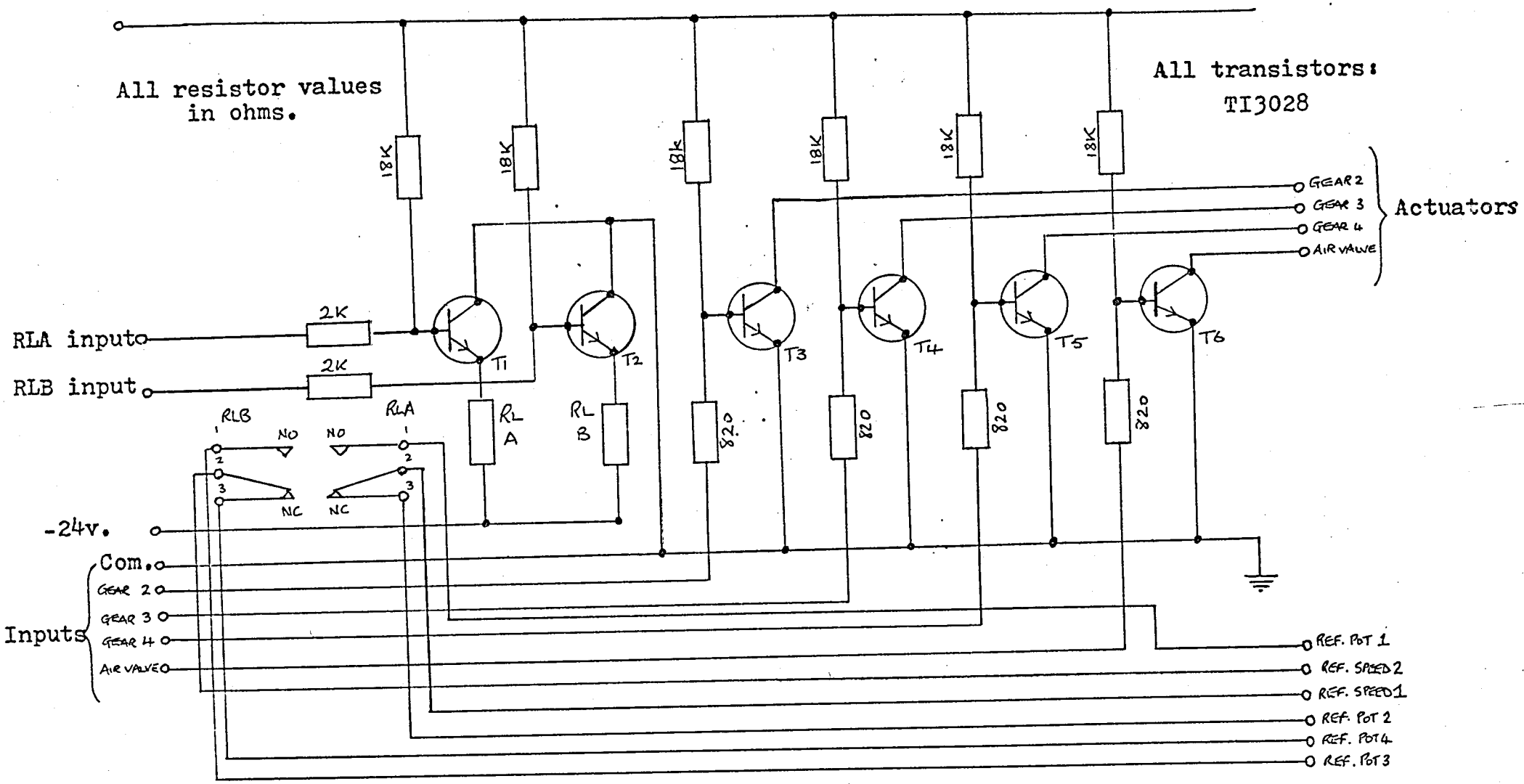

Figure 3.17 - Actuator Drive Circuit

A	B	C
1	1	1
0	1	0
0	0	1

Table 3.5 - Truth Table for Input Circuit

3.3.5 Logic Conversion Unit

Because the drive unit required input logic shgnals of 0v. and -10v., and because the logic signals provided by the logic units were 0v. and +4v., nominally, the circuit of figure 3.16 was devised and manufactured to provide the necessary conversion. The logic 1 input was permitted to be as low as+2.8v. and the logic 0 signal was allowed to have a value as great as+0.3v. The output logic was nominally logic 1 equalled -12v. This unit provided six identical channels to accommodate signals for:

gear-selection solenoids - 3

reference speed relays - 2

air valve solenoid - 1

3.3.6 Actuator and Relay Drive Unit

This unit switched the gear selection solenoids and the air valve to EARTH when the inputs were excited by a -12v. signal from the Logic Conversion Unit. The unit also contained the changeover relays which selected the potentiometers in the reference speed unit. (See figure 3.10). The circuit is shown in figure 3.17.

3.4 Gear Changing Performance

Using the simulation of figure 2.27 a number of computer runs were made to validate the mathematical model of the gear-changing system. Figure 3.18 shows the simulated engine speed and dynamometer speed for a constant speed demand at

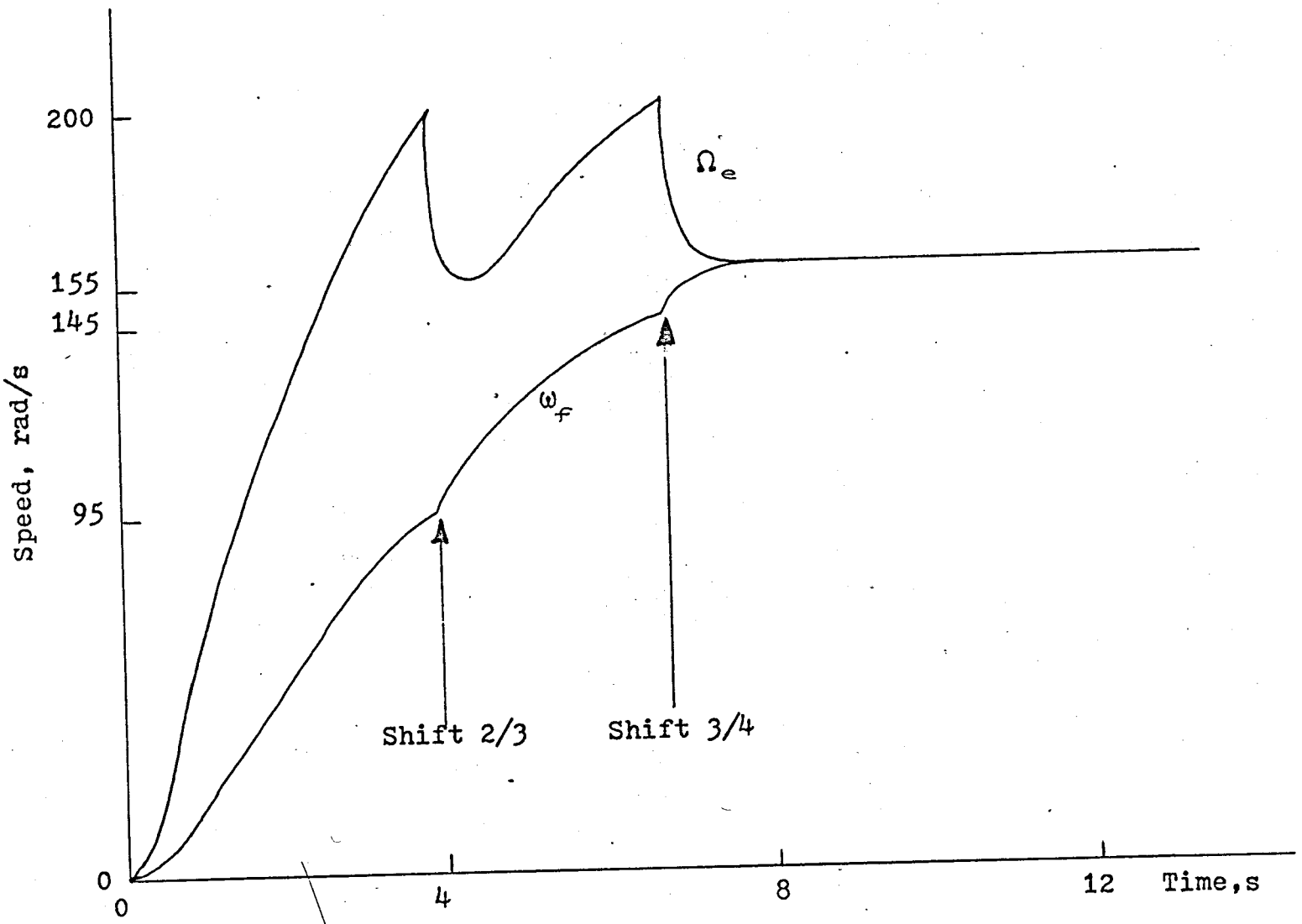

Figure 3.18 - Simulated Engine and Output Shaft Response to a Gearshift

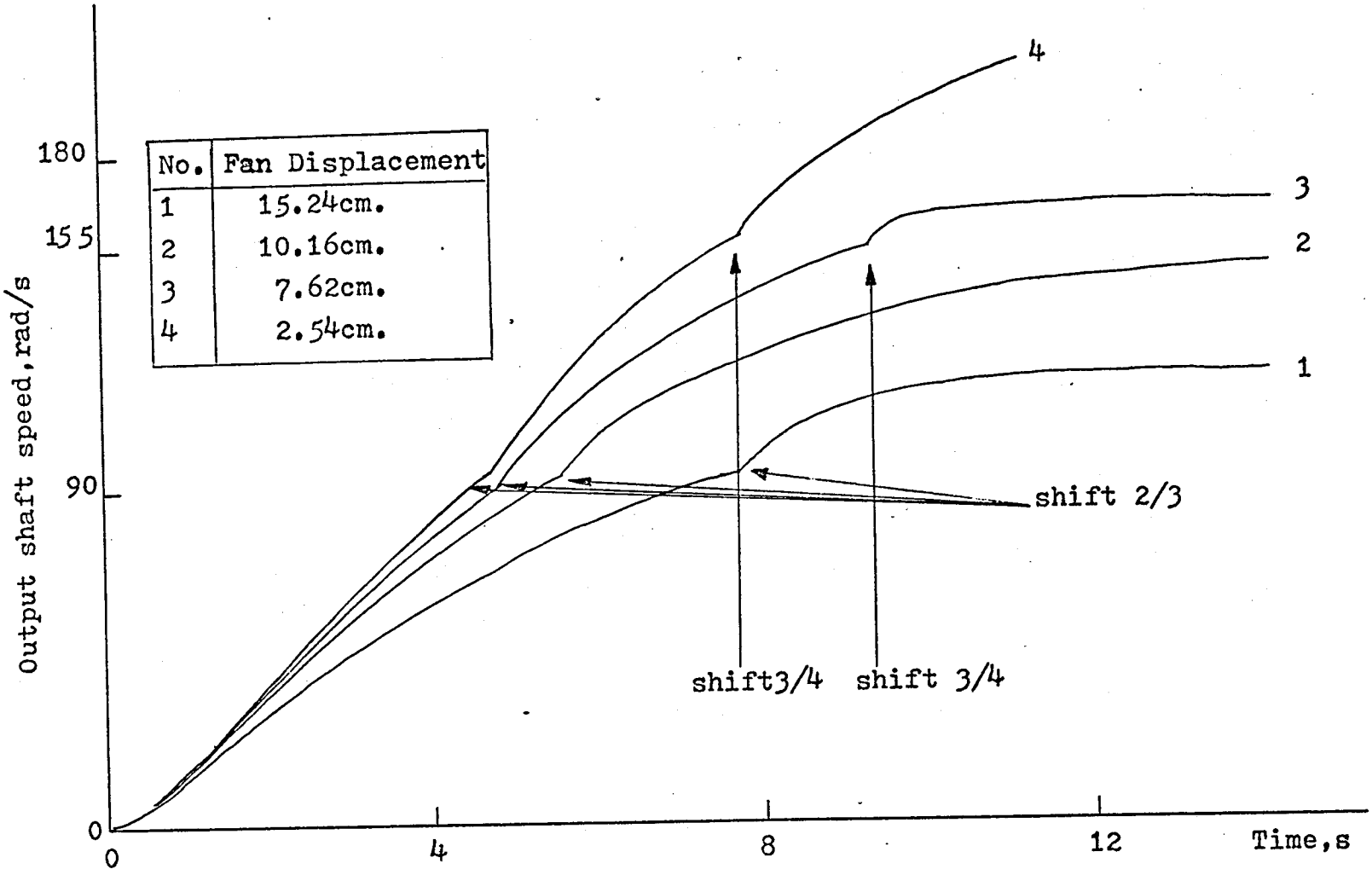

Figure 3.19 - Simulated Gearchange Responses

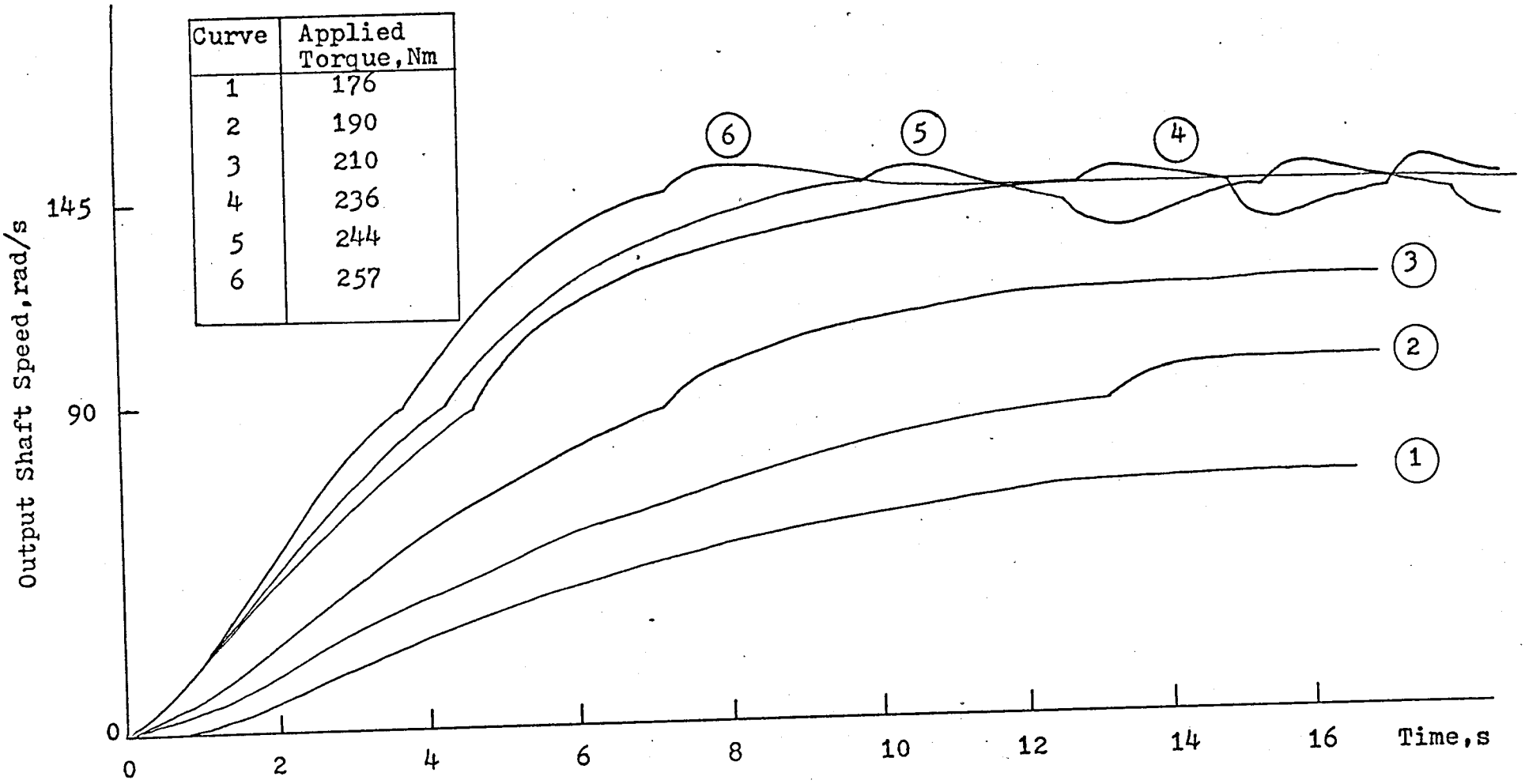

Figure 3.20 - Simulated Gearchange Responses

the input of the throttle servomechanism for a variety of load conditions. Note that for the least load, when the dynamometer setting is 1.27 cm., the engine system proceeded through the selection of all gears and the dynamometer was accelerating still after 12 seconds. For the greatest load, a dynamometer setting of 15.24 cm., the engine system did not change up to 4th gear and a lower final speed was obtained. In figure 3.20 the load was fixed but a wide variety of demanded speeds were input to the throttle servomechanism. In some cases 4th gear was not selected; in one case shown, (1), 3rd gear was not selected; and in two cases (4 and 5) hunting was observed. The period of the hunting was different in each case : for case 4 the period was 4.0 seconds, whereas for case 5 it was 5.375 seconds. The threshold due to different reference speeds for UP/DOWN changes can be observed on curves 4 and 5 at those parts of the responses where hunting occurs. By increasing the demanded final speed by a small amount (curve 6) the hunting could be removed. Equally effective in removing the hunting was to reduce the demanded final speed. Note that the overshoot due to gearshifting was observed on curves 4, 5 and 6. To evaluate the time required to reach a gearshift condition from rest in response to various demanded final speeds for a variety of load conditions, several computer runs were made. From the recordings (which were similar to figure 3.20) the graphs of figure 3.21 were obtained showing the time to gearshift, τ, as a function of throttle opening, θ. Both time and throttle opening have been plotted on a logarithmic (base 10) scale: time, τ, has the units of seconds, and throttle opening, θ, is given in degrees. The functional relationship between τ and θ was

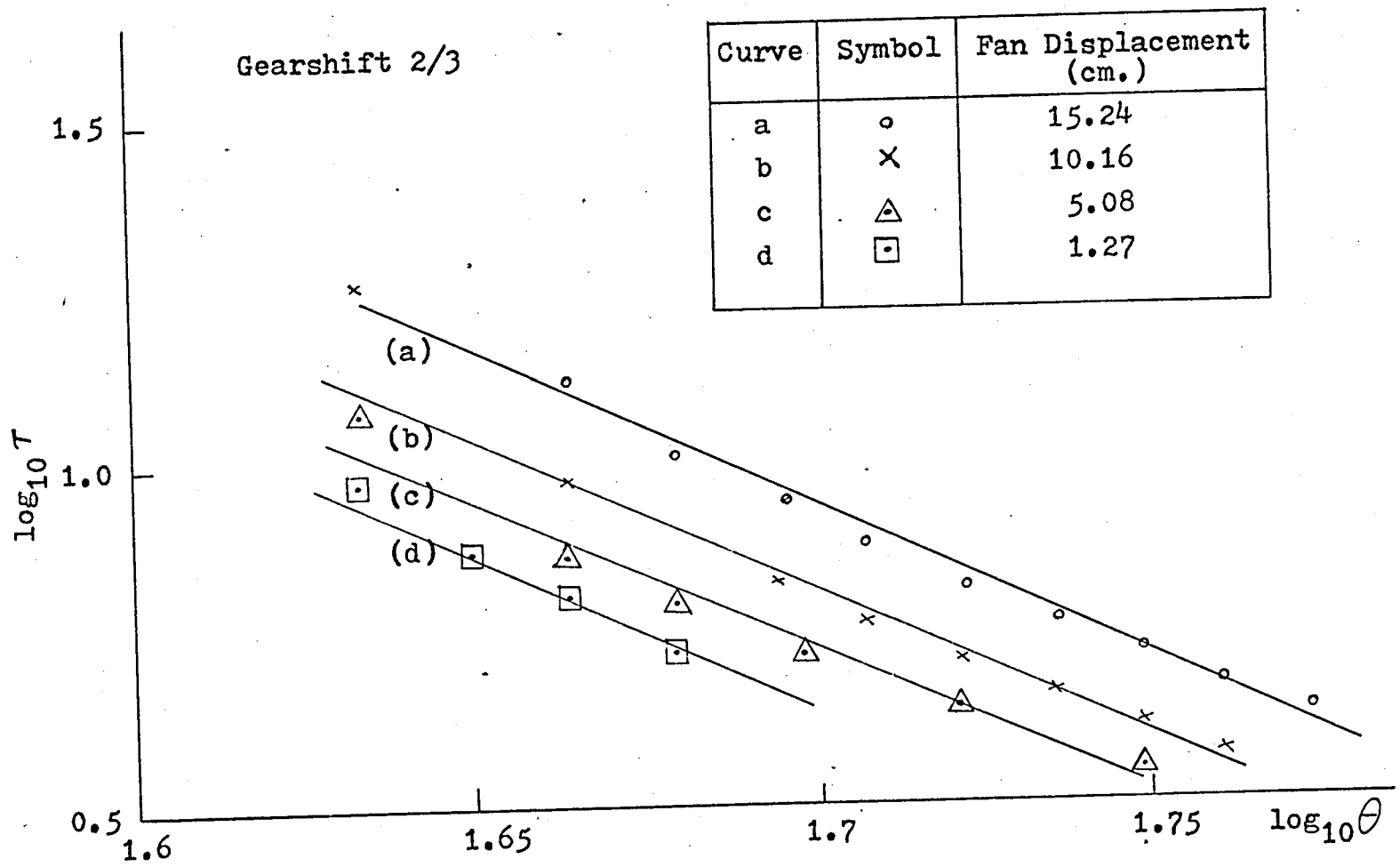

Figure 3.21a - Time-to-Gearshift vs. Throttle Opening

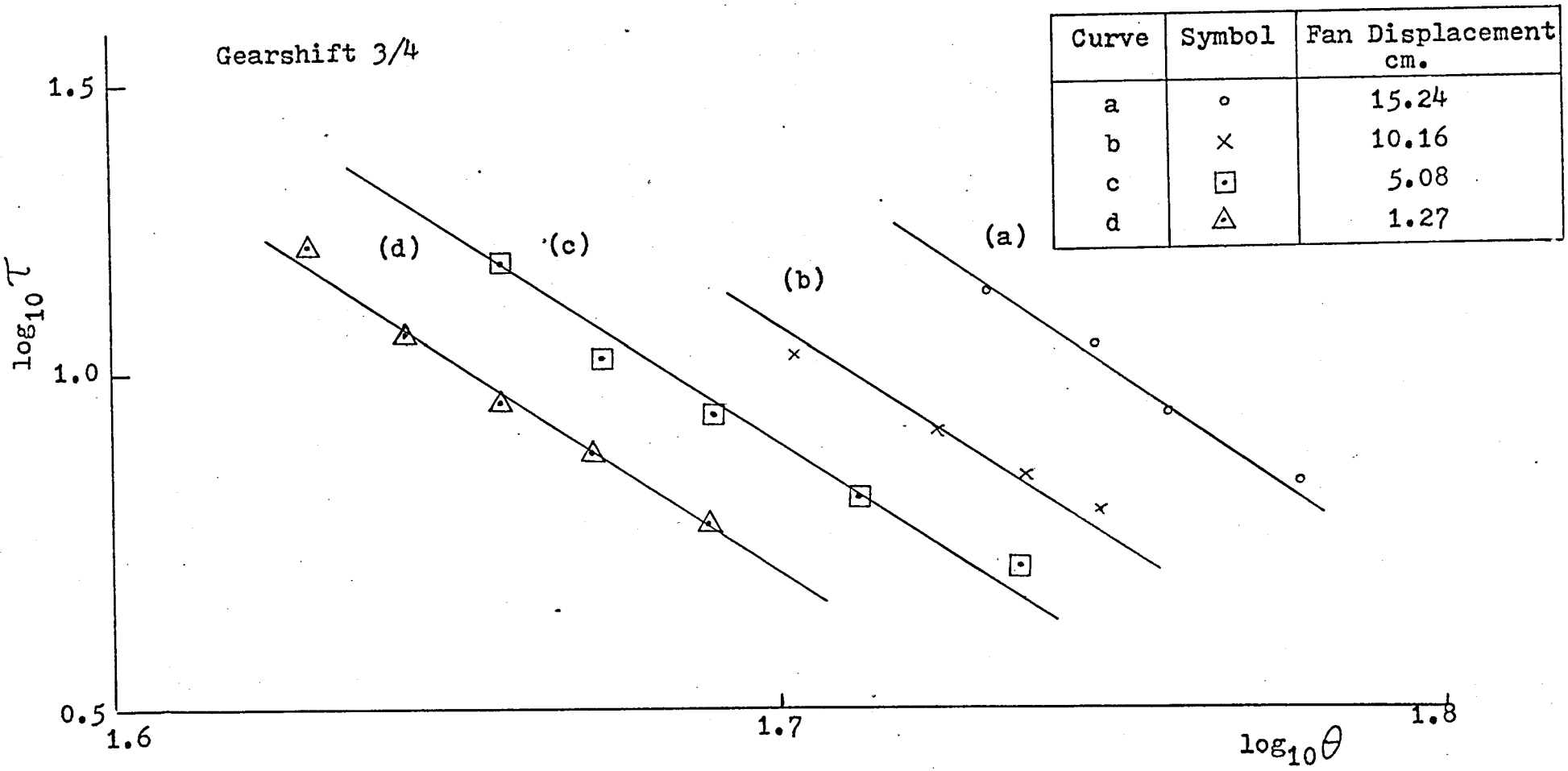

Figure 3.21b - Time-to-Gearshift vs. Throttle Opening

derived from the graphs as

$$\tau = \mu\theta^{\nu} \qquad (3.5)$$

The values of μ and ν depended upon whether the shift was from 2/3 or 3/4. The associated values are quoted in table 3.6.

Gearshift	Dynamometer Setting(cm.)	μ	ν
2/3	15.24	10.96×10^{7}	-4.2
	10.16	8.91×10^{7}	-4.2
	5.08	7.41×10^{7}	-4.2
	1.27	6.17×10^{7}	-4.2
3/4	15.24	5.75×10^{10}	-5.5
	10.16	2.95×10^{10}	-5.5
	5.08	2.24×10^{10}	-5.5
	1.27	1.48×10^{10}	-5.5

Table 3.6 - Gearshift Time Parameters

The effectiveness of the circuits described in this chapter is illustrated by the recordings of the output shaft response to gearchanges. These are shown in figures 3.22 and 3.23. Figure 3.22 shows the response to gear upshifts. These gearchanges were effected by the automatic gearchanging system. The throttle demand had to be reduced at the instant of gearchange to avoid the possible onset of hunting. Figure 3.23 shows the response to downshifts which were effected by the manual gear-shifting system.

The experimental work on optimal start-up used the system developed in this chapter and an account of the work is given in chapter five. The relationship of (3.5), and the associated figures, 3.21a and 3.21b, were used also in chapter five to establish the appropriate duration of gear-change intervals.

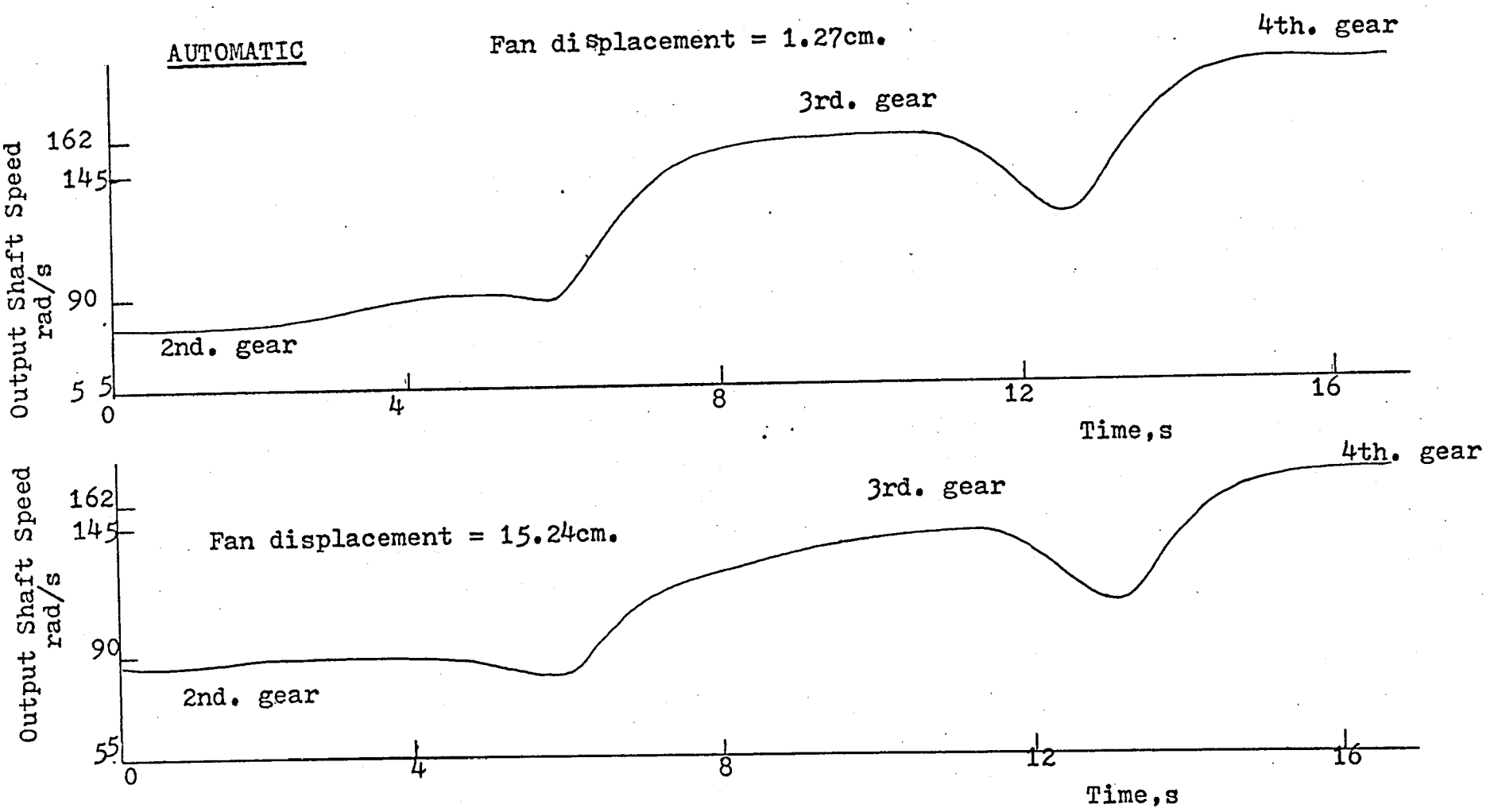

Figure 3.22 - System Response to Upshifts

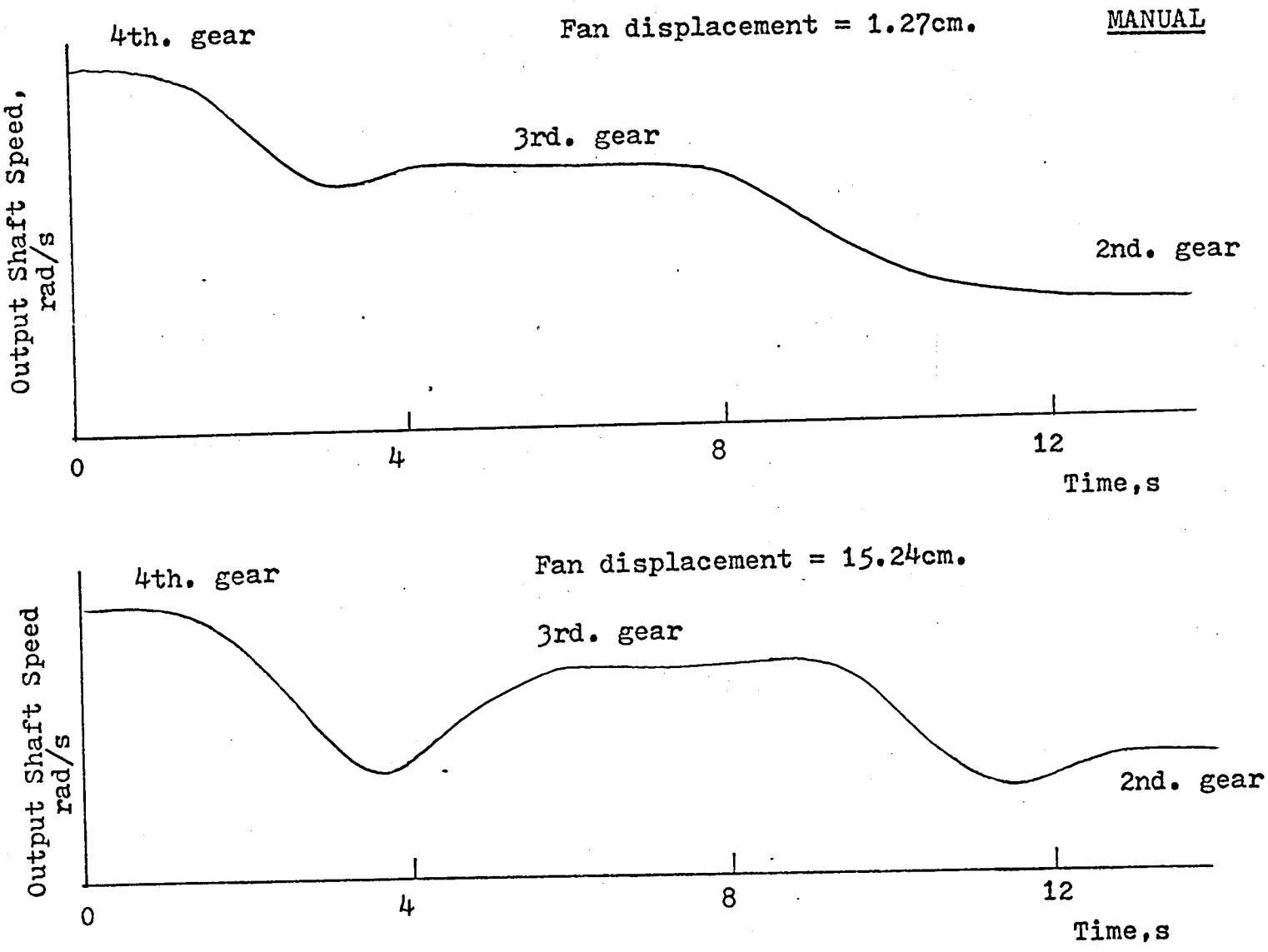

Figure 3.23 - System Response to Downshifts

CHAPTER 4 - DYNAMIC LOADING OF THE ENGINE

4.1 Introduction

It is usually difficult to load an engine on a test bed in any way corresponding closely to the kind of dynamic loading to which that engine would be subjected when it was installed in some vehicle which it drove. The analysis and simulation of diesel engine performance by EYMAN (1967) specified the use of a fixed load. The work of MONK and COMFORT (1970) which attempted, by the use of pseudo-random binary sequence test signals and direct computation of the resulting cross-correlation functions, to identify on-line the linear differential equation which described adequately the response of an i.c. engine also specified a fixed load. Such static loading is employed because it is not simple to provide adequate dynamic loading with the kinds of dynamometers which are used in work of this kind.

For the kind of optimal scheme that was envisaged for use with this study, however, it was considered to be desirable to provide a form of dynamic loading which was as simple and as realistic as possible. The Daimler engine was designed for use in a passenger saloon car; it was appropriate that any changes of the engine load should correspond as nearly as possible to the kind of changes experienced by the vehicle when travelling on the road. The engine loading which occurs due to the forces on the vehicle

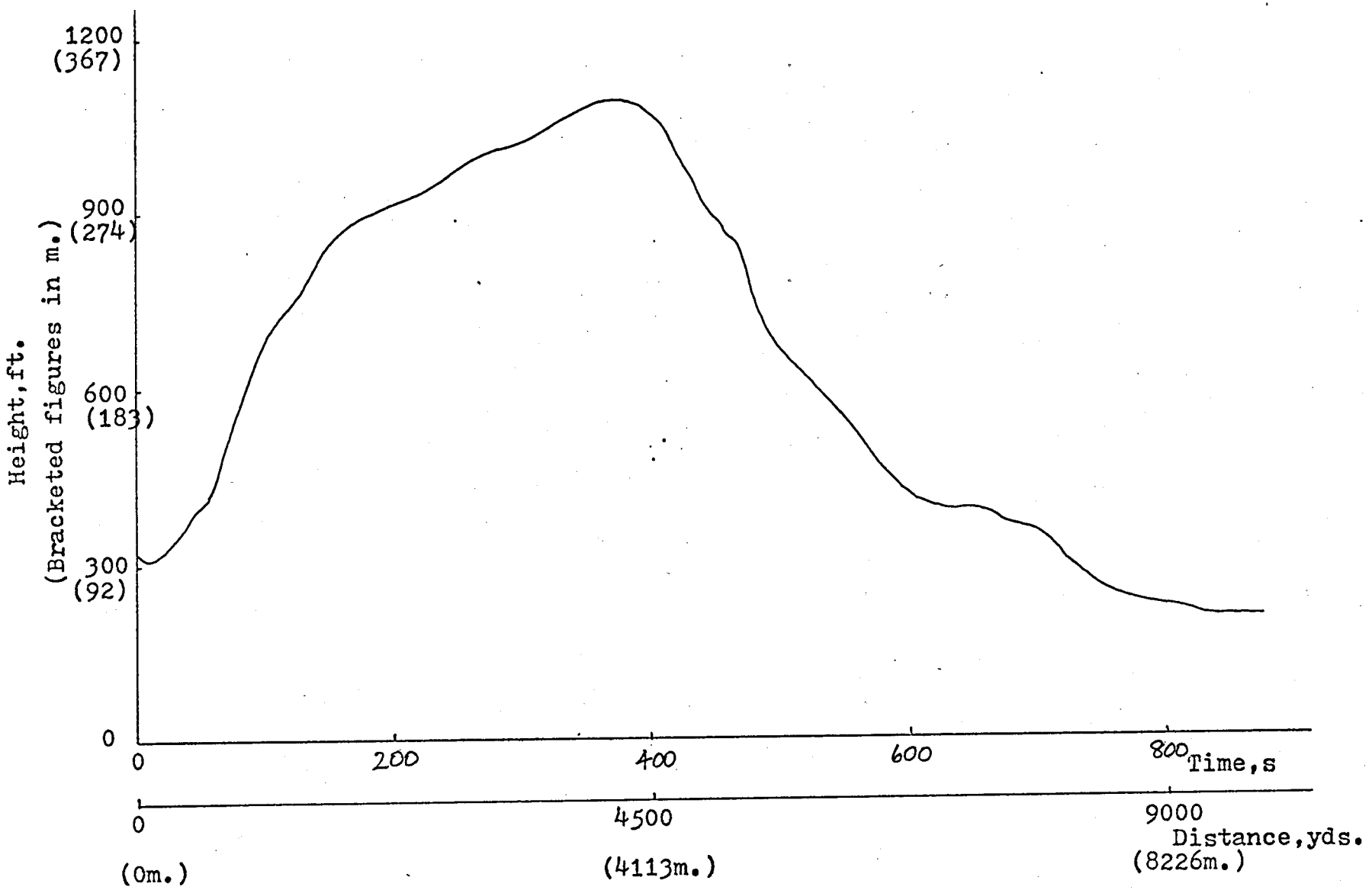

Figure 4.1 - Variation of Road Height with Time

during turning manoeuvres and/or braking periods were considered to be too complicated to simulate with the facilities available. As a first step to provide the required solution only changes with time in the gradient of the road were considered.

4.2 The Simulated Road

To provide large changes in road height over a fixed period of time a study of Ordnance Survey maps of the United Kingdom was made to find a section of road with the twin properties of straightness and hilliness. From this study it was decided that the best sections were :

(a) the B.4381 road from MARTON to WELSHPOOLS in Wales.

(b) the A.702 road from ST. JOHN'S TOWN of DALRY to MONIAIVE in Kirkcudbrightshire, Scotland.

Neither road is free entirely of curves but over the distances of about 6 and 10 miles* (9.6 and 16 km.) respectively the bends were considered to be of less significance than the changes of road gradient. Road (a) was chosen finally because its gradients were greater over a shorter distance. By using the Ordnance Survey sheet no. SJ 20, which has 25 ft. (8m.) contours, it was possible to draw up a graph showing the variation of road height with distance. This graph is shown as figure 4.1. The total length of the simulated road

---

*Heights and road distances are quoted in feet, yards, or miles in this section, because the scales upon the maps used these units. The S.I. equivalent unit has been given throughout in brackets and immediately following the Imperial quantities.

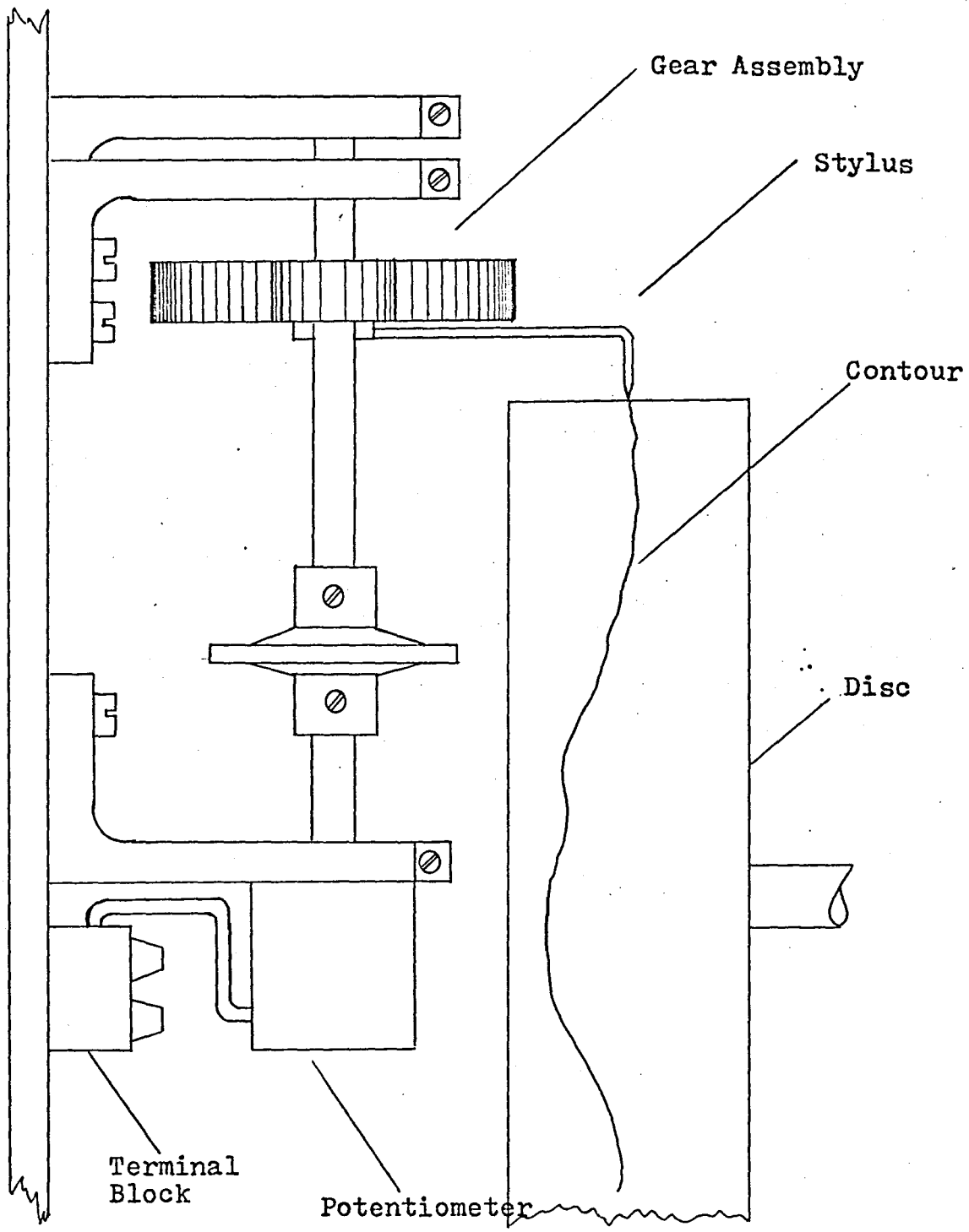

Figure 4.2 - Simulated Road Generator

was 10350yds. (9460m.) approximately, but, because the final section, of length 1350 yds. (1234m.), was almost straight and level it was not shown in figure 4.1; its effect upon the statistical properties of the road was taken into account however. The same level distance was also included in the contour disc used in the simulated road generator. The curve in figure 4.1 was cut as groove on a plastic sleeve mounted on a wooden mandrel of diameter 15 cm. and of width 4.5 cm. The disc assembly was mounted to the shaft of a synchronous electric motor which rotated at a constant speed of 1/15 rev/min. In the groove on the surface of the disc a stylus, connected to the armature of a potentiometer, was free to move to follow the contour. The potentiometer was excited with the mains voltage (230 volts, 50 hz.) and formed part of the error-sensing bridge circuit used in the servo-mechanism which positioned the fan dynamometer by the required amount. The simple scheme is illustrated in figure 4.2. The potentiometer is actually connected as a variable resistor whose resistance varies as a linear function of the contour. Because of the very slow rotation of the disc and because the slowest speed on any available chart recorder was 1.25 cm./sec. the recording of the variation of resistance with time is not shown. (Any segment of the recording would look very much like a straight line with an imperceptible slope). The merit of such a simple scheme of generating a simulated road, apart from its cheapness and reliability, is the great flexibility it can provide; different roads may be cut on separate discs which may be changed as required.

The constant speed rotation meant that any run over this

simulated road was carried out at an average road speed of 23 m.p.h. (37 k.p.h.) approximately. The times corresponding to road distance, for this speed, are shown also on figure 4.1. If the disc was driven by a rate servomechanism, rather than a synchronous motor different road speeds could be used.

4.3 The Statistical Properties of the Simulated Road

The probability density function, p(h), of the road contour, h(t), is given by :

$$p(h_1)dh = P(h_1 < h \leq h_1 + dh) \qquad (4.1)$$

$$= \lim_{\substack{T \to \infty \\ dh \to 0}} \frac{\Sigma \Delta t}{T} \qquad (4.2)$$

where h_1, h, dh, T, and Δt are all defined in figure 4.3.

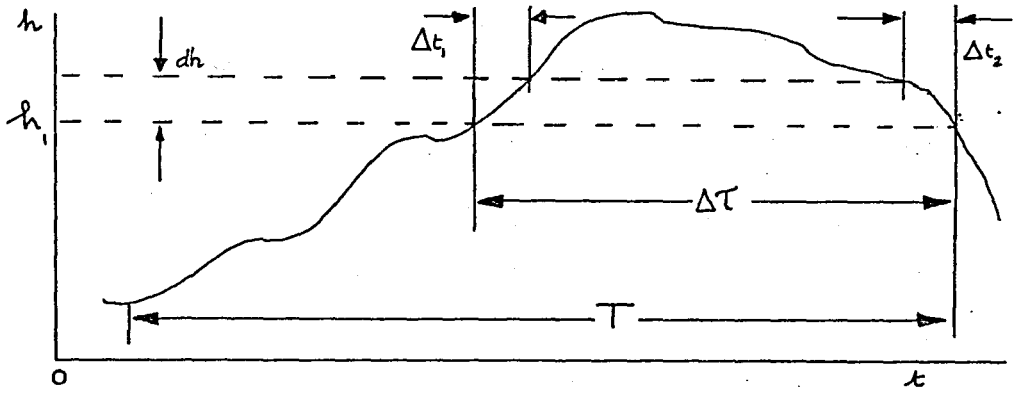

Figure 4.3 - Statistical Parameters

The fraction of the time that h(t) is greater than some value, h_1 say, is given by :

$$P(h_1 < h) = \lim_{T \to \infty} \frac{\Sigma \Delta \tau}{T} \qquad (4.3)$$

where $\Delta\tau$ is defined in figure 4.3 also.

To determine the probability distribution of the road, the mean height* and the variance** were determined from the equations given as (4.4) and (4.5) and from figure (4.1) :

---

*The mean height is denoted by μ.

**The variance is denoted by σ^2.

$$\mu = \frac{\sum_{i=1}^{N} x_i}{N} \qquad (4.4)$$

and

$$\sigma^2 = \frac{\sum_{i=1}^{N} (x_i - \mu)^2}{N} \qquad (4.5)$$

where x_i is the height of the road at the i^{th} sample and N is the total number of samples.

σ is the standard deviation of the contour. Because O.S. sheet, No. S.J.20, had 25 ft. (8m.) contours, the contour of the road was sampled at height intervals of 25 ft. (8m.). In this way any errors involved in the procedure were restricted to those due to measurement from the O.S. sheet and not to interpolation between the points read off to produce a smooth curve. The following results were obtained :

mean height, μ = 594.2 ft. (181m.) (4.6)

variance, σ^2 = 10.875×10^4 ft^2 (10.1×10^3 m^2) (4.7)

standard deviation, σ = 330 ft. (100.8m.) (4.8)

By using (4.2) and figure 4.1 the probability density function was evaluated for the same 25 ft. (8m.) height intervals. A graph of the probability density function versus height is shown in figure 4.4.

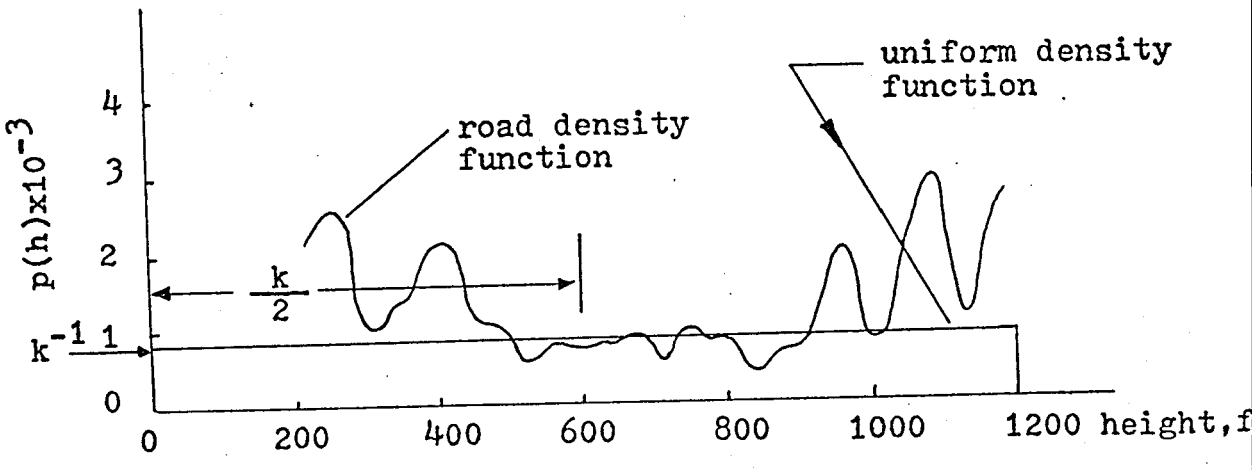

Figure 4.4 - probability density function

Although it seems that there is a great deal of variation displayed in the road density function it should be noted that the value of the function is never large. Consequently small numerical inaccuracies gave rise to proportionately large differences in p(h). The distribution was NOT Gaussian which was what had been expected a priori; the distribution was reasonably approximated however by a uniform, or rectangular distribution. From CRAMER (1946), if a random function has a uniform distribution, then the following properties pertain :

$$p(h) = \begin{cases} 1/k, & \mu-k/2 \leq h \leq \mu+k/2 \\ 0, & h>\mu+k/2,\ h<\mu-k/2 \end{cases} \qquad (4.9)$$

$$\int_{-\infty}^{\infty} p(h)dh = 1.0 \qquad (4.10)$$

$$E(h) = \mu \qquad (4.11)$$

$$E(h-\mu)^2 = \frac{k^2}{12} \qquad (4.12)$$

where E denotes the expected value.

For the distribution shown in figure 4.4

$$\mu = 600 \qquad (4.13)$$

$$\left.\begin{aligned} 1/k &= 0.8\times10^{-3} \\ \text{i.e. } k &= 1200 \text{ (appx.)} \end{aligned}\right\} \qquad (4.14)$$

Therefore,

$$E(x-\mu)^2 = \sigma^2 = 12\times10^4 \qquad (4.15)$$

From the numerical data obtained from figure (4.1)

$$\sum p(h)dh = 1.03 \qquad (4.16)$$

These results (4.6), (4.7), (4.8), and (4.16), which were all obtained from the numerical data extracted from figure 4.1, are compared in table 4.1 with the results (4.10), (4.11) and (4.12) which were obtained analytically under the assumption that the road density function had a uniform distribution.

Statistical Quantity	I From Numerical Data	II From Uniform Distribution
Mean Value, μ	594.2	600
Variance, σ^2	10.875×10^4	12×10^4
Standard Deviation, σ	330	345
$\int_0^\infty p(h)dh$	1.03	1.00

Table 4.1 - Comparison of Data

From table 4.1 it is evident that if a statistical model of the simulated road was chosen to be one with a uniform distribution the characteristics of which were defined by the parameters of column II of table 4.1 that model would be acceptable for analytical purposes. Further corroboration of the validity of this assumption was sought by evaluating (4.3) from the numerical data obtained from figure 4.1 directly. The graph showing the variation of $P(h_1<h)$ with h, is shown in figure 4.5. The theoretical variation of $P(h_1<h)$ with h, assuming a uniform distribution with the parameters of column II of table 4.1, has been drawn on the same graph for comparison.

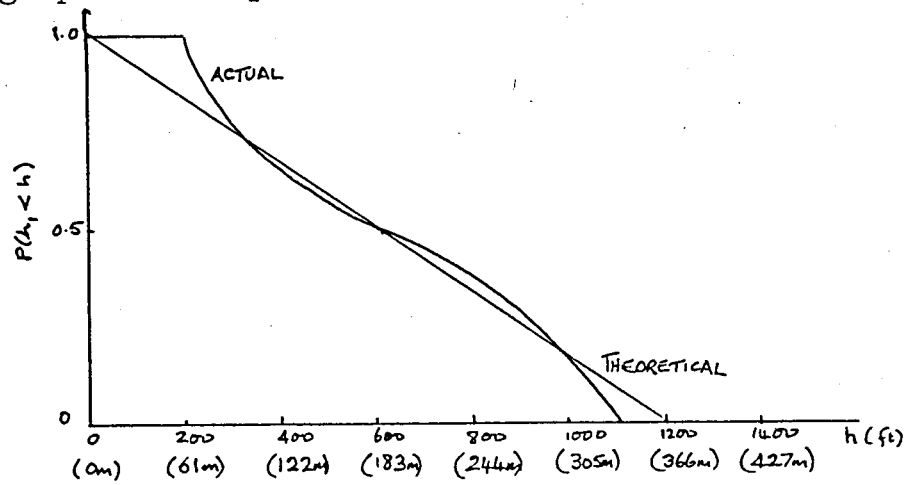

Figure 4.5 - $P(h_1<h)$ vs. h

It can be shown (LANNING and BATTIN (1956)) that by passing a uniform stationary random signal through a low-pass filter the resulting amplitude distribution of the output signal tends to be Gaussian. The frequency response characteristic of the dynamometer servomechanism approximated to the characteristic associated with a linear second order system even though the differential equation describing the behaviour of the servomechanism was non-linear. Hence it was assumed that in the appropriate range of dynamometer fan setting (see section 4.5) the load disturbance on the engine due to the simulated road was approximately Gaussian.

4.4 The Dynamometer Servomechanism

Because of the physical size of the dynamometer and its open-air siting the fan had to be positioned by means of an extended shaft driven from the output gear train of the servomechanism which was located inside the building which housed the experimental engine rig. The frictional forces associated with the fan, together with the mass to be positioned, required the use of a 250w. electric motor.

No servomotor of that size was available therefore a 250w., d.c. shunt motor surplus to the requirements of the Department, was used. It had an armature resistance of 25 ohms and required a supply of 220v. d.c. Such armature voltage and current levels precluded the possibility of designing a linear driving amplifier; it was decided therefore to design an ON/OFF servomechanism. The practical difficulties associated with the use of electromechanical relays to switch currents of 10A at 220v. d.c. are

All resistor values in ohms.

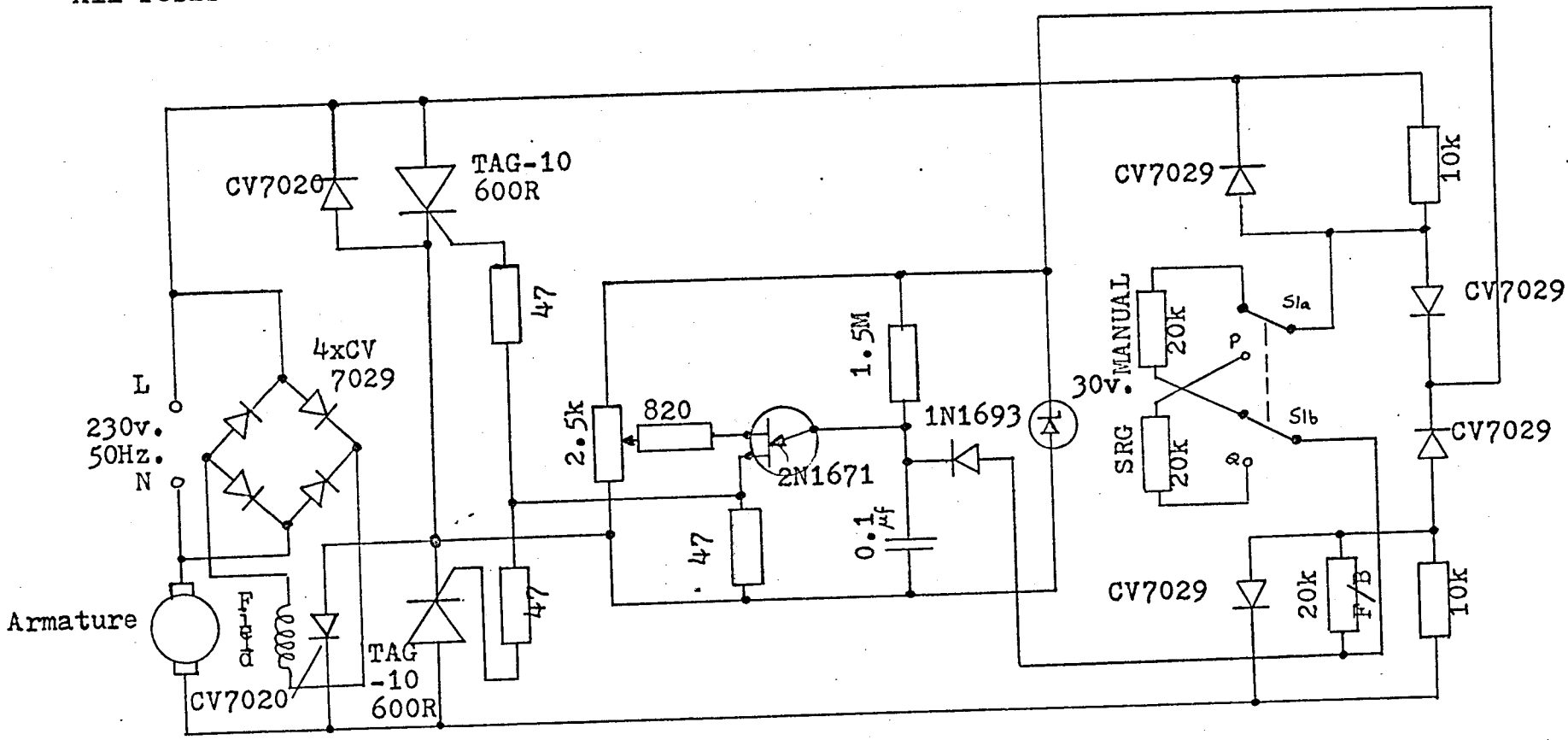

Figure 4.6 - Dynamometer Servomechanism Circuit Diagram

well-known to be formidable if correctly designed relays are not available. These difficulties were circumvented by employing thyristors to switch the current through the motor. The circuit diagram of the servomechanism is shown in figure 4.6. Its design was based on that given by GUTZWILLER (1967). A dead-zone width control was provided (the 2.5 kΩ variable resistor) to prevent the motor armature winding from drawing heavy current at standstill and thus burning out the winding. The existence of the dead-zone meant that there were small changes in road gradient to which there was no response; however, because of the nature of the simulated road these small dwell periods were not of primary significance in the overall system performance.

It was necessary to drive the fan of the dynamometer and the fan position potentiometer through gear trains. A schematic representation of the servomechanism gear unit which performed this function is shown in figure 4.7.

4.5 Dynamic Loading of the Engine

Because the lowest chart speed on the available recording apparatus was too high to permit an adequate recording of the simulated road it was not easy to see from recordings of engine response to fan loading (equilibrium speed of 2000 rev/min, 4th gear selected, and throttle setting fixed) that the correspondence of engine loading and simulated road signal was inexact. This was due to the non-linear relationship between fan opening and torque. From figure 2.12 it was seen that within the range of fan setting of 2.5 to 10cm. the relationship was very nearly linear. For the road speed chosen the bandwidth of the dynamometer servomechanism was

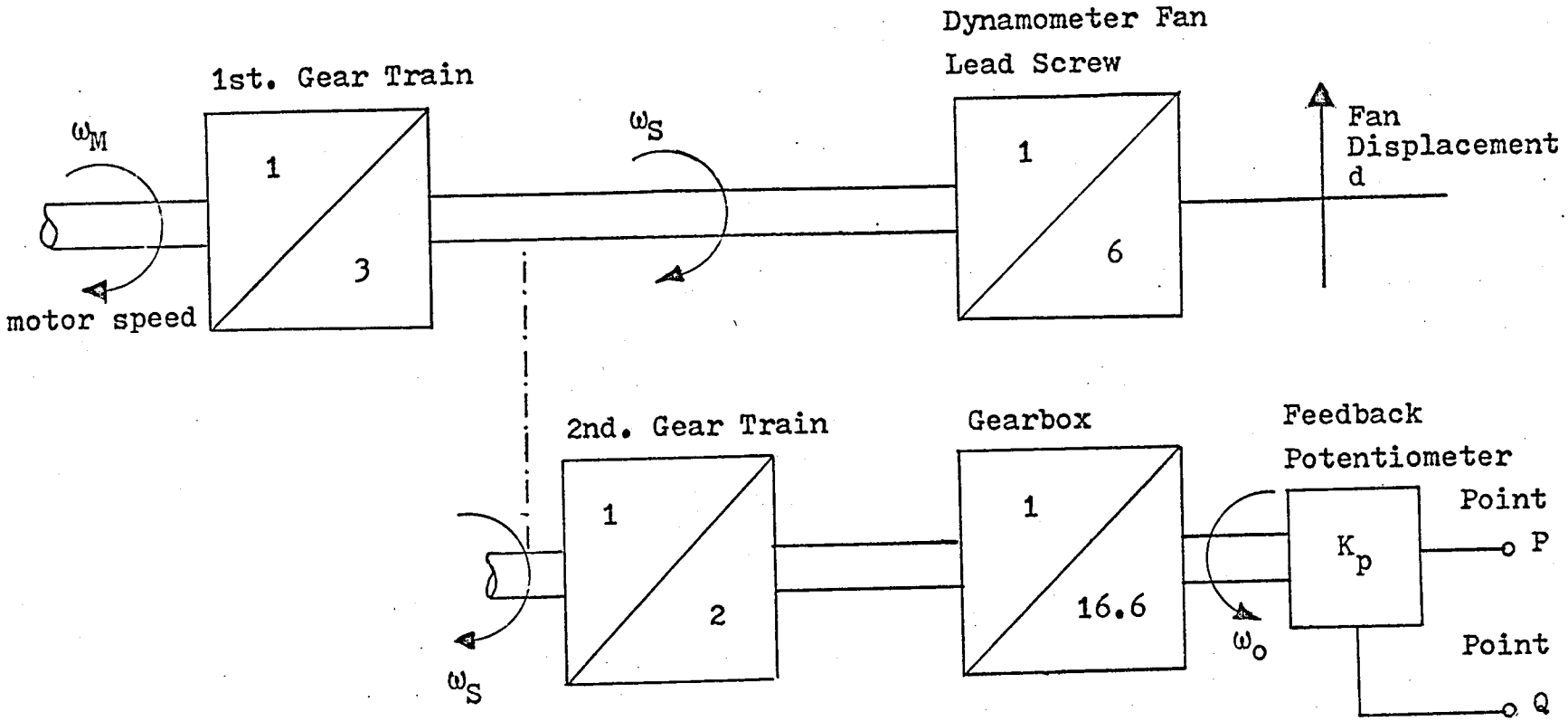

Figure 4.7 - Gear Unit for Dynamometer Servomechanism

adequate. If a different route, or higher road speed was used it might then be necessary to take into account in the system equations the dynamics of the fan servomechanism. If improved servomechanism response was needed the motor would have to be replaced and an alteration of the gear train ratios would be necessary also.

CHAPTER 5 - OPTIMAL STARTUP

5.1 Introduction

There are many applications for which optimal start-up of an engine may be required and it is the application that determines the appropriate definition of optimality. For some cases the shortest possible time to raise the engine speed from idling to equilibrium speed will be the proper criterion of performance, whilst for others it may be more important that the load should be brought to the desired speed without exceeding some stipulated limit of engine acceleration. In this presented work it was regarded as optimal to drive the load from idling up to a reference speed with the least expenditure of fuel. The problem was regarded as a member of the class of fuel optimal control problems. For convenience the control signal, u, was the throttle position which had to be as small as possible during the interval of start-up.

If the time to achieve the reference speed was left to be infinite obviously there could be no admissible solution to the optimal control problem because the fuel consumed in that time would be infinite also. Time has a pronounced effect upon the performance of any optimal system. From (2.38) it is seen that the time for the load to respond to any change of applied torque was infinite, theoretically. It was decided therefore to incorporate, if possible, in the subsequent

analysis some method by which the length of time spent in each successive gear during the start-up interval could be determined as well as the necessary history of the control function during that period.

A formal statement of the problem was to determine the optimal control function, $u^o(t)$, which would minimise the performance index :

$$J = \int_o^\infty L(\underline{x},u,t)dt \qquad (5.1)$$

subjected to the constraint of the engine equation;

$$\dot{\underline{x}} = \underline{f}(\underline{x},u,t) \qquad (5.2)$$

where u is the control function,

and $\underline{x}$ was the state vector of the system, of dimension 3.

The Hamiltonian of the system see e.g. ATHANS and FALB (1966a), BRYSON and HO (1969) and KIRK (1970) was given by :

$$H = \underline{\psi}'\underline{f}(\underline{x},u,t) + L(\underline{x},u,t) \qquad (5.3)$$

where $\underline{\psi}$ was the adjoint vector, of dimension 3.

The system was regarded as time invariant and therefore (5.3) was then re-expressible as

$$H = L(\underline{x},u) + \psi_1 f_1 + \psi_2 f_2 + \psi_3 f_3 \qquad (5.4)$$

The optimal control function was then determined from :

$$\frac{\partial H}{\partial u^o} = 0 \qquad (5.5)$$

Thus the optimal control function was influenced considerably by the choice of the cost functional, L. From ATHANS and FALB (1966b) it was noted that if L contained a term linearly proportional to u the resulting optimal control, u^o, would be a "bang-bang" function. If, however, L involved $|u|$ then the resultant optimal control involved a "dead-zone" function.

Instantaneous ON/OFF throttle action could not be achieved on an internal combustion engine and therefore the cost functionals mentioned were not of practical value for this reasearch. To obtain linear continuous control action required that there was a quadratic term in u contained in L. ATHANS (1971). Consequently it was decided to choose as the performance index to be minimised for optimal start-up :

$$J = 0.5\int_{o}^{T} gu^{2}\,dt \qquad (5.6)^{*}$$

where g was a weighting factor and T represented the interval over which start-up was to take place.

By forming the canonical optimal equations, from the application of the Principle of Maximum due to Pontryagin, the control function was determined in terms of the adjoint vector, Ψ. (ATHANS and FALB (1966c), SAGE (1968)). The resultant continuous control function was to be synthesised, approximately, in a function generator (see section 5.7) the output of which provided the command signal to the throttle servomechanism. This arrangement maintained compatibility with the optimal regulation schemes described in later chapters. At the outset of the research the interval over which start-up was to be achieved was unknown. Its determination was one aspect of the experimental investigations of this research.

The optimal start-up function was applied over the complete interval of T seconds, during which the engine shifted from 2nd to 3rd and from 3rd to 4th gear until the output shaft (and engine) speed was at 2000 rev/min. The requirement to determine each segment of the start-up trajectory was complicated by the need to ensure that a number of prescribed

---

*It is obvious that this performance index would be a minimum for Λ if no constraint was placed on the optimal trajectory. zero control

[illegible] when x(T) is specified.

conditions in some of the state variables occurred at each gearchange. All these conditions at internal points in the trajectory, when added to the known boundary conditions at the start and the finish of the optimal run-up, established this problem as a member of the class of variational problems known as multi-point boundary value problems (referred to hereafter as M.P.B.V.P.).

5.2 Conversion to a Fixed-End Time Problem

In the preceding section it was stated that the interval, T, over which the optimal control function was to be evaluated was unknown. The problem was regarded, then, as a free-end time problem. Application of the technique proposed by LONG (1965) transformed the problem to a fixed-end time problem with a resultant gain in computational convenience.

For start-up there were two segments upon which the boundaries occurred :

	UP	DOWN
gearshift	2→3	3→2
	3→4	4→3

The transformation consisted of letting

$$t = a\tau \tag{5.7}$$

where τ was a new independent variable and a was a constant, still to be determined.

If the end-times of each segment of start-up were taken as (fixed) values of 0, 1.0, 2.0, and 3.0.

$$t = a\tau \qquad 0 \leq \tau \leq 1 \tag{5.8}$$

and

$$t = a + b(\tau - 1), \quad 1 < \tau \leq 2 \tag{5.9}$$

and

$$t = a + b + c(\tau - 2), \quad 2 < \tau \leq 3 \tag{5.10}$$

where b and c were additional constants to be determined for the appropriate segment.

The boundary times were now

$$\left.\begin{aligned} \tau &= 0,1,2,3 \\ t_1 &= a \\ t_2 &= a + b \\ t_3 &= a + b + c \end{aligned}\right\} \qquad (5.11)$$

From (5.1), for $0 \leq \tau \leq 1$

$$\frac{dt}{d\tau} = a \qquad (5.12)$$

and from (5.9), for $1 < \tau \leq 2$

$$\frac{dt}{d\tau} = b \qquad (5.13)$$

Also from (5.10), for $2 < \tau \leq 3$

$$\frac{dt}{d\tau} = c \qquad (5.14)$$

Hence in the first interval the differential equation

$$\dot{\underline{x}}(t) = \underline{f}\{\underline{x}(t),u(t)\} \qquad (5.15)$$

became

$$\underline{x}'(\tau) = a\underline{f}\{\underline{x}(a\tau)u(a\tau)\} \qquad (5.16)$$

and in the 2nd interval

$$\underline{x}'(\tau) = b\underline{f}\{\underline{x}(a + b\tau),u(a + b\tau)\} \qquad (5.17)$$

and in the 3rd interval

$$\underline{x}'(\tau) = c\underline{f}\{\underline{x}(a + b + c\tau),u(a + b + c\tau)\} \qquad (5.18)$$

where, in this context, the prime (') denoted differentiation with respect to the independent variable, . The constants a, b, and c were treated as additional state variables in the appropriate segment of the state trajectory, i.e.

$$x'_{n+1} = 0 \qquad (5.19)$$

with

$$\left.\begin{aligned} x_{n+1}(0) &= a \\ x_{n+1}(1) &= b \\ x_{n+1}(2) &= c \end{aligned}\right\} \qquad (5.20)$$

Thus in each segment of the optimal start-up trajectory the system state equation was represented as :

$$\underline{x}' = \frac{d\underline{x}}{d\tau} = x_{n+1}\underline{f}\left\{\underline{x}(\varphi\tau), u(\varphi\tau)\right\} \qquad (5.21)$$

where the parameter φ depended upon the segment, Because of limited computer facilities this technique was used only with a single stage.

5.3 Corner Conditions

With internal boundary conditions on the optimal trajectory to be satisfied there existed some specific discontinuities in the adjoint variables which occurred at the instant of gearchange. It was possible to evaluate these "jump" conditions by the analytical methods proposed by BRYSON and HO (1969b) and VINCENT and MASON (1967). However, by adopting the method of quasilinearisation (section 5.4) as the basis of the computational method for determining the optimal start-up function it was possible to circumvent the additional complexity associated with the analysis when such "jump" conditions were included; sufficient boundary conditions were available from the problem statement to allow a solution to be found by using quasilinearisation.

5.4 Quasilinearisation

The method of quasilinearisation (Q.L. method) has been used widely heretofore in modern engineering studies {BELLMAN and KALABA (1965), LEE (1967), SAGE (1968b), BELTRAMI (1969), FALB and de JONG (1969), DYER and McREYNOLDS (1970), GREENSITE (1970), SPEEDY, GOODWIN and BROWN (1970), and RADBILL and McCUE (1970).} As a method it depends upon the formulation of the problem in the manner indicated in (5.1)

and (5.2). If the optimal control function, u^o, defined in (5.5), was substituted for u in (5.2) and in the associated equation for the adjoint vector, $\underline{\Psi}$, the equations which resulted provided the canonical equations of the optimal system. These equations were considered to form a single, new vector equation given by :

$$\dot{\underline{R}} = \underline{K}(\underline{R}) \tag{5.22}$$

where $\underline{R}$ was the new vector, of dimension 2n, defined as

$$\underline{R} = \begin{bmatrix} \underline{x} \\ \underline{\Psi} \end{bmatrix} \tag{5.23}$$

For the problem stated in this way the associated boundary conditions took the form :

$$R_j(t_i) = d_{ij} \tag{5.24}$$

where $j = 1,2,\ldots..2n$
and $t_i = 0$, or T

To apply the Q.L. method to the system of (5.21) it was necessary to start by finding some nominal solution which satisfied the boundary conditions, (5.24) but which did not, in general, satisfy (5.21). Then (5.21) was linearised about the nominal trajectory which was termed (for the purposes of this account) $\underline{R}^k$. The next trajectory which was evaluated was then $\underline{R}^{k+1}$ and this satisfied the linearised equation :

$$\dot{\underline{R}}^{k+1} = \underline{K}\Big|_{\underline{R}^k} + \underline{S}_{\underline{R}}\Big|_{\underline{R}^k} (\underline{R}^{k+1} - \underline{R}^k) \tag{5.25}$$

i.e.

$$\dot{\underline{R}}^{k+1} = \underline{S}_{\underline{R}}\Big|_{\underline{R}^k} \underline{R}^{k+1} + (\underline{K}\Big|_{\underline{R}^k} - \underline{S}_{\underline{R}}\Big|_{\underline{R}^k} \underline{R}^k) \tag{5.26}$$

where $\underline{S}_{\underline{R}}$ was the Jacobian matrix, of order 2n x 2n, the ijth component of which was given by $\dfrac{\partial K_i}{\partial R_j}$

The general solution of (5.26) has been shown (by the references given earlier in this section) to be of the form :

$$\underline{R}^{k+1}(t) = \Phi(t,t_0)\underline{R}^{k+1}(t_0) + \underline{P}(t) \qquad (5.27)$$

where $\Phi(t,t_0)$ was the transition matrix of the linearised system, of order 2n x 2n, and $\underline{P}(t)$ is the particular integral solution of (5.26) and is a vector of dimension, 2n.

Following the work of SPINGARN (1970), the transition matrix was evaluated by integrating (5.28)

$$\dot{\Phi}(t,t_0) = S_{\underline{R}}\Phi(t,t_0) \qquad (5.28)$$

where $$\Phi(t_0,t_0) \triangleq I \qquad (5.29)$$

The particular integral was determined from :

$$\dot{\underline{P}}(t) = S_{\underline{R}}\underline{P}(t) + (\underline{K}^k - S_{\underline{R}}\underline{R}^k) \qquad (5.30)$$

with

$$\underline{P}(t_0) = 0 \qquad (5.31)$$

The right hand side of (5.27) was equated to the given boundary conditions which resulted in 2n linear, simultaneous, algebraic equations, the solution of which provided the unknown vector $\underline{R}^{k+1}(t_0)$.

Thus :-

$$\Phi_{jz}(t_i,t_0)R_z^{k+1}(t_0) + P_j(t_i) = d_{ij} \qquad (5.32)$$

where $j = 1,2,\ldots\ldots\ldots\ldots\ldots$

$z = 1,2,\ldots\ldots\ldots\ldots\ldots$

Once $\underline{R}^{k+1}(t_0)$ was found it was used in (5.27) to determine $\underline{R}^{k+1}(t)$. The iterative process was continued then restarting with (5.26). The sequence of trajectories might converge to the solution of (5.21). If convergence was achieved then it has been shown [BELLMAN and KALABA (1969), KENNETH and McGILL

(1967) and FALB and de JONG (1969)] that convergence was quadratic*.

The Q.L. method formed the basis of the optimal start-up program which was developed for this research (BEARDM31EP - see Appendix A.3). It was also used in modified form for an investigation of a specific optimal control regulator for the engine system. (See chapter 8).

5.5 The Application of Quasilinearisation to the Optimal Start-Up Program

The solutions of such non-linear boundary value problems as the start-up problem have been solved, usually, by second variation methods employing Riccati transformations. [BRYSON and HO (1969b), DYER and McREYNOLDS (1970)]. Recent work by Tapley and Williamson [TAPLEY and WILLIAMSON (1971) and WILLIAMSON and TAPLEY (1971)] has demonstrated that the integration of these Riccati equations is frequently difficult because of instability of their solutions. The same work indicated the general superiority of linear equation methods, of which one example is the Q.L. method. It was suggested by LEE (1968) and by SAGE and MELSA (1971) that the Q.L. method might be useful for the solution of a M.P.B.V.P. However, the earliest treatment of such a problem by the method was that presented by VAN SCHIEREEN and KWAKERNAAK (1970) who solved a state-constrained optimal control problem. By employing the Q.L. method there seemed to be a better chance of obtaining more easily numerically-integrated equations, with the prospect of rapid convergence and fewer boundary conditions to be matched, than by alternative techniques.

---

*In a recent book ROBERTS and SHIPMAN (1972a) showed that the convergence of the Q.L. method could be inferred from the proof of the Newton-Raphson-Kantorovich method.

5.5.1 Preliminary Approach

To develop the program for the engine system the simple scalar non-linear model defined in (2.20) was considered as the plant. The problem solved was the determination of the torque function which would drive the dynamometer up to equilibrium speed and would minimise the performance index, which was chosen to be :

$$J = 0.5\int_0^T \{gu^2 + q(x - x_F)^2\}dt \qquad (5.33)$$

where x_F was the desired final speed up to which the dynamometer was to be driven,

x was the instantaneous speed of the dynamometer,

u was the applied torque,

and g was a weighting factor applied to the control.* The constant, q, placed a weighting on the state error of the system. When q = 0 the performance index (5.6) was obtained.

The upper limit of the integration, T, was left free at this point of the development; in the results to be quoted later the effect upon $u^o(t)$ of varying T will be indicated. The effect of the values assigned to g and to q upon the optimal choice of T will also be discussed.

For the performance index (5.33)

$$H = \frac{gu^2}{2} + \frac{q}{2}(x^2 + x_F^2 - 2xx_F) + \psi(-cx^2 + bu) \qquad (5.34)$$

$$\frac{\partial H}{\partial u^o} = gu^o + b\psi = 0 \qquad (5.35)$$

$$\therefore\ u^o = -\frac{b}{g}\psi \qquad (5.36)$$

Now

$$\dot{x} = -cx^2 - \frac{b^2}{g}\psi \qquad (5.37)$$

$$\dot{\psi} = -qx + qx_F + 2cx\psi \qquad (5.38)$$

Let $\underline{R} = [x \ \psi]'$ (5.39)

*The weighting factor, g, was included to permit flexibility in solving the problem. A value of unity was used subsequently.

Thence, the Jacobian matrix, $S_{\underline{R}}$, was found to be :

$$S_{\underline{R}} = \begin{bmatrix} -2cx & -\frac{b^2}{g} \\ (2c\psi - q) & 2cx \end{bmatrix} \tag{5.40}$$

and

$$\underline{K} - S_{\underline{R}} \cdot \underline{R} = \begin{bmatrix} cx^2 \\ -2cx\psi + qx_F \end{bmatrix} \tag{5.41}$$

$$\therefore \; x(0) = d_1 \tag{5.42}*$$

$$\Phi_{11}x(0) + \Phi_{12}(0) = d_2 - P_1(T)$$

where

$$d_2 = x_F \tag{5.43}$$

The upper limit, T, of the integration remained to be determined. One possible procedure was to select a value for T, find the optimal control function, and then evaluate (5.33) for specified q and g. The procedure would then be repeated with a different value of T, and so on, until a sufficient number of values J_{min} had been obtained to permit a graph to be plotted of J_{min} vs. T. Such a procedure is particularly expensive in computer time, especially with higher order systems. To avoid such a time expenditure the transformation proposed by LONG, and outlined briefly in section 5.2, was employed and the scaled canonical equations were

$$\underline{x}' = -acx^2 - \frac{ab^2}{g}\psi \tag{5.44}$$

$$a' = 0 \tag{5.45}$$

$$\psi' = -qax + qax_F + 2acx\psi \tag{5.46}$$

---

*d_1 and d_2 are the elements of the matrix, $\underline{d}$, defined in (5.24).

The associated Jacobian matrix was

$$S_{\underline{R}} = \begin{bmatrix} -2ac.x & (-cx^2 - \frac{b^2}{g}\psi) & -\frac{ab^2}{g} \\ 0 & 0 & 0 \\ (-qa + 2ac\psi) & (-qx + qx_F + 2cx\psi) & 2acx \end{bmatrix} \quad (5.47)$$

$$\underline{K} - S_{\underline{R}}.\underline{R} = \begin{bmatrix} 2acx^2 + \frac{ab^2}{g}\psi \\ 0 \\ qax - 4acx\psi \end{bmatrix} \quad (5.48)$$

The boundary conditions which corresponded to the introduction of the additional state variable was obtained from the value of the Hamiltonian at $\tau = 1$ viz :

$$H(1) = -\frac{b^2\psi^2(1)}{2g} + \frac{q}{2}\left\{x^2(1) + x_F^2 - 2x(1)x_F\right\} - cx^2(1)\psi(1) = 0. \quad (5.49)$$

From (5.49) it was possible to calculate $\psi(1)$; however the boundary condition of (5.49) was non-linear and the determination of $\psi(1)$ was avoided by applying the Long transformation <u>before</u> applying the maximum principle of Pontryagin. In the simple first order case considered here the gain was insignificant but for the full equations which were to follow the non-linear boundary condition was more involved and the benefit of pre-transformation as described here was realised. In that case the performance index to be minimised became :

$$J^{\#} = \tfrac{1}{2}\int_0^1 \left\{gu^2(a\tau) + q\left[x(a\tau) - x_F\right]^2\right\} ad\tau \quad (5.50)$$

$$= \tfrac{1}{2}a\int_0^1 \left\{gu^2(a\tau) + q\left[x(a\tau) - x_F\right]^2\right\} d\tau \quad (5.51)$$

$$H(\tau) = \frac{gau^2(\tau)}{2} + \frac{gax^2(\tau)}{2} + \frac{gx_F^2a}{2} - qax_Fx(\tau) - cax^2(\tau)\psi_1(\tau) + abu(\tau)\psi_1(\tau) \quad (5.52)$$

$$\frac{\partial H}{\partial u} = gau^{o}(\tau) + ab\psi_1(\tau) = 0 \qquad (5.53)$$

$$u^{o}(\tau) = -\frac{b}{g}\psi_1(\tau) \qquad (5.54)$$

Hence

$$H^{o}(\tau) = \frac{qax^2(\tau)}{2} + \frac{qax_F^2}{2} - qax_F x(\tau) - cax^2(\tau)\psi_1(\tau)$$

$$-\frac{ab^2\psi_1^2(\tau)}{2g} \qquad (5.55)$$

Thus :

$$x' = -cax^2(\tau) - \frac{ab^2}{g}\psi_1(\tau) \qquad (5.56)$$

$$a' = 0 \qquad (5.57)$$

$$\psi_1' = qax(\tau) + qax_F + 2acx(\tau)\psi_1(\tau) \qquad (5.58)$$

$$\psi_2' = -\frac{qx^2}{2}(\tau) - \frac{qx_F^2}{2} + qx(\tau)x_F + cx^2(\tau)\psi_1(\tau) + \frac{b^2\psi_1^2(\tau)}{2g} \qquad (5.59)$$

The Jacobian matrix, $S_{\underline{R}}$, (now of order 4 x 4) became :

$$S_{\underline{R}} = \begin{bmatrix} -2cax(\tau) & \left\{-cx^2(\tau) - \frac{b^2\psi_1(\tau)}{g}\right\} & -\frac{ab^2}{g} & 0 \\ 0 & 0 & 0 & 0 \\ \left\{-qa+2ca\psi_1(\tau)\right\} & \left\{-qx(\tau)+qx_F+2cx(\tau)\psi_1(\tau)\right\} & \left\{2cax(\tau)\right\} & 0 \\ \left\{-qx(\tau)+qx_F+2cx(\tau)\psi_1(\tau)\right\} & 0 & \left\{cx^2(\tau)+\frac{b^2\psi_1(\tau)}{g}\right\} & 0 \end{bmatrix} \qquad (5.60)$$

$$-S_{\underline{R}}\cdot\underline{R} = \begin{bmatrix} 2cax^2(\tau) + \frac{ab^2\psi_1(\tau)}{g} \\ 0 \\ qax(\tau) - 4acx(\tau)\psi_1(\tau) \\ \frac{qx^2}{2}(\tau) - \frac{qx_F^2}{2} - \frac{\psi_1^2(\tau)b^2}{2g} - 2cx^2(\tau)\psi_1(\tau) \end{bmatrix} \qquad (5.61)$$

The boundary conditions were obtained from :

$x(0)$ and $x(1)$ - both known

$\psi_2(0)$ and $\psi_1(1)$ - both zero*.

*See, for example, SAGE 1968b.

Note that the non-linear boundary conditions which, in the Q.L. method, had to be solved at the end of each iteration before the next could proceed, was avoided at the expense of increasing by one the dimension of the vector space. This fact has some importance when computer time is at a premium.

A program, BEARDM31F (see Appendix A.3), was written to obtain some idea of the optimal duration of the dynamometer start-up sequence: the program used the equations (5.47), (5.48) and (5.49). Another program, BEARDM31G, was written using the equations (5.60) and (5.61).

Because the same results were obtained with the use of either program only BEARDM31F was used extensively in view of its shorter execution time, and reduced storage requirement. A program, BEARDM31E, was written to evaluate the optimal start-up control when the interval of start-up was specified. This program was run many times with different values of T to confirm, for the single case of $q = 1.0$ and $g = 1.0$ with $k = 8 \times 10^{-3}$, corresponding to a fan displacement of 7.62 cm., that the minimum value of time, T, corresponded to the value obtained from BEARDM31F. The results of that series of numerical experiments are shown in figure 5.1; the result obtained from BEARDM31F was 9.284 seconds. A series of further experiments were conducted with BEARDM31F to check upon the effects on T of selecting different values for g. The results are shown in figure 5.2: the obvious physical fact that if there was a large penalty on the use of the throttle (i.e. that g was large) the time to reach final speed would increase is illustrated clearly. As a compromise a value for g of unity was used subsequently.

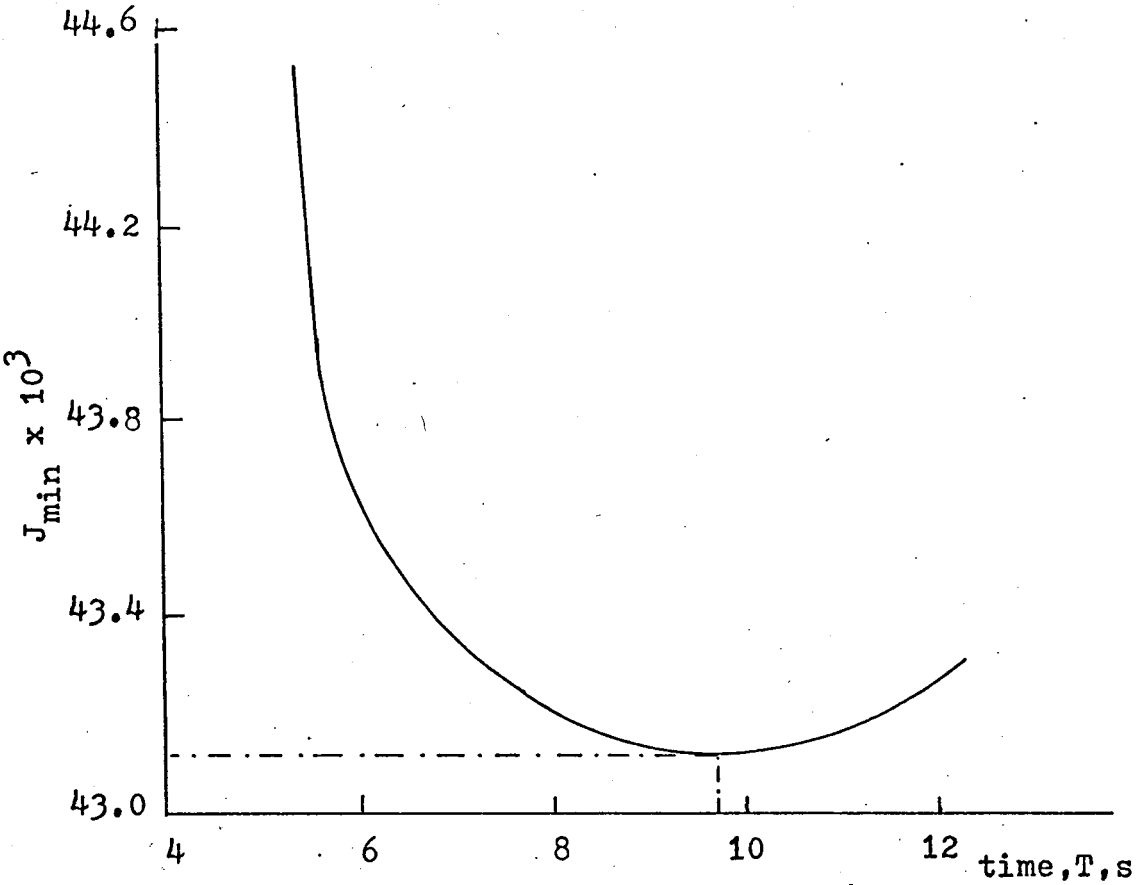

Figure 5.1 - Variation of J_{min} with T

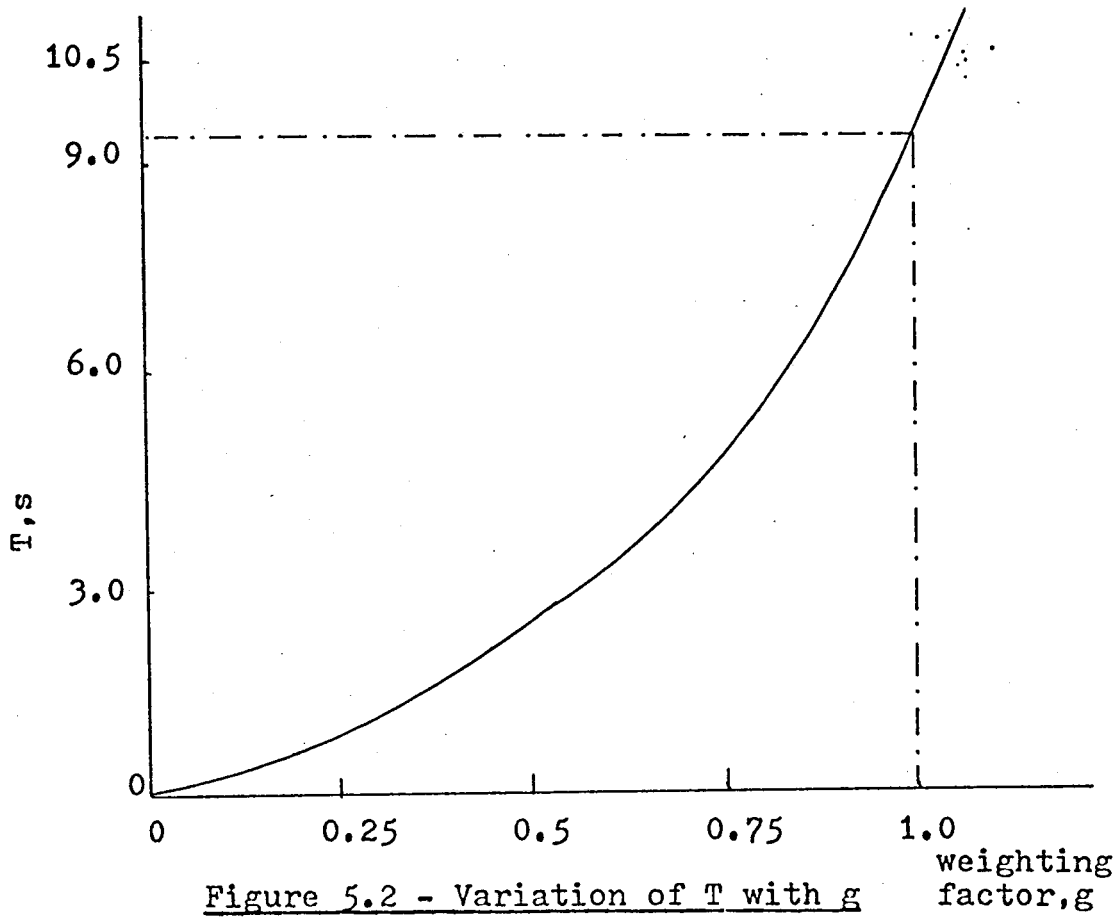

Figure 5.2 - Variation of T with g

5.5.2 Optimal Start-Up of Engine and Transmission System

In the course of the development of the optimal start-up program certain limitations upon what could be achieved with the computational facilities available at R.A.F. Cranwell became apparent. These limitations resulted in the deliberate decision to neglect from any further consideration in the start-up problem the dynamics associated with the throttle servomechanism in order that the problem could be solved, even if only approximately, on the available computer. From the work presented in chapter 2 it is plain that the assumption was unlikely to lead to gross inaccuracies because the settling time of the servomechanism in response to any sudden throttle demand was 0.65 sec. (see figure 2.12) whereas the total time to start-up the engine was unlikely to be less than 6.5 seconds (see figures 3.21a and 3.21b, table 3.6 and equation 3.5). The equations used as the mathematical model of the system for start-up were those of (2.80) and (2.81) which are repeated here for convenience :

$$\dot{x}_1 = -0.925x_1 + ax_2 + 1.894u \qquad (5.62)$$

$$\dot{x}_2 = dx_1 - cx_2 - bk_1x_2^2 \qquad (5.63)$$

where $x_1 = \Omega_e$, engine speed in rad/s (5.64)

$x_2 = \omega_f$, output shaft speed in rad/s (5.65)

$u = Q_e$, engine torque in Nm (5.66)

the coefficients a,b,c and d were listed in table 2.6. The damping coefficient of the fan, in Nms, was denoted by k_1^* and depended upon the fan displacement.

The performance index to be minimised was chosen to be :

$$J = \tfrac{1}{2}\int_0^T u^2 dt \qquad (5.67)$$

---

*Earlier in this thesis this coefficient was denoted as k. In order that the symbol, k, may be used to represent an iteration for the Q.L.method, the damping coefficient is denoted here as k_1.

and the Hamiltonian for the system was written as :

$$H = \tfrac{1}{2}u^2 + \psi_1(-0.925x_1 + ax_2\ 1.894u) + \psi_2(dx_1 - cx_2 - bkx_1^2) \tag{5.68}$$

$$\frac{\partial H}{\partial u^o} = u^o + 1.894\psi_1 = 0 \tag{5.69}$$

therefore, $u^o = -1.894\psi_1$ (5.70)

Also,

$$\frac{\partial H}{\partial x_1} = -\dot{\psi}_1 = 0.925\psi_1 + d\psi_2 \tag{5.71}$$

$$\frac{\partial H}{\partial x_2} = -\dot{\psi}_2 = -c\psi_2 + a\psi_1 - 2bkx_1x_2\psi_2 \tag{2.72}$$

Consequently,

$$\dot{x}_1 = -0.925x_1 + ax_2 - 3.587\psi_1 \tag{5.73}$$

$$\dot{x}_2 = dx_1 - cx_2 - bkx_1^2 \tag{5.74}$$

$$\dot{\psi}_1 = 0.925\psi_1 - d\psi_2 \tag{5.75}$$

$$\dot{\psi}_2 = -a\psi_1 + c\psi_2 + 2bkx_1x_2\psi_2 \tag{5.76}$$

By letting $\underline{R} = \left[x_1\ x_2\ \psi_1\ \psi_2\right]$, (5.77)

the quasilinearisation equation became :

$$\dot{\underline{R}}^{k+1} = S_{\underline{R}|\underline{R}^k} \cdot \underline{R}^{k+1} + \left(K_{|\underline{R}^k} - S_{\underline{R}|\underline{R}^k} \cdot \underline{R}^k\right) \tag{5.78}$$

where $S_{\underline{R}|\underline{R}^k}$ was the Jacobian matrix, of order 4 x 4, given by :

$$S_{\underline{R}|\underline{R}^k} = \begin{bmatrix} -0.925 & a & -3.587 & 0 \\ d & -(c + 2bkx_1^k) & 0 & 0 \\ 0 & 0 & 0.925 & -d \\ 0 & 2bk\psi_2^k & -a & (c + 2bkx_1^k) \end{bmatrix} \tag{5.79}$$

and

$$\left(\underline{K}\Big|_{\underline{R}^k} - S_{\underline{R}}\Big|_{\underline{R}^k}\cdot\underline{R}^k\right) = \begin{bmatrix} 0 \\ bk_1(x_2^k)^2 \\ 0 \\ -2bk_1x_2^k\psi_2^k \end{bmatrix} \qquad (5.80)$$

The boundary conditions for the quasilinearisation system for the segment were :

$$_{2/3}\underline{d}(0) = \left[x_1(0), x_2(0), x_1(t_1), x_2(t_1)\right]' \qquad (5.81)$$

$$_{3/4}\underline{d}(t_1) = \left[n_3x_2(t_1), x_2(t_1), x_1(t_2), x_2(t_2)\right]' \qquad (5.82)$$

$$_{4/t_2}\underline{d}(t_2) = \left[x_2(t_2), x_2(t_2), x_1(T), x_2(T)\right]' \qquad (5.83)$$

5.6 Computational Difficulties and Solutions

For each iteration of the quasilinearisation program there were three separate integrations which had to be carried out over the segment interval. The following were integrated :

(i) a matrix differential equation to obtain the matrix, Φ, of order 4 x 4

(ii) a vector differential equation to obtain the particular integral solution, P

(iii) a vector differential equation to obtain the next trajectory.

In the early stages of developing the program to find the optimal solution, a fourth order Runge-Kutta routine with fixed step length was used for integration. However, accuracy became a problem which manifested itself when solving the linear, simultaneous, algebraic equations at each iteration : it was a problem of "ill-conditioning". Both BELLMAN and KALABA(1969) and LEE (1968) have shown, by example, how the

method of complementary functions could fail to work. In their examples, each concerned with unstable differential equations, the integration procedure used was also Runge-Kutta with a fixed step length of 0.01 second. The same problems were solved using the integration routine and the same routine for solving linear simultaneous equations as had been used in the early Q.L. program. In this fashion it was intended to validate the method and the routines for achieving it. Near identical results to those quoted by Bellman and Kalaba were obtained. Some difference from the results quoted by Lee was found. The results are shown in tables 5.1 and 5.2.

	Bellman & Kalaba		McLean	
	$x_1(1)$	$x_2(1)$	$x_1(1)$	$x_2(1)$
h_3	1.95694×10^9	5.87083×10^{10}	1.956×10^9	5.867×10^{10}
h_4	3.26157×10^8	9.78472×10^9	3.259×10^8	9.778×10^9

Table 5.1 *

	Lee		McLean	
	$x_1(1)$	$x_2(1)$	$x_1(1)$	$x_2(1)$
h_3	-0.978575×10^4	-0.39146×10^6	-0.1038096	-33.913006
h_4	0.367115×10^{13}	0.146846×10^{15}	3.671×10^{12}	0.1468×10^{15}

Table 5.2 *

*The symbols h_3 and h_4 were used here to represent solutions of the homogeneous differential equations. These symbols, h_i, were used by the quoted authors, and maintenance of the convention permits easier comparison with the original papers.

In each case the matrix which had to be inverted to solve the simultaneous linear equations was near-singular : Because only single precision arithmetic was available on the Elliott 4120 computer when the matrix package was used, the results obtained by this author, by using that machine, were less accurate than the quoted results of the other authors* who both employed double precision arithmetic. Nevertheless, despite the exceedingly small pivot ratio of the example of Bellman and Kalaba, the solution for the unknown initial conditions being sought for in the example was found to be :

$$x_1(0) = 2.0791844 \qquad (5.84)$$

and

$$x_2(0) = 12.475106 \qquad (5.85)$$

The known analytical values were

$$x_1(0) = 2.0 \qquad (5.86)$$

$$x_2(0) = 12.0 \qquad (5.87)$$

The results obtained with the developed programs, although somewhat inaccurate, were superior to the results finally obtained by B. and K.** which they quoted as :

$$x_1(0) = 0.609136 \times 10^{-2} \qquad (5.88)$$

and

$$x_2(0) = 0.365481 \times 10^{-1} \qquad (5.89)$$

To improve such results B. and K. and CONTE (1966) suggested the use of a Gram-Schmidt orthonormalisation procedure in the integration routine to improve the step to step accuracy. They reported that such a technique had yielded substantial improvement in the results they had obtained. A similar routine, based upon ROSENBROCK and STOREY (1971), was prepared

---

*Some further remarks are made about Lee's results later.

**Bellman and Kalaba.

and is available as BEARDM37 (see Appendix A.3). Its use did improve accuracy as had been claimed; it also lengthened markedly the execution time of the integration routine, and, of course, of the entire program. Consequently an improved integration routine, which would improve accuracy and if possible speed, was sought. Before discussing this development it should be noted that the results for h_3, quoted by Lee, differ significantly from those obtained by the present author (see table 5.2). It is suggested that this must be an error in the book by Lee.* All other examples produced correct answers.

The improved integration procedure used was the algorithm proposed by HAMMING (1959) and is summarised below :

Hamming suggested the use of a predictor-corrector method which, in common with all numerical methods of this type, was not self-starting. If the first three steps in the integration process (which were derived from some alternative integration process - in this work, Runge-Kutta) were stable the remainder of the procedure was stable. At the start of the integration, when l = 0 say, the only known value was $\underline{x}^0$. Using Runge-Kutta, $\underline{x}^1$, $\underline{x}^2$, and $\underline{x}^3$ were evaluated and subsequent values were determined from the Hamming formulae :

Predictor formula

$$\underline{p}^{l+1} = \underline{x}^{k-3} + \frac{4h}{3}(2\dot{\underline{x}}^{l} + 2\dot{\underline{x}}^{l+2} - \dot{\underline{x}}^{l+1}) \qquad (5.90)$$

where $l = 4,5.....n$

h was the step length. n represented total number of steps.

Modification formula

$$\underline{m}^{l+1} = \underline{p}^{l+1} - \frac{112}{121}(\underline{p}^{l} - \underline{c}^{l}) \qquad (591)$$

---

* In a private communication with Lee (1972) it was acknowledged by him that the results might be in error.

$$\dot{\underline{m}}^{l+1} = \underline{f}(\underline{m}^{l+1}, t^{l+1}) \qquad (5.92)$$

t^{l+1} represented the value of t at the (l+1)th interval.

Corrector formula

$$\underline{c}^{l+1} = 0.125\left[9\underline{x}^{l} - \underline{x}^{l-2} + 3h(\dot{\underline{m}}^{l+1} - \dot{\underline{x}}^{l+1} + 2\dot{\underline{x}}^{l})\right] \qquad (5.93)$$

Final value formula

$$\underline{x}^{l+1} = \underline{c}^{l+1} + \frac{9}{121}(\underline{p}^{l+1} - \underline{c}^{l+1}) \qquad (5.94)$$

RALSTON (1960) noted that if the first three steps were computed with the same or less accuracy than the Hamming integration process to be employed, the most suitable choice for $(\underline{p}^3 - \underline{c}^3)$ was zero. This choice was used and consequently in the program

$$\underline{m}^4 = \underline{p}^4 \qquad (5.95)$$

The procedure was written as a program, BEARDM40 (see Appendix A.3), and it solved either vector or matrix differential equations. The examples of B. and K., and of Lee, were solved by the Hamming procedure by considering them to be :

(a) vector differential equations, in which the initial vector was either $[0\ 0\ 1\ 0]'$ or $[0\ 0\ 0\ 1]'$.

or (b) matrix differential equations, in which the initial matrix was the identity matrix.

For both examples the results obtained, using either vector or matrix formulation, were identical. The results are presented in tables 5.3 and 5.4.

	Bellman & Kalaba		McLean (Hamming)	
	$x_1(1)$	$x_2(1)$	$x_1(1)$	$x_2(1)$
h_3	1.95694×10^{9}	5.87083×10^{10}	1.958×10^{9}	5.783×10^{10}
h_4	3.26157×10^{8}	9.78472×10^{9}	3.263×10^{8}	9.785×10^{9}

Table 5.3

	Lee		McLean (Hamming)	
	$x_1(1)$	$x_2(1)$	$x_1(1)$	$x_2(1)$
h_3	-0.97875×10^{4}	-0.39146×10^{6}	0.24648119	-19.901373
h_4	0.367115×10^{13}	0.146846×10^{15}	3.68×10^{12}	1.472×10^{14}

Table 5.4

The accuracy of the Hamming procedure was better than that of the Runge-Kutta method** but there was an increase in execution time plus an increase in programming complexity*. It should be noted however, that use of the Hamming procedure to solve the matrix differential equation by taking a column at a time (i.e. solving it as a vector differential equation in which the vector is the appropriate column of the matrix) was slower by a factor of two than by solving the matrix differential equation as a matrix equation. Consequently this procedure was extremely useful for application in the Q.L. program because in that the transition matrix was evaluated using the matrix differential equation and then the particular integral was solved as a vector differential equation. Then, when the boundary conditions had been solved, the trajectory was determined next by solving a vector differential equation again. The use of the Hamming routine removed most of the numerical difficulties associated with the program.

One difficulty which remained was making an initial guess for the first trajectory. BELTRAMI (1967) suggested that the initial trajectory should be chosen to satisfy the boundary

---

*See later remarks however.
**It was faster than using the Runge-Kutta method with orthonormalisation.

conditions and should be a linear fit between these points. This technique was followed because experiment with other attempted guesses proved less successful. However, the linear fit method did not always produce a converging program. No definite statement about the choice of initial trajectory can be made; only numerical experiment provides an answer. This unsatisfactory feature of the Q.L. method had already been observed by FALB and de JONG (1969). Some indication of the likely success of the initial guess can always be found by printing out the solved initial conditions at the first iteration. If they are very large, and they most frequently will be, then the next iteration is unlikely to converge. Another choice of initial trajectory should be made and the procedure repeated. When convergence does occur it is very rapid. It was noticed that sometimes the program would fail to converge due to overflow in the machine solution*. Some results are presented in figure 5.4 of optimal start-up trajectories for gear 3, and a fan setting of 7.62 cm., and different start-up periods. When the interval was greater than 9 seconds the program always failed to converge and always in the same fashion. In the case quoted above, when the length of the segment was selected to be 10 seconds, the program had not converged after 7 iterations (i.e. a running time of 55 minutes). The symptom of this failure was that $\underline{x}(T)$ did not equal the read-in values by amounts which increased with each iteration.

---

*Both these features of convergence failure were also noted by ROBERTS and SHIPMAN (1972b.)

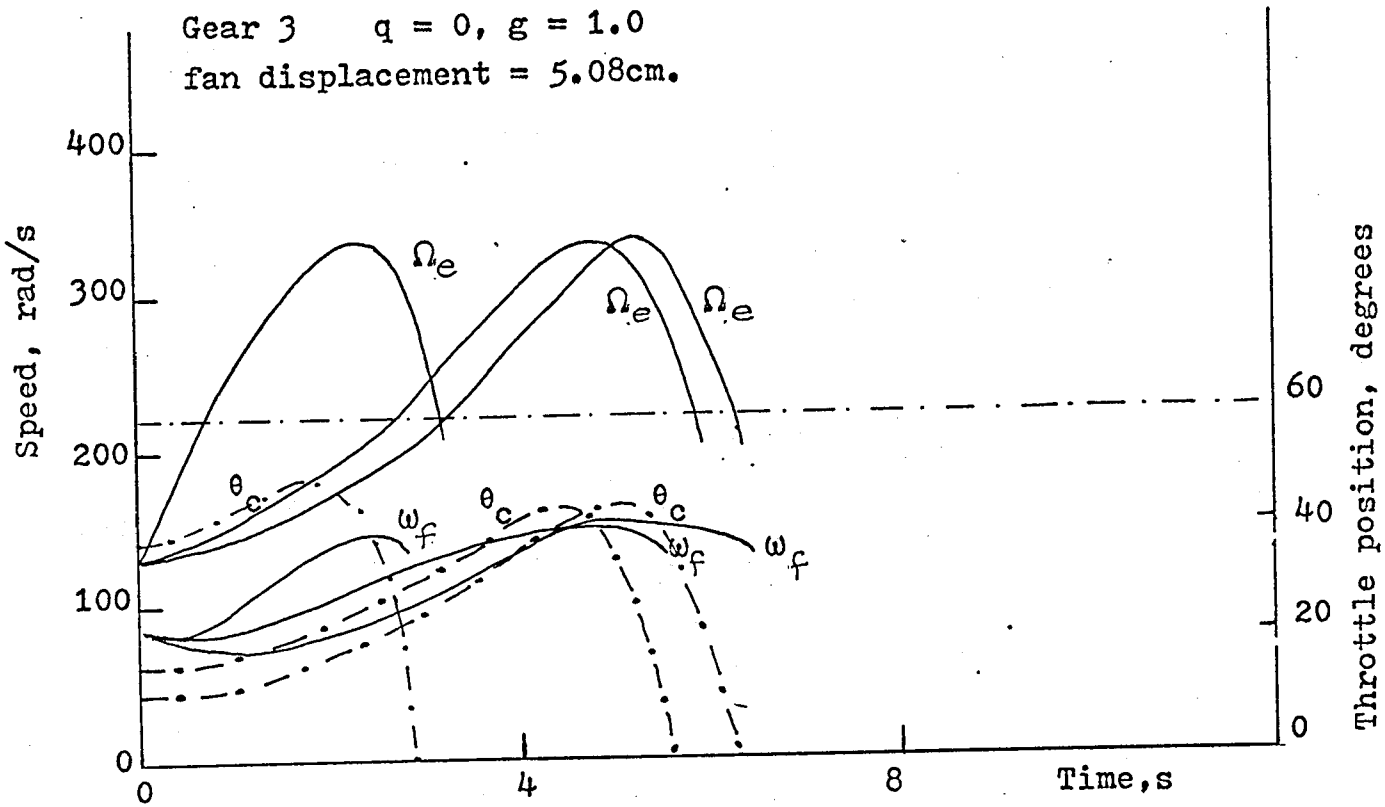

Figure 5.4 - Start-up Trajectories for Third Gear

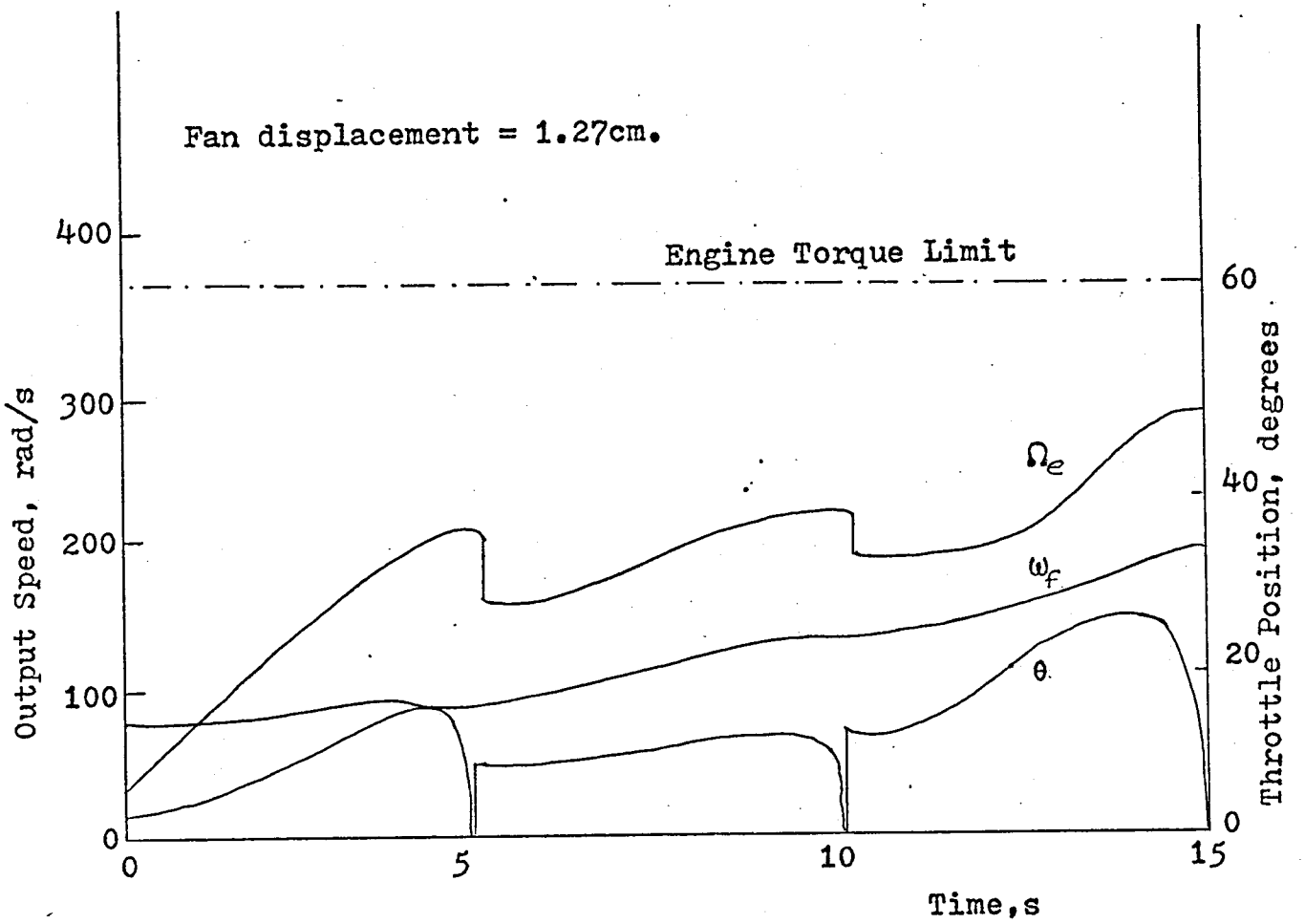

Figure 5.5 - Optimal Start -up Trajectory

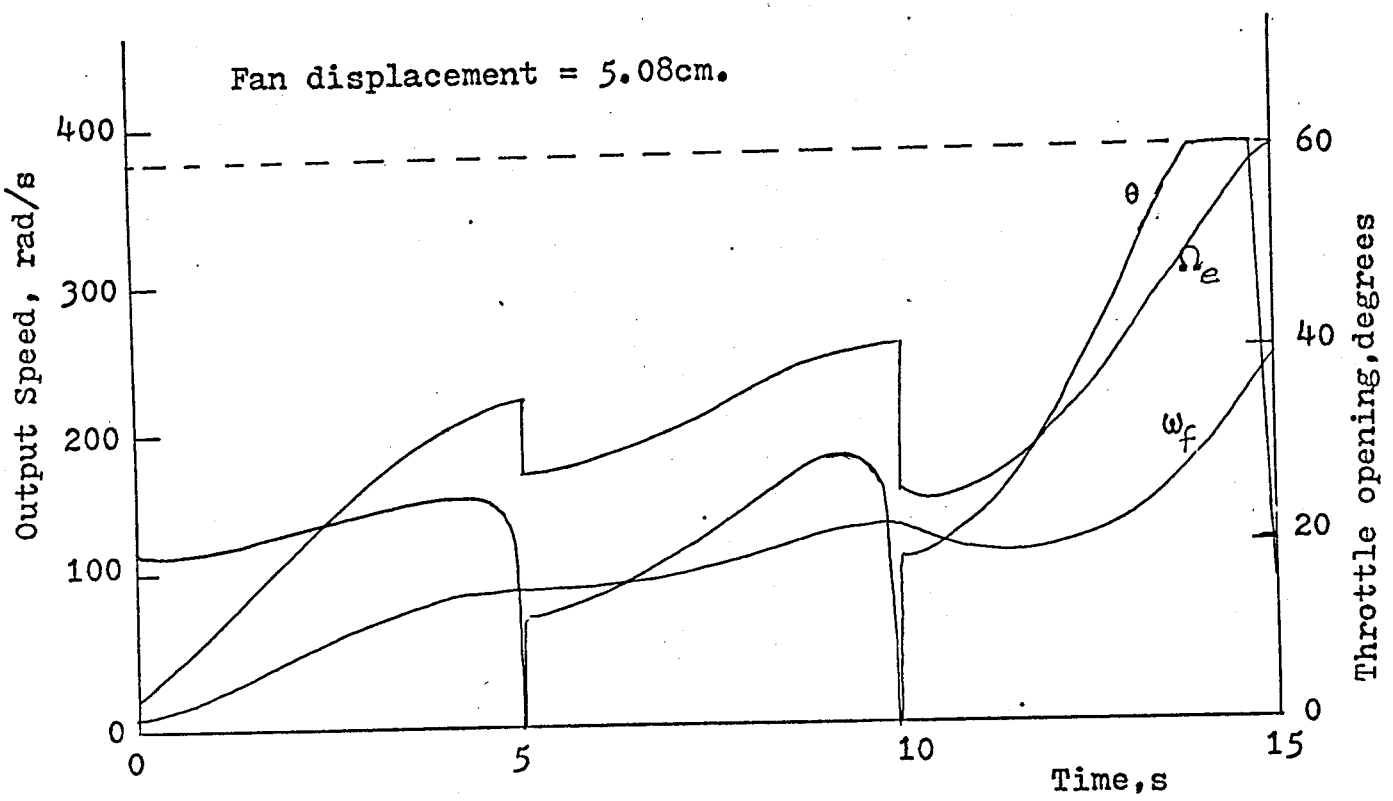

Figure 5.6 - Optimal Start-up Trajectory

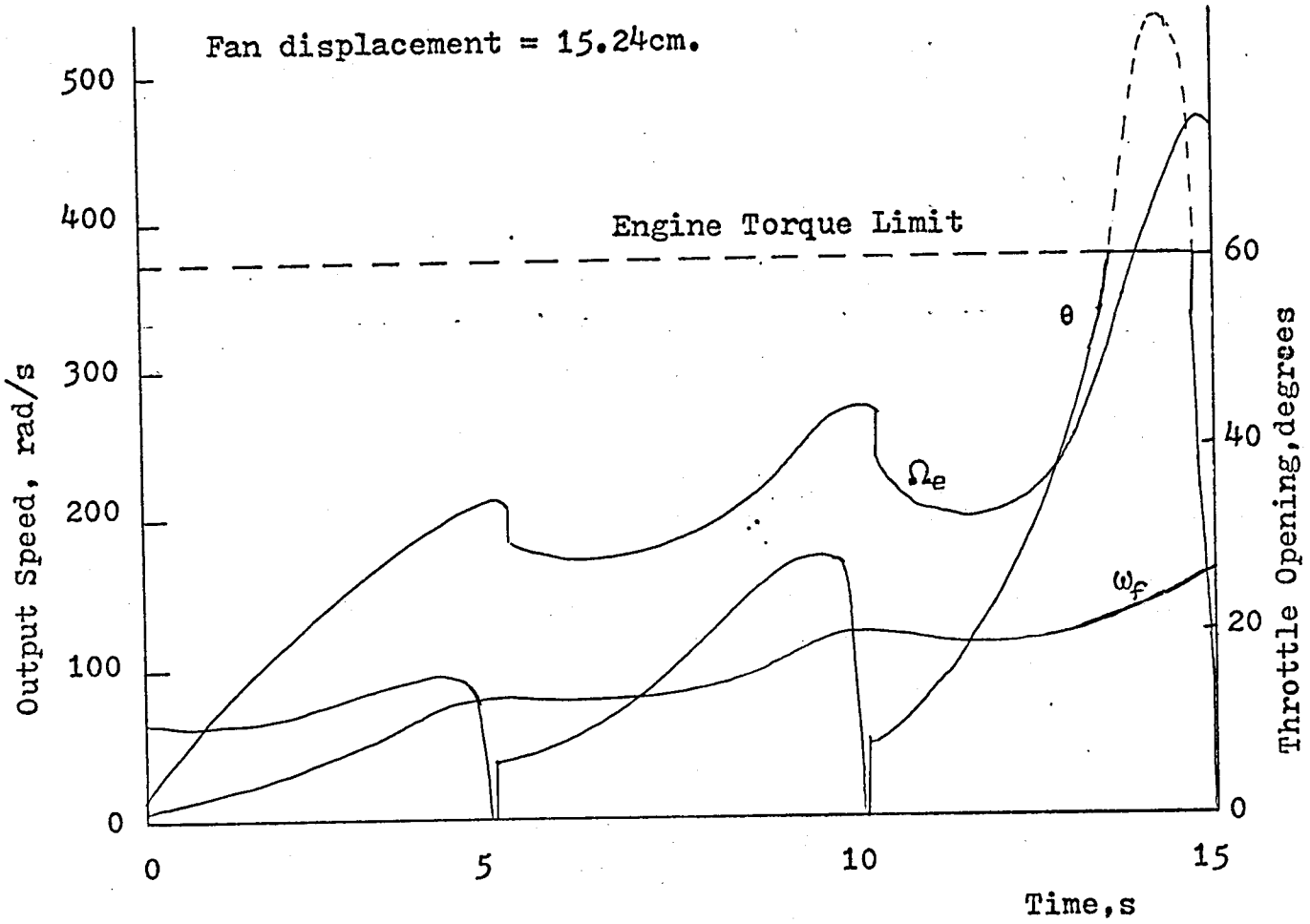

Figure 5.7 - Optimal Start-up Trajectory

The results for optimal start-up were weakened by a deliberate decision to limit the determination of the optimal start-up trajectory to fixed interval. If the Long transformation was used in this part of the work the dimension of the state vector was increased by two. This increase resulted in increased program time which was already very long. For some indication of how program execution time was affected consider table 5.5, which was derived from the results associated with the simple 3-state program, BEARDM31F, which used the Runge-Kutta integration scheme as well as the Long transformation. It should be appreciated that the execution time depended upon the integration step length and the stopping condition, both of which were associated with the achieved accuracy of the solution. Attempts to accept less accurate solutions, by lengthening the step or by opening out the stopping condition, were nullified usually by the failure of the program to converge with these adjustments.

Serial No.	Step Length	Stopping* Value	No. of Iterations	Execution Time
1	0.01	0.001	2	14m. 31s.
2	0.01	1×10^{-7}	7	49m. 12s.
3	0.1	0.001	4	3m. 14s.
4	0.01	0.001	4	28m. 21s.
5	0.1	0.001	10	7m. 57s.

Table 5.5

The use of the Hamming procedure, usually for the same stopping condition, resulted in a reduction of total execution time by about a half; the time per iteration was increased

*Norm of difference between current and previous trajectories.

but fewer iterations were required. Serial nos. 1 and 4 and 3 and 5 in table 5.5 which represent two pairs of comparative runs in which the step length and the stopping condition were maintained identical for each run, had different results. This was due to different initial trajectories being used. The need for an accurate guess for the initial trajectory has already been described as critical. A further adscititious consideration, which supported the decision to work in fixed intervals, was that the difficulty of synthesising the optimal control function would be lessened considerably. The particular choice of fixed interval was based upon examination of a series of curves for the different gears and the table 3.6. In some instances it was evident that too short an interval would result in the control function requiring levels of engine torque in excess of the capacity of the engine to deliver such torque values. Even with the choice of 5.0 seconds for each interval, which produced for d = 1.27 cm. a smooth, almost continuous trajectory for the dynamometer shaft speed with relatively easily synthesised control signals (see figure 5.5), there resulted for moderate loads (d = 5.08 cm.) a control function which exceeded the engine torque limit (see figure 5.6). Even this moderate torque limiting did not affect seriously the start-up of the engine system other than to result in the dynamometer shaft speed being less than the specified 200 rad/sec at t = 15 seconds. (See figure 5.8).* If the torque had been maintained at maximum for a few more seconds then the desired final speed could

---

*Gearshifts occur later than specified chiefly due to the finite duration of travel of the gear selector lever. (See chapter 3).

have been reached. Thus the torque limiting may be regarded as being analogous to the introduction of a finite time delay in the optimal control function. This idea is strengthened if the case for full fan displacement , i.e. maximum loading , is considered : see figure 5.7. Note that the final segment of the optimal control function was limited for almost half the interval and that the maximum throttle position attainable was only 60% of the computed value. The result of this limiting was to have introduced effectively a pronounced time delay in the control action which resulted in violent oscillation between 3rd and 4th gears in the recorded optimal start-up sequence shown in figure 5.9 which was obtained from the engine rig using that control function of figure 5.7. The time axis in figure 5.9 has been labelled from 0 to 16 seconds; the origin corresponds to the start of the oscillations. By maintaining the throttle at the fully open position the oscillation was maintained beyond 15 seconds. From figure 5.9 it is seen that as time progresses the hunting was becoming unstable. The recording could not be continued beyond this point because of the certainty of severe damage to the gearbox and engine with such conditions prevailing. A modest reduction of the load, the dynamometer displacement was altered to 12.7 cm., resulted, with the same optimal start-up program, in an acceptable start-up trajectory. Because the start-up program for d = 15.24 cm. was used with the reduced load setting the gearshifts occurred a fraction earlier than at the specified times. A description of how the control functions were synthesised is given in the final section of this chapter.

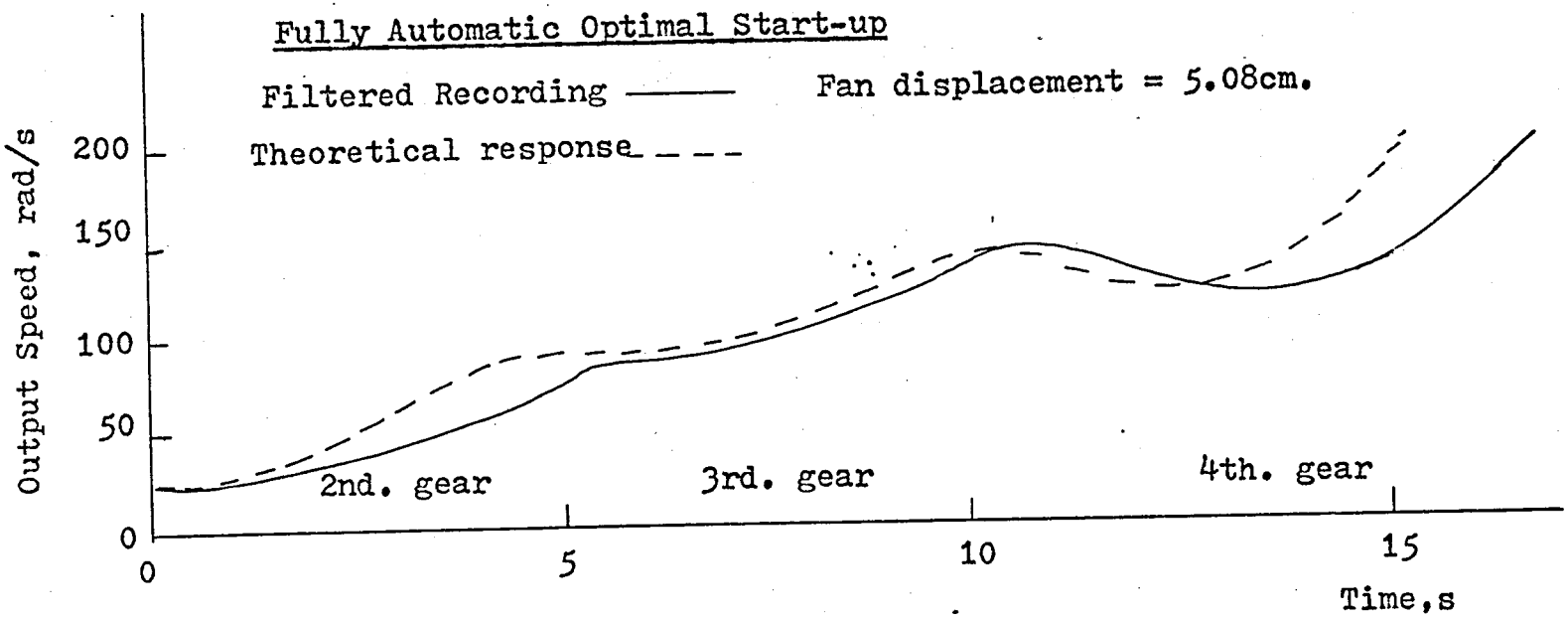

Figure 5.8 - Recorded Start-up Response

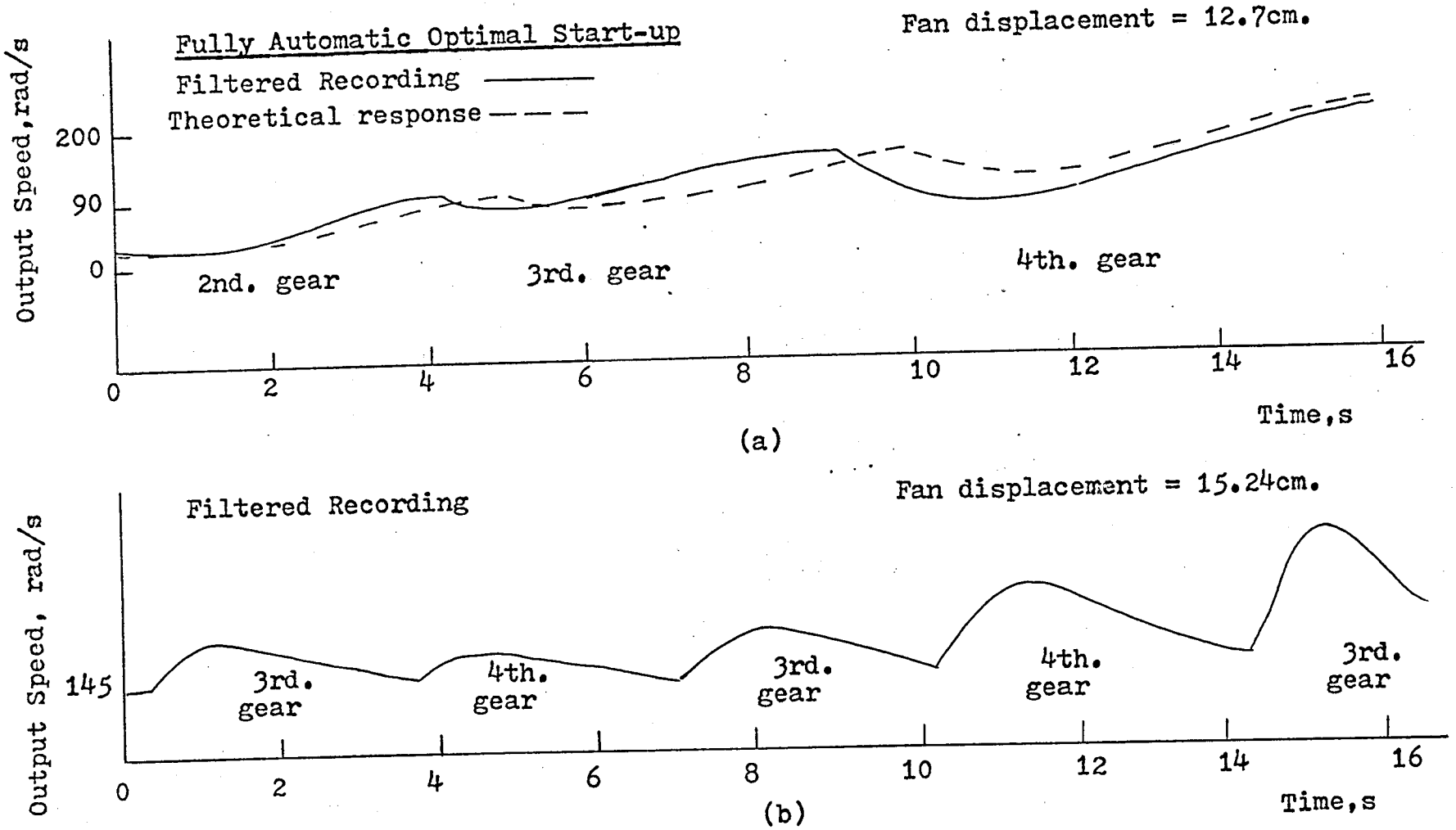

Figure 5.9 - Recorded Start-up Responses

5.7 Synthesis of Optimal Start-Up Function Generator

Only analogue devices were available to synthesise the optimal control functions. The resulting generated function was an approximation therefore, the nature of which is illustrated in figure 5.10

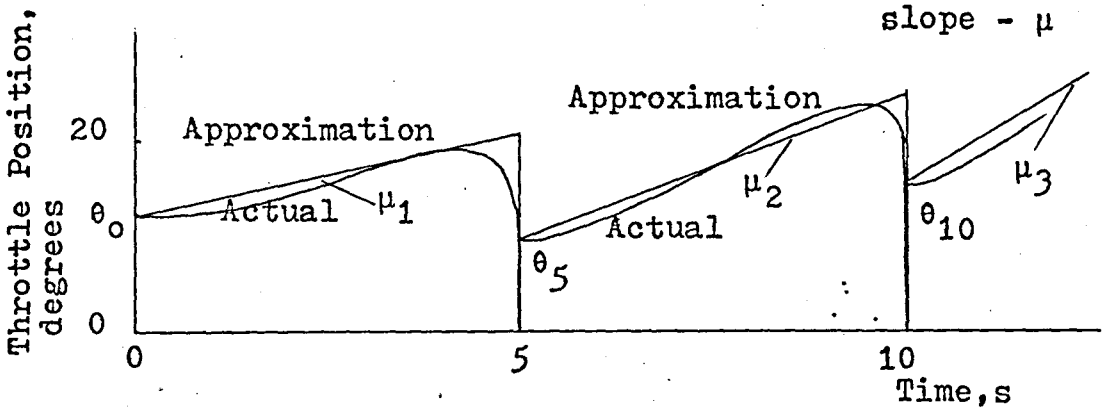

Figure 5.10 - Control Function Approximation

The approximation consisted of representing the optimal control function by a sum of singularity functions, which is an established practice in engineering analysis. (See deRUSSO, ROY, and CLOSE (1964)). The chief singularity function used was the ramp and consequently the active devices in the generator were integrators. Because the slope of the ramps were event-dependent logic-controlled integrators were used. Comparators provided the necessary event switching. A schematic diagram of the generator is shown in figure 5.11. The time generator was a simple unity gain integrator (A1) composed of a 100kΩ input resistor, a 10μf feedback capacitor and a Burr-Brown operational amplifier (model no. 3317/14) with a voltage swing of ± 15v. The output amplifier (A2) was the same type of operational amplifier with input resistors of 100kΩand a feedback resistor of 100kΩ. The two comparators

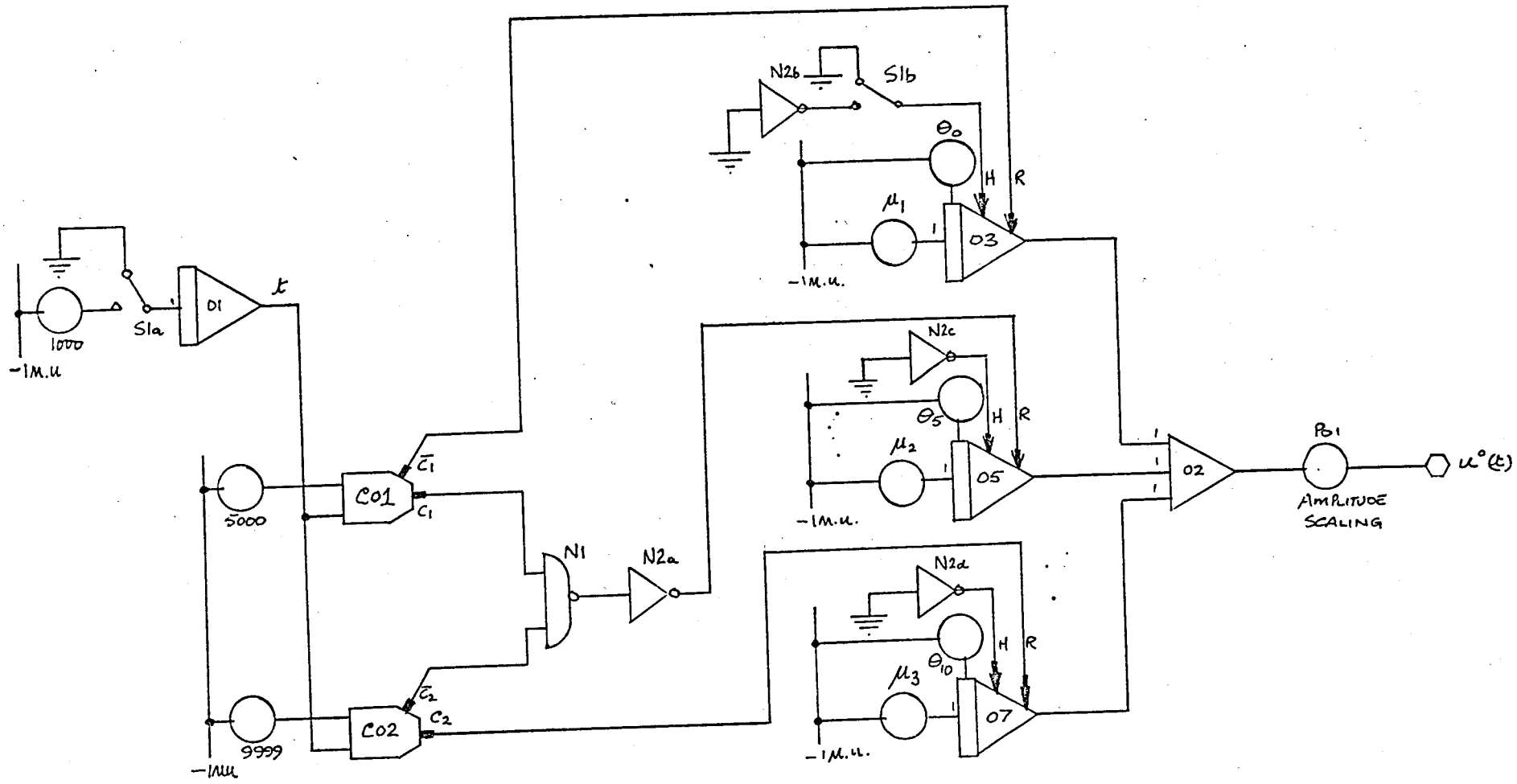

Figure 5.11 - Optimal Start-up Function Generator

were Burr-Brown comparator units (model nos. 4032/12C). The logic elements were a dual input Nand gate and a quad inverter, (Texas Instrument model nos. SN74H20 and SN74H00 respectively). The three logic-controlled integrators were Analog Devices 165A. The appropriate logic diagrams are given in the tables 5.6 and 5.7.

Input	C_1	$\overline{C}_1$	C_2	$\overline{C}_2$
$t < 5$	0	0	0	1
$5 \leqslant t < 10$	1	0	0	1
$10 \leqslant t < 15$	1	0	1	0

Table 5.6 - Comparator Logic Table

t	A3		A5		A7	
	H	R	H	R	H	R
$t < 5$	1	1	1	0	1	0
$5 \leqslant t < 10$	1	0	1	1	1	0
$10 \leqslant t < 15$	1	0	1	0	1	1

Table 5.7 - Logic Table for Three Mode Integrators

The switch S1 started the time generator and switches A1 from HOLD to COMPUTE. The m.u. is 10 volts. Scaling of the output voltage, $u^o(t)$, was necessary to match the sensitivity of the throttle servomechanism; P01 was set to 2000. At t = 15 seconds A1 overloads (indicated by a lamp circuit) and S1 was used to reset the generator.

CHAPTER 6 - OPTIMAL ENGINE REGULATION - LINEAR MODEL AND QUADRATIC PERFORMANCE INDEX

6.1 Introduction

It was outlined in chapter 2 how the engine system could be described by a linear model, the most appropriate definition of which was given in equations (2.5), (2.82) and (2.83). Also the effect upon the form of any resulting optimal control for a particular choice of performance index was discussed in chapter 5. In this chapter it is intended to discuss the design of controllers which resulted in continuous regulation of the engine about some equilibrium speed. By the work of chapter 5 the engine was arranged to have reached this desired equilibrium speed with least expenditure of fuel; it was essential to further maintain the cost of fuel at a minimum over a lengthy period of time by controlling optimally the performance of the engine. Consequently an integral cost criterion was chosen and to ensure continuous control a quadratic form was used again. From figure 2.5 it may be noted that the equilibrium speed was 2000 rev/min. The controllers developed by the methods of this and subsequent chapters were designed to ensure that the engine speed was maintained as close to the equilibrium as possible, otherwise specific fuel consumption would have been raised and the resulting performance would not have been optimal. By

choosing to penalize the use of the throttle it was intended to secure tight regulation and lowest s.f.c.

The work presented in this chapter was concerned with deriving, synthesising, and using linear optimal control laws which were applied to the engine system under the assumption that it was linear. Several different methods of obtaining the optimal control law were considered and a comparison of the efficiency of the associated computational schemes is here presented. The practical effects and limitations of providing linear control* for a non-linear system are represented also.

6.2 Optimal Regulator

The work of this section is essentially that of KALMAN (1960). It is outlined briefly for two reasons :

(i) it represents the foundation of other methods to be discussed in later sections

(ii) it provides the basis for some of the programs which were devised to synthesise the controller.

The engine and load system** was assumed to be described by :

$$\dot{\underline{x}} = A\underline{x} + Bu \qquad (6.1)$$

where $\underline{x}$ was the state vector, of dimension 3, which represents the deviations from the reference, or equilibrium, state, and where u represented the command input to the throttle servomechanism.

---

* derived under the assumption of system linearity.

** In this and all subsequent chapters it is assumed that 4th gear was selected. The methods would remain applicable if other gears were used : only the coefficient matrix, A, would be altered.

The performance index was selected to be

$$J = \tfrac{1}{2}\int_0^{\infty}\{\underline{x}'Q\underline{x} + gu^2\}dt \qquad (6.2)$$

In (6.2) Q was positive definite and of order, 3 x 3; g was a weighting factor on the control. The factor 0.5 was included for analytical convenience. Because the period of time over which the engine system would run was lengthy, when compared to the time constants associated with this system, the regulation interval (i.e. T) was taken to be infinite.* The analytical (and more important, the practical) convenience which resulted from this choice in some measure counterbalanced the errors which would result from short time engine operation.

From (6.1) and (6.2)

$$H(\underline{x}, \underline{\psi}, u) = \tfrac{1}{2}\underline{x}'Q\underline{x} + \tfrac{1}{2}gu^2 + \underline{\psi}'(A\underline{x} + Bu) \qquad (6.3)$$

$$\frac{\partial H}{\partial u}_o = gu^o + B'\underline{\psi} = 0 \qquad (6.4)$$

$$\frac{\partial H}{\partial \underline{\psi}} = \dot{\underline{x}} = A\underline{x} + Bu \qquad (6.5)$$

$$-\frac{\partial H}{\partial \underline{x}} = \dot{\underline{\psi}} = -A'\underline{\psi} + Q\underline{x} \qquad (6.6)$$

where

$$\underline{\psi}(\infty) = 0 \qquad (6.7)$$

The solution to (6.6) was

$$\underline{\psi}(t) = K\underline{x}(t) \qquad (6.8)$$

The matrix, K, was positive definite and the steady-state solution to the matrix equation :

$$\dot{K} = -KA - A'K - Q + KB\, g^{-1}B'K \qquad (6.9)$$

For (6.8) and (6.4)

$$u^o = -g^{-1}B'K\underline{x} = D\underline{x} \qquad (6.10)$$

---

*The choice avoided the difficulty associated with attempts to synthesise a controller with time-varying gains; such gains result if the upper limit of (6.2) is finite.

D was a rectangular matrix, of order 1 x 3.

To determine D required the solution of the matrix Riccati equation (6.9).

6.3 Numerical Solution of the Optimal Control Law

6.3.1 Approximate Integration

To solve the matrix Riccati equation a program, BEARDM11, (see Appendix A.3) was written based on the algorithm proposed by ATHANS and FALB (1966d) viz :

$$\frac{K(t+\triangle t) - K(t)}{\triangle t} = -KA - A'K - Q + KB\, g^{-1} B'K \qquad (6.11)$$

$$K(t+\triangle t) = K(t) + \triangle t\left\{-KA - A'K - Q + KB\, g^{-1} B'K\right\} \qquad (6.12)$$

with $K(\infty) = 0$ (6.13)

This simple Euler integration formula was evaluated backwards in time by choosing the integration step length, $\triangle t$, to be a small negative value. Although easy to program it was not an accurate method and the choice of $\triangle t$ was critical. With the matrices, A and B, of (2.83) and (2.84) the program "blew-up" although it had performed satisfactorily, if slowly, with a simple benchmark program*. To counteract this effect, due to accumulated and uncontrollable round-off error (only single precision arithmetic was available at the computing facility of R.A.F. Cranwell) the suggestion proposed by KALMAN and ENGLAR (1966) was adopted, viz. at every step the matrix K was symmetrisised by replacing it with

$$K(t) = \frac{K(t) + K'(t)}{2} \qquad (6.14)$$

This palliative proved to be ineffective and it was evident some transformation was needed to enable the program to solve the equation (6.9) both quickly and accurately. It should be noted here that only the steady-state solution was required although this program solved from ∞ (actually some guessed,

*The problem was Q7.3.6 on p.275 of SCHULTZ and MELSA (1967).

time) to 0. Consequently a large amount of unrequired data was generated. The program was used later with transformed equations.

6.3.2 Transformation of State Variables

It was decided to use the transformation

$$\underline{x} = T\underline{z} \tag{6.15}$$

$\underline{z}$ was the transformed state vector of the same dimension, 3, and T was a constant, non-singular matrix, of order 3 x 3.

If $$\dot{\underline{x}} = A\underline{x} + Bu \tag{6.16}$$

then $$\dot{\underline{x}} = T\dot{\underline{z}} = AT\underline{z} + Bu \tag{6.17}$$

hence $$\dot{\underline{z}} = T^{-1}AT\underline{z} + T^{-1}Bu \tag{6.18}$$

or $$\dot{\underline{z}} = E\underline{z} + Fu \tag{6.19}$$

To ensure that T was non-singular it was taken to be diagonal, i.e.

$$T = \text{diag}(t_1, t_2, t_3) \tag{6.20}$$

Hence $$T^{-1} = \text{diag}(t_1^{-1}, t_2^{-1}, t_3^{-1}) \tag{6.21}$$

If

$$A = \begin{bmatrix} a_{11} & a_{12} & a_{13} \\ a_{21} & a_{22} & a_{23} \\ a_{31} & a_{32} & a_{33} \end{bmatrix} \tag{6.22}$$

$$B' = \begin{bmatrix} 0 & 0 & b_{31} \end{bmatrix} \tag{6.23}$$

then

$$E = \begin{bmatrix} a_{11} & \frac{a_{12}t_2}{t_1} & \frac{a_{13}t_3}{t_1} \\ \frac{a_{21}t_1}{t_2} & a_{22} & \frac{a_{23}t_3}{t_2} \\ \frac{a_{31}t_1}{t_3} & \frac{a_{32}t_2}{t_3} & a_{33} \end{bmatrix} \tag{6.24}$$

$$F = \begin{bmatrix} 0 & 0 & \frac{b_{31}}{t_3} \end{bmatrix} \tag{6.25}$$

For this research, from equation (2.83),

$$A = \begin{bmatrix} -1 & 400 & 0 \\ 0 & 0 & 1 \\ 0 & -130 & -16 \end{bmatrix} \tag{6.26}$$

Obviously $a_{13} = a_{21} = a_{22} = a_{31} = 0$ (6.27)

hence $e_{13} = e_{21} = e_{22} = e_{31} = 0$ (6.28)

$$E = \begin{bmatrix} -1 & \frac{a_{12}t_2}{t_1} & 0 \\ 0 & 0 & \frac{a_{23}t_3}{t_2} \\ 0 & \frac{a_{32}t_2}{t_3} & -16 \end{bmatrix} \tag{6.29}$$

For good conditioning, it was decided that :

$$\frac{400t_2}{t_1} \leq 20 \tag{6.30}$$

$$\frac{t_3}{t_2} \leq 20 \tag{6.31}$$

$$\frac{130t_2}{t_3} \leq 10 \tag{6.32}$$

$$\frac{b_{31}}{t_3} \leq 5.0 \tag{6.33}$$

The choice of $t_3 = 10.0$ (6.34)

yielded $\frac{b_{31}}{t_3} = 4.33$ (6.35)

and $\frac{t_3}{t_2} = 13$ (6.36)

$$t_1 = \frac{400}{13} \tag{6.37}$$

and $\frac{a_{12}t_2}{t_1} = 10.0$ (6.38)

Thus $$T = \text{diag}\{37.69237, 0.769237, 10.0\} \quad (6.39)$$

$$T^{-1} = \text{diag}\{0.0265306, 1.29999, 0.1\} \quad (6.40)$$

$$E = \begin{bmatrix} -1 & 10 & 0 \\ 0 & 0 & 13 \\ 0 & -10 & -16 \end{bmatrix} \quad (6.41)$$

$$F = \begin{bmatrix} 0 & 0 & 4.33 \end{bmatrix}' \quad (6.42)$$

The optimal control law was determined in terms of the original state vector and was given by :

$$u^o = \hat{D}\underline{z} = \hat{D}T^{-1}\underline{x} \quad (6.43)$$

6.3.3 Integration of Transformed Riccati Equation

To obtain an accurate evaluation of the optimal control law the equation (6.9), with substitution of (6.41) for A, and (6.42) for B, was integrated using a specially written program, BEARDM40 (see Appendix A.3) which used the Hamming algorithm. BEARDM40 was described in section 6 of chapter 5. Only the sub-routine which generated the Riccati equation had to be altered from the program description of the earlier chapter. It ought to be remembered, when comparing the performance of the various programs, that the first three steps of the Hamming routine were generated in BEARDM40 by a fixed step, 4th order Runge-Kutta routine.

6.3.4 Dynamic Programming

Since the problem to be solved was a Linear Quadratic Problem (the L.Q.P. of MAYNE (1970)) a closed form solution could be obtained by the method of dynamic programming. From the algorithm of NICHOLSON (1964), outlined briefly in Appendix A.5.2, it was evident that the recursion formula

involved only speedy algebraic operations once the transition matrix, Φ, and the driving matrix, Δ, had been determined. A program, BEARDM15, (see Appendix A.3) was written and results therefrom are presented in table 6.1.

6.3.5 Solution of the Steady-State Matrix Equation

(a) The iterative method proposed by KLEINMAN (1968) was used to solve the steady-state matrix Riccati equation :

$$A'K + KA + Q = KB\, g^{-1} B'K \qquad (6.44)$$

This algorithm required a procedure for obtaining a solution, say P, to the Lyapunov matrix equation :

$$A'P + PA = -Q \qquad (6.45)$$

where A and Q are given. A special program based on the work of DAVISON and MAN (1968) was written to solve (6.45). This was incorporated then as a sub-routine in BEARDM33 (see Appendix A.3) the program written using the Kleinman algorithm. The program required* that a starting guess for the matrix, D, had to ensure that the coefficient matrix of the closed-loop system, (A + BD) was a stability matrix i.e.

$$\mathrm{Re}(\lambda_i) < 0 \qquad (6.46)$$

where the λ_i were the eigenvalues associated with (A + BD). If a poor choice of D was made the program failed to converge. Comparative results obtained from this program are quoted in table 6.1. The initial starting guess was chosed to be a null matrix since it had been determined earlier that the eigenvalues of the matrix A (hence E) were all negative or had negative real parts.

---

*A later note by Kleinman (1970) provided a modification to remove the need to guess at a starting value of matrix D.

(b) Eigenvector Solution

From (6.4) it was easily shown that

$$u^o = -g^{-1}B'\underline{\psi}^o \tag{6.47}$$

hence (6.5) could be re-expressed as :

$$\dot{\underline{x}} = A\underline{x}^o - B\,g^{-1}B'\underline{\psi}^o \tag{6.48}$$

Combining (6.48) and (6.6) yielded :

$$\begin{bmatrix} \dot{\underline{x}}^o \\ \dot{\underline{\psi}}^o \end{bmatrix} = \begin{bmatrix} A & -Bg^{-1}B' \\ Q & -A' \end{bmatrix} \begin{bmatrix} \underline{x}^o \\ \underline{\psi}^o \end{bmatrix} \tag{6.49}$$

An eigenvector solution of (6.49) was available. MARSHALL and NICHOLSON (1970) showed that the optimal control law derived from such an eigenanalysis was :

$$u^o = -g^{-1}B'U_{21}U_{11}^{-1}\underline{x} \tag{6.50}$$

U_{11} and U_{21} represented sub-matrices of the model matrix, U, the columns of which were formed from the eigenvectors of the coefficient matrix, M, of the canonical system, viz.

$$M = \begin{bmatrix} A & -Bg^{-1}B' \\ Q & -A' \end{bmatrix} \tag{6.51}$$

To produce the solution (6.50) required :

(i) the determination of the 3 eigenvectors associated with the 3 eigenvalues (of the associated system matrix, M) which had negative real parts.*

(ii) the inversion of the matrix, U_{11}, which was complex.

A numerical procedure which provided the eigenvalues and eigenvectors of any real matrix, up to order 20 x 20, was available at R.A.F. Cranwell. This procedure, EIGEN, was

---

*This choice follows from the knowledge that the optimal system should be stable.

written in Fortran IV, a computing language used irregularly at Cranwell. Consequently both the eigenvalues and eigenvectors were evaluated separately before being used as input data for BEARDM36 (see Appendix A.3) the program written to produce the optimal control law. Within the program there is contained a procedure* for the inversion of complex matrices, based on the method proposed by LANCZOS (1957), viz :

letting Z be a complex matrix of order n x n it was denoted also by

$$Z = R + jS \tag{6.52}$$

which allowed Z to be represented by an equivalent matrix, X, of order 2n x 2n, where X was defined as :

$$X = \begin{bmatrix} R & -S \\ S & R \end{bmatrix} \tag{6.53}$$

The inversion of the real matrix X provided

$$X^{-1} = \begin{bmatrix} N & P \\ -P & N \end{bmatrix} \tag{6.54}$$

thence

$$Z^{-1} = N - jP \tag{6.55}$$

(6.53) and (6.54) were the basis of the algorithm upon which the routine was established. Because only algebraic operations were involved the method was intended to be fast and accurate.

---

*The program as written is limited to problems in which the state dimension does not exceed ten, because the real matrix inversion routine used was limited to matrices of order, 20 x 20. The restriction does not affect the work of this research but, because the program was written for general use, the restriction must be remembered. If larger systems are to be dealt with in some other application, another procedure for the inversion of complex matrices should be written based on the algorithm proposed by CROSSLEY and PORTER (1971) for example.

6.3.6 Comparison of Methods

The weighting matrix used for comparison was

$$Q = \text{diag}\{9.156, 1, 1\}$$

and the weighting factor, g, was chosen to be

$$g = 1.0$$

The results obtained by each of the methods outlined in this section are quoted below in table 6.1.

	ATHFALB[1]	HAMMING[1]	DYN.PROG	KLEINMAN	MARNICH
$\hat{d}_1$	-2.6964178	-2.69641778	-2.365828	-2.8487640	-2.6963468
$\hat{d}_2$	-3.3198137	-3.31981373	-2.9983304	-3.506573	-3.3197205
$\hat{d}_3$	-2.1860360	-2.18603605	-2.029744	-2.334205	-2.185967
TIME	14m 38s[2]	7m 15s[2]	1m 28s[3]	0m 20s[4]	0m 15s[5]

Table 6.1 - Comparison of Methods of Obtaining Optimal Control Laws

NOTES : (1) Both procedures "blew-up" with a choice for step-length of 0.1 second. Quoted results were obtained for a 0.01 second step-length.

(2) The interval of time over which the equation was integrated was 5.0 seconds. From the printout it was evident that K_{ss}^* had been obtained by 1.25 seconds. Thus these figures could be reduced by approximately 0.75 i.e. for ATHFALB a time of 4 minutes (approx.) and for HAMMING a time of 1m 45s would be representative. However the value of any reasonable approximation to infinite time is not known a priori.

*K_{ss} means the steady-state value of the Riccati matrix.

(3) The accuracy of the method could be improved by the inclusion in the matrix Φ, and hence Δ, of further terms in the exponential series expansion used to evaluate this transition matrix. The increase in computing time would be insubstantial.

(4) The accuracy of KLEINMAN could be improved further by a reduction of the value of the stopping condition in the routine for solving the Lyapunov matrix equation (6.45). There would then be an increase of computing time : approximately double for each order reduction.

(5) This figure was approximate; 7 seconds were needed to evaluate the eigenvectors with EIGEN. 8 seconds were required by BEARDM36.

For speed and accuracy the method proposed by Marshall and Nicholson* should be used. However, because the eigenvectors had to be processed separately at R.A.F. Cranwell and then had to be used as input to the main program this method was used only infrequently in the research. The eigenanalysis program could be run only when the computing laboratory used the FORTRAN compiler. The major portion of the computing work at Cranwell was carried out in ALGOL and therefore the day-to-day delays in processing such dual-language programs were such that the bulk of the computation for the optimal regulator was carried out using BEARDM33, which was the next

---

*The technique had been developed implicitly, before Marshall and Nicholson, by MacFarlane (1963). Independently, in the U.S.A., POTTER (1966) proposed a similar method.

most efficient method (KLEINMAN). Later algorithms proposed by FATH (1969) and MAKI (1972) for use with single-input systems were also studied but, although both were found to be effective, their use did not provide any real improvement upon the choice of methods already indicated. Indeed the method proposed by Fath was just a slight extension of the method used in BEARDM36.

6.4 Fixed Structure Optimal Feedback Controller

From section 2 of this chapter the optimal control law had the form :

$$u^o = D\underline{x} \qquad (6.56)$$

A technique, proposed by PURI (1966), of determining a set of fixed feedback gains was investigated such that the set of evaluated gains would provide D without the need to solve the matrix Riccati equation.

The model of the engine system could be transformed into the required phase-variable form either by using the transformation proposed by WONHAM and JOHNSON (1964), or by representing the system in block diagram form and deriving from the diagram the overall transfer function which can be manipulated into phase-variable form easily. With the system description in the phase-variable form the derived feedback gains operated upon the system output and its derivatives. The requirement to produce for the feedback control law the acceleration of the output shaft would result in some severe practical difficulties. To avoid these a post transformation from phase to state variables* was employed to obtain the results in state

---

*It is known, from KALMAN (1963), that the state variables ought to be regarded as abstract variables. In this research the particular choice of variables was coloured by the knowledge that the variables were easy to measure and to transduce.

feedback form. The block diagram of the system was represented in figure 6.1

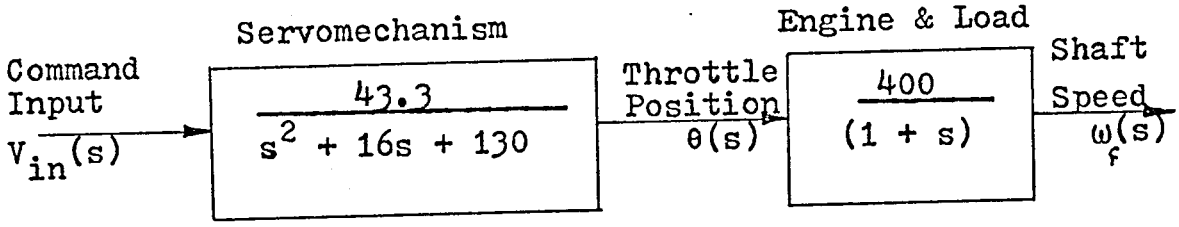

Figure 6.1 - Block Diagram of System

It was simple to obtain from figure 6.1, by the rules of block diagram algebra (d'AZZO and HOUPIS 1966), the overall transfer function :

$$\frac{\omega_f(s)}{V_{in}(s)} = \frac{17320}{s^3 + 17s^2 + 146s + 130} \qquad (6.57)$$

Letting

$$\omega_f = y_1 \qquad (6.58)$$

$$\dot{\omega}_f = \dot{y}_1 = y_2 \qquad (6.59)$$

$$\ddot{\omega}_f = \dot{y}_2 = y_3 \qquad (6.60)$$

then

$$\begin{bmatrix} \dot{y}_1 \\ \dot{y}_2 \\ \dot{y}_3 \end{bmatrix} = \begin{bmatrix} 0 & 1 & 0 \\ 0 & 0 & 1 \\ -130 & -146 & -17 \end{bmatrix} \begin{bmatrix} y_1 \\ y_2 \\ y_3 \end{bmatrix} + \begin{bmatrix} 0 \\ 0 \\ 1 \end{bmatrix} \hat{u} \qquad (6.61)$$

i.e $$\dot{\underline{y}} = C\underline{y} + B_o\hat{u} \qquad (6.62)$$

where C was the companion matrix of (6.61) and the matrix B_o was represented by

$$B_o = \begin{bmatrix} 0 & 0 & 1 \end{bmatrix} , \qquad (6.63)$$

N.B. $$\hat{u} = 17320\, V_{in} \qquad (6.64)$$

The performance index to be minimised was chosen to be

$$J = 0.5\int_{o}^{\infty} \{ \underline{y}'\hat{Q}\underline{y} + g\hat{u}^2 \} \, dt \qquad (6.65)$$

By using the method of the calculus of variations with undetermined Lagrange multipliers, the performance index (6.65) was augmented viz :

$$J = 0.5 \int_{o}^{\infty} \{ \underline{y}'\hat{Q}\underline{y} + g\hat{u}^2 + 2\sum_{j=1}^{3}\lambda_j(t) f_j(\underline{y},\hat{u},t) \} \, dt \qquad (6.66)$$

where $\lambda_j(t)$ were the Lagrange multipliers. The index J was minimised subject to the constraint

$$\underline{f}(\underline{y},\hat{u},t) = 0 \qquad (6.67)$$

The variational equations required for the solution were defined in terms of the integrand of (6.66) viz :

$$F = \tfrac{1}{2}\{\underline{y}'\hat{Q}y + g\hat{u}^2\} + \lambda_1 f_1 + \lambda_2 f_2 + \lambda_3 f_3 \qquad (6.68)$$

They were given by the Euler-Lagrange equations :

$$\left.\begin{aligned} \frac{\partial F}{\partial y_i} &= \frac{d}{dt}\left[\frac{\partial F}{\partial \dot{y}_i}\right] \quad i = 1,2,3 \\ \frac{\partial F}{\partial \lambda_j} &= \frac{d}{dt}\left[\frac{\partial F}{\partial \dot{\lambda}_j}\right] \quad j = 1,2,3 \\ \frac{\partial F}{\partial u} &= \frac{d}{dt}\left[\frac{\partial F}{\partial \dot{u}}\right] \end{aligned}\right\} \qquad (6.69)$$

The complete augmented set of equations for the variational system was obtained from (6.62) and (6.69) : it was

$$\begin{bmatrix} \dot{\underline{y}} \\ \dot{\underline{\lambda}} \end{bmatrix} = \Theta \begin{bmatrix} \underline{y} \\ \underline{\lambda} \end{bmatrix} \qquad (6.70)^*$$

where Θ was a coefficient matrix, of order 6 x 6, and its characteristic determinant was given by :

$$\Delta(s) = \left| sI - \Theta \right| \qquad (6.71)$$

---

*(6.70) is not given in detail - an alternative, simpler equation to evaluate the optimal control law is developed. The derivation of 6.70 is given in Appendix A.5.4.

If $\triangle_1(s)$ was defined as a polynomial with all its roots in L.H. of s-plane then

$$\triangle(s) = \triangle_1(s)\triangle_1(-s) \tag{6.72}$$

and if u was determined correctly $\triangle_1(s)$ would be the characteristic determinant of the optimised closed-loop system.

The system represented in figure 6.1 was represented by a transfer function

$$G_1(s) = \frac{N_1(s)}{D_1(s)} \tag{6.73}$$

The optimal feedback controller was chosen a priori to be a dynamic controller operating only upon the system output, i.e. the optimal feedback controller was chosen to be :

$$G_2(s) = \frac{N_2(s)}{D_2(s)} = \sum_{i=1}^{m} k_i s^{(i-1)} \tag{6.74}$$

where k_i represented the controller gains which had to be chosen for specific q_{ii} and g such that (6.65) was minimised. From (6.73) and (6.74) the characteristic function of the optimised closed-loop system was :

$$\triangle_1(s) = D_1(s)D_2(s) + N_1(s)N_2(s) \tag{6.75}$$

However Puri had shown that

$$\triangle(s) = \triangle_1(s)\triangle_1(-s) = D_1(s)D_1(-s)g + N_1(s)N_1(-s)x \; (-1)^{(i-1)} q_i s^{2(i-1)} \tag{6.76}$$

For this engine system it was supposed that

$$\triangle_1(s) = s^3 + a_2 s^2 + a_1 s + a_o \tag{6.77}$$

It was derived then from (6.76), (6.57), that

$$\triangle(s) = (-s^6 - 3s^4 - 16896s^2 + 16900)g + (q_1 - q_2 s^2 + q_3 s^4) = 0 \qquad (6.78)$$

Further when it was taken that

$$g = 1, \qquad q_{11} = 100, \quad q_{22} = 10, \quad q_{33} = 10 \qquad (6.79)$$

then

$$\triangle(s) = -s^6 + 7s^4 - 16906s^2 + 17000 = 0 \qquad (6.80)$$

However, from (6.76) and (6.77)

$$\triangle(s) = -s^6 + (a_2^2 - 2a_1)s^4 - (a_1^2 - 2a_o a_2)s^2 + a_o^2 \qquad (6.81)$$

Comparison of the coefficients of (6.80) and (6.81) yielded :

$$a_2^2 - 2a_1 = 7$$

$$a_1^2 - 2a_o a_2 = 16906 \qquad (6.82)$$

$$a_o^2 = 17000$$

Hence,

$$a_o = 130.4 \qquad (6.83)$$

and

$$a_2^4 - 14a_2^2 + 1043.2a_2 - 67575 = 0 \qquad (6.84)$$

Use of Bairstow's procedure to evaluate the zeros of the polynomial (BECKETT and HUNT 1967) showed that the largest positive root of (6.84) was 17.3124 which was the value taken for a_2. Therefore

$$a_1 = 146.355 \qquad (6.85)$$

The closed-loop system was represented as :

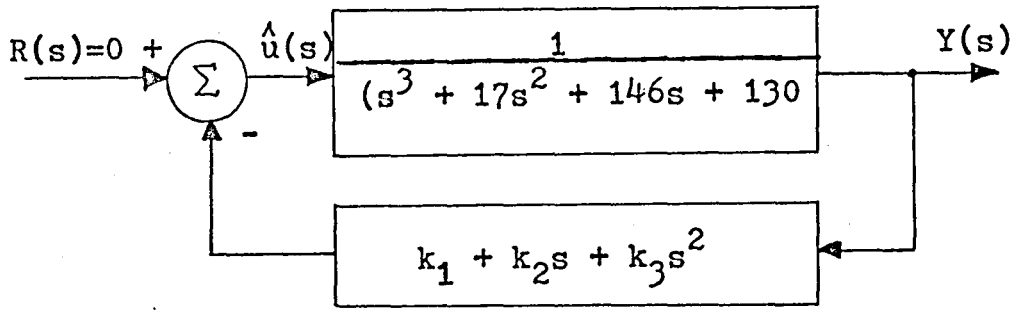

Figure 6.2 - Block Diagram of Closed Loop System

For this system the characteristic equation was found to be :

$$s^3 + (17 + k_3)s^2 + (146 + k_2)s + (130 + k_1) = 0 \quad (6.86)$$

Thus, (cf,(6.81))

$$a_2 = 17 + k_3 = 17.3124$$

hence $k_3 = 0.3124$ (6.87)

Also $a_1 = 146 + k_2 = 146.355$

and $k_2 = 0.355$ (6.88)

Finally $a_o = 130 + k_1 = 130.4$

yielded $k_1 = 0.4$ (6.89)

Therefore, $u^o = -\left[0.4 \quad 0.355 \quad 0.3124\right] \underline{y}$ (6.90)

Some convenient transformation from phase to state variables was required to provide a state feedback law. It was decided to let

$$\underline{x} = T\underline{y} \quad (6.91)$$

where $\underline{x}$ was the state vector, of dimension 3

$\underline{y}$ was the phase vector, of dimension 3

and T was a non-singular transformation matrix, of order 3 x 3. From GREENSITE (1970) the transformation matrix was defined as :

$$T = RS \quad (6.92)$$

where $R = \left[B \vdots AB \vdots A^2B\right]$ * (6.93)

and where A and B were the matrices in (6.1), the characteristic equation associated with which was :

---

*This transformation method works for A and B matrices of orders, [n x n] and [n x m] respectively.

$$\det\left[\lambda I - A\right] = \lambda^3 - \sum_{i=1}^{3} w_i \lambda^{i-1} = 0 \qquad (6.94)$$

The matrix S was formed from (6.94) thus :-

$$S = \begin{bmatrix} -w_2 & -w_3 & 1 \\ -w_3 & 1 & 0 \\ 1 & 0 & 0 \end{bmatrix} \qquad (6.95)$$

For the engine system being considered :

$$R = \begin{bmatrix} 0 & 0 & 17320.0 \\ 0 & 43.3 & -692.8 \\ 43.3 & -692.8 & 5455.8 \end{bmatrix} \qquad (6.96)$$

It was established earlier in this chapter that the system characteristic equation was given by :

$$s^3 + 17s^2 + 146s + 130 = 0 \qquad (6.97)$$

therefore

$$\begin{aligned} w_1 &= -130 \\ w_2 &= -146 \\ w_3 &= -17 \end{aligned} \qquad (6.98)$$

Thus

$$S = \begin{bmatrix} 146 & 17 & 1 \\ 17 & 1 & 0 \\ 1 & 0 & 0 \end{bmatrix} \qquad (6.99)$$

$$\text{and } T = RS = \begin{bmatrix} 17320 & 0 & 0 \\ 43.3 & 43.3 & 0 \\ 0 & 43.3 & 43.3 \end{bmatrix} \qquad (6.100)$$

Therefore

$$\underline{y} = T^{-1}\underline{x} \qquad (6.101)$$

where
$$T^{-1} = \frac{1}{17320}\begin{bmatrix} 1 & 0 & 0 \\ -1 & 400 & 0 \\ 1 & -400 & 400 \end{bmatrix} \qquad (6.102)$$

The validity of the calculated matrix, T, was confirmed by checking that

$$B_o = T^{-1}B \qquad (6.103)$$

and that
$$C = T^{-1}AT \qquad (6.104)$$

From the relationship
$$u = V_{in} = 17320\,\hat{u} = -K\hat{T}^{-1}\underline{x} \qquad (6.105)$$

where
$$\hat{T}^{-1} = \begin{bmatrix} 1 & 0 & 0 \\ -1 & 400 & 0 \\ 1 & -400 & 400 \end{bmatrix} \qquad (6.106)$$

From (6.90) and (6.106)
$$u = -\begin{bmatrix} 0.3574 & 17.04 & 124.96 \end{bmatrix}\underline{x} \qquad (6.107)$$

It will be noted, from comparison with the results presented in section 6 of this chapter, that the gain operating upon the rate of change of throttle position is very much greater in (6.107) than in any other result. This stemmed from the choice of weighting matrix (6.79). To compare the optimal control law found by this method with that found by any other method requires that the same performance index should be minimised. For the Puri algorithm the phase variables were weighted : if a comparison with state variables is required the weighting matrix should be modified so that the performance index would become

$$J = 0.5\int_0^\infty \left\{\underline{x}'(T^{-1})'\hat{Q}(T^{-1})\underline{x} + g\hat{u}^2\right\} dt$$
$$= 0.5\int_0^\infty \left\{\underline{x}'Q\underline{x} + g\hat{u}^2\right\} dt \qquad (6.108)$$

in which
$$Q = (T^{-1})'\hat{Q}(T^{-1}) \qquad (6.109)$$

In this case

$$Q = \frac{1}{(17320)^2}\begin{bmatrix} 210 & -8000 & 4000 \\ -8000 & 32\times10^5 & -16\times10^5 \\ 4000 & -16\times10^5 & 16\times10^5 \end{bmatrix} \quad (6.110)^*$$

Use of this matrix and g set at unity in BEARDM33 produced the following control law

$$u^o = -\begin{bmatrix} 0.3469 & 16.924 & 125.104 \end{bmatrix}\underline{x} \quad (6.111)$$

The method therefore was equivalent to those presented already but it suffered from the disadvantage of requiring phase variable representation which meant that there was no immediate relationship with the state weighting matrix elements. Another disadvantageous fact was the need to evaluate numerically the coefficients (prior to the determination of the largest positive root) which was sometimes difficult, particularly so if approximations were made for analytical convenience for then the root value might be affected and consequently the values of the gain factors. It proved to be a useful method when computational facilities were not available. Because a range of optimal control laws were provided already from the earlier work of this chapter the method was not proceeded with but the work of transformation of phase to state variables was employed later in chapter 7.

---

*The off-diagonal terms in the Q matrix do not influence the resulting control law. A proof of this statement is to be found in KALMAN and ENGLAR (1966).

6.5 Some Computational Results

The results obtained for a range of choices for Q and g are shown in table 6.2.

Serial No.	Q	g	d_1	d_2	d_3
01	1,1,1,	1.0	-0.01874392	-1.4029931	-0.07935012
02	10,1,1,	1.0	-0.07932972	-4.6306788	-0.23642939
03	10,1,1	10.0	-0.01896485	-1.2137097	-0.06943526
04	1,1,0	10.0	-0.00376475	-0.26755704	-0.01636467
05	10,1,0	20.0	-0.0215821	-0.782717	-0.04697808
06	10,100,0	1.0	-0.06613816	-13.759723	-0.53168752
07	10,10,0	1.0	-0.07206332	-5.6007329	-0.26280872
08	10,1,0	100.0	-0.00378037	-0.24434472	-0.01496975

Table 6.2 - Optimal Control Gains

It was noted in the course of numerical experiments that there was a well-defined relationship between the value of the gains and the control weighting factor. The relationship is shown graphically in figure 6.3. The control gain was not transformed and only the gain corresponding to x_1 was plotted; same slope was obtained for other gains d_2 and d_3.

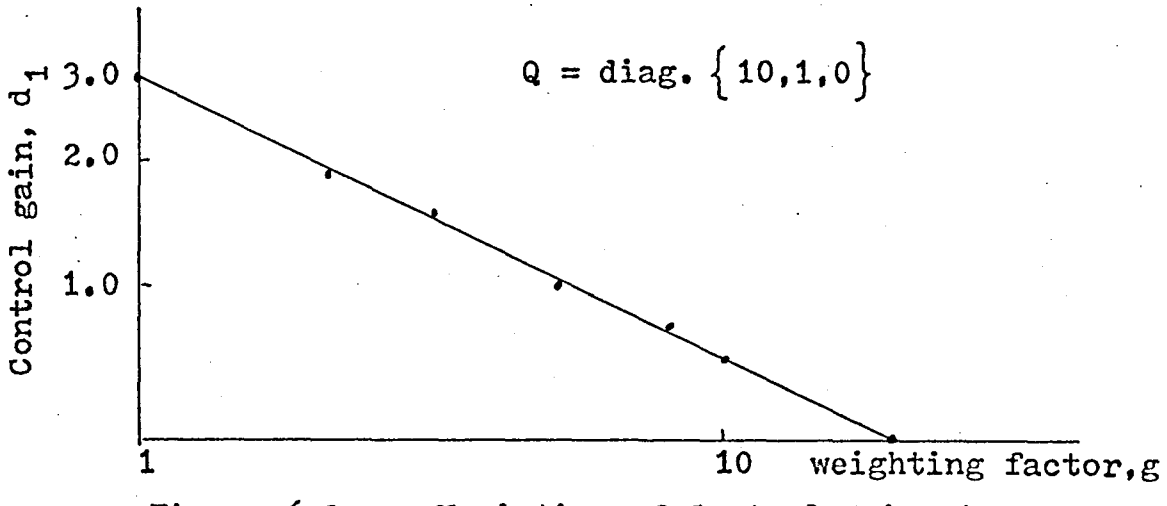

Figure 6.3 - Variation of Control Gain with g

Figure 6.3 was most useful for it reduced substantially the computational load; only two runs, for widely different values of g, for any diagonal Q matrix were required. A straight line graph could then be drawn on a log-log scale and the values of gain corresponding to intermediate values of weighting factor were available immediately without further computation. From these numerical studies it may be stated that increasing the elements of the Q matrix resulted in increased control gains and consequently reduced deviations from the equilibrium of the state variables. On the other hand an increase of g reduced the control used and hence the state deviations were larger. A compromise choice was necessary.

Although the disturbances in this regulation were statistical in nature no attempt was made to develop a stochastic controller. First, the disturbance was not stationary but was obviously periodic, by nature of the method of its generation; this was contrary to some of the assumptions necessary to design an optimal stochastic controller by using the Separation Theorem of LEE (1964), which permits the synthesis of the controller by cascading an optimal estimator with a deterministic optimum controller. Such a scheme requires that the estimator, which has its own dynamics, is synthesised as well as the controller. In the second place the noise due to the engine vibration, which was present on the transducer signals, was of prime importance, but was also periodic in nature. The filtration of such unwanted signals has been dealt with already in chapter 2. It was decided to be guided by the heuristic principle, enunciated by WONHAM and CASHMAN (1969), that an apparently crude approximation to the optimal

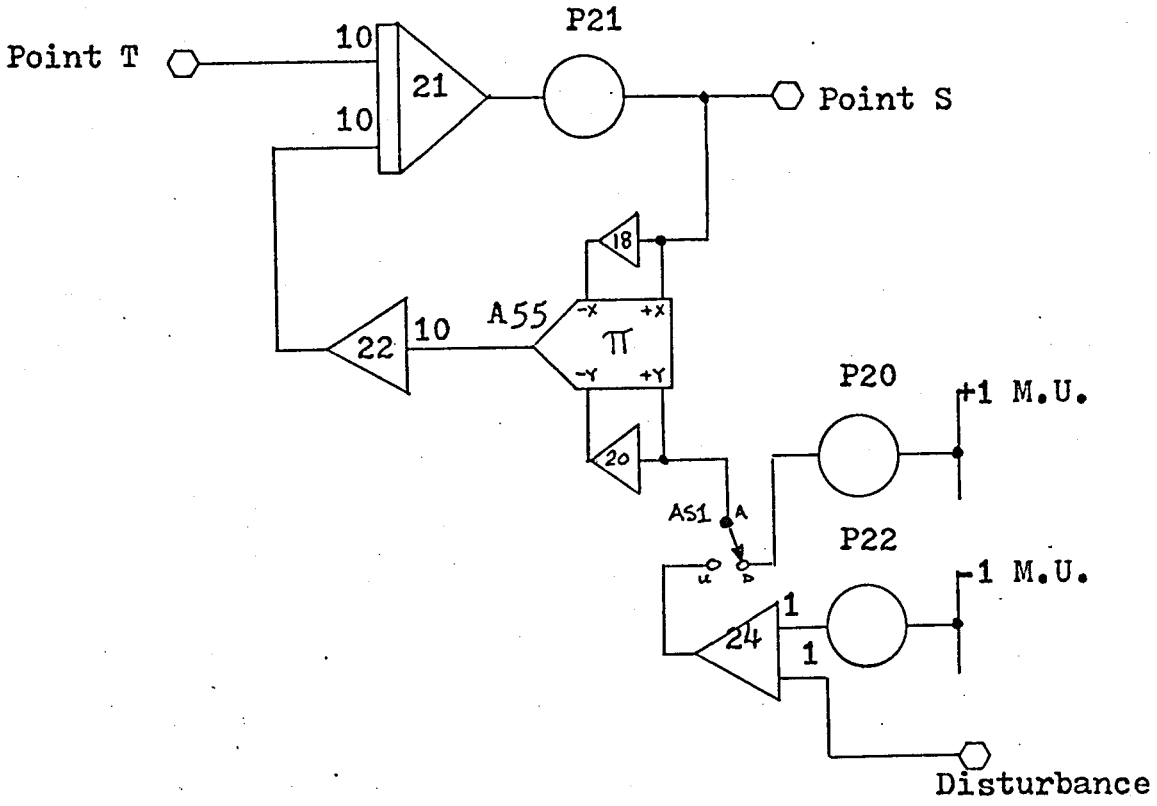

Figure 6.4 - Simulation Of Linear Model of Engine and Load System

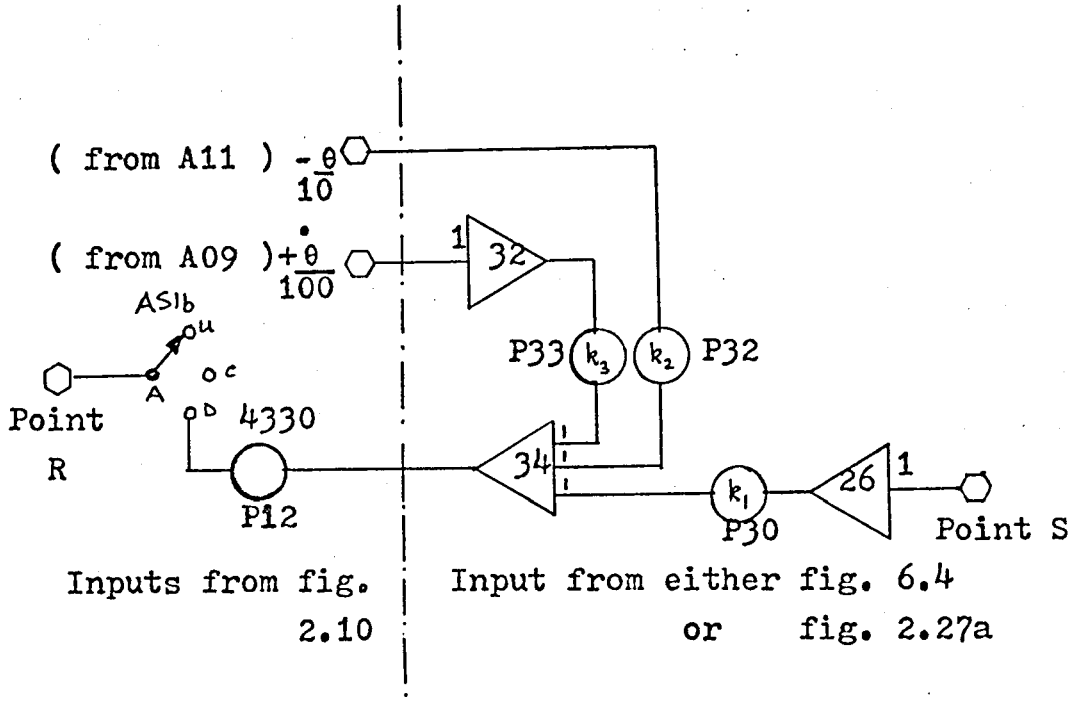

Figure 6.5 - Simulated Regulator Controller

stochastic control may, if properly chosen, yield near-optimal results. The effects of the load changes were regarded as causing changes in some of the parameters of the system and in the next chapter attention is given to obtaining some controller which would provide optimal control and would be minimally sensitive to such parameter changes.

6.6 Controller Synthesis and Experimental Results

To confirm experimentally the validity of the regulator gains listed in table 6.2 a study was undertaken first on the analogue computer. Figure 6.4 shows the diagram of the simulation of the linear model. Points T and S correspond to the input and output points indicated on figure 2.27a, the full engine, transmission, and load simulation. Point T was driven from the output of the simulation of the throttle servomechanism shown in figure 2.10. P20 and P22 were changed to alter fan setting. Figure 6.5 is a diagram of the simulated regulator with gains suitably adjusted to take into account the appropriate analogue scaling.

In figure 6.4 the point marked Disturbance was used to inject external load disturbances into the engine/load systems to test the effectiveness of the regulation property of the derived control law. A random signal generator was designed (see Appendix A.4) for use as a disturbance source and its signal was injected into the simulation at the point mentioned. All the control laws derived were found to be fully effective. The simulation of figure 6.4 was next replaced by the full simulation of figure 2.27a; the load disturbances were again injected into the terminal D at the input of A24. AS3 was switched to ensure that 4th gear was selected. The effects

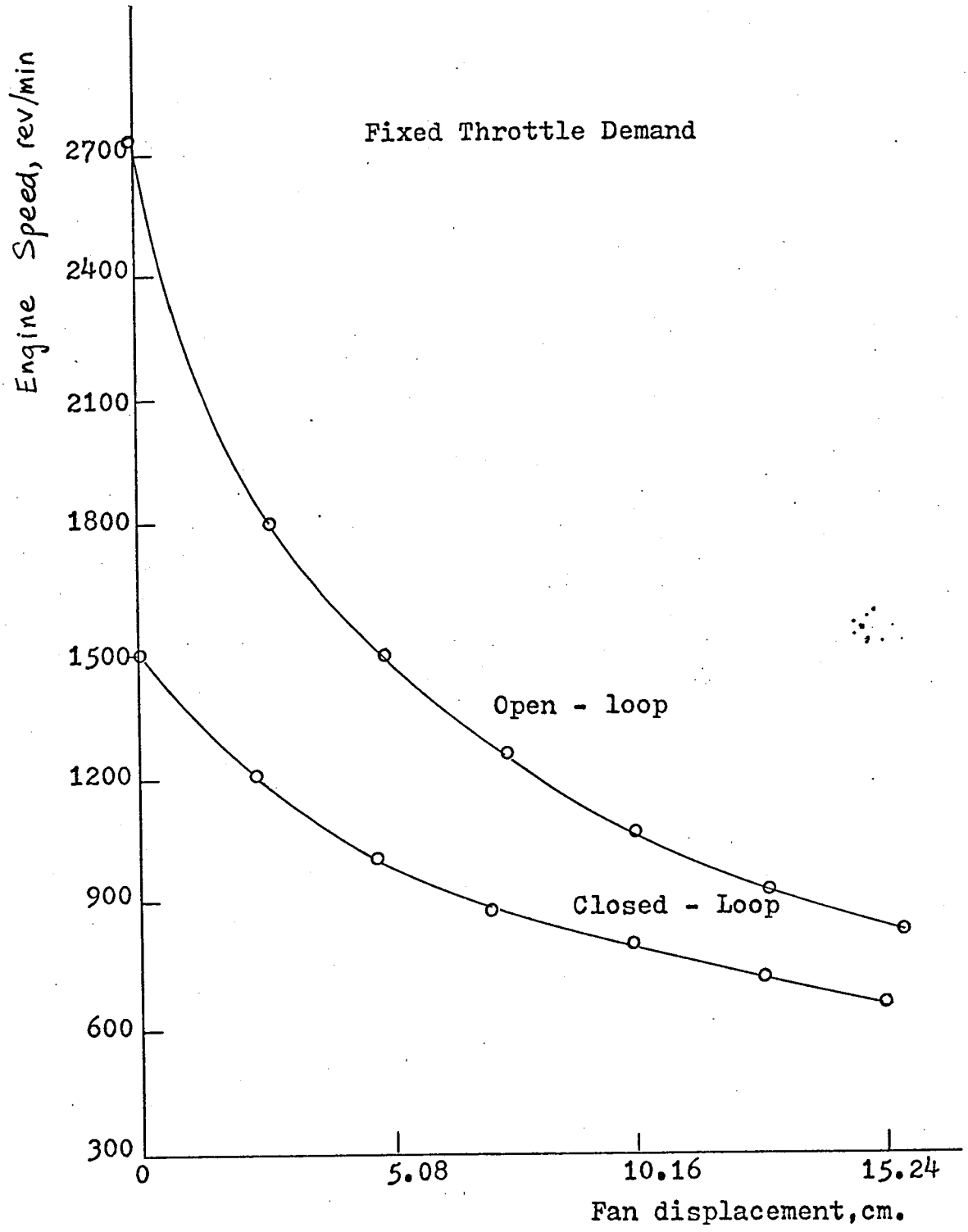

Figure 6.6 - Steady -state Regulation

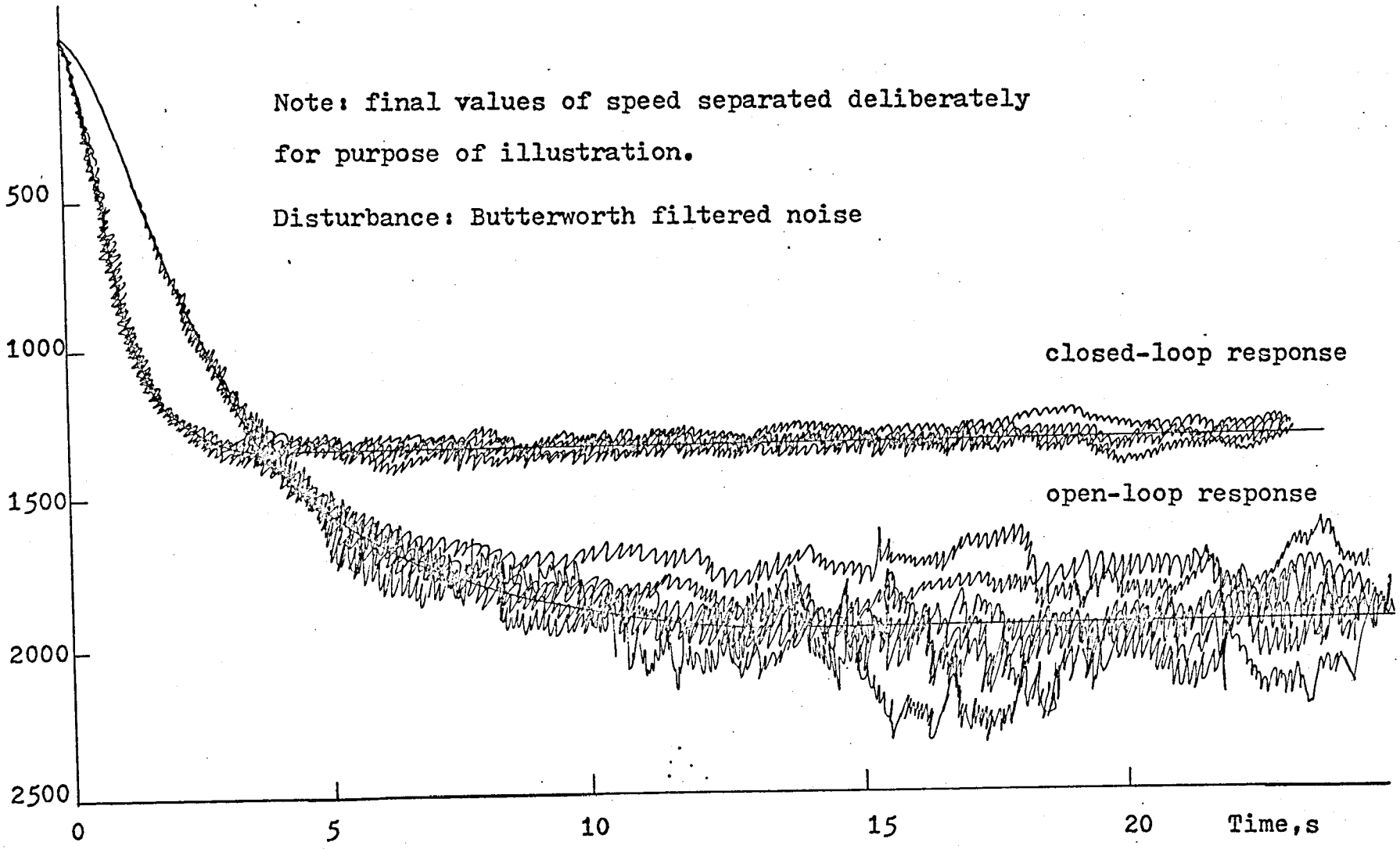

Figure 6.7 - Simulation Responses for L.Q.P. Regulator

upon the steady-state speed of the engine of changing the fan setting for open and closed-loop operation are shown in figure 6.6 which corresponds to case 03 of table 6.2. The resulting change of output speed due to a dynamometer setting change of 7.62 cm. (from 2.54 cm. to 10.16 cm.) in closed-loop operation was 300 rev/min compared to a change of 830 rev/min open-loop. The effectiveness of the controller was checked also for the situation where a random signal was injected into A24. The effectiveness of the regulation is evident from figure 6.7. From this evidence it was clear that the regulator scheme should be effective when applied to the experimental engine rig. A controller was synthesised using operational amplifiers (Burr-Brown model no. 3317/14); the schematic diagram is shown below in figure 6.8.

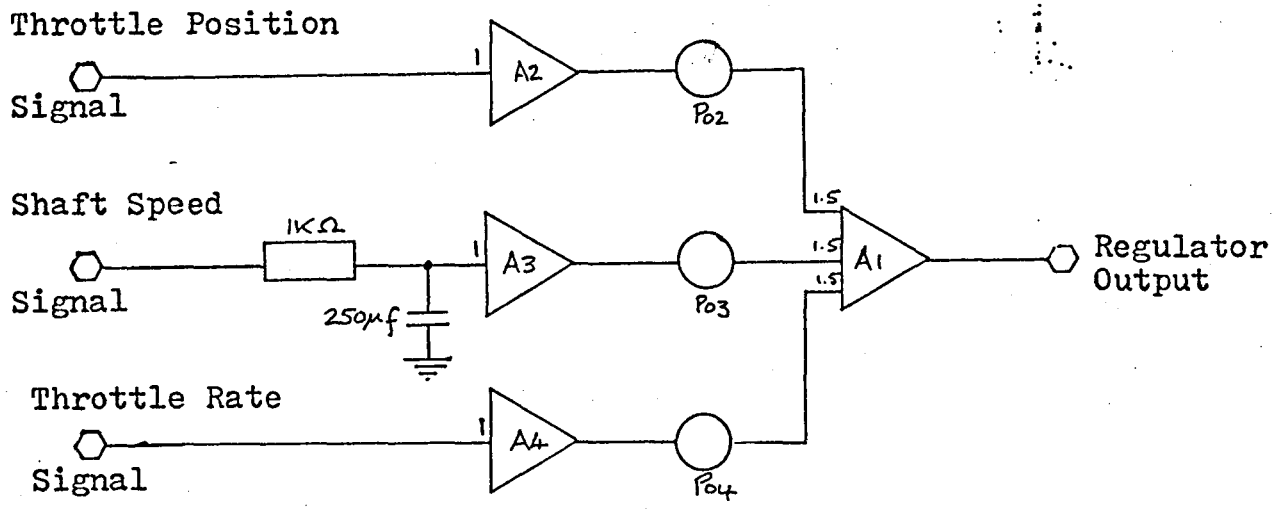

Figure 6.8 - Optimal Regulator Controller

The gains required scaling before application to the experimental rig because of the sensitivity of the tachogenerator and potentiometer transducer associated with the engine and servomechanism. The results of using the controller are

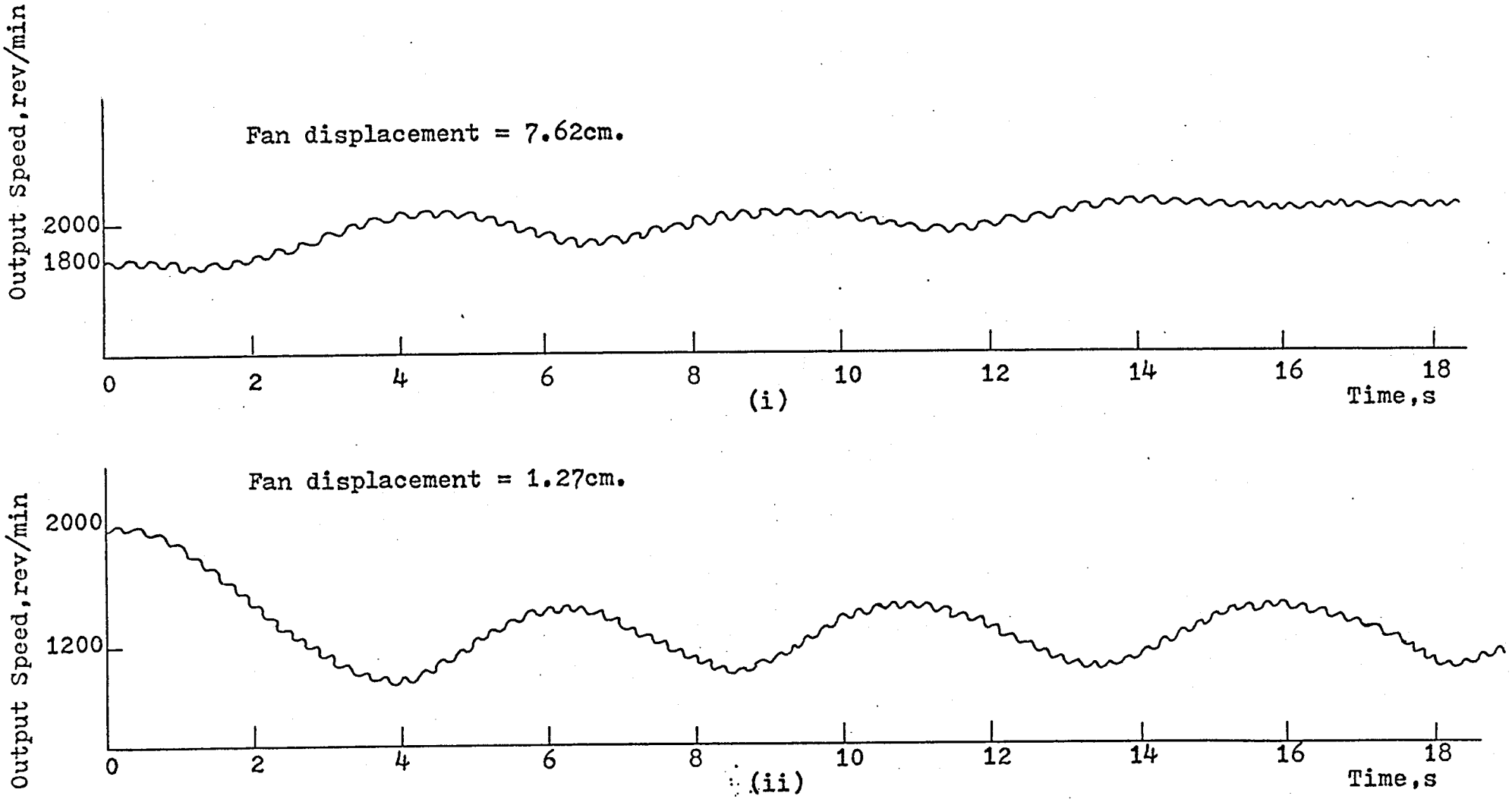

Figure 6.9a - Optimal Engine Regulation Responses

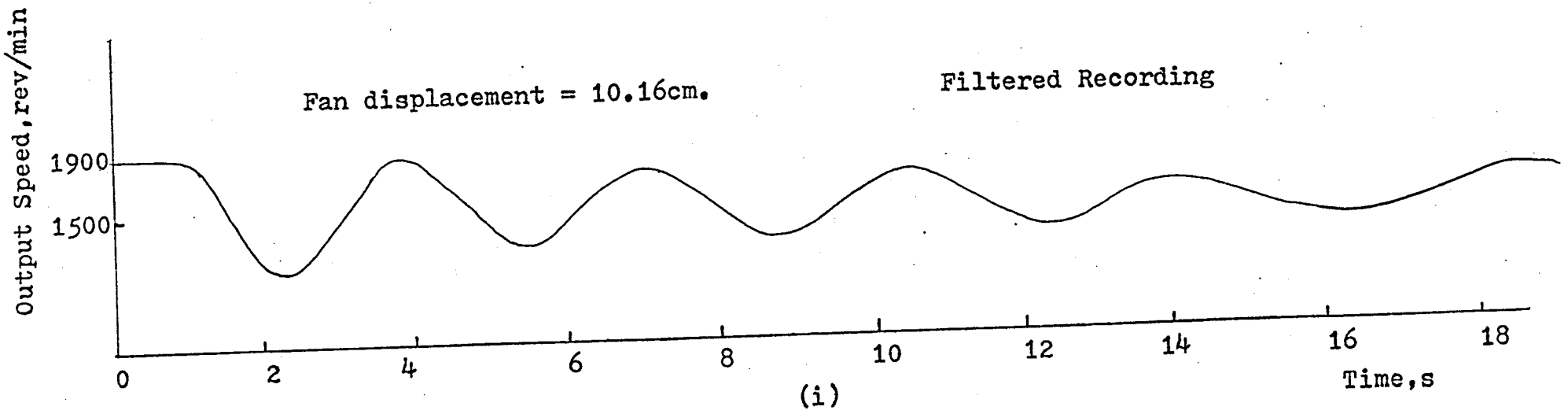

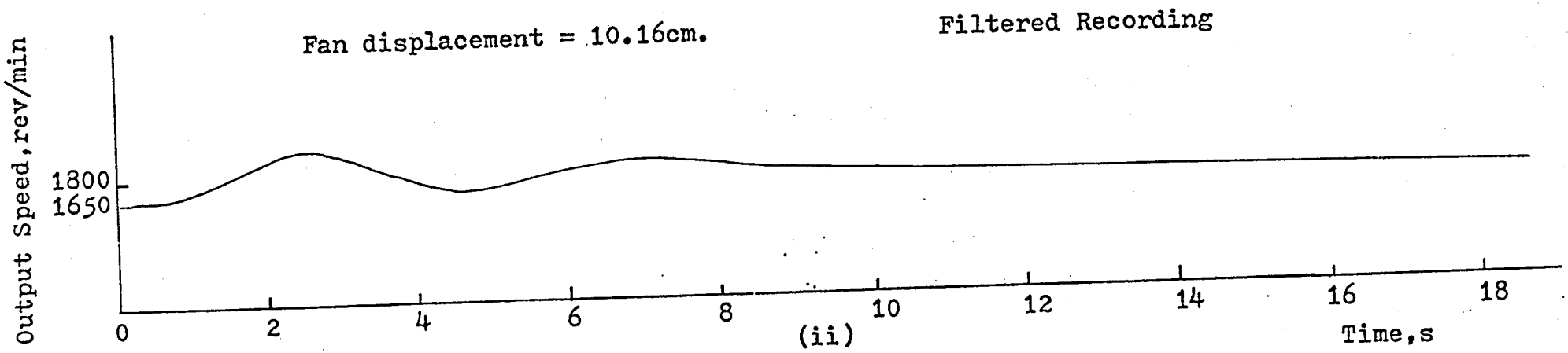

Figure 6.9b - Optimal Engine Regulation Responses

shown in figure 6.9 a and b. In figure 6.9b and subsequent figures the engine noise has been removed by filtration for ease of illustration. It was noted that use of control law no. 05 resulted in hunting (see figure 6.9a) when the dynamometer fan setting was changed from 7.62 cm. to 1.27 cm. (The fixed throttle demand signal was also reduced to ensure that the operating speed was also approximately the same). For the same control law (serial no. 03) and the same fan setting (d = 10.16 cm.) figure 6.9b illustrates an unexpected phenomenon associated with this experimental work : the response was less stable for "step-downs" in equilibrium speeds. Further experimental investigations merely confirmed this observation for all settings of the dynamometer. Figure 6.10 illustrates some typical results : control law (serial no. 04) was employed and different steady speeds were used. For responses a and b the demanded speed was stepped from 1750 to 1850 rev/min and from 1900 to 1600 rev/min respectively. For the upward step the response was stable and settled in 11 s. For the downwards step the response was much more oscillatory and settled in 14 s. In case a the period of the oscillation was 5 s.; in case b it was about 4 s. in the early part of the response and lengthened to 5 s. as the speed settled. Similar results were obtained for responses c and d. However for c the response had settled in 5 s. and for d the period of oscillation had been reduced to 3.5 s. There had been no evidence from the analogue computer studies to indicate the existence of such results. Although the effects of the filter in the shaft speed signal channel had not been considered in the early studies its inclusion in the simulation did not alter

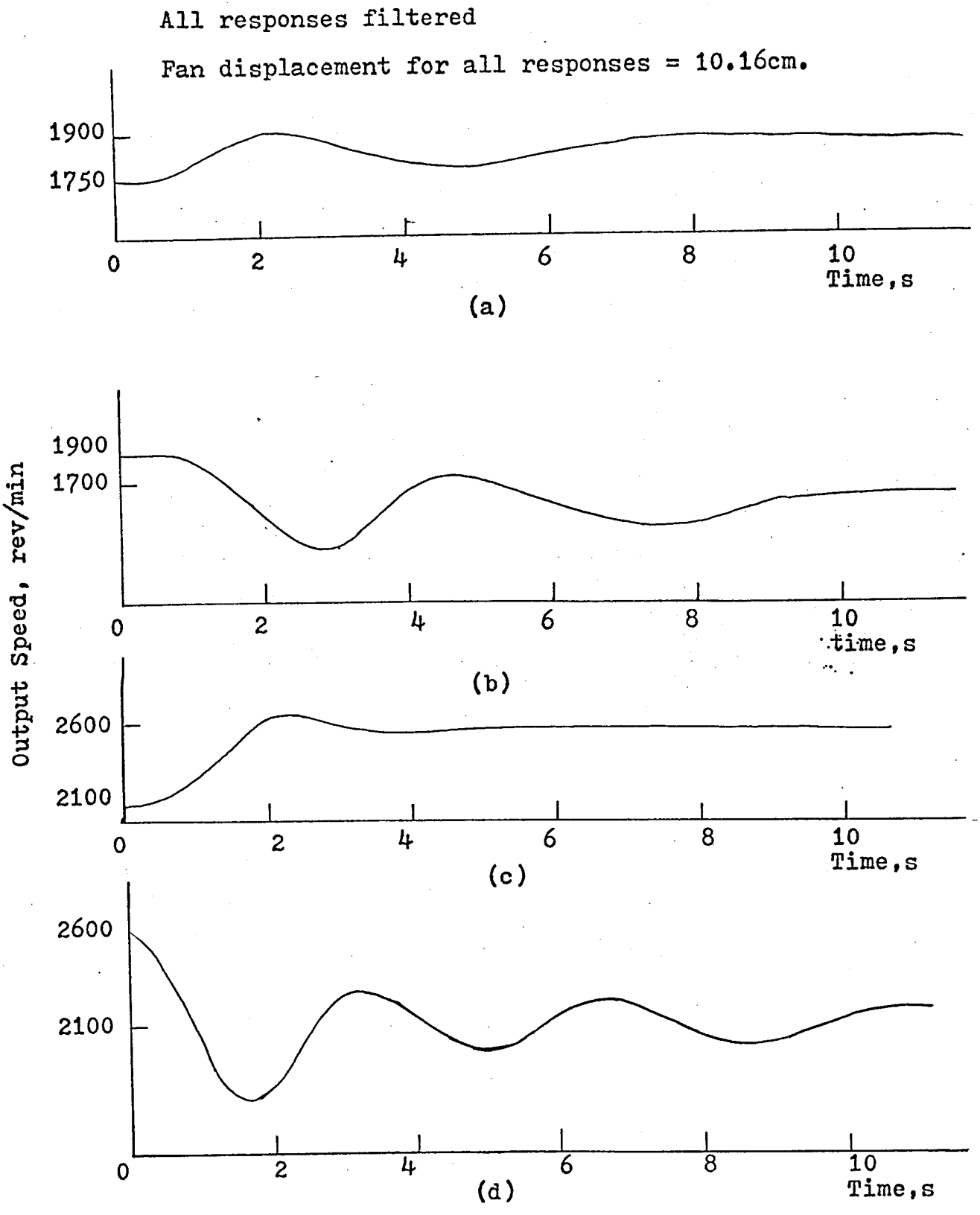

Figure 6.10 - Optimal Engine Regulation Responses

the computed results in any observable way. The different engine responses exhibited for higher or lower demanded steady speeds indicate that the phenomenon is non-linear in nature : there appeared to be a failure to satisfy the homogeneity property which characterises the linear system. A further series of tests, with the load being varied in response to the simulated road signal, generated as outlined in chapter 4, did not reveal such oscillatory response. With the throttle demand set for a speed of 2000 rev/min, with the fan set at 7.62 cm. and the simulated road at the centre of its height contour, the engine and load speeds were held relatively constant; a section of the response is shown in figure 6.11. No evidence of hunting was found. The earlier results must have resulted therefore from the changes of reference speed and from interaction between the internal loops of the engine/load system and those added by the addition of the controller to the rig. The failure to reproduce hunting of any kind from the simulation indicates that the models derived in chapter 2 require refinement.

It was not possible, with the fuel-measuring techniques being used, to obtain acceptable quantitative evidence of improved fuel-consumption. The fuel used over a complete run of the simulated road, using manual speed control, could not be measured accurately because the operator was necessarily occupied in monitoring engine speed and making the associated throttle adjustments and was unable to record visually the fuel consumed per unit time. To obtain a qualitative assessment of the performance a measured amount of fuel was placed in the fuel tank and the run was made with

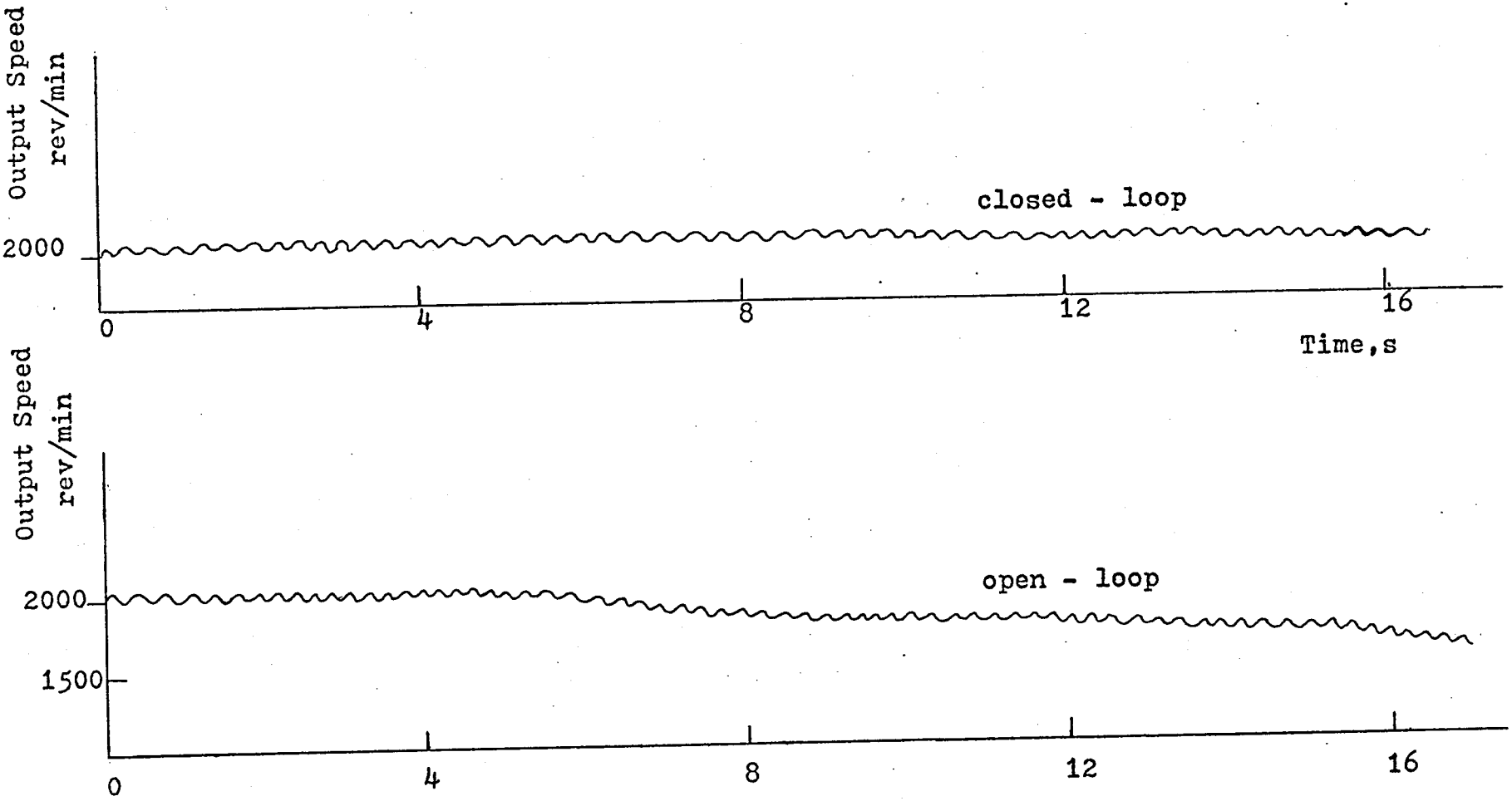

Figure 6.11 - Response to Simulated Road Signal

manual and with closed-loop control. In the event the closed-loop control run covered about 250 yards further along the simulated road. Actually the engine ceased to run about 250 yards before the end of the road for the manual case. The run had been completed in the closed-loop case before engine shut-down.

This qualitative result is not wholly conclusive however, because the performance index included a speed term in addition to the throttle term. It is conceivable that the speed may have been regulated better manually than automatically, but with greater throttle useage. Nevertheless it was evident that a reduced fuel expenditure was possible; less satisfactory speed regulation might be acceptable in many circumstances if fuel savings were assured.

CHAPTER SEVEN - OPTIMAL ENGINE REGULATION-LINEAR MODEL, QUADRATIC PERFORMANCE INDEX, AND MINIMAL SENSITIVITY

7.1 Introduction

The increase in the complexity of the overall control system, which would have resulted if an attempt to produce a stochastic controller had been made, suggested the need to look at alternative schemes which could achieve optimal-in-the-mean performance with simple controllers.* It is even a matter of some doubt [WONHAM (1969)] whether the control system, which would result from taking into direct account the stochastic signals, would be significantly superior to any system designed on the assumption that there were no stochastic signals present. Additionally, if the random disturbances cannot be considered to be Gaussian the stochastic control problem cannot be solved analytically. MORTENSEN (1968) indicated also, that if the plant was not linear (or could not be treated as linear) there would be great difficulty in handling white noise signals because it turned out that it was possible to have as solutions to the same non-linear stochastic, differential equation two different answers depending upon whether the Ito or the Stratonovich integral had been employed in the analysis. To avoid these difficulties an

---

* Simple in the special sense of being easy to synthesise.

approach first suggested by LUH and CROSS (1967) was tried, viz. : the problem was regarded as being a minimal trajectory sensitivity problem. Such a procedure is appropriate only if the dynamic system can accommodateitself to relatively slow variations in its parameters. From the work of chapter 2, section 3 it is clear that the parameters of the linear model of the engine/load system did change slowly with time when the engine was subjected to dynamic loading. Consequently the approach seemed to be justified.

The minimal sensitivity problem is discussed in detail below but the controller provided system performance which, although less sensitive to parameter variations than other controllers used, was not optimal.

7.2 Minimal Sensitivity Systems

7.2.1 Problem Statement

The engine and load described by (2.5) was re-expressed as :

$$\dot{\underline{x}} = A(t,\mu)\underline{x}(t) + B(t,\mu)u(t) \qquad (7.1)$$

where $\underline{x}$ and u had the usual meanings and dimensions. μ was a scalar parameter of the engine and load combination and was regarded as a constant i.e. it was assumed that the variation of μ from its nominal value was very slow. This assumption was weakened when the interval of the integral in the performance index was considered to be semi- finite. Both A and B were assumed to be continuous in time and differentiable in μ. Although the state vector $\underline{x}$ was an implicit function of μ, $\dot{\underline{x}}$ still denoted differentiation with respect to time because μ was taken as a constant.

The performance index to be minimised was

$$J = 0.5\int_{o}^{\infty}\left\{\underline{x}'(t)Q\underline{x}(t) + gu^2(t) + \underline{s}'(t)V\underline{s}(t)\right\} dt \qquad (7.2)$$

where Q and g had the same meanings and restrictions as in section 6.2 and where $\underline{s}(t)$ was the trajectory sensitivity vector defined here as :

$$\underline{s}(t,\mu) = \frac{\partial \underline{x}(t,\mu)}{\partial \mu} \qquad (7.3)$$

The sensitivity weighting matrix was V, of order 3 x 3, and it was chosen to be positive definite.

The differential equation describing the trajectory sensitivity was expressed as :

$$\frac{\partial \dot{\underline{x}}(t,\mu)}{\partial \mu} = \dot{\underline{s}}(t,\mu) = \frac{\partial A(t,\mu)}{\partial \mu}\underline{x}(t,\mu) + A(t,\mu)\frac{\partial \underline{x}(t,\mu)}{\partial \mu}$$

$$+ \frac{\partial B(t,\mu)}{\partial \mu}\, u(t) + B(t,\mu)\frac{\partial u(t)}{\partial \mu} \qquad (7.4)$$

By inference it was established that parameter variations would not affect $\underline{s}$ at t = 0; therefore

$$\underline{s}(0,\mu) = 0 \qquad (7.5)$$

Because the control function, u, to be determined, was not considered to be a function of the parameter, μ, the result of differentiating u with respect to μ was zero. A further simplifying assumption was made LAMONT and KAHNE (1967), DOMPE and DORF (1967) and KREINDLER (1968a) viz. that changes in the driving matrix, B, due to changes in μ were negligible. Hence

$$\frac{\partial B(t,\mu)}{\partial \mu} = 0 \qquad (7.6)$$

This assumption was not altogether reasonable however. BARNETT and STOREY (1966) had shown that for an optimal

system (7.1) with performance index (7.2) in which the matrix V was null, the system was more sensitive to changes in B than in changes in A. Although B will vary the assumption of (7.6) was followed briefly but the consequences of that assumption will be dealt with later in this section.

With these simplifications (7.4) became :

$$\dot{\underline{s}}(t,\mu) = \frac{\partial A(t,\mu)}{\partial \mu}\,\underline{x}(t,\mu) + A(t,\mu)\underline{s}(t,\mu) \qquad (7.7)$$

Combining (7.1) and (7.7) yielded :

$$\begin{bmatrix} \dot{\underline{x}}(t,\mu) \\ \dot{\underline{s}}(t,\mu) \end{bmatrix} = \begin{bmatrix} A(t,\mu) & 0 \\ \dfrac{\partial A(t,\mu)}{\partial \mu} & A(t,\mu) \end{bmatrix} \begin{bmatrix} \underline{x}(t,\mu) \\ \underline{s}(t,\mu) \end{bmatrix} + \begin{bmatrix} B \\ 0 \end{bmatrix} u(t) \qquad (7.8)$$

Let

$$\underline{\chi}(t,\mu) = \begin{bmatrix} \underline{x}(t,\mu) \\ \underline{s}(t,\mu) \end{bmatrix} \qquad (7.9)$$

$$H(t,\mu) = \begin{bmatrix} A(t,\mu) & 0 \\ \dfrac{\partial A(t,\mu)}{\partial \mu} & A(t,\mu) \end{bmatrix} \qquad (7.10)$$

$$N(t) = \begin{bmatrix} B \\ 0 \end{bmatrix} \qquad (7.11)$$

Therefore, $$\dot{\underline{\chi}} = H\underline{\chi} + N\,u \qquad (7.12)$$

Equation (7.2) was re-written as :

$$J = 0.5\int_0^\infty \left\{ \underline{\chi}' Z\, \underline{\chi} + gu^2 \right\} dt \qquad (7.13)$$

where

$$Z = \begin{bmatrix} Q & 0 \\ 0 & V \end{bmatrix} \qquad (7.14)$$

By minimising (7.13), subject to the constraint of (7.12), the minimal sensitivity control was found to be :

$$u^o(\underline{\chi},t) = D^*(t,\mu)\underline{x}(t,\mu) \qquad (7.15)$$

in which $D^*(t,\mu) = -g^{-1}N'(t)K(\mu)$ (7.16)

The matrix $K(\mu)$ was the solution of the matrix Riccati equation :

$$K(\mu)N(t)g^{-1}N'(t)K(\mu) - K(\mu)H(t,\mu) - H'(t,\mu)K(t,\mu) - Z = 0 \quad (7.18)$$

The solution was partitioned thus :

$$K(\mu) = \begin{bmatrix} K_{11}(\mu) & K_{12}(\mu) \\ K_{21}(\mu) & K_{22}(\mu) \end{bmatrix} \quad (7.17)$$

From (7.11), (7.15), (7.16) and (7.17) the optimal control law was expressed :

$$u^o(t,\mu) = -g^{-1}B'K_{11}(\mu)\underline{x}(t,\mu) - g^{-1}B'K_{12}(\mu)\underline{s}(t,\mu) \quad (7.19)$$

7.2 Lack of Optimality

Dompe and Dorf considered as an example a simple second-order system and noted that the control derived from (7.19) did not result in optimality i.e. they noted that other values for gains in the control law resulted in a lower value of performance index.

The example they chose was :

$$\dot{\underline{x}} = \begin{bmatrix} 0 & 1 \\ -0.5 & -\mu \end{bmatrix} \underline{x} + \begin{bmatrix} 0 \\ 1 \end{bmatrix} u \quad (7.20)$$

Nominal values of μ was 2.0 and for definiteness

$$g = 0.1 \quad (7.21)$$

$$Q = \begin{bmatrix} 1 & 0 \\ 0 & 0.25 \end{bmatrix} \quad (7.22)$$

and

$$V = \begin{bmatrix} 1 & 0 \\ 0 & 1 \end{bmatrix} \quad (7.23)$$

Using this data in BEARDM33 (see Chapter 6) the optimal control law was obtained; some discrepancies between the

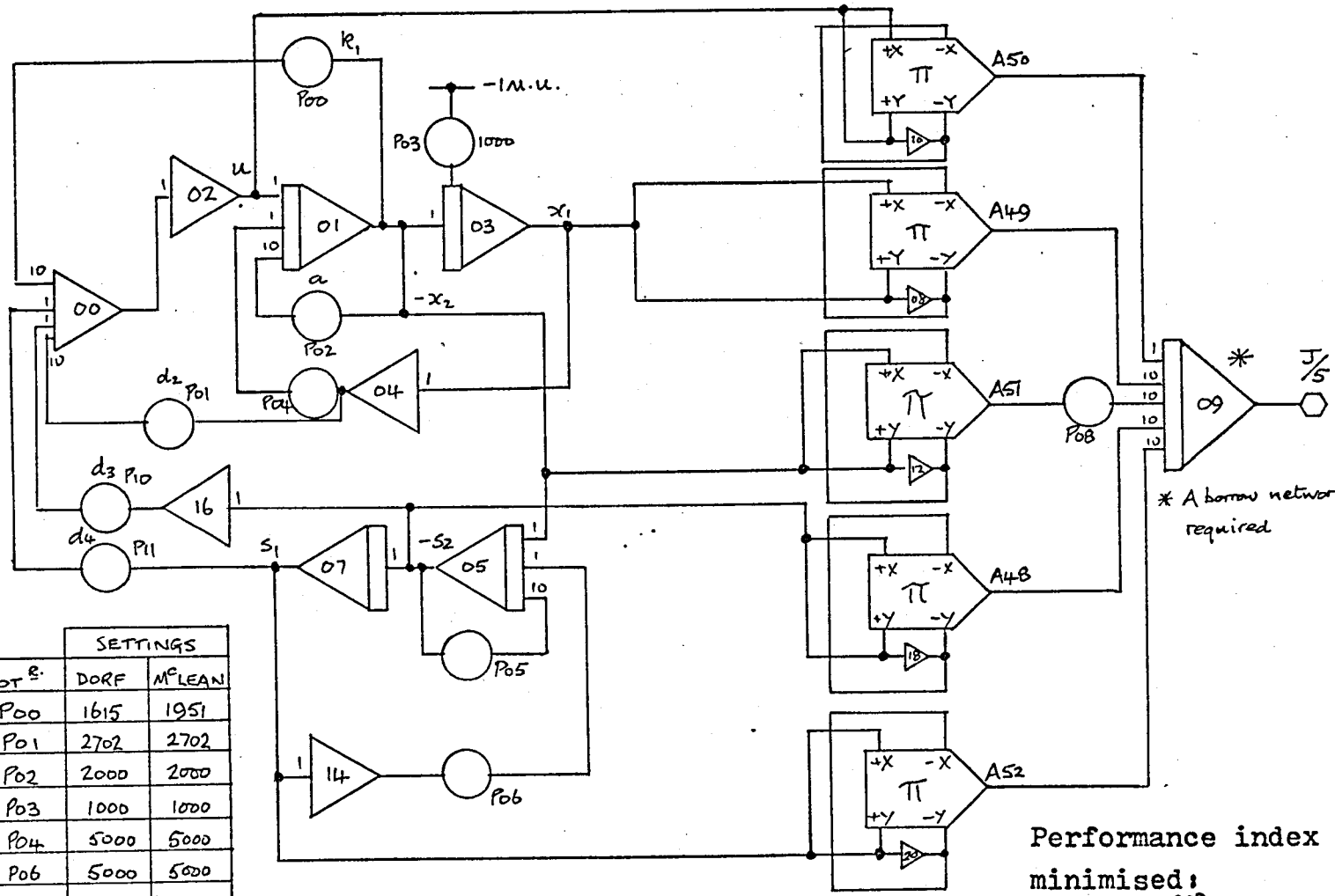

Pot R.	SETTINGS	
	DORF	McLEAN
P00	1615	1951
P01	2702	2702
P02	2000	2000
P03	1000	1000
P04	5000	5000
P06	5000	5000
P08	2500	2500
P09	2000	2000
P10	6196	6019
P11	6821	6673
P05	2000	2000

Performance index being minimised:

$$J = 0.5\int_0^\infty \{x_1^2+0.25x_2^2+0.1u^2+s_1^2+s_2^2\}\,dt$$

Figure 7.1 - Minimal Sensitivity System Simulation

results of the present author and those of the paper by Dompe and Dorf occurred. These can be seen in table 7.1.

	I	II
	DOMPE & DORF	McLEAN
d_1	-2.70156	-2.701525
d_2	-1.62524	-1.9505566
d_3	+0.68214	+0.6672860
d_4	+0.61964	+0.6019240

Table 7.1 - Comparison of Results

An analogue computer simulation, shown in figure 7.1, was set up to test both sets of results. From this simulation it was observed the use of the Dompe and Dorf values did result in non-optimal performance. For example, with d_1, d_3 and d_4 set at the values given by DOMPE and DORF the value of d_2 which resulted in a minimum value of J was -1.95 not -1.62524. However, when the values shown in column II of table 7.1 were employed optimality was achieved : the lowest value of J was achieved using the computed gains. It was observed that widely varying values of the sensitivity control coefficient did not affect significantly the value of the performance index, which remained at the minimum value, provided that the feedback gains, d_1 and d_2, were at their correct values. In this sense then, optimality has not been achieved : the values of d_3 and d_4 were not critical. The simulation experiments were carried out as indicated above, but for every test the parameter, μ, was

not changed. This lack of optimality is discussed in the next section but attention is drawn here to a secondary disadvantage of the approach. The control law is a function not only of the state but of the sensitivity vector also. In general, the sensitivity vector is not available from the system and it has to be simulated by an analogue model. This is an additional complexity in synthesis of the same magnitude as the provision of an estimator for a stochastic controller : the problem it was intended to avoid.

7.3 Closed-Loop Sensitivity

The method of the previous section contained some flaw in its development because optimality had not been achieved. This flaw stemmed basically from a confusion by earlier workers between

$$\underline{s} \triangleq \frac{\partial \underline{x}}{\partial \mu} \tag{7.24}$$

which was the sensitivity vector of the open-loop trajectory and

$$\underline{\sigma} \triangleq \frac{\partial \underline{x}_c}{\partial \mu} \tag{7.25}$$

the sensitivity vector of the closed-loop system of which $\underline{x}_c$ was the state vector. The distinction between these two vectors had been emphasised by KREINDLER (1968b,1969) who further suggested that the problem of closed-loop minimal sensitivity would require an approximate solution. Because a sensitivity model was required to provide the sensitivity vector, and because this model required as its input the system state vector, the only available state vector was that from the closed-loop system and was a function of the control signal which was, of course, a feedback signal. Consequently it was inappropriate

to employ the sensitivity vector, $\underline{s}$, and an amended analysis employing $\underline{\sigma}$ is outlined below. First, however, it should be mentioned that in the papers by Lamont and Kahne, and Dompe and Dorf it was proposed that the reason for the non-optimal solution was the neglect of the $\frac{\partial B}{\partial \mu}$ term. The correct reasons have been given above.

The form of the optimal control law for minimal closed-loop sensitivity was assumed a priori to have an identical form to that obtained from the earlier analysis viz :

$$u = D_1 \underline{x}_c + D_2 \underline{\sigma} \tag{7.26}$$

Consequently

$$\dot{\underline{x}}_c = A\underline{x}_c + BD_1\underline{x}_c + BD_2\underline{\sigma} \tag{7.27}$$

and

$$\dot{\underline{\sigma}} = \frac{\partial A x_c}{\partial \mu} + BD_1\underline{\sigma} + A\underline{\sigma} + BD_2\frac{\partial \sigma}{\partial \mu} \tag{7.28}$$

$\frac{\partial B}{\partial \mu}$ terms were ignored. If only small variations in parameter were considered then, to a first order approximation, (7.28) could be expressed as

$$\dot{\underline{\sigma}} = \frac{\partial A}{\partial \mu}\underline{x}_c + (A+BD_1)\underline{\sigma} \tag{7.29}$$

Letting

$$\underline{\Gamma} = \begin{bmatrix} \underline{x}_c \\ \underline{\sigma} \end{bmatrix} \tag{7.30}$$

then the minimal sensitivity, closed-loop optimal control system was described by the following differential equation :

$$\dot{\underline{\Gamma}} = \begin{bmatrix} (A + BD_1) & BD_2 \\ \frac{\partial A}{\partial \mu} & (A + BD_1) \end{bmatrix} \underline{\Gamma} \tag{7.31}$$

or more appropriately for the optimal control problem,

$$\dot{\underline{\Gamma}} = \begin{bmatrix} A & 0 \\ \frac{\partial A}{\partial \mu} & (A + BD_1) \end{bmatrix} \underline{\Gamma} + \begin{bmatrix} B \\ 0 \end{bmatrix} u \tag{7.32}$$

$$\dot{\underline{\Gamma}} = \Xi\underline{\Gamma} + Wu \tag{7.33}$$

From (7.33) and (7.32) it was apparent that the coefficient matrix, Ξ, was a function of the control gain matrix, D_1, which had yet to be determined. It can be shown (NEWMANN (1970)) that this problem may not be solved by simply solving the matrix Riccati equation, as in the deterministic case. Some iterative method is required : a not unexpected result since it had been predicted earlier by KREINDLER (1968b). While trying to establish some iterative method it was also worthwhile trying to find a means whereby the need to provide in the controller at least a measure of the sensitivity vector could be avoided.

The method proposed by HENDRICKS and d'ANGELO (1967) provides minimal sensitivity optimal control. It has the desirable feature that there is a constraint applied to the feedback signal so that it must be a linear function of the system state only. There is then no need to provide a sensitivity model in the synthesis of the optimal controller. Use of such a fixed structure controller also provides performance which is optimal in the mean in the sense of PROPOI and TSYPKIN (1968).

Letting $u = D'\underline{x}_c$ (7.34)

then $\dot{\underline{x}}_c = (A + BD')\underline{x}_c = A^*\underline{x}_c$ (7.35)

The sensitivity equation with respect to μ for (7.35) was given by :

$$\dot{\underline{\sigma}} = \frac{\partial A^*}{\partial \mu}\,\underline{x}_c + A^*\underline{\sigma} \tag{7.36}$$

$$\begin{bmatrix} \dot{\underline{x}}_c \\ \dot{\underline{\sigma}} \end{bmatrix} = \begin{bmatrix} A^* & 0 \\ \frac{\partial A^*}{\partial \mu} & A^* \end{bmatrix} \begin{bmatrix} \underline{x}_c \\ \underline{\sigma} \end{bmatrix} \tag{7.37}$$

The performance index (7.2) was then re-written as

$$J = 0.5\int_0^\infty \left\{ \underline{x}_c'(Q + gDD')\underline{x}_c + \underline{\sigma}'V\underline{\sigma} \right\} dt \qquad (7.38)$$

Using (7.30), (7.37) and (7.38) were expressed thus

$$\dot{\underline{\Gamma}} = \tilde{A}\underline{\Gamma} \qquad (7.39)$$

and

$$J = 0.5\int_0^\infty \left\{ \underline{\Gamma}'\Phi\underline{\Gamma} \right\} dt \qquad (7.40)$$

where

$$\tilde{A} = \begin{bmatrix} A^* & 0 \\ \frac{\partial A^*}{\partial \mu} & A^* \end{bmatrix} \qquad (7.41)$$

$$\Phi = \begin{bmatrix} (Q + GDD') & 0 \\ 0 & V \end{bmatrix} \qquad (7.42)$$

The minimisation of (7.40) was achieved by some optimal choice of D'. The evaluation of D' was carried out iteratively using the algorithm proposed by Hendricks and d'Angelo viz :

$$D^{j+1} = \{P^j\}^{-1}\{K^j + \Upsilon^j\} \qquad (7.43)$$

where the matrices P,K, and Υ are defined later.

(7.43) was terminated when

$$\|D^{j+1} - D^j\| \leq \epsilon \qquad (7.44)$$

ϵ was a small positive number. At each step in the iteration two algebraic equations, of order 2n, had to be solved :

$$\tilde{A}'H + H\tilde{A} + \Phi = 0 \qquad (7.45)$$

$$\hat{H}\tilde{A}' + \tilde{A}\hat{H} + \begin{bmatrix} \underline{x}_o\underline{x}_o' & \underline{0} \\ 0 & \underline{0} \end{bmatrix} = 0 \qquad (7.46)$$

where the matrices H and $\hat{H}$ had the property of positive definiteness. They were of order 2n x 2n, were symmetric and were partitioned thus :

$$H = \begin{bmatrix} H_1 & H_2 \\ H_2' & H_3 \end{bmatrix} \qquad (7.47)$$

$$\hat{H} = \begin{bmatrix} \hat{H}_1 & \hat{H}_2 \\ \hat{H}_2' & \hat{H}_3 \end{bmatrix} \tag{7.48}$$

$$P = \hat{H} \tag{7.49}$$

$$K = (\hat{H}_1 H_1 + \hat{H}_2 H_2')B \tag{7.50}$$

$$\Upsilon = (\hat{H}_2' H_2 + \hat{H}_3 H_3)B \tag{7.51}$$

(7.45) and (7.46) were not matrix Riccati equations because $\tilde{A}$ depended upon D which had yet to be evaluated. But (7.45) was a Lyapunov matrix equation and (7.46) was the same type of equation which may be seen by making the simple substitution

$$Y = \tilde{A}' \tag{7.52}$$

Then (7.46) becomes

$$\hat{H}Y + Y'\hat{H} + \begin{bmatrix} \underline{x}_o\underline{x}_o' & 0 \\ 0 & 0 \end{bmatrix} = 0 \tag{7.53}$$

Some method of solving the Lyapunov matrix equation had to be found which was fast and accurate because the unknown matrices H and $\hat{H}$ needed to be found at each step of the iteration. The methods outlined in the study by ROTHSCHILD and JAMESON (1970)* were considered. However, of the four methods outlined in that paper the most efficient required the use of triple

---

*A more recent survey by PACE and BARNETT (1972) established that for low order systems i.e. the dimension of the system state space less than 10, the direct methods were superior. However the order of improvement over a method using the infinite series expansion was only a factor of two; Davison and Man's method was used still therefore.

precision arithmetic to achieve satisfactory numerical accuracy. Consequently the algorithm of DAVISON and MAN, used in the program BEARDM33 (discussed in section 6.3) was again employed although it needed an initial guess for the matrix D to ensure that $\mathcal{X}$ was a stability matrix.*

The algorithm for the solution of the Lyapunov matrix equation viz.

$$KA + A'K = -Q \tag{7.54}$$

was given by :

$$K = \lim_{k\to\infty} K_k \tag{7.55}$$

where

$$K_{k+1} = \pi'^{2k} K_k \pi^{2k} + K_k \tag{7.56}$$

$$k = 0,1,2,3,.....$$

and where

$$K_o = hQ \tag{7.57}$$

$$\pi = (I - \frac{hA}{2} + \frac{h^2A^2}{12})^{-1}(I + \frac{hA}{2} + \frac{h^2A^2}{12}) \tag{7.58}$$

and

$$h \longrightarrow 0 \tag{7.59}$$

The choice of h was not critical; the algorithm was numerically stable for any positive value of h. In this research h was chosen to be 0.001.

The choice of $\underline{x}_o$ did not affect the optimal sensitivity control gains so that any convenient choice of $\underline{x}_o$ was used in the program BEARDM28 (see Appendix A.3) which was written based on this algorithm.

7.4 Computational Results

A wide variety of conditions were studied using the program BEARDM28. To assist the presentation of results the various different elements of the problem are listed and coded first, before listing the corresponding control laws.

---

*$\mathcal{X}$ necessary and sufficient condition for A to be a stability matrix was that $\lambda_i + \lambda_j \neq 0$ where the $\lambda_{i,j}$ were the eigenvalues.

(a) The matrix $\frac{\partial A^*}{\partial \mu}$

In the program this always had the form

$$\frac{\partial A^*}{\partial \mu} = \begin{bmatrix} \alpha_{11} & \alpha_{12} & 0 \\ 0 & 0 & 0 \\ 0 & 0 & 0 \end{bmatrix} \qquad (7.60)$$

because it was considered that only the parameters associated with the engine and load description would vary. From chapter 2 section 3 it is obvious that, depending upon speed and dynamometer setting, the linear model coefficients may be in error. This could be regarded as a slow parameter change.

CODE	α_{11}	α_{12}
A1	-0.2	0
A2	0.4	0
A3	0.6	0
A4	0.8	0
A5	1.0	0
A6	0	-9.0
A7	0	9.0
A8	-0.4	-2.0
A9	-0.4	2.0
A10	-0.4	5.0

Table 7.2 $\frac{\partial A^*}{\partial \mu}$ matrices elements

(b) The Sensitivity Weighting Matrix, V

V was chosen to be a diagonal matrix. 3 values were used :

$$V_1 = \text{diag}\ [10^{-4}, 10^{-4}, 10^{-4}] \qquad (7.61)$$

$$V_2 = \text{diag}\ [10^{-3}, 10^{-3}, 10^{-3}] \qquad (7.62)$$

$$V_3 = \text{diag}\ [10^{-7}, 10^{-7}, 10^{-7}] \qquad (7.63)$$

(c) The State Weighting Matrix, Q

This matrix was chosen to be a diagonal matrix thus :

CODE	q_{11}	q_{22}	q_{33}
Q1	10	1	0
Q2	7	2	0
Q3	10	10	1
Q4	10	1	1
Q5	100	1	1
Q6	1000	1	1

Table 7.3 - State Weighting Matrix Elements

(d) Initial Condition Vector $\underline{x}_o$

It was determined after extensive numerical experimentation that different $\underline{x}_o$ did not affect the final control laws. Consequently the value of $\underline{x}_o$ was the same for each entry and for the results presented in table 7.3 was given by :

$$\underline{x}_o' = [10, 0.1, -0.01] \qquad (7.64)$$

(e) The Optimal Control Laws

Using the program BEARDM28 the optimal control laws presented in table 7.4 were obtained. The starting guess for the D matrix was taken as

$$D' = [-1.0, -1.0, -1.0] \qquad (7.65)$$

in every case.

Serial No.	Q	A*	V	Control Gain Matrix			
				$-d_1$	$-d_2$	$-d_3$	
1	Q1	A1	V1	2.7553691	3.3663570	2.1442847	
2	Q1	A2	V1	2.7553691	3.3663571	2.1442847	
3	Q1	A3	V1	2.7553693	3.3663572	2.1442854	
4	Q1	A4	V1	2.7553695	3.3663574	2.1442848	
5	Q1	A5	V1	2.7553693	3.3663576	2.1442849	
6	Q4	A6	V2	2.7603464	3.4140693	2.2855068	
7	Q4	A6	V2	2.7600352	3.4143392	2.2847941	*
8	Q4	A6	V2	2.7599292	3.4138702	2.2846471	**
9	Q4	A10	V2	2.7592566	3.4135186	2.2842961	
10	Q2	A9	V3	2.2448397	2.9538445	1.9225799	
11	Q1	A8	V1	2.7553690	3.3663582	2.1442846	
12	Q3	A7	V2	2.7152722	4.3395876	2.7541167	
13	Q5	A10	V2	10.223866	10.019123	5.1973698	
14	Q5	A10	V2	10.223347	10.019496	5.1981884	**
15	Q6	A10	V2	———	diverged	———	

Table 7.4 - Optimal Control Gains for Minimal Sensitivity System

Using the same data as serial no. 7 and the formulation of (7.12) and (7.13) [the method of Dompe and Dorf] the optimal control law was obtained, derived from BEARDM33, viz :

$$u = [-2.7620447, -3.4166854, -2.2874913, +0.00624766, +0.0002929, +0.0001884]\begin{bmatrix}\underline{x}\\ \underline{s}\end{bmatrix} \qquad (7.66)$$

*Element, b_{31}, of driving matrix was 5.33 in this case.

**Element, b_{31}, of driving matrix was 6.83 in this case.

The gains which operate on the system states were very nearly the same as those obtained from the fixed structure controller. It is interesting to note that the small sensitivity gains were positive. They always were when this Dompe and Dorf method was used. Even though the change in a_{12} of the transformed coefficient matrix was as great as -90% of the nominal value the sensitivity gains remained very small. It should be noted that the gains shown in table 7.4 were not greatly affected by changes in the system parameters; this was the very desirable property of minimal sensitivity. Note also that when Q6 was used the program diverged. It is worth emphasising that the restriction of the structure in the way outlined resulted in a deterministic optimal regulator which, for some specific weighting matrix, and range of parameter changes, was minimally sensitive. The lack of sensitivity to parameter changes is of course one of the principal properties of feedback control. Because of the structure of this controller no special or additional engineering is needed on the engine rig. The gains were set on and results much similar to those obtained already in chapter 6 were obtained ; good regulation of speed errors due to external load disturbances, and marked destabilisation with changes of reference speed.

7.5 Model-Following System

7.5.1 Theory of Model-Following

As an alternative approach to providing minimal sensitivity the technique was considered of determining some optimal control law to control the engine system so that its output variables would follow faithfully the output variables

of some specified model. That model could have been a part of the control scheme and could have been placed ahead of the engine system as a pre-filter (TYLER (1964)). An alternative view of the same method was that the engine system must follow a desirable response to command inputs to the model (KREINDLER (1969). This kind of model-following is referred to as "explicit model-following". Several authors* however, ASSEO (1968), ERZBERGER (1968), WILKIE and PERKINS (1969) and MARKLAND (1970), considered the use of a "conceptual" model which appears, not in the physical system, but only in the performance index : in the mathematical statement of the problem. This type is referred to as "implicit model-following".

One of the principal results of the analysis of explicit model-following systems was that, in addition to the feedback gains, feedforward gains, operating upon the model-states, must be determined. Generally, for these feedforward gains, the derivatives of the system inputs have to be generated to implement the model-following control. Because derivatives were not easily synthesised, only the implicit model-following technique was considered for research.

The method used was that proposed by Erzberger which, because it was algebraic, was fast, efficient and direct in its method. An alternative method, due to Tyler, could be used with BEARDM33, the only modification required being a slight precomputation of the matrix input data to the program. The work of Asseo was an extension of the earlier work by Tyler and was concerned principally with the conditions to be satisfied for perfect

---

*including Tyler (1964).

model-following. That method required a considerable increase in the program working space because the state vector was augmented (with a consequent increase in the order of the associated matrices). Because Erzberger's method did not require state augmentation, provided a means to check the conditions for perfect matching, and was purely algebraic, it was the method preferred. A check for perfect matching was incorporated in BEARDM26 (see Appendix A3) the program written to determine the model-following control law. The algebraic method presented by MARKLAND is discussed also in this chapter and is shown to be very similar to the method proposed by Erzberger which is outlined next.

The solution was required to result in a perfect match between the controlled system and the model equation; in other words, the model equation

$$\dot{\underline{y}} = L\,\underline{y} \tag{7.67}$$

where $\underline{y}$ represented the system output vector, was required to result when the control, u^o, forced the engine system, i.e.

$$\dot{\underline{y}} = C\dot{\underline{x}} = CA\underline{x} + CBu^o \tag{7.68}$$

where the system output vector was related to the state vector by

$$\underline{y} = C\underline{x} \tag{7.69}$$

Thus $$u^o = [CB]^{+}(LC - CA)\underline{x} \tag{7.70}$$

where $[CB]^{+}$ meant the pseudo-inverse* of the matrix product $[CB]$. From (7.70) and (7.68)

$$\left[[CB][CB]^{+} - I\right](LC - CA)\,\underline{x} = 0 \tag{7.71}$$

---

*A brief statement on some methods of evaluating the pseudo-inverse of a matrix is given in Appendix A.4.

Consequently, if

$$\left[[CB][CB]^{+} - I\right](LC - CA) = 0 \qquad (7.72)$$

perfect matching was achieved. If perfect matching was not achieved by the method the feedback matrix which did result was guaranteed, by the properties of the pseudo-inverse of a matrix, to yield a weighted least squares match between the response of the engine system and the model.

Markland proposed a scheme to minimise a weighted least squared error criterion viz :

$$R = \underline{e}'Q\underline{e} \qquad (7.73)$$

where Q was a symmetric, positive definite matrix and where

$$e = (LC - CA)\underline{x} - CBu \qquad (7.74)$$

Now
$$\frac{\partial R}{\partial u} = \left(\frac{\partial e}{\partial u}\right)'\left(\frac{\partial R}{\partial \underline{e}}\right) \qquad (7.75)$$

$$\frac{\partial R}{\partial \underline{e}} = Q\underline{e} + Q'\underline{e} = 2Q\underline{e} \qquad (7.76)$$

$$\frac{\partial \underline{e}}{\partial u} = -CB \qquad (7.77)$$

$$\frac{\partial R}{\partial u} = -2B'C'Q\left[(LC - CA)\underline{x} - CBu\right] \qquad (7.78)$$

If

$$\frac{\partial R}{\partial u} = 0 \qquad (7.79)$$

then

$$(LC - CA)\underline{x} - CBu = 0 \qquad (7.80)$$

hence
$$u^{o} = [CB]^{+}(LC - CA)\underline{x} \qquad (7.81)$$

which was identical, of course, to (7.70).

In the paper by Markland he defined

$$\frac{\partial R}{\partial \underline{e}} = \underline{e}'(Q + Q') \qquad (7.82)$$

$$\frac{\partial R}{\partial \underline{e}} = \underline{e}'2Q \qquad (7.83)^{*}$$

$\frac{\partial R}{\partial \underline{e}}$ is a row vector.

*Q was symmetric.

and $$\frac{\partial R}{\partial u} = (\underline{x}'[CA - LC]' + uB'C')2QCB = 0 \qquad (7.84)$$

whence $$2\underline{x}'[CA - LC]'QCB + 2uB'C'QCB = 0 \qquad (7.85)$$

thus $$u = -(B'C'QCB)^{-1}B'C'Q[CA - LC]\underline{x} \qquad (7.86)$$

It shold be noted that the transpose of (7.83) equals (7.76) i.e.

$$\frac{\partial R}{\partial \underline{e}}\Big|_{(7.76)} = \frac{\partial R'}{\partial \underline{e}}\Big|_{(7.82)} \qquad (7.87)$$

It may be concluded therefore that

$$[CB]^{+} = (B'C'QCB)^{-1}B'C'Q \qquad (7.88)$$

and that the work of Markland was similar to that of Erzberger.

The control law of (7.86) required that (B'C'QCB) be non-singular which implied that CB must not be zero in the research work. However, for the engine system C was of order 1 x 3, and from (2.84) B was of order 3 x 1; the product, CB, was a scalar. From (2.84) it can be observed that B had some zero rows; care had to be exercised in the choice of an appropriate C matrix else (7.86) would have been invalidated. The same property of the B matrix gave some trouble with the Erzberger method; care was taken with the choice of matrix, C, therefore.

It should be noted that with the Erzberger method it was possible to admit to the class of admissible control functions impulse-gains. Such controls were arrived at in a solution only when the engine system was required to match the response of a model system of order lower than the engine system. Such a situation is pathological from the mathematical point of view; it is a natural requirement in engineering practice. In this research the model order was taken as three, thus

assuming that no impulse-gains would need to be synthesised.

7.5.2 Some Numerical Results

With engine system equations (2.83) and (2.84) an attempt was made to obtain the control law using as a model one of several choices of the form :

$$L = \begin{bmatrix} \lambda_M & 400 & 0 \\ 0 & 0 & 1 \\ 0 & -150 & -25 \end{bmatrix} \qquad (7.89)$$

in which λ_M was taken as -0.5, -1.0, or -2.0 respectively. It was assumed that the output vector and the state vector were identical; in other words the output matrix, C, was chosen to be the identity matrix. From Appendix A.4 it is clear that if the pseudo-inverse of some matrix, say, W, of order n x m, has to be determined then, if $n > m$ the pseudo-inverse would be given by :

$$W^+ \triangleq (W'W)^{-1}W' \qquad (7.90)$$

Although the program BEARDM26 has been written for general use (i.e. it will determine the pseudo-inverse of matrix, W, even if $n < m$) it was the case for this research that $n = 3$ and $m = 1$. Thus the pseudo-inverse of CB was simply

$$[CB]^+ = [0 \quad 0 \quad (b_3)^{-1}] \qquad (7.91)$$

Therefore

$$u^o = [0 \quad 0 \quad (b_3)^{-1}](L - A)\underline{x} \qquad (7.92)$$

The simplicity of (7.92) resulted from the nature of the driving matrix and the choice of the output matrix; there was no necessity to use BEARDM26 for the research. But the program contained useful checks for perfect matching and because all the operations were algebraic it was extremely fast. It was used therefore for all the work of this section.

To confirm the program the optimal control laws were determined for a series of model matrices which corresponded to the coefficient matrices of the closed-loop system when the control laws of table 6.2 were used. Obviously the same control laws should have resulted - this was the situation that pertained. As a further check the companion matrix form was used by employing the transformation matrix of (6.100) and specifying the model equation as a 3rd order homogeneous differential equation. Control laws, identical to those of table 6.2 were obtained, after post-transformation. The program confirmation emphasised the confidence which could be placed upon the results obtained by this very fast procedure. A series of further numerical experiments were conducted to investigate the effects on the resulting optimal control laws when parameter variations* were present. The model inverse time constant λ_M was assumed to vary about its nominal value (see (7.89)). The control laws corresponding to the three cases are shown in table 7.5.

	Control Gains		
λ_M	d_1	d_2	d_3
-0.5	+0.004125	-0.8.83	-0.1963
-1.0	0	-0.8776	-0.2079
-2.0	-0.00936	-1.479	-0.231

Engine inverse time constant, $\lambda = 1.0\ sec^{-1}$

Table 7.5 - Model-Following Gains**

*It was not time-varying parameters which were considered here but the cases where parameter values were different from their nominal values by some specified, fixed amount.

**These gains were evaluated by transforming the system and model-equations to phase-variable form and then applying a post-transformation to the results of processing the phase-variables.

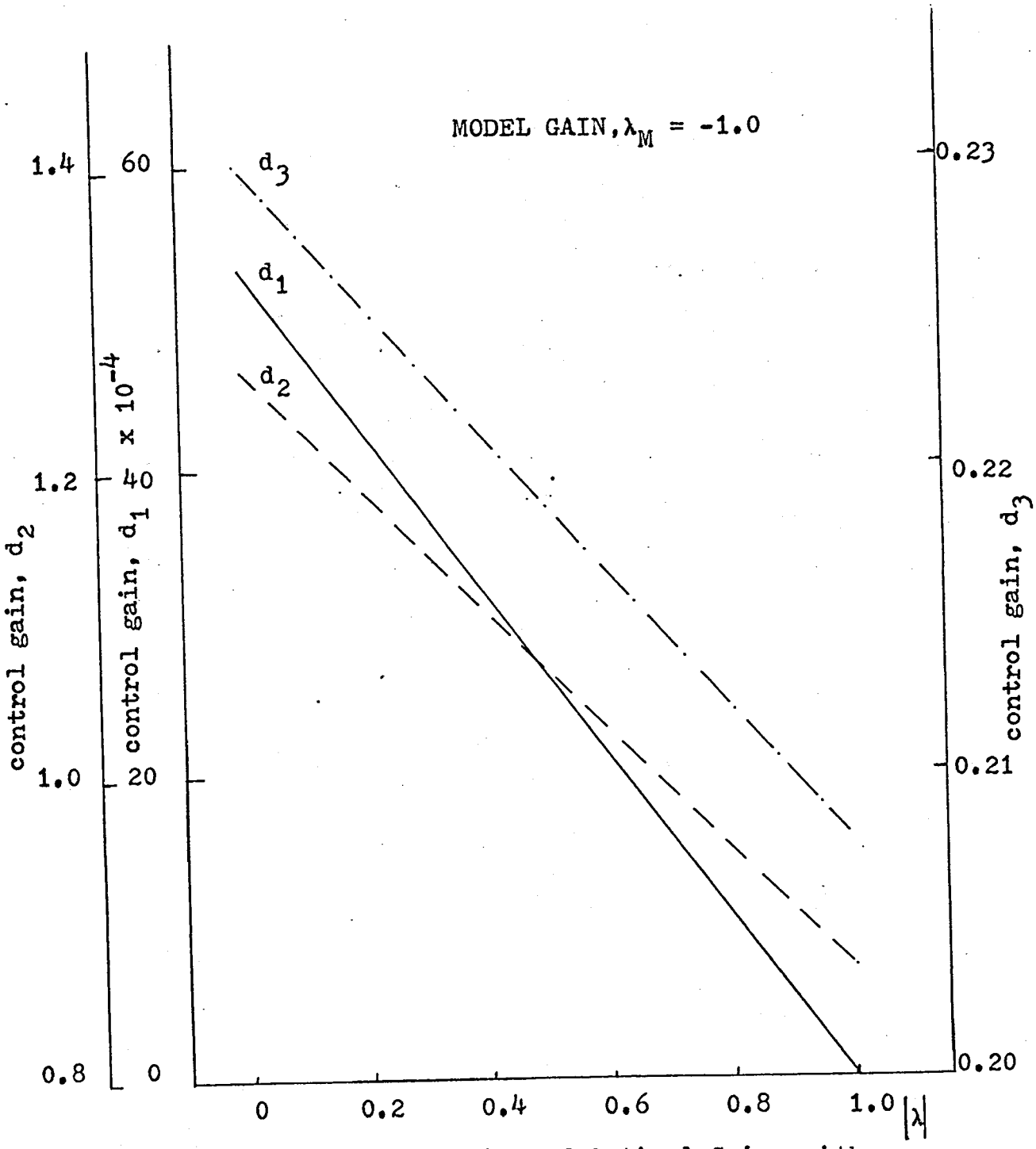

Figure 7.2 - Variation of Optimal Gains with Plant Parameter

It is of interest to note that a zero gain* resulted when the engine parameter was identical to the model parameter viz. $\lambda = \lambda_M$. Note also that when $\lambda_M > -1.0$ (this corresponded to the situation when the fan setting was 2.5 cm. or less : see figure 2.20) the resulting gain* was positive, because the model-following control gain was required to effectively destabilise the system. The gains, d_2 and d_3, which resulted with $\lambda_M \triangleq -1.0$ were required to match the servo response to the model servo response of (7.89). For a change of parameter in the engine gain then all the control gains were affected equally, see (7.92). The variations of control gains d_1, d_2, and d_3 with change of engine parameter, λ, for a model equation of (7.89) with $\lambda_M = -1.0$ are shown in figure 7.2. It is to be noted that a linear variation of the gains occurred in the circumstances. The absolute values of the gain changes for such very large changes in plant parameters were not very great, and the resulting closed-loop system matrix was not greatly different from the specified model matrix. When the elements of the companion matrix, representing the model, are more than the corresponding elements of the companion matrix of the plant then positive feedback results. Because λ did not exceed -1.0 (see figure 2,20) this situation did not occur in the engine work. A disadvantage of the method was that it was difficult to relate the specified model matrix to any cost function although the requisite dynamic response was easily assured.

In this work the method was used in conjunction with the work of chapter 6. For a given performance index the optimal control law for the nominal plant parameters was obtained from

---

* The gain is d_1.

BEARDM33. The optimal closed-loop system matrix was used then as the model matrix for BEARDM26 and the effects of altered plant parameters upon the derived control gains were then assessed swiftly by the use of the methods of this section.

CHAPTER EIGHT - OPTIMAL ENGINE REGULATION - NON-LINEAR MODEL AND QUADRATIC PERFORMANCE INDEX

8.1 Introduction

In chapter 6 optimal engine regulation was considered for the engine system using a linear model to describe the engine system dynamics. Several different schemes were considered to take account of the random changes of engine parameters and also the limitations imposed by the need for ease of synthesis of the resulting optimal controller. These schemes assumed that the regulation was effective and that any deviations from the equilibrium speed were never large. Subsequent experiment confirmed substantially these assumptions. Nevertheless some features of the resulting control suggested that there was an inadequacy in the engine mathematical model and that some further investigation was required. The nature of the system response when there were present some parameter deviations was investigated therefore, and, from the use of optimal sensitivity studies, it was established in chapter 7 that the deterministic control laws found in chapter 6 also provided inherently desirable minimal sensitivity properties. But with such similar control laws the features of concern in the experimental investigation still remained.

In this chapter therefore consideration is given to the problem of providing optimal regulation but specifically taking into account the non-linear nature of the engine and

load system. There has been keen interest in recent years in this kind of control problem typified by the papers of such writers as SIMS and MELSA (1968), BURGHART (1969a,b), GARRARD (1969), GUSTAFSON and HARDWOOD (1969), LUKES (1969), SALMON and KOKOTOVIC (1969) and FOOTE (1972).

In the papers by Burghart, Garrard, and Salmon and Kokotovic the optimal controls which resulted from their analyses were sub-optimal and the gain matrix obtained in each case was an infinite Taylor's series expanded about some nominal value of the state. The methods of Burghart depended upon the availability of a linear model of the plant although the feedback gains operated upon non-linear functions of the state. Foote assumed a priori a truncated power series for which the necessary values of the coefficients were determined for optimal control. In this scheme Foote admitted explicit functions of time as control functions. For all practical synthesis the Taylor series was truncated necessarily. It was this feature of the work which resulted in sub-optimality. The entire approach of these papers was dealt with rigorously in the paper by Lukes.

A novel method of using additional states to represent approximately the non-linearities of the system was proposed by Gustafson and Harwood and this scheme was considered first. In common with all the methods presented in the quoted references (except the paper by Sims and Melsa) the synthesis of the controller required the use of either multipliers* or

---

*It should be noted that control laws of similar form (i.e. non-linear functions of the output state) are obtained when dealing with linear plants and non-quadratic performance criteria. (e.g. see ASSEO (1969)).

function generators to produce the required non-linear function of the state.

8.2 Controller Derived Using Auxiliary State Variables

For this method the non-linear engine and load system was described by a linear state equation which had been augmented by the addition of auxiliary state variables to represent, in a way outlined briefly below, the residual non-linearity. Once the engine and load system were described in this fashion the optimal control problem was identical to that outlined in chapter 6. The authors of the reference suggested that dynamic programming should be used to obtain a solution. Any of the methods of chapter 6, section 3 could also be used as effectively.

The results presented in this section were obtained by using the method of dynamic programming (BEARDM15) described in 6.3.4. Once the feedback gains were determined the residual non-linearity was recreated from measured values of the other state variables. The re-established non-linearity was multiplied then by the appropriate coefficient and processed with the other signals to produce the control signal. Thus the closed-loop control system depended upon the system non-linearity even though the controller was derived from a problem formulated on the basis of plant linearity.

The method of handling the non-linearity was to represent it as the sum of two components : a linear term and a component of residual non-linearity. In this work the non-linearity was essentially a squared function i.e.

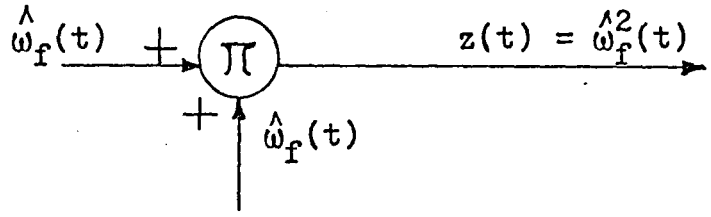

Figure 8.1 - Non-linear Function Representation

The squared function was linearised about the equilibrium value of output speed, viz :

$$\hat{\omega}_f(t) = \hat{\omega}_f(t) - \Omega_E + \Omega_E \qquad (8.1)$$

Therefore,

$$z(t) = 2\Omega_E\hat{\omega}_f(t) + (\hat{\omega}_f^2(t) - 2\Omega_E\hat{\omega}_f(t)) \qquad (8.2)$$

The linear component, μ, of $z(t)$ was given by

$$2\Omega_E\hat{\omega}_f(t) = \mu \qquad (8.3)$$

The non-linear residue was given then by :

$$\hat{\omega}_f^2(t) - 2\Omega_E\hat{\omega}_f(t) = \Psi \qquad (8.4)$$

The linearised squared function was represented therefore by

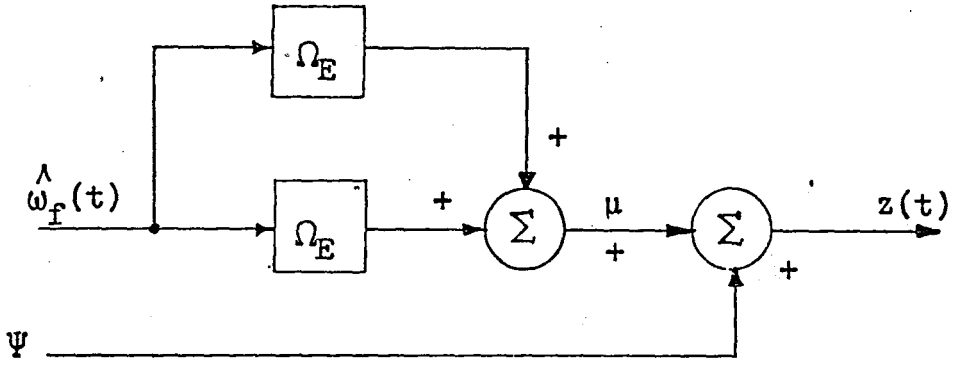

Figure 8.2 - Representation of Linearised Squared Function

The term, Ψ, was regarded as a d.c., or bias, offset. If Ψ was a constant offset then the most convenient method of including its effect in the system was to designate Ψ as an extra state variable. In the optimal controller this additional bias state was multiplied by the appropriate feedback gain to cancel out its effect in the steady-state. If Ψ changed more quickly than the linear component, μ, then that

cancellation would not be effected, and severe stability problems sometimes ensued.

The equation of the non-linear engine and load system given in (2.20) was considered viz.,

$$\dot{\hat{\omega}}_f = -3.33k\hat{\omega}_f^2 + 3.33u \qquad (8.5)$$

Linearisation of the equation about the equilibrium speed of Ω_E = 210 rad/sec resulted in the non-linearity's being replaced by :

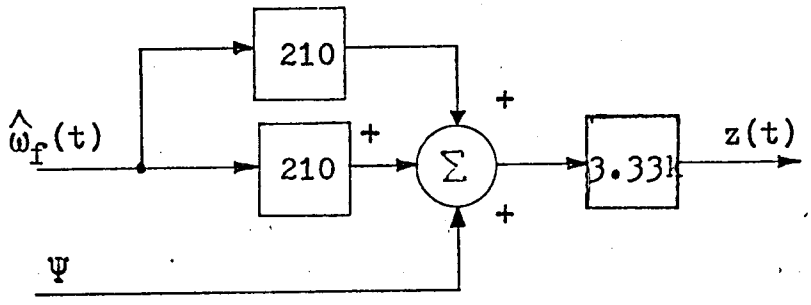

Figure 8.3 - Linearised Engine/Load System

(8.6) was represented by the new block diagram of the pseudo-linear engine/load system, given as figure 8.4.

$$\dot{\hat{\omega}}_f = 3.33u - 1398.6k\hat{\omega}_f - 3.33k\Psi \qquad (8.6)$$

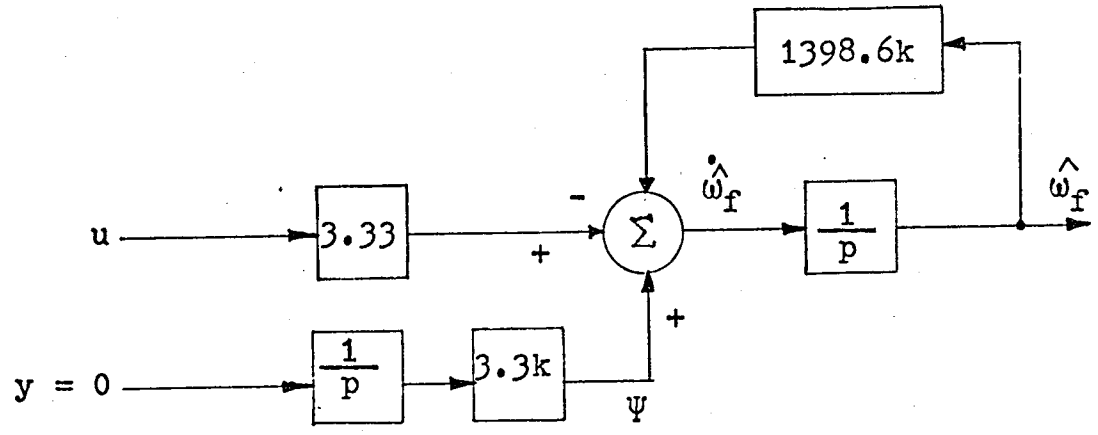

Figure 8.4 - Block Diagram of the Pseudo-Engine/ Load System

Thus the pseudo-engine/load system was represented by the linear state equation :

$$\begin{bmatrix} \dot{\hat{\omega}}_f \\ \dot{\Psi} \end{bmatrix} = \begin{bmatrix} 1398.6k & -3.33k \\ 0 & 0 \end{bmatrix} \begin{bmatrix} \hat{\omega}_f \\ \Psi \end{bmatrix} + \begin{bmatrix} b \\ 0 \end{bmatrix} u \qquad (8.7)$$

where $\hat{\omega}_f$ was the deviation from equilibrium speed, in rad/s

Ψ was the auxiliary state variable in rad/s^2

u was the torque in N m

By addition of the equations associated with the throttle servo-mechanism, (2.4) and (2.79), to (8.7), with the meaning of the variable, u, taken now to mean V_{in}, the command signal to the servomechanism, the state equation became :

$$\begin{bmatrix} \dot{x}_1 \\ \dot{x}_2 \\ \dot{x}_3 \\ \dot{x}_4 \end{bmatrix} = \begin{bmatrix} 1398.6k & 400 & 0 & -3.33k \\ 0 & 0 & 1 & 0 \\ 0 & -130 & -16 & 0 \\ 0 & 0 & 0 & 0 \end{bmatrix} \begin{bmatrix} x_1 \\ x_2 \\ x_3 \\ x_4 \end{bmatrix} + \begin{bmatrix} 0 \\ 0 \\ 43.3 \\ 0 \end{bmatrix} u \qquad (8.8)$$

For a nominal setting of the fan displacement of 7.62 cm. the control laws which resulted, and which corresponded to the indicated weighting matrices and factors, are quoted in table 8.1.

CASE	d_1	d_2	d_3	d_4
I	-0.16102113	-8.2961903	-0.37098617	+0.00022597
II	-0.16050978	-8.2751289	-0.3703255	-0.00022555
III	-0.12356413	-6.7071729	-0.32080342	-0.00019388

Case I Q = diag(100,10,0) g = 0.1

Case II Q = diag(100,1,0) g = 1.0

Case III Q = diag(10,1,0) g = 10.0

Table 8.1 - Optimal Gains for Augmented Engine System

The gains, d_4, were all too small to permit satisfactory synthesis of the non-linear terms. Their omission from the experimental arrangements did not affect perceptibly the system performance. On the analogue computer simulation their inclusion did not result in any significant improvement over the performance of the system when they were omitted*. The gains d_1, d_2 and d_3 almost exactly correspond to the values found by the methods of chapter 6.3 for the same weightings. Thus it was demonstrated that the linear optimal control law derived from an L.Q.P. formulation has a strong tolerance to unaccounted-for plant non-linearity. From this conclusion it was taken as logical to attempt to find the optimal linear control law when the engine/load system was described as accurately as possible. Such an approach required the technique of specific optimal control.

8.3 Specific Optimal Control

8.3.1 Introduction

Specific optimal control (s.o.c.) is a method of determining a linear control law to regulate a non-linear system. It was proposed first by EISENBERG and SAGE (1966) and its distinctive feature is the requirement for a priori specification of the feedback control structure. The optimal values of the selected controller are determined by using the technique of quasilinearisation, an account of which was given in section 4 of chapter 5.

---

*The evaluation of the performance index with and without the non-linear terms was identical when it was carried out on the analogue computer.

The engine/load system may be described by the usual vector differential equation, viz :

$$\dot{\underline{x}} = \underline{f}(\underline{x},u) \tag{8.9}$$

in which the vector $\underline{x}(0) = \underline{x}_o$ (8.10)

The problem is to find then a specific optimal control law

$$u^o = \underline{K}'\underline{x} \tag{8.11}$$

in which the vector, $\underline{K}$, represents the parameters k_1, k_2, and k_3 which have to be chosen to minimise the integral (8.12)

$$J = \int_o^T \varphi(\underline{x},u)dt \tag{8.12}$$

The method of obtaining a solution is started by adding the unknown parameters k_1, k_2 and k_3 to the state vector, thus augmenting it :

$$\left.\begin{aligned} \dot{x}_4 &= \dot{k}_1 = 0 \\ \dot{x}_5 &= \dot{k}_2 = 0 \\ \dot{x}_6 &= \dot{k}_3 = 0 \end{aligned}\right\} \tag{8.13}$$

The problem then is treated thereafter as a TPBVP to be solved by the Q.L. method. The boundary conditions associated with this TPBVP are composed of the given initial state vector, $\underline{x}_o$ the boundary values of the adjoint variables associated with the augmenting vector, $\underline{K}$ and the final values of the adjoint variables associated with the first three states :

$$\begin{cases} \psi_4(0) = \psi_5(0) = \psi_6(0) = 0 \\ \psi_1(T) = \psi_2(T) = \psi_3(T) = \psi_4(T) = \psi_5(T) = \psi_6(T) = 0 \end{cases} \tag{8.14}$$

This set of boundary conditions resulted because neither $\underline{K}(0)$ nor $\underline{K}(T)$ was fixed. [CITRON (1969)].

8.3.2 The S.O.C. of the Dynamometer

It was decided initially to develop the necessary program by finding a feedback control law to regulate the speed of the dynamometer only. (The throttle servomechanism

and the engine dynamics were not taken into account at this stage). What was attempted was to determine a value for the feedback gain, k, such that in restoring the deviated speed of the dynamometer, x(0) = 10.0, to equilibrium the performance index of (8.15) was minimised.

$$J = 0.5 \int_0^2 (x^2 + u^2)dt \qquad (8.15)$$

The system equation (from (2.20)) was expressed as

$$\dot{x} = -cx^2 + bu \qquad (8.16)$$

where c depended upon the fan setting and b = 3.33. Without invalidating the solution it proved convenient to consider b as unity : the reasons for this convenience are discussed later. The problem became that of finding some s.o.c. law

$$u^o = kx \qquad (8.17)$$

where the gain, k, had to be chosen to minimise J(k), i.e.

$$J(k) = 0.5 \int_0^2 (1 + k^2)x^2 dt \qquad (8.18)$$

The unknown gain was represented as an additional state variable;

$$\dot{k} = 0 \qquad (8.19)$$

Therefore, the Hamiltonian was

$$H = 0.5x^2 + 0.5k^2x^2 + \psi_1 (-cx^2 + kx) \qquad (8.20)$$

from which were obtained the canonical equations :

$$\dot{x} = -cx^2 + kx \qquad x(0) = 10.0 \qquad (8.21)$$

$$\dot{k} = 0 \qquad \psi_2(0) = 0 \qquad (8.22)$$

$$\dot{\psi}_1 = -x - k^2x + 2cx\,\psi_1 - k\psi_1 \qquad \psi_1(2) = 0 \qquad (8.23)$$

$$\dot{\psi}_2 = -kx^2 - \psi_1 x \qquad \psi_2(2) = 0 \qquad (8.24)$$

(8.21) to (8.24) were combined into a single vector equation

$$\dot{z} = f(z) \qquad (8.25)$$

where $$\underline{z} = \begin{bmatrix} x \\ k \\ \psi_1 \\ \psi_2 \end{bmatrix} \tag{8.26}$$

$\underline{f}(\underline{z})$ was given by the r.h.s. of the equations (8.21) to (8.24). From (8.25) the Q.L. equation was formed as

$$\dot{\underline{z}}^{i+1} = \underline{f}(\underline{z}^i) + J_{\underline{z}^i}\underline{f}(\underline{z}^i)\ (\underline{z}^{i+1}-\underline{z}^i) \tag{8.27}$$

where $J_{\underline{z}^i}$ was the Jacobian matrix defined as $\frac{\partial \underline{f}}{\partial \underline{z}^i}$. Thence

$$\dot{\underline{z}}^{i+1} = A\underline{z}^{i+1} + \underline{v} \tag{8.28}$$

where $$A = J_{\underline{z}^i}\underline{f}(\underline{z}^i) \tag{8.29}$$

and $$\underline{v} = \underline{f}(\underline{z}^i) - J_{\underline{z}^i}\underline{f}(\underline{z}^i)\underline{z}^i \tag{8.30}$$

(8.29) was shown to be :

$$A = \begin{bmatrix} (-2cx^i + k^i) & x^i & 0 & 0 \\ 0 & 0 & 0 & 0 \\ (-1-[k^i]^2+2c\psi_1^i) & (-2k^ix^i - \psi_1^i) & (2cx^i-k^i) & 0 \\ (-2k^ix^i-\psi_1^i) & -(x^i)^2 & -x^i & 0 \end{bmatrix} \tag{8.31}$$

Similarly (8.30) was evaluated as

$$\underline{v} = \begin{bmatrix} c(x^i)^2 - k^ix^i \\ 0 \\ 2(k^i)^2x^i + k^i\psi_i^i - 2cx^i\psi_1^i \\ 2k^i(x^i)^2 + \psi_1^ix^i \end{bmatrix} \tag{8.32}$$

The program BEARDM31, described in section 5 of chapter 5, was modified and the problem was solved for $c = 8 \times 10^{-3}$ which corresponded to a fan setting of 7.62 cm. The solution was

$$k_1 = -0.7054 \times 10^1 \qquad (8.33)^*$$

The solution was obtained in 4 iterations using a Runge-Kutta fourth order integration routine with a step length of 0.05s from an initial guess of k =-1.0. This guess presupposed negative feedback. The stopping condition was when the latest value of k differed from previous value by less than 0.001. Figure 8.5 shows the trajectory of the dynamometer speed in response to s.o.c.

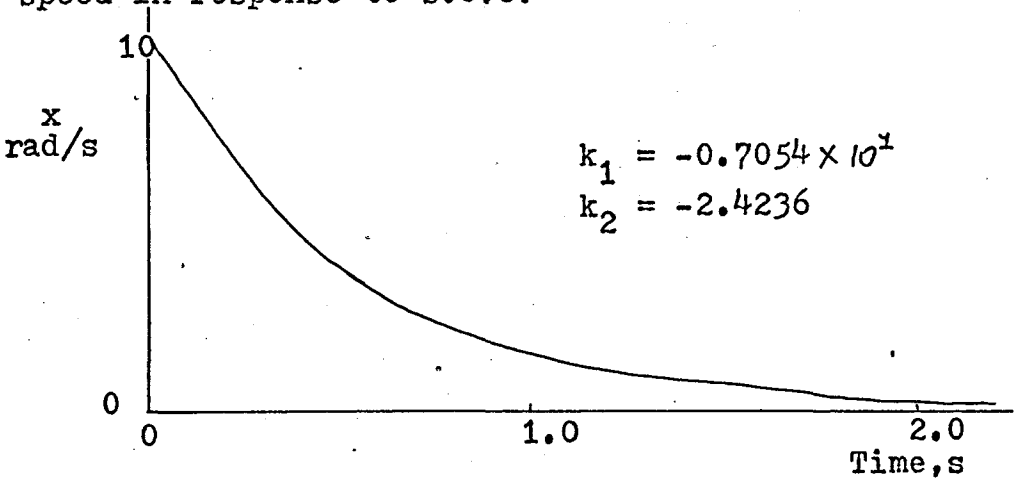

Figure 8.5 - S.O.C. - Optimal Trajectory

To use the program successfully required a good initial guess for the unknown gain, k. Depending upon the quality of the guess and also upon the value chosen for the stopping value, the number of iterations and, as a consequence, the execution time of the program varied considerably. A series of runs were carried out to investigate thiscomputational problem (using c = 1.0 for convenience). The results obtained are presented in table 8.2.

---

*The subscript 1 was used merely to identify this value of s.o.c. gain which will be discussed later.

Serial No.	Initial Guess	Final S.O.C. Value	Integration Step Length	Stopping Condition	No.of Iter.	Execution Time
1	-0.1	-0.11657259	0.01	0.001	2	14m 31s
2	-0.1	-0.10392092	0.01	10^{-7}	7	49m 12s
3	-0.1	-0.11505328	0.1	0.001	4	3m 14s
4	-1.0	-0.10433740	0.01	0.001	4	28m 21s
5	-1.0	-0.11332862	0.1	0.001	10	7m 57s

Table 8.2 - Program Parameters

It may be deduced from these results that

(a) the number of iterations required for convergence increases as the trial guess gets worse

(b) the execution time increases markedly with the requirement for increased accuracy (i.e. with a reduced stopping value)

(c) the execution time increases with reduced step length

It should be noted however that the choice of step length does affect whether the program converges at all : any choice of step length depends upon the problem being solved. This consideration will be dealt with later in this chapter.

In the basic dynamometer problem it was stated that it was advantageous to consider b to be unity. If b had a non-unity value (8.31) and (8.32) would have become :

$$A = \begin{bmatrix} (-2cx^i+bk^i) & bx^i & 0 & 0 \\ 0 & 0 & 0 & 0 \\ -1-(k^i)^2+2c\psi_1^i & -2k^ix^i-b\psi_1^i & 2cx^i-bk^i & 0 \\ -2k^ix^i-b\psi_1^i & -(x^i)^2 & -bx^i & 0 \end{bmatrix} \qquad (8.34)$$

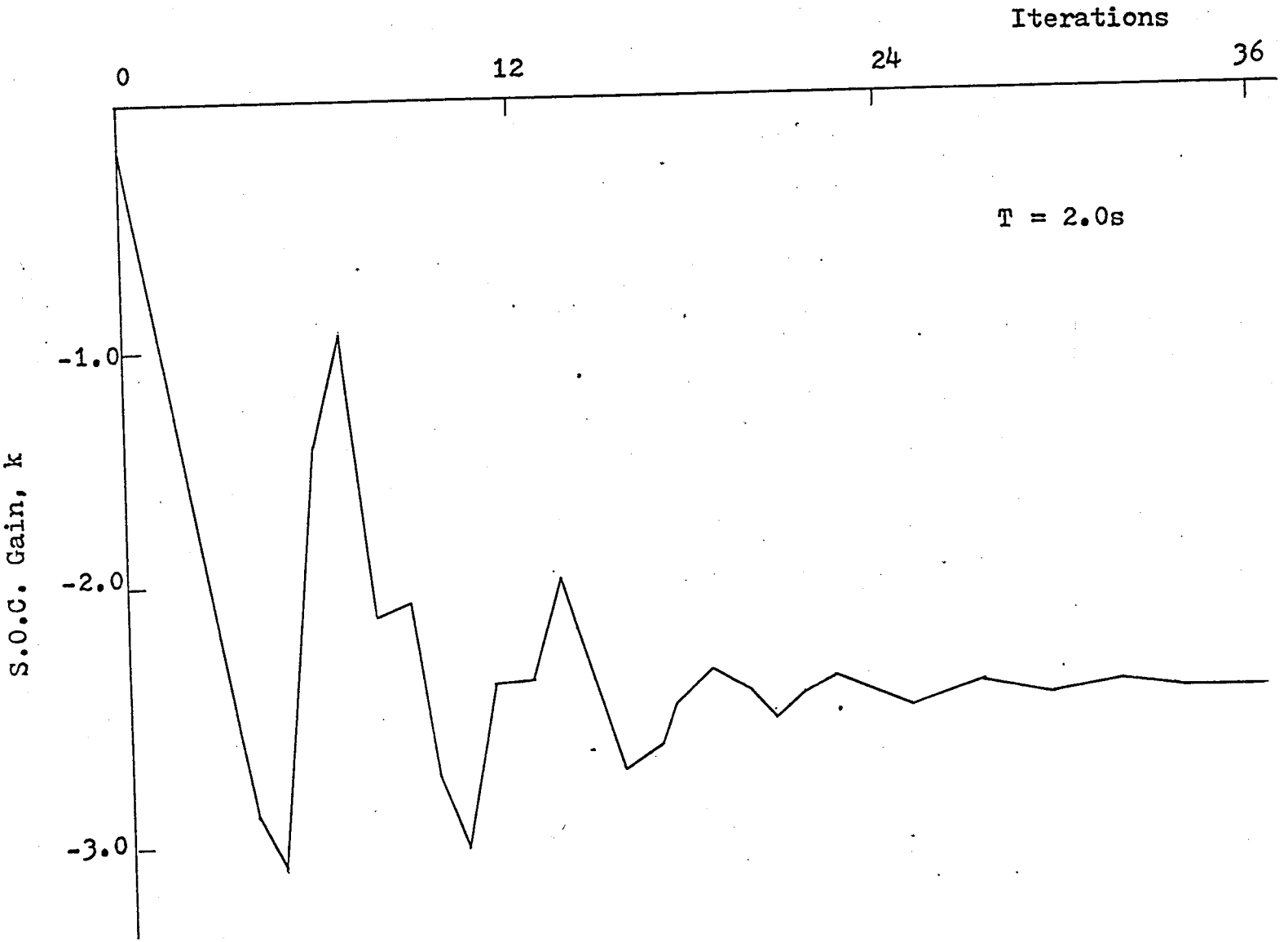

Figure 8.6 - Convergence Characteristic of S,O,C. Program

$$\underline{v} = \begin{bmatrix} -c(x^i)^2 - k^i b x^i \\ 0 \\ 2(k^i)^2 x^i + bk^i \psi_1^i - 2cx^i \psi_1^i \\ 2k^i (x^i)^2 + b\psi_1^i x^i \end{bmatrix} \qquad (8.35)$$

Use of these equations in the program provided a final s.o.c. gain of :

$$k_2 = -2.4236 \qquad (8.36)$$

The trajectory of x(t) returning to equilibrium was identical to that obtained for k_1 (see (8.33)). If it turned out (as it did) that

$$k_1 = bk_2 \qquad (8.37)$$

then the dynamic equation would be identical for each case, viz :

$$\dot{x} = -cx^2 - kx \qquad (8.38)$$

where, in case 1, k_1 was substituted for k and, in case 2, bk_2 was substituted for k. In figure 8.6 it displayed the value of k_2 obtained by the program at the end of each iteration. The program was stopped after 38 iterations because there was a time limit of 1 hour for any program run at R.A.F. Cranwell. The oscillatory pattern observed was a feature of this program when non-unity values of b were used. Figure 8.7 shows the feature for the same problem but with the upper limit of integration increased to 3.0. Also shown in figure 8.7 is the convergence curve for a different initial guess for the value of k. Note that the solution for a starting value of $k_2 = -1.0$ converged sooner although it started off initially in the wrong direction. It has always been the experience of the author with this program that, when the coefficient of the single input control is non-unity oscillatory convergence

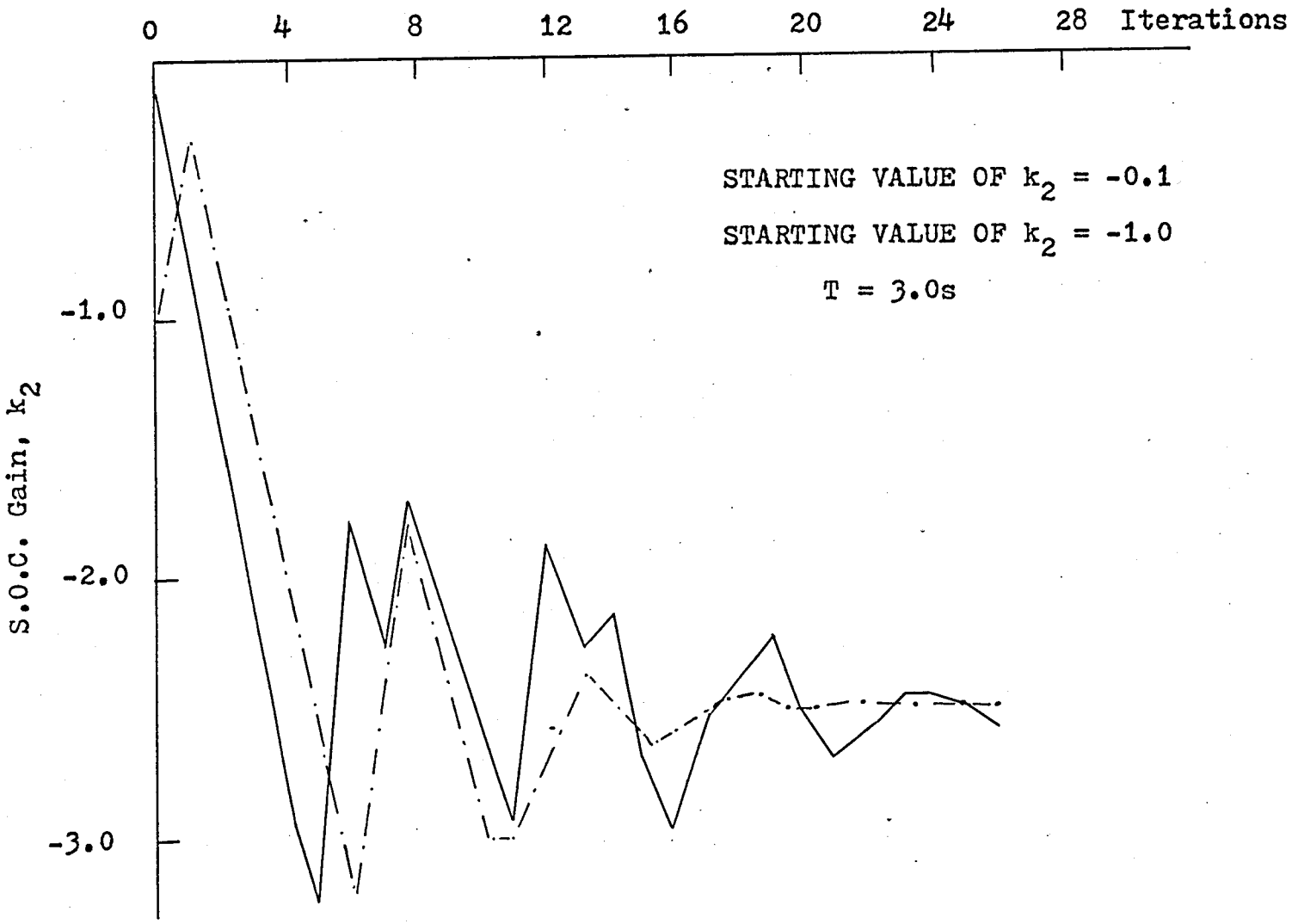

Figure 8.7 - Comparison of S.O.C. Convergence Characteristics

occurred with the associated large number of iterations and the increased execution time. It is to avoid, or at least to minimise the effects of this feature that b should always be taken as unity and some appropriate adjustment made to the final computed value, k.

For the dynamometer the required control law (case 2) was

$$u = Q_f = Q_e = -2.4236\omega_f \qquad (8.39)^*$$

The production of torque from a speed deviation signal is shown in a schematic in figure 8.8 in which the dynamics of the throttle servomechanism have been ignored.

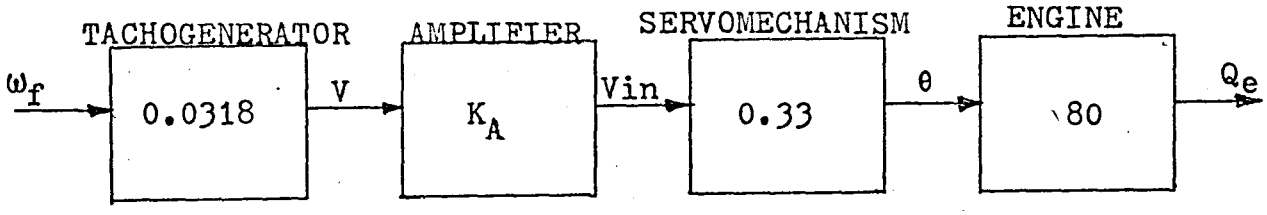

Figure 8.8 - Control Signal Transduction

From figure 8.8 it can be derived that

$$Q_e = 0.83952K_A\omega_f \qquad (8.40)$$

Therefore, from a comparison of (8.39) and (8.40) the value of the gain of the feedback amplifier was found to be

$$K_A = 2.89 \qquad (8.41)$$

---

*This assumes that 4th gear was selected.

8.3.3 S.O.C. of Engine and Dynamometer

The engine/load system equation was given in (2.85). The performance index chosen for minimisation was :

$$J = 0.5 \int_0^T (x_1^2 + V_{in}^2)dt \tag{8.42}$$

where $$V_{in} = kx_1 \tag{8.43}$$

Hence $$J(k) = 0.5\int_0^T ([k^2 + 1]x_1^2)dt \tag{8.44}$$

The additional state variable, x_4, was defined to be k and therefore the Hamiltonian was found to be :

$$H = 0.5(k^2 + 1)x_1^2 + \psi_1(-cx_1^2 + 267x_2) + \psi_2 x_3 + \psi_3(-130x_2 - 16x_3 + 43.3x_1 k) \tag{8.45}$$

The canonical equations were :

$$\dot{x}_1 = -cx_1^2 + 267x_2 \tag{8.46}$$

$$\dot{x}_2 = x_3 \tag{8.47}$$

$$\dot{x}_3 = -130x_2 - 16x_3 + 43.3kx_1 \tag{8.48}$$

$$\dot{x}_4 = 0 \tag{8.49}$$

$$\dot{\psi}_1 = -(k^2+1)x_1 + 2cx_1\psi_1 - 43.3k\psi_3 \tag{8.50}$$

$$\dot{\psi}_2 = -267\psi_1 + 130\psi_3 \tag{8.51}$$

$$\dot{\psi}_3 = -\psi_2 + 16\psi_3 \tag{8.52}$$

$$\dot{\psi}_4 = -kx_1^2 - 43.3x_1\psi_3 \tag{8.53}$$

Application of the Q.L. method to these equations produced :

$$\dot{\underline{z}}^{i+1} = A\underline{z}^{i+1} + \underline{v} \tag{8.54}$$

where

$$\underline{z}' = [x_1\ x_2\ x_3\ x_4\ \psi_1\ \psi_2\ \psi_3\ \psi_4] \tag{8.55}$$

and the matrix A was given by :

$$A = \begin{bmatrix} -2cz_1 & 267 & 0 & 0 & 0 & 0 & 0 & 0 \\ 0 & 0 & 1 & 0 & 0 & 0 & 0 & 0 \\ 43.3z_4 & -130 & -16 & 43.3z_1 & 0 & 0 & 0 & 0 \\ 0 & 0 & 0 & 0 & 0 & 0 & 0 & 0 \\ (-z_4^2+1)+2cz_5 & 0 & 0 & -(2z_4z_1+43.3z_7) & 2cz_1 & 0 & -43.3z_4 & 0 \\ 0 & 0 & 0 & 0 & -267 & 0 & 130 & 0 \\ 0 & 0 & 0 & 0 & 0 & -1 & 16 & 0 \\ (-2z_4z_1-43.3z_7) & 0 & 0 & -z_1^2 & 0 & 0 & -43.3z_1 & 0 \end{bmatrix} \tag{8.56}$$

and

$$\underline{v} = \begin{bmatrix} cz_1^2 \\ 0 \\ -43.3z_4z_1 \\ 0 \\ 2z_1z_4^2-2cz_1z_5+43.3z_4z_7 \\ 0 \\ 0 \\ 2z_1^2z_4+43.3z_1z_7 \end{bmatrix} \tag{8.57}$$

The associated boundary conditions were selected to be

$$\underline{c}'(0) = [2.000\ 0\ 0\ 0\ 0\ 0]^* \tag{8.58}$$

For the same state equations and performance index it is possible to use a different control law. E.g. consider

$$V_{in} = k_1x_1 + k_2x_2 + k_3x_3 \tag{8.59}$$

---

*The selection of the boundary conditions is restricted to the initial states; the final values of the adjoint variables were fixed by the problem. Therefore the boundary conditions were:

$$\underline{c} = [x_1(0), x_2(0), x_3(0), \psi_4(0), \psi_1(T), \psi_2(T), \psi_3(T), \psi_4(T)]$$

thus :

$$\dot{x} = (43.3k_2-130)x_2 + (43.3k_3-16)x_3 + 43.3k_1x_1 \qquad (8.60)$$

and

$$J = 0.5\ (k_1^2x_1^2+k_2^2x_2^2+k_3^2x_3^2+2k_1k_2x_1x_2+2k_1k_3x_1x_3+2k_2k_3x_2x_3+x_1^2)dt \qquad (8.61)$$

The canonical equations become then :

$$\dot{x}_1 = -cx_1^2 + 267x_2 \qquad (8.62)$$

$$\dot{x}_2 = x_3 \qquad (8.63)$$

$$\dot{x}_3 = (43.3k_2-130)x_2 +(43.3k_3-16)x_3 +43.3k_1x_1 \qquad (8.60)$$

$$\dot{x}_4 = 0 \qquad (8.64)$$

$$\dot{x}_5 = 0 \qquad (8.65)$$

$$\dot{x}_6 = 0 \qquad (8.66)$$

$$\dot{\psi}_1 = -k_1^2x_1-k_1k_2x_2-k_1k_3x_3-x_1+2cx_1\psi_1-43.3k_1\psi_3 \qquad (8.67)$$

$$\dot{\psi}_2 = -k_2^2x_2-k_1k_2x_1-k_2k_3x_3-267\psi_1+130\psi_3-43.3k_2\psi_3 \qquad (8.68)$$

$$\dot{\psi}_3 = -k_3^2x_3-k_1k_3x_1-k_2k_3x_2-\psi_2+16\psi_3-43.3k_3\psi_3 \qquad (8.69)$$

$$\dot{\psi}_4 = -k_1x_1^2-k_2x_1x_2-k_3x_1x_3-43.3x_1\psi_3 \qquad (8.70)$$

$$\dot{\psi}_5 = -k_2x_2^2-k_1x_1x_2-k_3x_2x_3-43.3x_2\psi_3 \qquad (8.71)$$

$$\dot{\psi}_6 = -k_3x_3^2-k_1x_1x_3-k_2x_2x_3-43.3x_3\psi_3 \qquad (8.72)$$

Thus the canonical vector is of dimension 12. The A matrix is given as figure 8.9 and the vector, $\underline{v}$ is :

$$\underline{v} = \begin{bmatrix} cz_1^2 \\ 0 \\ -43.3(z_1z_4+z_2z_5+z_3z_6) \\ 0 \\ 0 \\ 0 \\ 2z_1z_4^2+2z_2z_4z_5+2z_3z_4z_6-2cz_1z_7+43.3z_4z_9 \\ 2z_2z_5^2+2z_1z_4z_5+2z_3z_5z_6+43.3z_5z_9 \\ 2z_3z_6^2+2z_1z_4z_6+2z_2z_5z_6+43.3z_6z_9 \\ 2z_1^2z_4+2z_1z_2z_5+2z_1z_3z_6+43.3z_1z_9 \\ 2z_2^2z_5+2z_1z_2z_4+2z_2z_3z_6+43.3z_2z_9 \\ 2z_3^2z_6+2z_1z_3z_4+2z_2z_1z_6+43.3z_3z_9 \end{bmatrix} \qquad (8.73)$$

$$
\begin{bmatrix}
-2cz_1 & 267 & 0 & 0 & 0 & 0 & 0 & 0 & 0 & 0 & 0 & 0 \\
0 & 0 & 1 & 0 & 0 & 0 & 0 & 0 & 0 & 0 & 0 & 0 \\
43.3z_4 & (43.3z_5-130) & (43.3z_6-16) & 43.3z_1 & 43.3z_2 & 43.3z_3 & 0 & 0 & 0 & 0 & 0 & 0 \\
0 & 0 & 0 & 0 & 0 & 0 & 0 & 0 & 0 & 0 & 0 & 0 \\
0 & 0 & 0 & 0 & 0 & 0 & 0 & 0 & 0 & 0 & 0 & 0 \\
0 & 0 & 0 & 0 & 0 & 0 & 0 & 0 & 0 & 0 & 0 & 0 \\
(2cz_7-1-z_4^2)-z_4z_5 & -z_4z_6(-2z_1z_4-z_2z_5-z_3z_6-43.3z_9)-z_2z_4 & -z_3z_4 & 2cz_1 & 0 & -43.3z_4 & 0 & 0 & 0 \\
-z_4z_5 & -z_5^2 & -z_5z_6 & -z_1z_5 & (-2z_2z_5-z_3z_6-z_1z_4-43.3z_9) & -z_3z_5 & -267 & 0 & (130-43.3z_5) & 0 & 0 & 0 \\
-z_4z_6 & -z_5z_6 & -z_6^2 & -z_1z_6 & -z_2z_6 & (-2z_3z_6-z_1z_4-z_2z_5-43.3z_9 & 0 & -1 & (16-43.3z_6) & 0 & 0 & 0 \\
(-2z_1z_4-z_2z_5-z_3z_6-43.3z_9) & -z_1z_9 & -z_1z_6 & -z_1^2 & -z_1z_2 & -z_1z_3 & 0 & 0 & -43.3z_1 & 0 & 0 & 0 \\
-z_2z_4 & (-2z_2z_5-z_1z_4-z_3z_6-43.3z_9) & -z_2z_6 & -z_1z_2 & -z_2^2 & -z_2z_3 & 0 & 0 & -43.3z_2 & 0 & 0 & 0 \\
-z_3z_4 & -z_3z_5 & (-2z_3z_6-z_1z_4-z_2z_5-43.3z_9) & -z_1z_3 & -z_2z_3 & -z_3^2 & 0 & 0 & -43.3z_3 & 0 & 0 & 0
\end{bmatrix}
$$

Figure 8.9 - S.O.C. A Matrix

Because of its size this problem could not be run on the computing facilities at R.A.F. Cranwell. The problem outlined in (8.42)-(8.58) was solved however, for a fan setting of 7.62 cm. The results are summarised in table 8.3 and in figure 8.10 which shows the output shaft speed trajectory.

Serial No.	T	Initial Guess, k_o	Execution Time	Iterations	S.O.C. Value
1	1.5	-0.03	53m 03s	5	-0.01930167
2	3.0	-0.03	58m 04s	5	-0.01277291
3	1.0	-0.019	21m 39s	2	-0.03296742
4	3.0	-0.012	60m 38s	5	-0.01332018

Table 8.3 - S.O.C. Results for Engine/Load System

It must be emphasised that when the program was attempted with the Runge-Kutta routine it did not appear to converge. There were several occasions however when it was impossible to state that the program was not converging; on those occasions only a single iteration had been completed by the time the maximum allowable computing period had expired. The program was modified to use the Hamming integration routine described in section 6 of chapter 5 to improve the convergence time. Even with this procedure however it should be noted that when an integration step length of 0.1 second

was utilised the program (see serial nos. 1 and 2 of table 8.3) had not converged in 60 minutes. In serial nos. 3 and 4 the program diverged and computation ceased because of floating point overflows. For serial nos. 2 and 4 the step length was 0.05 second, and for serial nos. 1 and 3 the step length was reduced to 0.025 second. From the results shown in table 8.3 it is plain that :

(i) when the initial guess was good (i.e. "close" to the final s.o.c. value) convergence was rapid.

(ii) the shorter the period over which the performance index was evaluated, and consequently the shorter the time available to restore the system to equilibrium, the greater was the s.o.c. value.

(iii) when the initial guess was below the s.o.c. value (but was close enough to ensure convergence) the convergence was most rapid.*

Another feature of ensuring convergence lies in the interplay between the given initial conditions and the guessed initial trajectory. In every case considered the initial solution was chosen to be a ramp function descending from some specified initial deviation of output shaft speed to zero value at the terminal time. With this choice it was essential that the value of the initial deviation of shaft speed had been chosen with care : for all cases considered $x_1(0)$ was taken

---

*This appears to be the case on almost every occasion with Q.L. techniques : values below the optimum give rise to smaller deviations and hence the Taylor's series approximation still retains its validity.

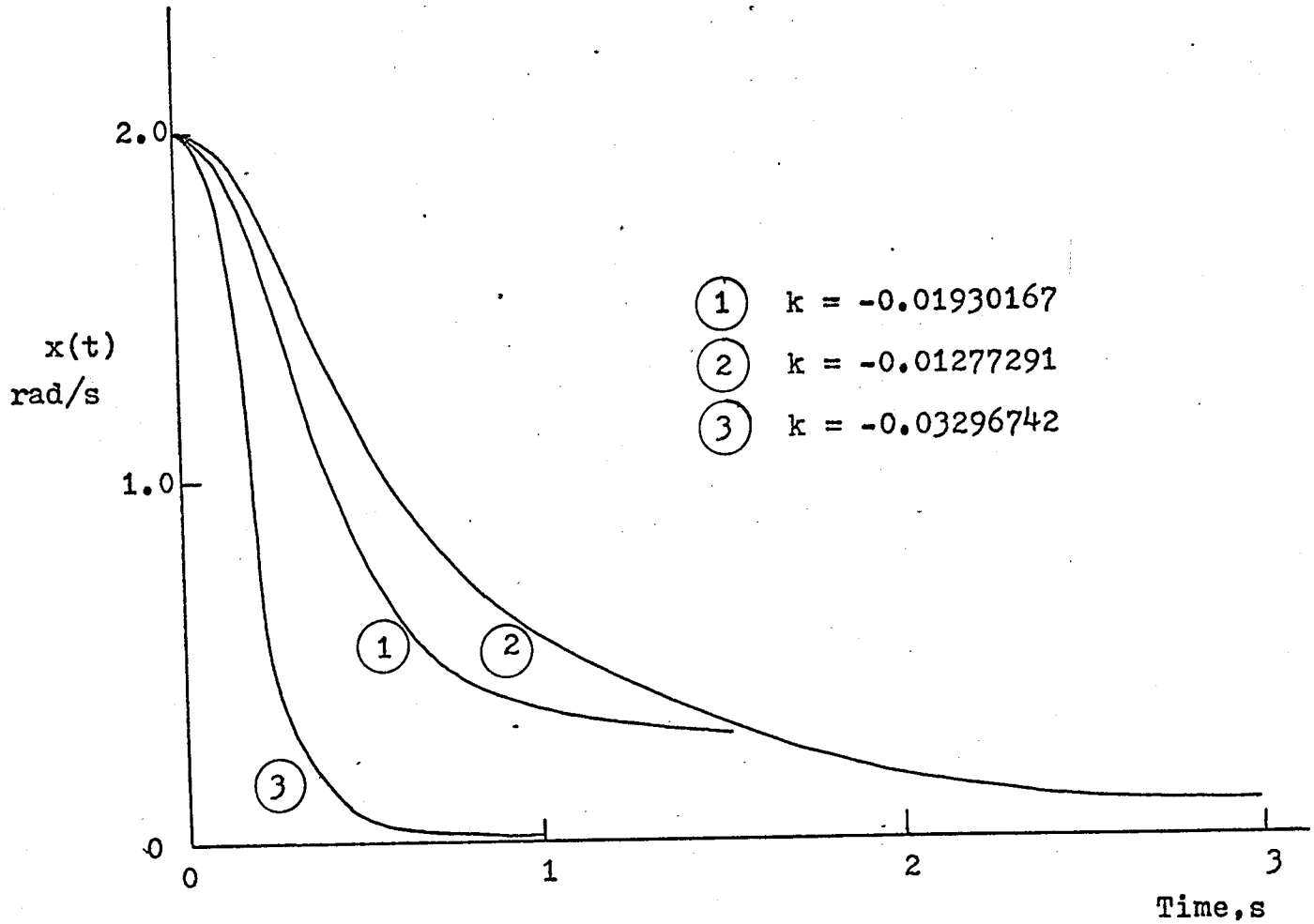

Figure 8.10 - S.O.C. Trajectories

as 2.0. When $x_1(0)$ was selected to be 10.0 the program diverged. Attempts to improve the solution by reducing the step length in half, and by using as initial values the s.o.c. values already obtained, were thwarted because such changes resulted in the available storage of the 4120 computer being exceeded; the program was not then processed. However, the values obtained for the s.o.c. of the dynamometer alone were used to provide the initial guesses for the s.o.c. of the engine/load system with the throttle servomechanism. The influence upon the s.o.c. gain of the choice of final time, T, is shown in figure 8.10.

When the gains of table 8.3 were tried on the experimental rig, using the controller of figure 6.6, the trajectories which resulted are shown in figure 8.11. The same phenomenon of destabilised response with change of reference speed was again observed. A run over the simulated road with this s.o.c. resulted in good response with no evidence of the destabilisation. It was not possible to demonstrate on the engine rig the sub-optimailty of this scheme in comparison with the optimal schemes derived in chapter 6.

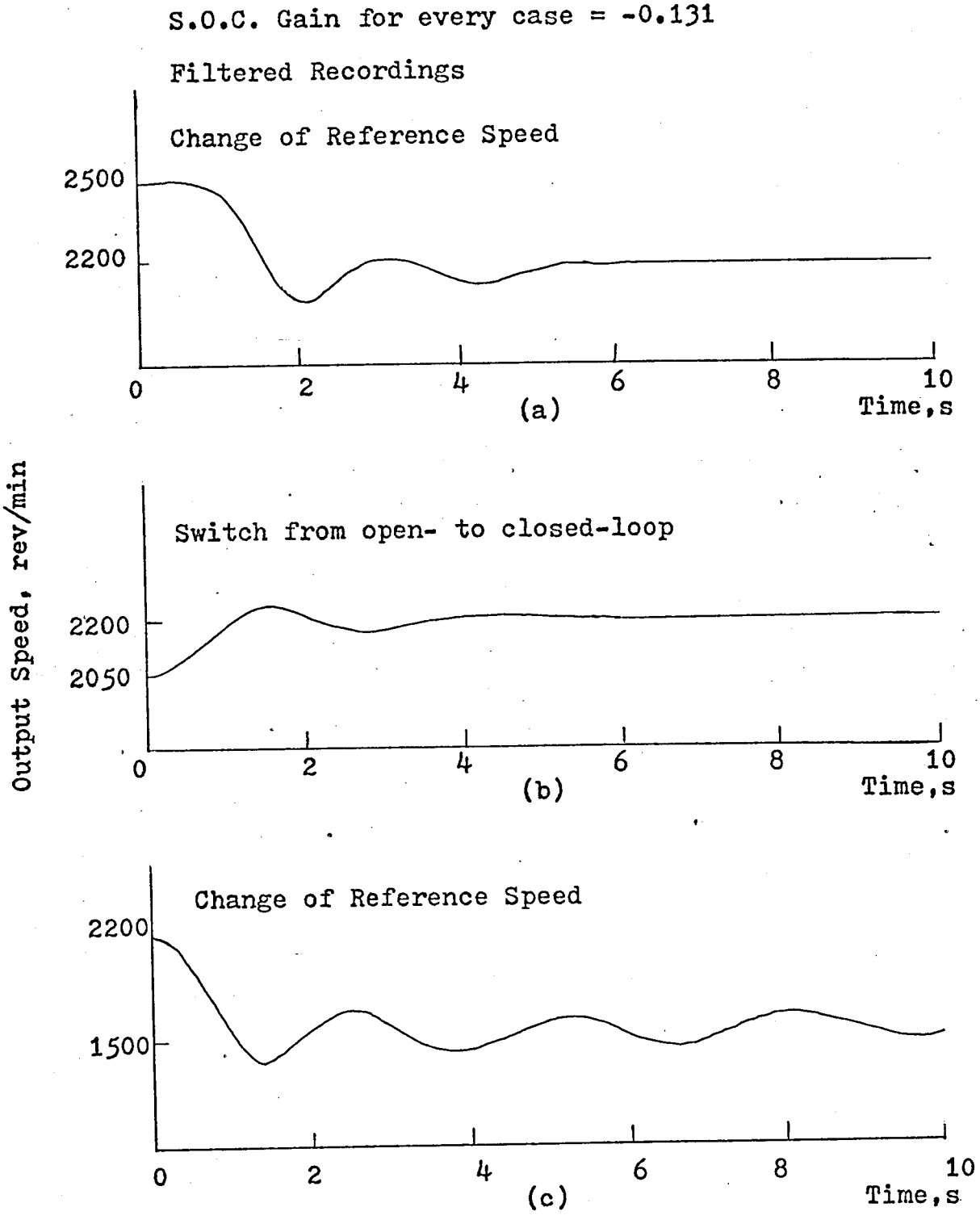

Figure 8.11 - Engine System Responses with S.O.C. Regulation

CHAPTER NINE - CONCLUSIONS

9.1 Concluding Summary and Discussion

The work undertaken in the conduct of this research involved extensive experimental testing and analogue simulation studies to develop adequate mathematical models of the engine, load and transmission system. In particular in chapter 2 three mathematical models were established :

(a) a pseudo-linear model which was used in the regulation studies considered in the research; and which assumed the engine transmission system was operating in fourth gear

(b) a non-linear model which was used in the regulation studies and which assumed the engine transmission system was operating in fourth gear

(c) a non-linear model which accounted for the behaviour of the engine and load during gear changes.

This non-linear model was used exclusively in the consideration of the problem of optimal start-up. All the mathematical models were obtained from matching simulation results with data obtained from experimental studies on the engine rig. The pseudo-linear model was established in an optimal sense in that it minimized the ISE which existed between the linear and non-linear model of the load.

The non-linear gear-changing model was used successfully to establish, by means of the method of quasilinearisation, an optimal start-up control function. A considerable

amount of work was carried out in developing suitable programs to determine this optimal start-up control function. Many of the difficulties associated with obtaining solutions were associated with the computational facilities available to the author at the time of the research. The optimal control function was synthesised and some of the experimental results obtained were presented in chapter five. The implementation of this optimal start-up scheme required the development and construction of an automatic gear-changing scheme the details of which were presented in chapter three together with some computer results used to confirm the validity of the gear-changing scheme.

In order to provide as realistic a method of loading the engine as the facilities available would permit, a scheme for generating a simulated 'road' function was developed and an account of its implementation, and of the statistical properties of the generated function, was given in chapter five.

The optimal regulation of the engine in the presence of load disturbances was considered extensively in chapter six. Five methods of computing the optimal control gains, assuming that the problem could be considered as a linear quadratic problem, were studied and corresponding digital computer programs were developed. These programs were compared from the standpoints of accuracy, execution time and ease of programming. The most effective method was found to be that developed by Marshall and Nicholson from earlier work by MacFarlane. Because all the computational work for this research was programmed in Algol 60 and because the eigen-analysis program available to the author was written in

Fortran IV, and required therefore separate processing, it proved too inconvenient to perform by this method at RAF Cranwell the bulk of the numerical experiments. Consequently the next most effective method, that due to Kleinman, was employed extensively in determining the control laws for this part of the work. An analytical method which required little computation was considered also : control laws similar to those found already were obtained but the method was judged to be cumbersome and is not recommended therefore for further use. Analogue computer studies and experimental engine runs were undertaken using the control laws already determined : both the corresponding simulation and experimental rig results showed that good regulation was obtained. The tolerance of the feedback control laws to the presence of unaccounted-for non-linearities was demonstrated. However, study of the responses obtained from the engine rig did show the existence of limit cycling and an associated destabilisation whenever the reference speed was changed from the design figure by too great an amount. All the schemes of regulation presented in chapter six were successful in the presence of load variations. They were less effective when the reference speed was changed.

The study of minimal sensitivity optimal control scheme, reported in chapter seven, revealed that earlier studies of this problem which were presented in the literature of the subject were erroneous. A satisfactory engineering method of designing a controller, the structure of which was defined a priori, was used. The results obtained indicated that the optimal control gains were not affected greatly by changes in the value of the parameters of the system or by the initial

conditions assumed. This is the property of minimal sensitivity. However, with control laws similar to those found earlier the results obtained from experimental engine runs using these gains were essentially the same as those obtained with the control laws of chapter six; destabilised response with changed reference speed. The method of model-following was used next to produce control laws to ensure the correct dynamic response; the study showed that zero sensitivity could not be obtained but that specified dynamic response could be achieved. The results from the engine rig with these control laws were similar to the results obtained already using other methods. The method did not in any way predict existence of a limit cycle. However, the cumulative evidence of all these approaches, allied to analogue computer studies, support the view that the limit cycle or associated destabilisation of the response, was not due to incorrect parameter values in the pseudo linear models (which could be regarded as a parameter variation). In chapter ~~nine~~ eight therefore, an attempt was made to take into account specifically the true, non-linear nature of the load by using the non-linear regulation model established in chapter two. A novel scheme, proposed by Gustafson and Harwood, was essayed first but the resulting non-linear controller did not prove satisfactory : the associated analogue computer study showed no benefit from including the non-linear term and the value of non-linear control gain was so small that the difficulty of implementing the controller physically was acute. By modifying extensively the programs of chapter five the method of specific optimal control was considered next. A linear controller was derived

but, because of the computational complexity associated with the method of quasilinearisation, only a single gain controller could be determined. Because it was necessary to include load effects the control gain chosen was that operating on the load speed. Satisfactory results were obtained from this scheme but the same destabilising effect due to change of reference speed was again observed. Extensive investigation using the computer model of figure 2.27 did not produce this limit cycling when using any of the controllers established by the methods of chapters six, seven and eight. The inclusion in the simulation of simple first order terms in the feedback lines or between throttle position and engine torque (to represent the time delay due to the combustion process or neglected time lags in the measurement paths) did not produce the effect. It is then an effect due to the non-linear nature of the load and to the dynamics of the engine. The practical regulation schemes all worked in the way intended. However, it is evident that the same control laws do not permit satisfactory operation as servomechanisms : for the LQP there is no resulting change of feedback gains if the reference is changed. For a non-linear system this is not true generally; consequently further study is needed to develop the necessary feedforward control law necessary to ensure that the scheme will work also as a servomechanism.

9.2 Suggestions for Further Research

9.2.1 Refinement of Models

Further studies are required to produce a more detailed model of the engine to take into account the slow dynamics associated with changes of engine timing and to

account for the dynamics associated with the combustion process. Such studies will require the development of a more robust program for system identification. However, if the suggestions of 9.2.3 in respect of the dynamometer are adopted the program BEARDM20 would be more effective but should be modified so that the program will select on the basis of the input data the sampling interval to be used. This modification will improve the convergence, speed and accuracy of the problem.

9.2.2 Computational Methods

(a) Quasilinearisation

Because of the length of time required to obtain a solution using the programs as developed it is suggested that an investigation should be undertaken to employ the method of particular solutions proposed recently by MIELE and IYER and their co-workers (1970 a,b , 1971) at Rice University of Houston, Texas. This method appears to offer significant improvements in the associated convergence properties and in lack of sensitivity to the initial trial solution which were both severe problems with the method of quasilinearisation. Such an investigation will permit the optimal start-up problem to be considered exclusively from the point of view of providing minimal time gear-changing which could not be done in this research because of the restricted computational facilities. Also the investigations using specific optimal control could be completed.

(b) Specific Optimal Control

The investigation carried out so far could be extended usefully to include consideration of dynamic controllers. Of particular interest would be a study to determine the

effectiveness of using the traditional three-term controller, with optimal gains; there is no analytical justification in modern control theory for an integral term although its use is almost always required in practice.*

(c) LQP and Model-Following

An extensive investigation relating the control gains to the elements of the weighting matrices should be undertaken in conjunction with corresponding engine runs to determine the global relationship of fuel consumption to weighting matrices for a step load change. (This can be accomplished only if the recommendation of section 9.2.3 is implemented). This would permit the development of explicit relationships between the parameters of the performance index and the characteristics of the optimal closed-loop system. With the use of the model-following program studies could be made to develop a relationship between desirable closed-loop response and resulting fuel consumption performance.

9.2.3 Improvements to the Engine Rig

For further work it would be helpful to replace the present fan dynamometer with an electric dynamometer. Engine loading would then be linear with a consequent reduction in computational difficulties. Control of engine loading would also be greatly simplified. However, because of power output from the engine a 100 KW generator would be required; this would require a new site for the engine rig.

---

* In the studies presented in this thesis it was present in that some crude filter was already in use to remove engine vibration noise from the tach signal.

For the refinement of engine models (proposed in section 9.2.1) it will be necessary to design, construct and install a new electronic ignition system to replace the present electro-mechanical system. To model the manifold dynamics requires only a pressure transducer (in the range 0 - 450 kilopascals with a d.c. electrical output voltage) to be connected to the manifold. (On the existing rig there is a pressure meter already fitted : the pressure line to that instrument can be used as the input to the electrical pressure transducer). The output from this device, when recorded in response to throttle action, would provide sufficient data to allow an attempt at identifying the dynamics. Since it is known that a pure time delay (although small) exists it would be preferable possibly to attempt the identification by means of frequency response analysis in which the phase contribution of the time delay is most easily detected.

An unsatisfactory feature of the present work has been the crude measurement of fuel consumption. Turbulent flow of the petroleum does occur with demands for large values of engine acceleration. This turbulence makes measurement difficult and this accounts for the uncertainty in the fuel consumption data used in this work. It is recommended that for future work a flowmeter with an electrical output should be designed and developed for use with the rig : if the flowmeter output is either a pulse rate or a d.c. voltage proportional to fuel flow rate, then the fuel consumed in any given period can be determined by integrating, in an integrating amplifier, the flowmeter output.

The air consumed by the engine was not measured in the

present work since the mechanical efficiency of the engine cannot be improved by external controllers without modifying the engine, the air breathing system or the manifold arrangement. It is believed, however, that for future work the provision of some arrangement to measure air consumption would provide additional information for refinement of the mathematical models, particularly in respect of the attempt to identify the manifold dynamics.

9.3 Conclusions

From the nature of the results obtained from many of the optimisation programs it is evident that future engineering applications will require, for the successful implementation of the control schemes, digital controllers rather than the logic-controlled analogue controllers used in this work. It should be stressed too that mathematical modelling must be regarded now as an essential part of any control system design : the successful application of control theory depends almost entirely upon the adequacy of the model of the physical system to be controlled. In this work the three major branches of control engineering have been involved viz :

mathematical modelling

optimisation

computation

It has been shown that the application of the results of analysis does permit the practical solution of one engineering problem in ways that could not be arrived at properly by other methods.

REFERENCES

ANSDALE R.

(1964) AUTOMATIC TRANSMISSIONS

FOULIS, LONDON, 1964, pp. 31-44

ASSEO S.J.

(1968) "Applications of Optimal Control to Perfect Model-Following"

JACC(1963), 1056-1070

(1969) "Optimal Control of a Servo Derived from Nonquadratic Performance Criteria"

Trans IEE, 1969, Vol.AC-14, No.3,404-407

ATHANS M.

(1971) "The Role and Use of the Stochastic Linear Quadratic Gaussian Problem in Control System Design"

Trans IEEE, 1971, Vol.AC-16, No.6 pp.529-552

ATHANS M. and P.L. FALB

(1966) OPTIMAL CONTROL

McGRAW-HILL, N.Y., 1966

a pp. 245-246
b pp. 451-456
c pp. 269-291
d p. 767

BANHAM J.W. and W.L. SMITH

(1966) "A Practical Approach to Adaptive Control"

Control Engineering, 1966, May, 97-102

BARNETT S. and C. STOREY

(1966) "Insensitivity of Optimal Linear Control Systems to Persistent Changes in Parameters" Int.J.Control, 1966, Vol.4, No.2, 179-184

BECKETT R. and J. HUNT

(1967) NUMERICAL CALCULATIONS and ALGORITHMS McGRAW-HILL, N.Y., 1967, pp. 70-74

BELLMAN R.

(1960) INTRODUCTION TO MATRIX ANALYSIS McGRAW-HILL, N.Y., 1960

a pp. 165-169
b pp. 230-231

BELLMAN R. and R.E. KALABA

(1965) QUASILINEARISATION and NONLINEAR BOUNDARY VALUE PROBLEMS ELSEVIER, N.Y., 1965, pp. 99-102

BELTRAMI E.J.

(1970) AN ALGORITHMIC APPROACH TO NONLINEAR ANALYSIS AND OPTIMIZATION ACADEMIC PRESS, N.Y., 1970, p. 205

BLACQUIERE A.

(1962) "Une Nouvelle Methode de Linearisation Locale des Operateurs NonLineaires Approximations Optimale" NONLINEAR VIBRATION PROBLEMS. 2nd CONFERENCE NONLINEAR VIBRATIONS, WARSAW, 1962

BURGHART J.G.

(1969) a "Sub-Optimal Linear Regulation for System Subject to Parameter Variations"

Trans IEE, 1969, Vol.AC-14, No.6, 285-289

b "A Technique for Sub-Optimal Feedback Control of Non-Linear Systems"
Trans IEE, 1969, Vol.AC-14, No.10, 530-533

BRYSON A.E. and Y.C. HO

(1969) APPLIED OPTIMAL CONTROL
BLAISDELL, WALTHAM, 1969, pp. 42-89

CANNON R.H.

(1967) DYNAMICS OF PHYSICAL SYSTEMS
McGRAW-HILL, N.Y., 1967, pp. 561-562

CITRON S.J.

(1969) ELEMENTS OF OPTIMAL CONTROL
HOLT, RINEHART and WINSTON, N.Y.19, pp. 90-91

CONTE S.D.

(1966) "The Numerical Solution of Linear Boundary Value Problems"
S.I.A.M. Review, 1966, Vol.8, No.3, 309-321

CRAMER H.

(1946) MATHEMATICAL METHODS OF STATISTICS
PRINCETON UNIVERSITY PRESS, 1946, pp. 244-246

CROSSLEY T.R. and B. PORTER

(1970) "Inversion of Complex Matrices"
Electronics Letter, 1970, Feb., Vol.6, No.4

CUNNINGHAM W.J.

(1958) INTRODUCTION TO NONLINEAR ANALYSIS
McGRAW-HILL, N.Y., 1958, pp. 163-164

DAVISON E.J. and F.T. MAN

(1969) "The Numerical Solution of A'Q+QA = -C
Trans IEE, 1969, Vol. AC-13, No.4, 448

d'AZZO and C.H. HOUPIS

(1966) FEEDBACK CONTROL SYSTEM ANALYSIS AND SYNTHESIS

McGRAW-HILL, N.Y., 1966, pp. 136-161

deRUSSO P.M., R.J. ROY and C.M. CLOSE

(1965) STATE VARIABLES FOR ENGINEERS

J. WILEY, N.Y., 1965, pp. 20-25

DEUTSCH R.

(1969) SYSTEM ANALYSIS TECHNIQUES

PRENTICE HALL, N.J., 1969, 338-346

DOMPE R.J. and R.C. DORF

(1967) "The Design of Optimal Low Sensitivity Linear Control Systems"

Proc. 5th Allerton Conference, 1967, 170-180

DYER P. and S.R. McREYNOLDS

(1970) THE COMPUTATION AND THEORY OF OPTIMAL CONTROL

ACADEMIC PRESS, N.Y., 1970, pp. 218-219

EISENBERG B.R. and A.P. SAGE

(1966) "Closed Loop Optimization of Fixed Configuration Systems"

Int.J.Control, 1966, Vol.3, No.2, 183-194

ERZBERGER H.

(1968) "On the Use of Algebraic Methods in the Analysis and Design of Model-Following Control Systems"

NASA TN - D4663, July 1968

EVERSHED (Anon)

(1964/65) "Equivalent Circuit Analysis of Clutch Controls : Parts 1 and 2"

Evershed News, 1964, Vol.8, No.1, 18-20
Vol.8, No.2, 19-20

EYMAN D.E.

(1968) "Analogue Computer Study of Some Fundamental Control Relations Involving Alternators and Diesel Engines"
Int.J.Control, 1968, Vol.7, No.3, 201-221

FALB P.L. and J.L. de JONG

(1969) SOME SUCCESSIVE APPROXIMATION METHODS IN CONTROL AND OSCILLATION THEORY
ACADEMIC PRESS, N.Y., 1969, pp. 196-218

FATH A.F.

(1969) "Computational Aspects of the Linear Optimal Regulator Problem"
Trans IEEE, 1969, Vol. AC-14, No.5, 547-550

FOOTE A.L.

(1972) "Truncated Power Series Control Representations for Optimization of Dynamic Systems"
AFAL-TR-191, August 1972

GARRARD W.L.

(1969) "Additional Results on Sub-Optimal Feedback Control of Non-Linear Systems"
Int.J.Control, 1969, Vol.10, No.6, 657-663

GILES J.G.

(1961) AUTOMATIC and FLUID TRANSMISSIONS
ODHAMS, LONDON, 1961, pp. 17, 50-54, 77-81

GREENSITE A.L.

(1970) ELEMENTS OF MODERN CONTROL THEORY
SPARTAN PRESS, N.Y., 1970, pp. 126-127

GUSTAFSON R.D. and R.A. HARWOOD

(1969) "Nonlinear Optimal Control by Use of Extra Linear States to Represent Nonlinearities" Trans ASME,J.BAS.ENG., 1969, Vol.91, Ser.D, No.2, 139-148

GUTZWILLER F.W.(ed.)

(1967) SILICON CONTROLLED RECTIFIER MANUAL G.E.Co., N.Y., 1967, 4th Ed., pp. 217-218

HAMMING R.W.

(1959) "Stable Predictor-Corrector Methods for Ordinary Differential Equations" J.Assoc.Computing Mach. 1959, Vol.6, 37-47

HENDRICKS T. and H. d'ANGELO

(1967) "An Optimal Fixed Control Structure Design With Minimal Sensitivity for a Large Elastic Booster" Proc. 5th Allerton Conference, 1967, 142-151

KALMAN R.E.

(1960) "Contributions to the Theory of Optimal Control" Bol.Soc.Mat.Mex. 1960, Vol.5, 102-119

(1963) "Mathematical Description of Linear Dynamical Systems" S.I.A.M. J.Cont., 1963, Ser.A, Vol.1, No.2, 152-192

KALMAN R.E. and T.S. ENGLAR

(1966) "A User's Manual for the Automatic Synthesis Program" NASA CR-475, June 1966, 213

KENNETH P. and R. McGILL

(1966) "Two-point Boundary-Value-Problem Techniques"
ADVANCES IN CONTROL, 3, 1966, 69-109
ACADEMIC PRESS, N.Y.

KLEINMAN D.L.

(1968) "On an Iterative Technique for Riccati Equation Computations"
Trans IEEE, 1968, Vol.AC-13, No.1, 114-115

(1970) "An Iterative Technique for Riccati Equation Computations"
BBN* TECH.MEMO. No. DLK-1, June 1970
(*BOLT, BERANEK and NEWMAN)

KIRK D.E.

(1970) OPTIMAL CONTROL THEORY
PRENTICE-HALL, N.Y., 1970, pp. 357-371

KREINDLER E.

(1968) a "Closed Loop Sensitivity Reduction of Linear Optimal Control Systems"
Trans IEEE, 1968, Vol.AC-13, No.3, 254-262

b "On Minimization of Trajectory Sensitivity"
Int.J.Control, 1968, Vol.8, No.1, 89-96

(1969) "On the Linear Optimal Servo Problem"
Int.J.Control, 1969, Vol.9, No.4, 465-472

LAMONT G.B. and S.J. KAHNE

(1967) "Time Domain Sensitivity Comparisons"
Proc. 5th Allerton Conference, 1967, 161-169

LANCZOS C.

(1957) APPLIED ANALYSIS
PITMAN, LONDON, 1957, pp. 139-140

LANNING J.H. and R.H. BATTIN

(1956) RANDOM PROCESSES IN OPTIMAL CONTROL
McGRAW-HILL, N.Y., 1956, pp. 68-69

LEE, E.S.

(1968) QUASILINEARISATION AND INVARIANT IMBEDDING
ACADEMIC PRESS, N.Y., 1968, pp. 109-113

LEE R.C.K.

(1964) OPTIMAL ESTIMATION, IDENTIFICATION AND CONTROL
M.I.T. RESEARCH MONOGRAPH No.28, pp. 131-135

LONG R.S.

(1965) "Newton-Raphson Operator; Problems with Undetermined End-Points"
J.AIAA, 1965, Vol.3, 1351-1352

LUH J.Y.S. and E.R. CROSS

(1967) "Optimal Controller Design for Minimum Trajectory Sensitivity"
Proc. 5th Allerton Conference, 1967, 152-160

LUKES D.L.

(1969) "Optimal Regulation of Nonlinear Dynamical Systems"
S.I.A.M. J. Control, 1969, Vol.7, No.1, 75-100

MacFARLANE A.G.J.

(1963) "An Eigenvector Solution of the Optimal Linear Regulator Problem"
J.Elec. and Cont. 1963, Vol.14, 643-654

MAKI M.C.

(1972) "Numerical Solution of the Algebraic Riccati Equation for Single-Input Systems:
Trans IEEE, 1972, Vol.AC-17, No.4, 264-265

MANKIN J.R. and J.C. HUNG

(1969) "On Round Off Errors in Computation of Transition Matrices"
10th JACC. 1969, 60-64

MARKLAND C.A.

(1970) "Optimal Model-Following Control System Synthesis Techniques"
Proc. IEE, 1970, Vol.117, No.3, 623-627

MARSHALL S.A. and H. NICHOLSON

(1970) "Optimal Control of Linear Multivariable Systems With Quadratic Performance Criteria"
Proc. IEE, 1970, Vol.117, No.8, 1705-1713

MAYNE D.Q.

(1970) "Methods for Optimizing Dynamic Systems"
IEE Conf. Publication No.66, 1970, 15-23

MIELE A. and R.R. IYER

(1970) "A General Technique for Solving Nonlinear Two Point Boundary Value Problems Via the Method of Particular Solutions"
J.O.T.A., 1970, Vol.5, 382-399

MIELE A.A., R.R. IYER and K.H. WELL

(1970) "Modified Quasilinearisation and Optimal Initial Choice of the Multipliers.
Part 2 : Optimal Control Problems"
Rice University Report, 1970, AAR-77,
Rice University, Houston, Texas

MIELE A.A., S. NAQVI, A.V. LEVY and R.R. IYER

(1971) "Numerical Solution of Non-Linear Equations and Non-Linear Two Point Boundary Value Problems
ADVANCES IN CONTROL, 8, 1971, pp. 189-215
ACADEMIC PRESS, N.Y.

MOLINARI B.E.

(1969) "Algebraic Solution of Matrix Linear Equations in Control Theory"
Proc. IEE, 1969, Vol.116, No.10, 1748-1754

MONK H. and J. COMFORT

(1970) "Mathematical Model of an Internal Combustion Engine and Dynamometer Test Rig"
Trans Inst.M.C., 1970, Vol.3, No.6, 93-100

MORTENSEN R.E.

(1968) "Mathematical Problems of Modelling Stochastic Non-Linear Dynamic Systems"
NASA CR-1168, 1968

NEWMANN M.M.

(1970) "On Attempts to Reduce the Sensitivity of the Optimal Linear Regulator to a Parameter Change"
Int.J.Control, 1970, Vol.11, No.5, 1079-1084

NICHOLSON H.

(1964) "Dynamic Optimisation of a Boiler"
Proc. IEE, 1964, Vol.111, No.8, 1479-1499

PACE I.S. and S. BARNETT

(1972) "Comparison of Numerical Methods of Solving Lyapunov Matrix Equations"
Int.J.Control 1972, Vol.15, No.5, 907-915

PEARSON J.D.

(1962) "Approximation Methods in Optimal Control"
J. Electron Control, 1962, Vol.13, 453-469

PENROSE R.

(1955) "A generalized inverse for matrices"
Proc.Camb.Phil.Soc. 1955, Vol.51, 406-413

POTTER J.E.

(1966) "Matrix quadratic solutions"
S.I.A.M. J.Appl.Math., 1966, Vol.14, 496-501

PROPOI A.I. and Ya. Z. TSYPKIN

(1968) "Synthesis of Optimal-in-the-Mean Automatic Systems"
Doklady, 1968, Vol.12, No.8, 768-769

PURI N.N.

(1966) "Optimal Design of Regulators"
J.Frank.Inst., 1966, Vol.281, No.6, 499-513

RADBILL J.R. and G.A. McCUE

(1971) QUASILINEARISATION AND NONLINEAR PROBLEMS IN FLUID and ORBITAL MECHANICS
ELSEVIER N.Y., 1971, pp. 8-21

RALSTON A.

(1960) "Numerical Integration Methods for the Solution of Ordinary Differential Equations"
MATH. METHODS FOR DIGITAL COMPUTERS
(ed. RALSTON & WILF)
J. WILEY, N.Y., 1960, pp. 101-103

RICARDO H.

(1953) HIGH SPEED INTERNAL COMBUSTION ENGINE
BLACKIE, GLASGOW, 1953, pp. 57-58

ROBERTS S.M. and J.S. SHIPMAN

(1972) TWO POINT BOUNDARY VALUE PROBLEMS - SHOOTING METHODS

ELSEVIER, N.Y., 1972

a pp. 101-106
b p. 91

ROSENBROCK H.H. and C. STOREY

(1971) MATHEMATICS OF DYNAMICAL SYSTEMS

NELSON, EDINBURGH, 1971, pp. 68-69

ROTHSCHILD D. and A. JAMESON

(1970) "Comparison of Four Numerical Algorithms for Solving the Lyapunov Matrix Equation"

Int.J.Cont., 1970, Vol.11, No.2, 181-198

SALMOND M. and P.V. KOKOTOVIC

(1969) "Design of Linear Controllers for Nonlinear Plants"

Trans IEEE, 1969, Vol.AC-14, No.6, 289-292

SAGE A.P.

(1968) OPTIMUM SYSTEMS CONTROL

PRENTICE HALL, N.Y., 1968

a pp. 66-70
b pp. 439-456

SAGE A.P. and J.L. MELSA

(1971) SYSTEM IDENTIFICATION

ACADEMIC PRESS, N.Y., 1971, pp. 152-167

SCHULTZ D.G. and J.L. MELSA

(1967) STATE FUNCTIONS and LINEAR CONTROL SYSTEMS

J. WILEY, N.Y., 1967, p. 275

SHANNON C.E.

(1948) "A Mathematical Theory of Communication"
Bell STJ, 1948, Vol.27, 379-623

SIMS C.G. and J.L. MELSA

(1968) "Sensitivity Reduction in Specific Optimal Control by the Use of a Dynamical Controller"
Int.J.Control, 1968, Vol.8, No.5, 491-502

SPEEDY C.B., R.F. BROWN, and G.C. GOODWIN

(1970) CONTROL THEORY : IDENTIFICATION and OPTIMAL CONTROL
OLIVER and BOYD, EDINBURGH, 1970, pp. 259-264

SPINGARN K.

(1970) "Some Numerical Aspects of Optimal Control"
J.Frank.Inst., 1970, Vol.289, No.5, 351-359

TAPLEY B.D. and W.E. WILLIAMSON

(1971) "A Comparison of Linear Systems and Riccati Equations Used to Solve Optimal Control Problems"
AMRL Report 1036, June 1971, University of Texas, Austin, Texas

TYLER J.S.

(1964) "The Characteristics of Model Following Systems as Synthesized by Optimal Control"
Trans IEEE, 1964, Vol. AC-9, No.4, 485-498

VAN SCHIEVEEN H.M. and H. KWAKERNAAK

(1970) "Solution of State-Constrained Optimal Control Problems through Quasilinearisation"
J.Eng.Maths., 1970, Vol.4, No.1, 87-94

WILLIAMSON W.E. and B.D. TAPLEY

(1971) "Riccati Transformations for Control Optimization Using the Second Variation"
AMRL Report 1035, June 1971, University of Texas, Austin, Texas

WILKIE D.F. and W.R. PERKINS

(1969) "Design of Model-Following Systems Using the Companion Transformation"
Automatica, 1965, Vol.5, 615-622

WONHAM W.M.

(1969) "Optimal Stochastic Control"
Automatica 1969, Vol.5, No.1, 113-118

WONHAM W.M. and CASHMAN W.F.

(1969) "A Computational Approach to Optimal Control of Stochastic Saturating Systems
Int.J.Control, 1969, Vol.10, No.1, 77-98

WONHAM W.M. and C.D. JOHNSON

(1964) "A Note on the Transformation to Canonical (Phase Variable) Form"
Trans IEEE, 1964, Vol.AC-9, No.3, 312-313

YORE E.E. and Y. TAKAHASHI

(1967) "Identification of Dynamic Systems by Digital Computer Modelling in State Space"
Trans ASME, J.Bas.Eng., 1967, Vol.89, No.2, Ser.D, 295-299

APPENDICES

APPENDIX A.1. NOTATION*

a	constant, coefficient
a_{ij}	element of system coefficient matrix, A
b	constant, coefficient
b_i	element of system driving matrix, B
c	constant, coefficient
d	fan displacement, in cm.
d_i	optimal regulator control gains
d_{ij}	boundary values in Q.L. method
g	control input weighting factor
h	road height, in ft.(m.)
i,j,k	integers
k	fan damping coefficient
k_i	controller gain
l,m,n	integers
n	order of system, gear ratio
q	constant
q_{ii}	element of state weighting matrix, Q
r	constant
s	Laplace variable
t	time
u	command input, torque input
w_i	polynomial coefficient
x_i	element of state vector
y_i	element of phase variable vector
z_i	element of augmented Q.L. vector
F	augmented cost function
F_e	engine viscous friction, N m s
H	Hamiltonian function
J	performance index, inertia (kg m^2)

*All vector quantities are underlined

L	cost functional
Q_e	torque delivered by engine, N m
Q_c	slip torque of coupling, N m
Q_l	load torque applied by fan, N m
R	performance index
T	time interval, sampling period
V_{in}	throttle servomechanism command voltage
Eps	A small positive number
γ	coupling coefficient, N m s
ϵ	a small positive number
θ	throttle position, rad
λ, λ_M	inverse time constant, s^{-1}; λ_M refers to model
λ_i	Lagrange multipliers
μ	scalar parameter, mean value, slope
ν	a positive number
ξ	dummy variable, coefficient
σ	standard deviation
τ	time to gearshift
ψ_i	costate variable
ω_e	speed of gearbox input shaft, rad/s
ω_f	speed of dynamometer shaft, rad/s
Ψ	non-linear residue
Δ	increment e.g. Δu
Ω	equilibrium speed, rad/s
Ω_e	engine shaft speed, rad/s
$E(')$	expected value operator
$G_1(s)$	plant transfer function
$G_2(s)$	controller transfer function

$N_1(s)$, $N_2(s)$, $D_1(s)$, $D_2(s)$	polynomials in s
$p(\cdot)$	probability function
$\Delta(s)$	characteristic polynomial
$\Delta_1(s), \Delta_1(-s)$	components of characteristic polynomial
$\epsilon(t)$	an error function
$\varphi(t)$	model function
dez(·)	dead-zone function
sgn(·)	signum function
$A, A_c, \tilde{A}, A^*, A_{mod}$, B, C, DA, D, D^*, $E, F, H, \tilde{H}, HA, AH, K, M, N, P, Q, S$, $T, V, W, Z, S_R, X_{orig}, \Phi, \Delta, \theta, \Xi, L$	matrices
$\underline{e}$	error vector
$\underline{f}$	vector function
$\underline{s}$	sensitivity vector
$\underline{v}$	engine system vector, Q.L. vector
$\underline{w}$	white noise vector
$\underline{x}$	state vector
$\underline{x}_m$	measured state vector
$\underline{x}_c$	estimated state vector, closed-loop vector
$\underline{y}$	phase variable vector, model state vector
$\underline{z}$	augmented Q.L. vector
$\underline{R}$	an augmented state vector
$\underline{\gamma}$	an augmented state vector
$\underline{K}$	augmented state vector function
$\underline{\xi}$	model state vector
$\underline{\Psi}$	adjoint vector
$\underline{T}$	closed-loop, minimum-sensitivity vector
$\underline{\sigma}$	sensitivity vector

APPENDIX A.2 - SOME SYMBOLS USED WITH ITERATIVE ANALOGUE COMPUTER DIAGRAMS (INCLUDING APPROPRIATE LOGIC DEFINITIONS)

The elements described in this appendix are defined for the Redifon-Astrodata analogue computer, ci-175.

1. NAND gate

Symbol :

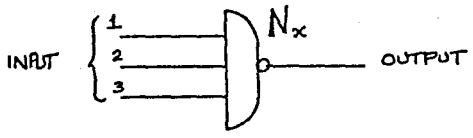

Logic definition :

Input Condition	Output State
Every input = logic 1	logic 0
Any input = logic 0	logic 1

2. COMPARATOR

Symbol :

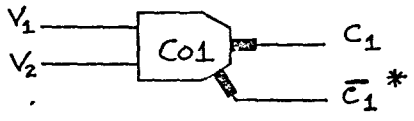

*Note : complementary logic output provided.

Logic definition

(Analogue) Input Condition	Output State
$(V_1 + V_2) > 0$	logic 1
$(V_1 + V_2) < 0$	logic 0

3. DIGITAL - TO - ANALOGUE SWITCH

Symbol :

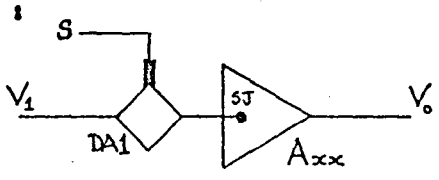

Note : A_{xx} is a normal analogue inverting amplifier.

SJ means SUMMING JUNCTION

Definition of Operation :

Input Logic(S) State	Analogue Output(V_o)
logic 1	0
logic 0	$-V_1$

4. RELAY

Symbol :

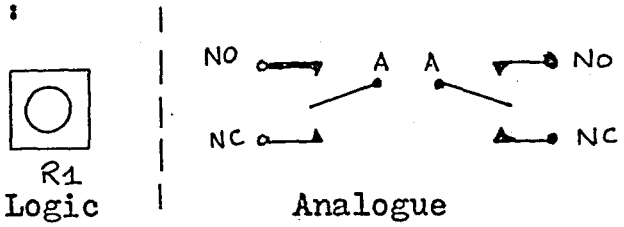

Logic Definition

Logic Input	Relay Switch State
0	R1 switched to NC
1	R1 switched to NO

5. LOGIC - CONTROLLED INTEGRATOR

Symbol :

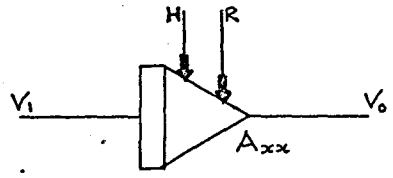

Definition of Operation :

Logic Input Signals		Integrator
H	R	Mode
1	0	RESET*
0	1	HOLD
1	1	COMPUTE

*Reset mode also obtained with H = R = 0.

6. LOGIC - CONTROLLED SUMMING AMPLIFIER

Symbol :

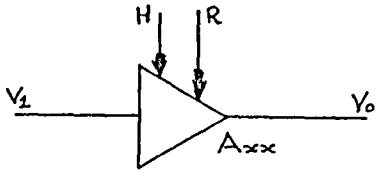

Note : this element is actually a logic-controlled integrator patched as a summing amplifier.

Definition of Operation*:

Logic Input Signals		Analogue Output
H	R	V_o
1	0	0
1	1	$-V_1$

*This operation is identical to that of the D/A switch. This configuration is used to supplement the limited number of D/A switches (8) available on the Ci-175.

APPENDIX A.3 - COMPUTER PROGRAMS

A feature of this research was the extensive use of digital computation. Many programs were written to perform the necessary computations involved in the work. All the computing was carried out at R.A.F. Cranwell on the Elliott 4120 computer with a 16k store for which each ADD instruction took 12 micro seconds and each MULTIPLY instruction took about 68 micro seconds. The programming language used for the programs was ALGOL 60 and extensive use was made of the matrix package provided by the computer manufacturer.

The complete set of programs (print-up, example problem print-out, and data input format explanation) is held at the Department of Electrical Engineering, University of Technology, Loughborough. To identify each program the Cranwell job number identifier was used. A list of these programs, with identifier and simplified flow-chart where appropriate, is given below.

Identifier	Program Name	Program Function
BEARDM11	ATHFALB	Solution of matrix Riccati eqn.
BEARDM15	DYNPROG	Solution of L.Q.P.
BEARDM20	LINAUTOIDENT	Identification of Lin. Syst.
BEARDM26	MODELFOLLOW	Erzberger's Model Scheme
BEARDM28	MINSENSOPT	Optimal Control with Minimum Sensitivity
BEARDM31EP	OSU	Fixed Interval O.S.U.
BEARDM31F	DYNOSU(LONG)	Dynamometer O.S.U.-T_f unknown
BEARDM33	KLEINMAN	Solution of Matrix Riccati eqn.

BEARDM34	STATRAN	Solution of State Transition eqn.
BEARDM36	MARNICH	Solution of L.Q.P. - Eigenvalues
BEARDM37	ORTONORM	Orthonormalisation Procedure
BEARDM40	HAMMING	Hamming Integration Procedure
BEARDM60	S.O.C.	Specific Optimal Control
BEARDM98	LYAMAT	Solution of Lyapunov Matrix eqn.
BEARDM08	RUNKUT	Runge-Kutta Integration Procedure

For completeness a brief explanation of the statements associated with the matrix package is given below. These procedures are called by listing them by name after the program call "LIBRARY" which appears with the initial declarations in each program. The statements may be used then as required subsequently within the body of the program.

STATEMENT	MEANING
MXSUM(A,B,C)	A becomes (B+C)
MXDIFF(A,B,C)	A becomes (B-C)
MXCOPY(A,B)	A becomes B
MXNEG(A,B)	A becomes -B
MXPROD(A,B,C)	A becomes B*C
MXTRANS(A,B)	A becomes A'
MXQUOT(B,A,C,)	Solves equation AB = C with results in B. A and C are preserved.
SCPROD(A,t)	A becomes tA. t is a scalar.
FORMMX(A,x,I,J)	a_{ij} becomes x. (x is a real variable)
READMX(A)	a_{ij} read in by rows from data tape
PRINTMX(A)	a_{ij} printed out in rows and columns
INVMX(A)*	A becomes A^{-1} (Note : A must be real, square, and non-singular)

*In this package A must be a matrix of order not less than 2x2.

In several programs the possibility occurs of the matrix A being of order 1x1 (i.e. a scalar). To maintain the generality of these programs provision has been made to handle this special situation by means of a switch statement which, when A is a scalar, avoids the use of the procedure INVMX and instead assigns

```
A:= 1/A;
```

If A is rectangular the inverse of the matrix does not exist, although its pseudo-inverse may. The pseudo-inverse is found from the technique outlined in Appendix A.5.3.

FLOW DIAGRAM OF BEARDM15

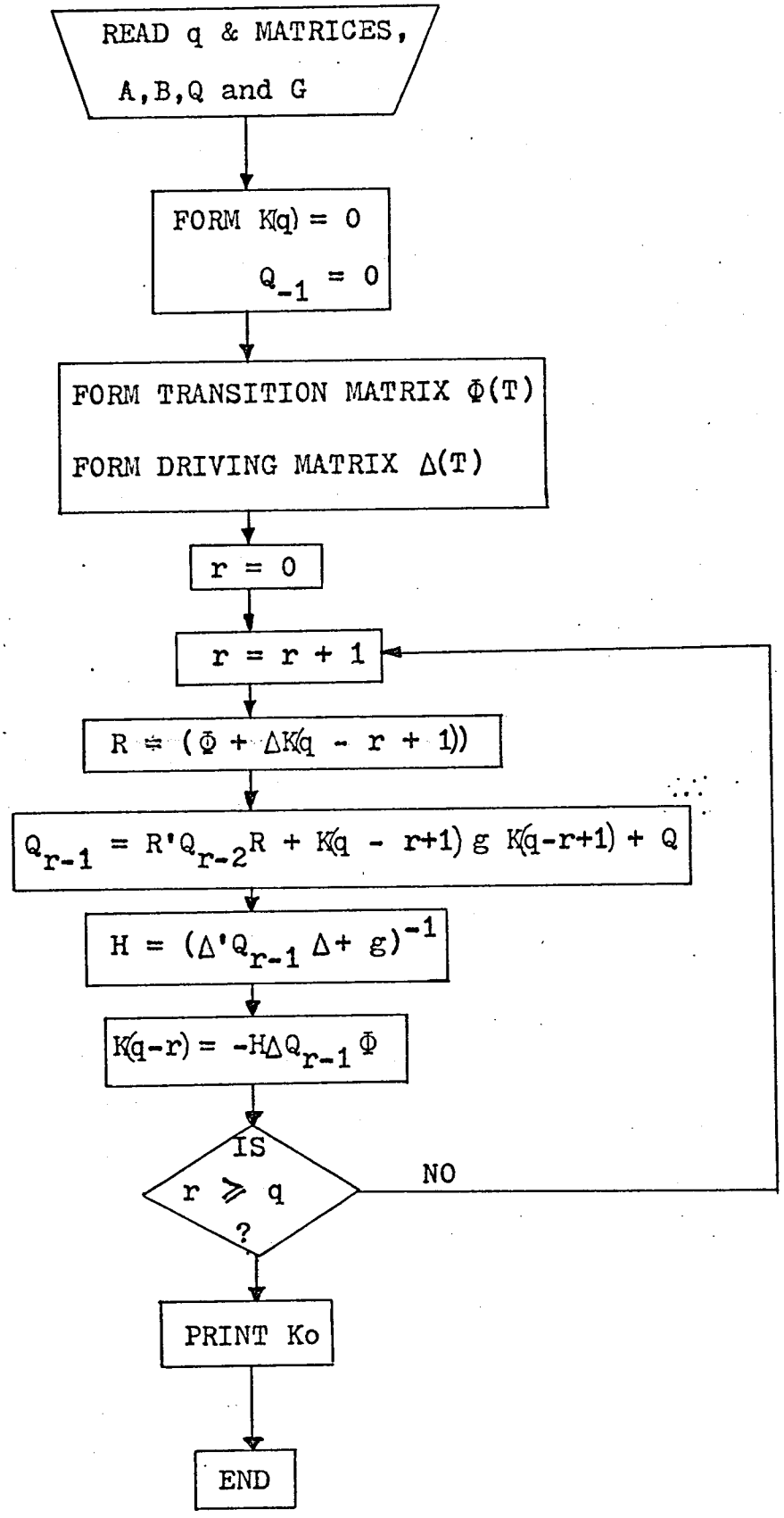

FLOW DIAGRAM OF BEARDM20

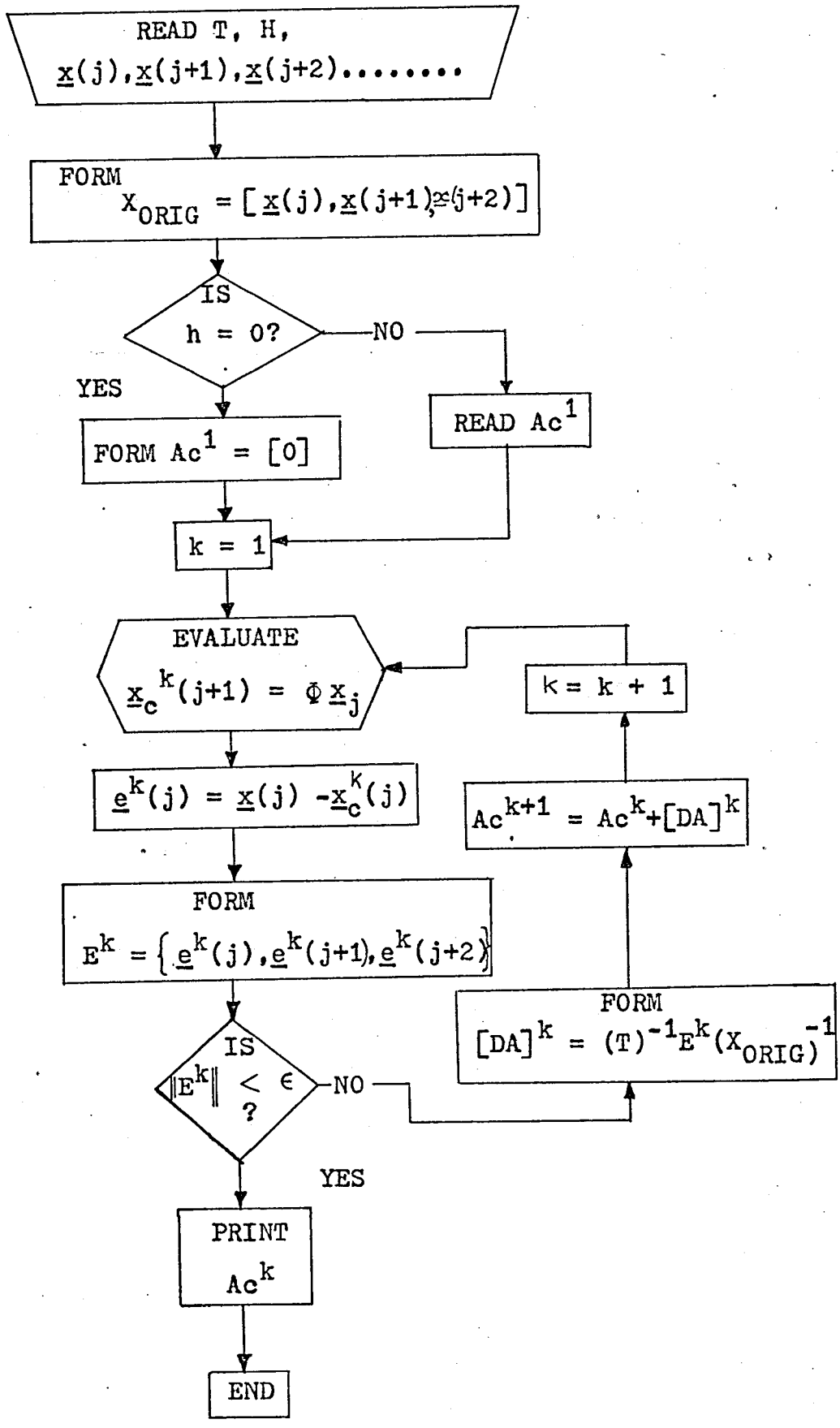

FLOW DIAGRAM OF BEARDM26

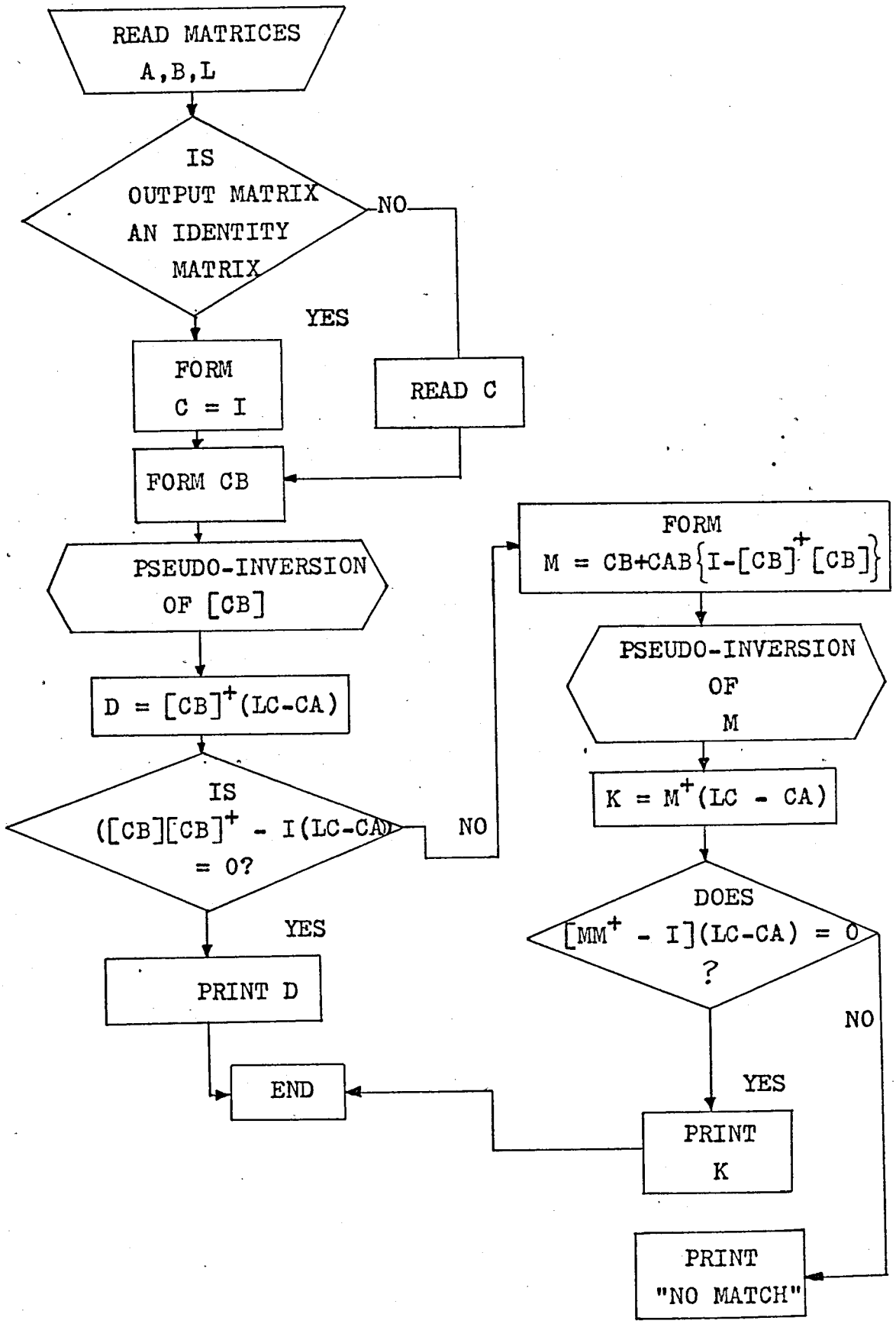

FLOW DIAGRAM OF BEARDM28

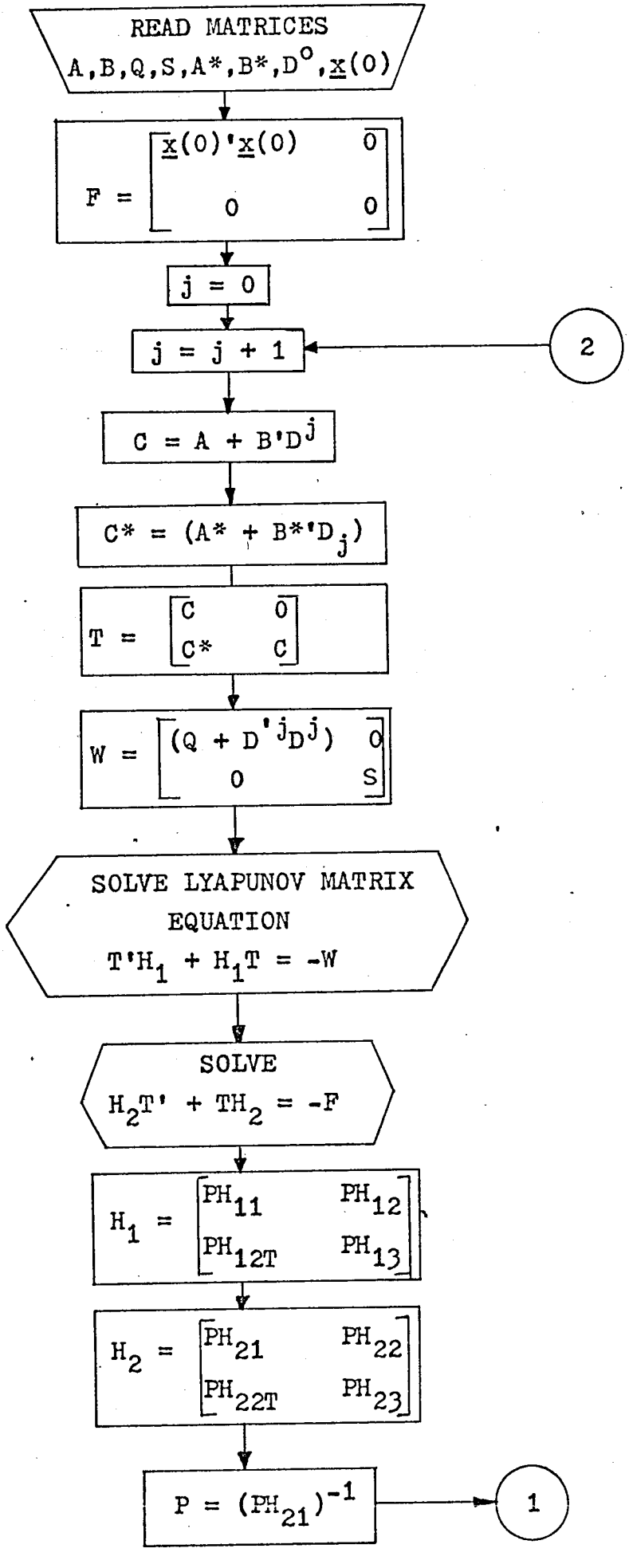

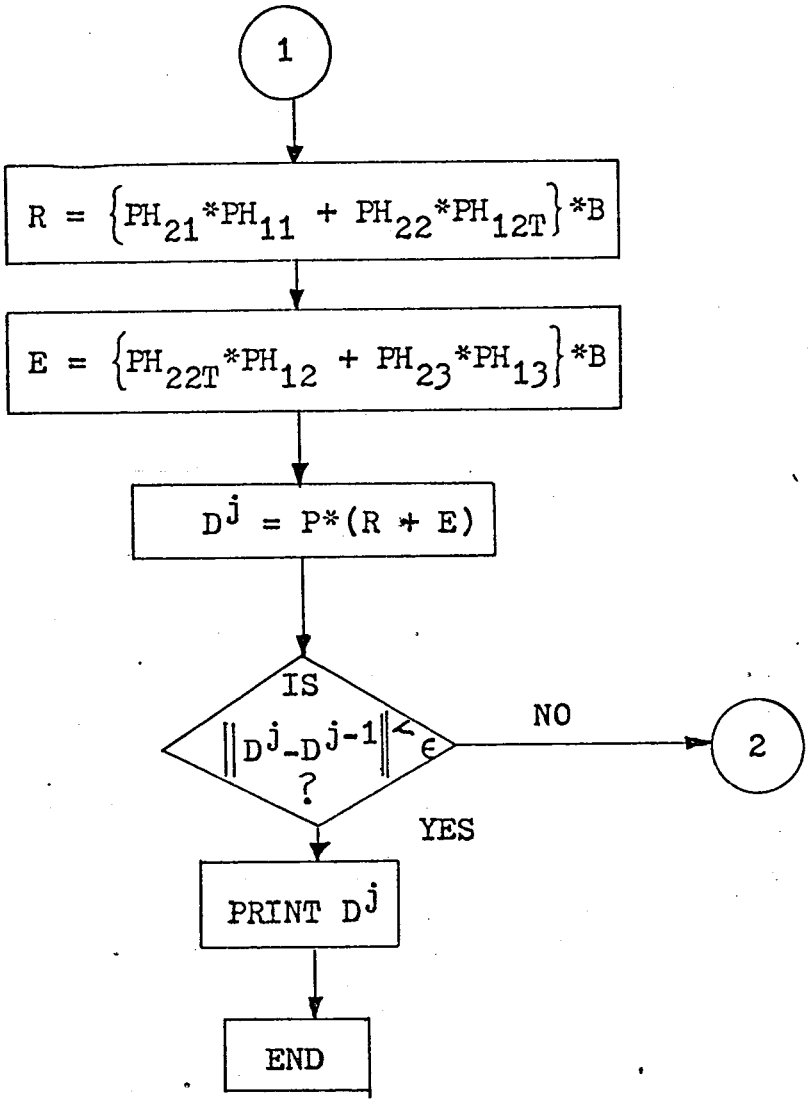
1
R = {PH21*PH11 + PH22*PH12T}*B
E = {PH22T*PH12 + PH23*PH13}*B
D^j = P*(R + E)
IS
||D^j-D^j-1|| < ε
?
NO
2
YES
PRINT D^j
END

FLOW DIAGRAM OF BEARDM31 SERIES

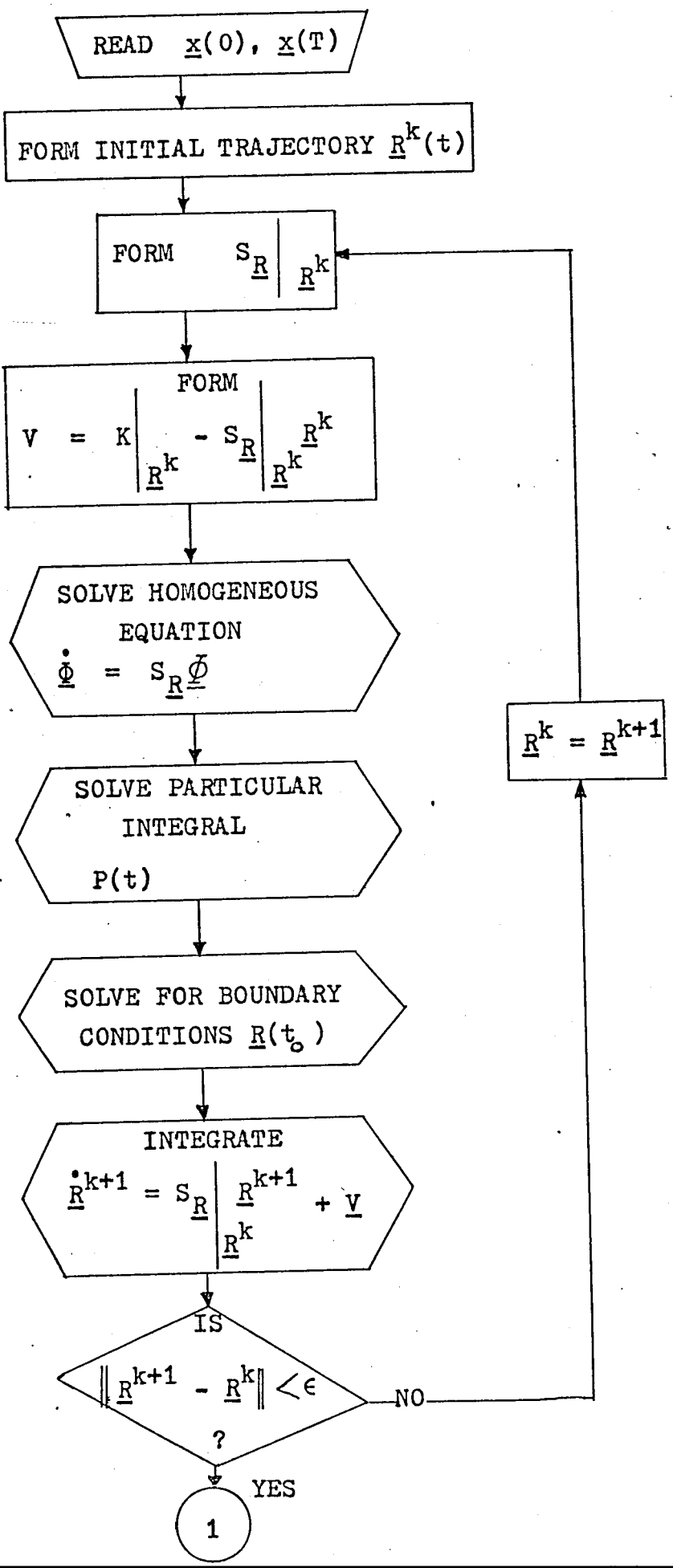

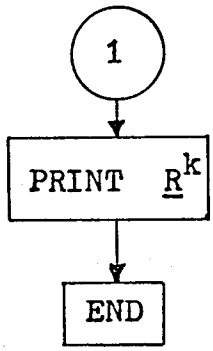

This flow diagram essentially governs BEARDM60 also.

FLOW DIAGRAM OF BEARDM34

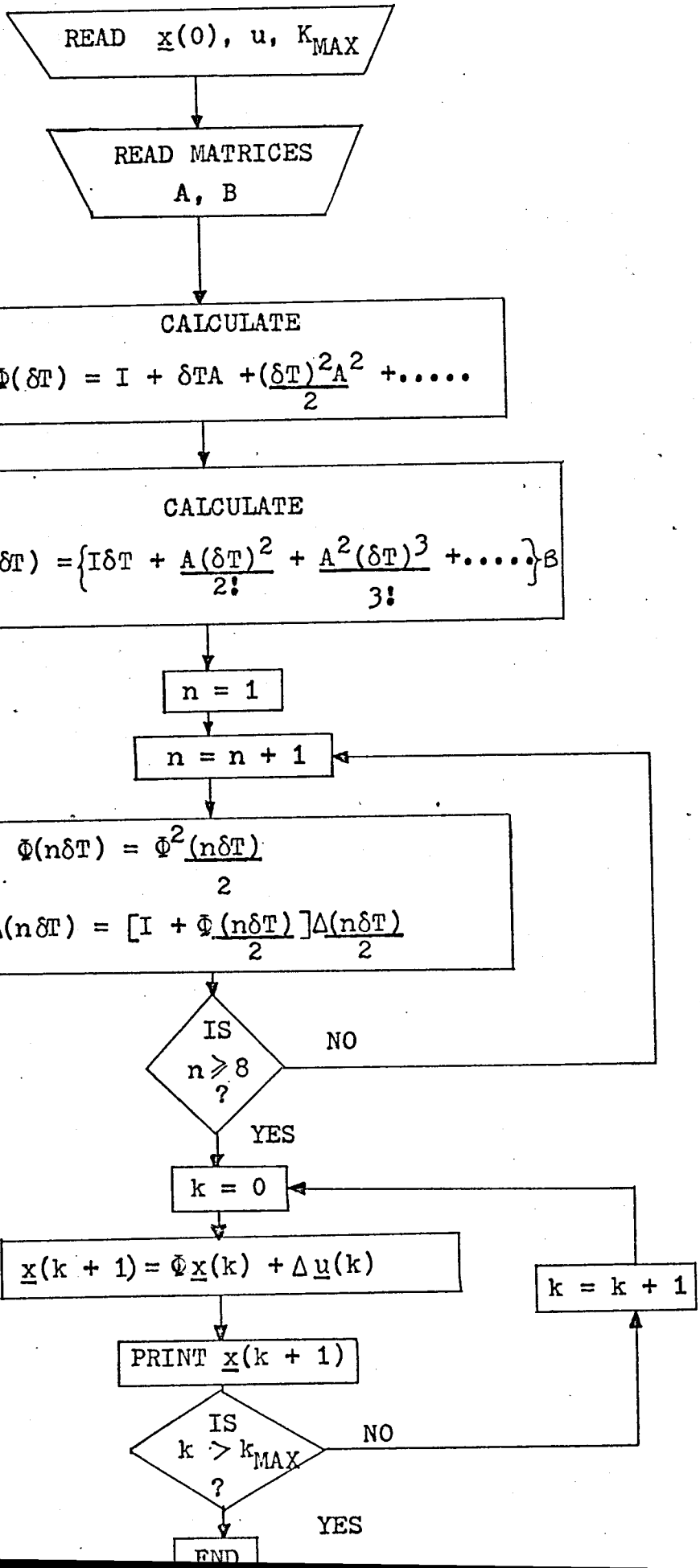

FLOW DIAGRAM OF BEARDM36

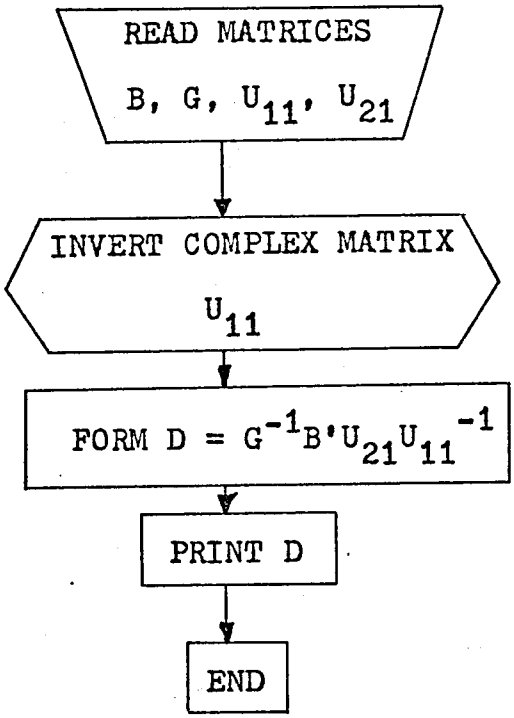

FLOW DIAGRAM OF BEARDM33

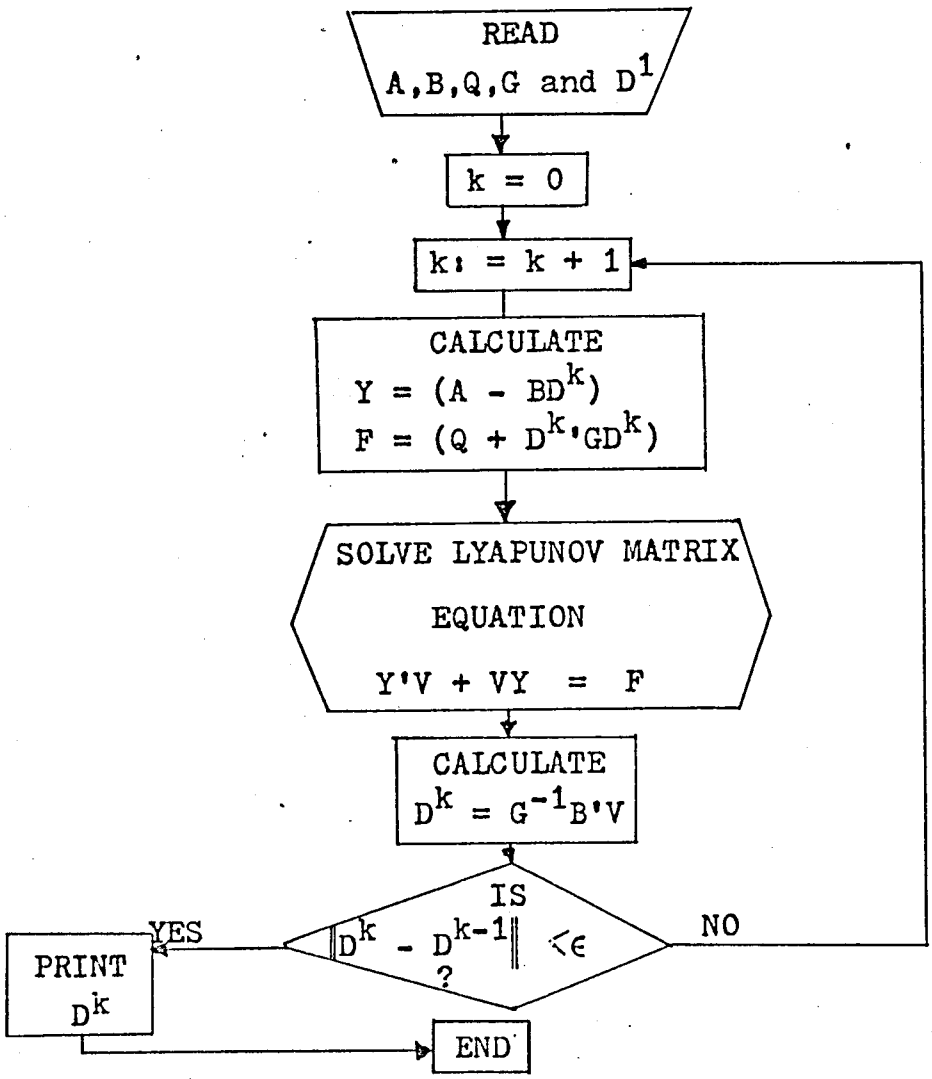

FLOW DIAGRAM OF BEARDM37

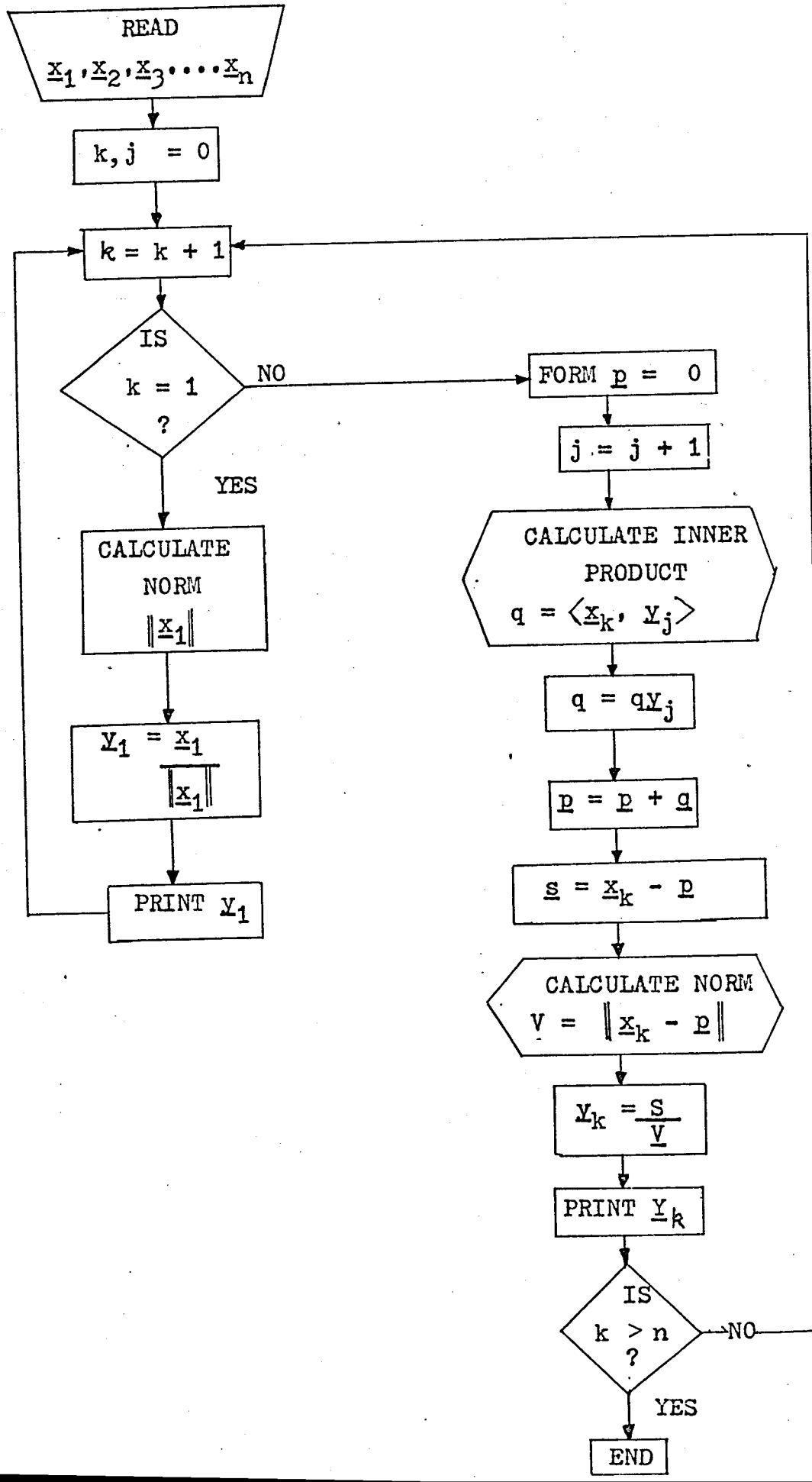

APPENDIX A.4 - RANDOM SIGNAL GENERATOR

A random signal generator was constructed for use with the simulation studies. Based upon a proprietary binary noise device (Burr-Brown model no. 4006/25) the signal generator produced a random telegraph wave derived from a clock signal of 1hz. The clock pulses were in turn derived from a crystal oscillator within the instrument. Provision was made to provide internal filtering of the noise signal by either an active low-pass 1st order filter, with a corner frequency of 0.05hz., or by a low-pass Butterworth filter with an approximate bandwidth of 1.5hz. The maximum output voltage from any of the signal sources was ± 12 volts which could be reduced continuously by means of a 10-turn potentiometer. The block diagram of the generator is given in figure A.1; the circuit diagram of the filter and output stages is given as figure A.2.

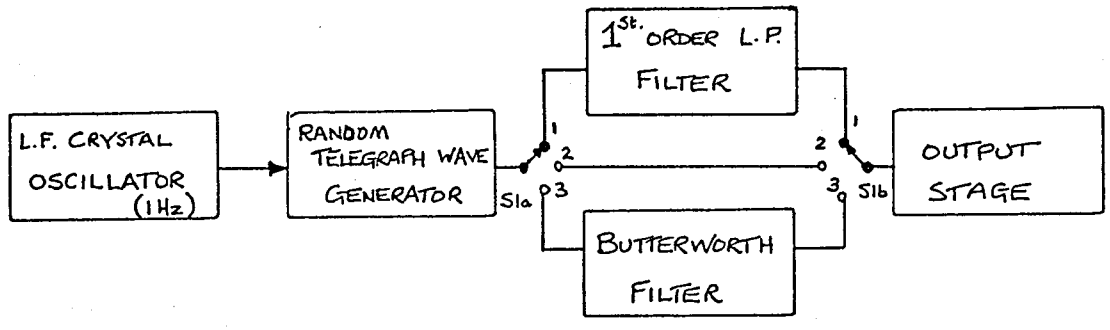

Figure A.1 - Block Diagram of Random Signal Generator

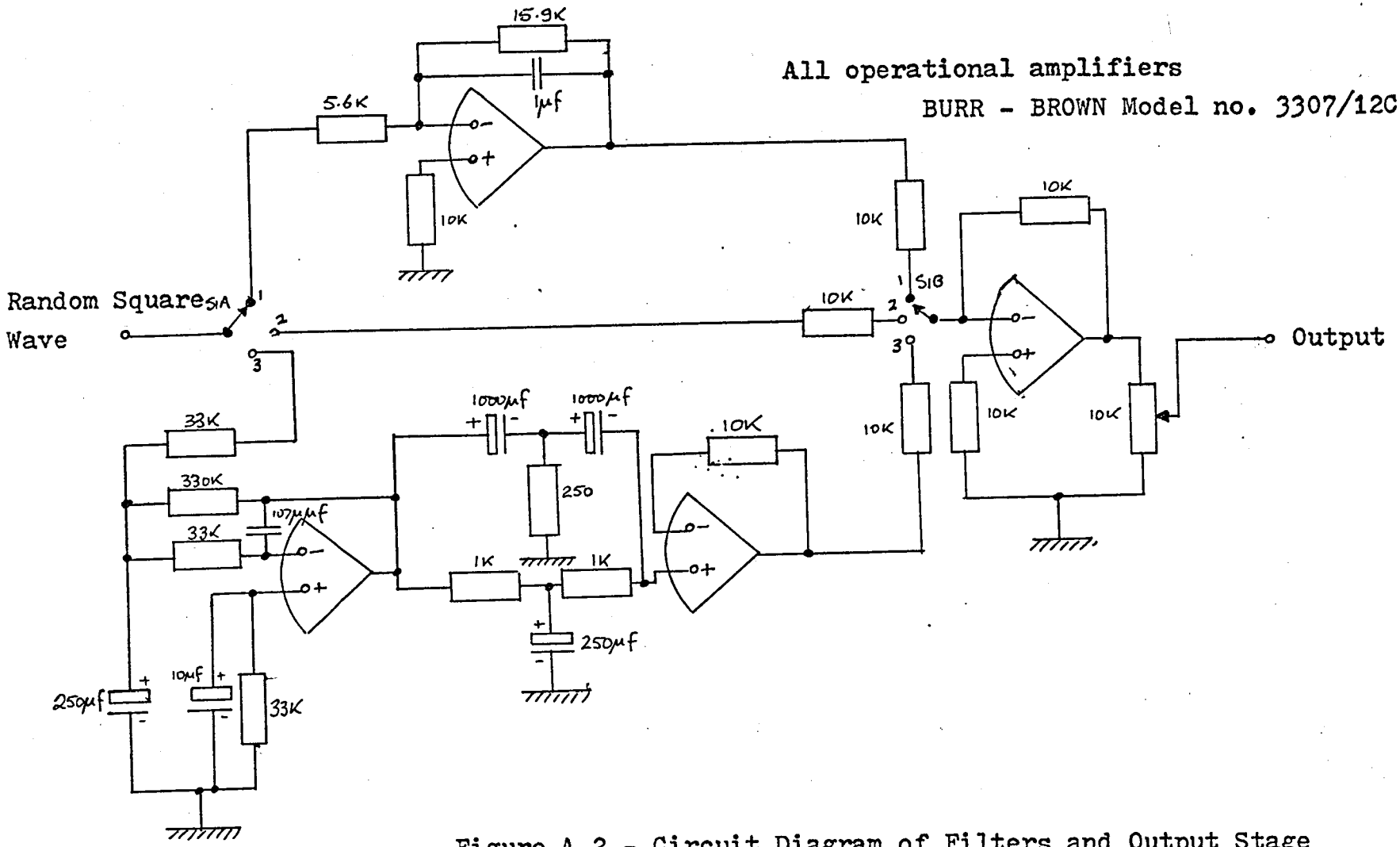

Figure A.2 - Circuit Diagram of Filters and Output Stage

The theoretical probability of the positive and negative levels of the random telegraph wave is 0.5. From a recording of the output over 5 seconds the measured value of probability for the positive level was 0.47826; the value measured for the negative level was 0.5131. With a longer duration recording these figures would approach more closely the theoretical value. The average output voltage was zero.

APPENDIX A.5 - SPECIAL ELEMENTS OF THEORY (associated with particular programs)

A.5.1 TRANSITION AND DELTA MATRICES

Transition and delta matrices are used in BEARDM34, BEARDM15, and BEARDM20.

The solution to the equation

$$\dot{\underline{x}} = A\underline{x} + Bu \qquad (A.5.1)$$

has been shown (BELLMAN (1960)) to be :-

$$\underline{x}(t) = \Phi(t-t_o)\underline{x}(t_o) + \int_{t_o}^{t} \Phi(t-\tau)Bu(\tau)d\tau \qquad (A.5.2)$$

where

$\Phi(t-t_o)$ is the TRANSITION matrix.

The delta matrix is defined as :

$$\Delta(T) = \int_{o}^{T} \Phi(T-\tau)Bd\tau \qquad (A.5.3)$$

If the system is regarded as discrete and if the forcing function, u(t), is taken to be piecewise constant the (A.5.2) may be re-expressed as :

$$\underline{x}\,(k+1)T = \Phi(T)\underline{x}(kT) + \Delta(T)u(kT) \qquad (A.5.4)$$

or, when T is known and fixed,

$$\underline{x}(k+1) = \Phi\underline{x}(k) + \Delta u(k) \qquad (A.5.5)$$

The transition matrix may be represented by a series expansion, viz.

$$\Phi(T) = \exp(AT) = I + AT + \frac{A^2T^2}{2!} + \frac{A^3T^3}{3!} + \frac{A^4T^4}{4!} \qquad (A.5.6)$$

The size of the elements of A, and the choice of T, can affect the convergence of the matrix series. To guarantee convergence in a limited number of iterations a very small step size, δT, is used to find first $\Phi(\delta T)$. Repeated squaring of $\Phi(\delta T)$ will result in the desired $\Phi(T)$ because

$$\Phi(n\delta T) = \Phi^2(n\delta T/2) \qquad (A.5.7)$$

For a discrete interval of 0.1 second the choice of

$$T = 0.00078125 \text{ second} \qquad (A.5.8)$$

will ensure that Φ (0.1) is determined in 7 iterations. The accuracy to which Φ (0.1) is determined can be controlled by means of setting in a round-off error bound in the program. (MANKIN J.B. and J.C. HUNG (1969).

If A is non-singular then

$$\Delta(T) = A^{-1}\left[\exp(A\left[T-\tau\right])\right]_0^T B \qquad (A.5.9)$$

$$= A^{-1}(\Phi - I)B \qquad (A.5.10)$$

Alternatively, as a series expansion, with the reduced step size δT, then

$$\Delta(T) = \Delta(n\delta T) = I+\Phi(n\delta T/2)\Delta(n\delta T/2) \qquad (A.5.11)$$

Consequently Δ is determined from Φ. The algorithms used to evaluate both Φ and Δ in each program were

$$\Phi(\delta T) = I + A\delta T + (A\delta T)(A\delta T/2) + (A^2\delta T^2/2)(A\delta T/3)+ \qquad (A.5.12)$$

and

$$\Delta(\delta T) = \left\{I\delta T + \delta T(A\delta T/2) + (A\delta T^2/2)(A\delta T/3) + \ldots\right\}B \qquad (A.5.13)$$

A.5.2 Dynamic Program

In this procedure, due to NICHOLSON (1964), it is assumed that the linear process will be restored to equilibrium in say, q sampling periods. The state trajectory is traversed backwards in time from the final state to the equilibrium state to determine the optimum discrete input sequence. The performance index to be minimised is taken as the discrete version of (6.2), namely

$$J = \min_u \sum_{k=0}^{q} \left\{\underline{x}'(k)Q\underline{x}(k) + gu^2(k-1)\right\} \qquad (A.5.14)$$

The discrete equation is

$$\underline{x}(q) = \Phi\,\underline{x}(q-1) + \Delta u(q-1) \qquad \text{(A.5.15)}$$

$$J_q^o = \min_{u(q-1)} \left\{ \left[\Phi\,\underline{x}(q-1) + \Delta u(q-1)\right]' Q \left[\Phi\,\underline{x}(q-1) + \Delta u(q-1)\right] + g u^2(q-1) \right\} \qquad \text{(A.5.16)}$$

Now,

$$\frac{\partial J_q^o}{\partial u(q-1)} = \left\{ \left[\Phi\,\underline{x}(q-1) + \Delta u(q-1)\right] Q\Delta' + \Delta' Q \left[\Phi\,\underline{x}(q-1) + \Delta u(q-1)\right] + 2gu(q-1) \right\} \qquad \text{(A.5.17)}$$

For optimality (A.5.17) must be zero, and the only control which will satisfy this condition is :

$$u^o(q-1) = -(\Delta' Q\Delta + g)^{-1}\Delta' Q\Phi\,\underline{x}(q-1) \qquad \text{(A.5.18)}$$

$$= K_{q-1}\underline{x}(q-1) \qquad \text{(A.5.19)}$$

where

$$K_{q-1} = -(\Delta' Q\Delta + g)^{-1}\Delta' Q\Phi \qquad \text{(A.5.20)}$$

By continuing thus for every successive backwards sampling interval the general result was established that

$$u^o(q-r) = K_{q-r}\underline{x}(q-r) \qquad \text{(A.5.21)}$$

where

$$K_{q-r} = (\Delta' Q_{r-1}\Delta + g)^{-1}\Delta Q_{r-1}\Phi \qquad \text{(A.5.22)}$$

and

$$Q_{r-1} = (\Phi + \Delta K_{q-r+1})' Q_{r-2}(\Phi + \Delta K_{q-r+1}) + K'_{q-r\ 1} g K_{q-r+1} + Q_o \qquad \text{(A.5.23)}$$

As $q \to \infty$ the entire control sequence of gains viz. K_{q-1}, K_{q-2}, K_{q-3}, ... converges to some limiting value K^o. J_q^o will also converge to a value J^o. (A.5.21), (A.5.22) and (A.5.23) form the basic algorithm used in the program, BEARDM15. In BEARDM15 the matrices Φ and Δ are computed using the expansions (A.5.11) and (A.5.12).

A.5.3 Pseudo-Inversion of a Matrix

It is well known that the inverse of a rectangular matrix does not exist; e.g. the system of equations

$$A\underline{x} = \underline{y} \qquad (A.5.24)$$

where $\underline{y}$ is a vector of dimension, m

and $\underline{x}$ is a vector of dimension, n

does NOT have a unique solution

$$\underline{x} = A^{-1}\underline{y} \qquad (A.5.25)$$

However, the system of equations (A.5.24) does have solutions. A solution is

$$\underline{x} = A^{+}\underline{y} \qquad (A.5.26)$$

where A^{+} is the matrix pseudo-inverse. If A is a matrix of order m x n, and of rank $r>0$, a factorisation of A exists such that

$$A = BC \qquad (A.5.27)$$

where B is a matrix of order m x r

C is a matrix of order r x n

and the rank of both B and C is r.

The pseudo-inverse of a matrix is defined by PENROSE (1955), from (A.5.27), as

$$A^{+} = C'(CC')^{-1}(B'B)^{-1}B' \qquad (A.5.28)$$

The pseudo-inverse is required also to satisfy the definition of a generalised inverse : it is defined (DEUTSCH (1969)) as the matrix, A*, of rank r, such that :

$$A = AA^{*}A \qquad (A.5.29)$$

From (A.5.27), (A.5.28) and (A.5.29) it may be shown that the pseudo-inverse does meet the requirement of being also a generalised inverse.

Thus :

$$AA^{+}A = A\,C'(CC')^{-1}(B'B)^{-1}\,A$$
$$= BCC'(CC')^{-1}B'B)^{-1}B'BC = BC = A \qquad (A.5.30)$$

(A.5.28) is used in the program BEARDM26.

When m>n then C is an identity matrix and

$$A^{+} = (A'A)^{-1}A' \qquad (A.5.31)$$

A.5.4 Derivation of Equation (6.70)

Equation (6.68) was re-expressed as :

$$F = 0.5\left\{q_{11}\,y_1^2 + q_{22}\,y_2^2 + q_{33}\,y_3^2 + g\hat{u}^2\right\} + \lambda_1 f_1 + \lambda_2 f_2 + \lambda_3 f_3 \qquad (A.5.32)$$

From (6.61) it is apparent that :

$$\left.\begin{aligned} f_1 &= \dot{y}_1 - y_2 = 0 \\ f_2 &= \dot{y}_2 - y_3 = 0 \\ f_3 &= \dot{y}_3 + 130y_1 + 146y_2 + 17y_3 - \hat{u} = 0 \end{aligned}\right\} \qquad (A.5.33)$$

However, it is known a priori that the control law will be constrained to have the form :-

$$\hat{u} = -k_1\,y_1 - k_2\,y_2 - k_3\,y_3 \qquad (A.5.34)$$

This equation is imbedded into the problem so that

$$f_3 = \dot{y}_3 + (130 + k_1)y_1 + (146 + k_2)y_2 + (17 + k_3)y_3 = 0 \qquad (A.5.35)$$

From the variational equations, quoted as (6.69), it may be shown that :-

$$\left.\begin{aligned} \dot{y}_1 &= y_2 \\ \dot{y}_2 &= y_3 \\ \dot{y}_3 &= -(130 + k_1)y_1 - (146 + k_2)y_2 - (17 + k_3)y_3 \\ \dot{\lambda}_1 &= q_{11}\,y_1 + (130 + k_1)\lambda_3 \\ \dot{\lambda}_2 &= q_{22}\,y_2 - \lambda_1 + (146 + k_2)\lambda_3 \\ \dot{\lambda}_3 &= q_{33}\,y_3 - \lambda_2 + (17 + k_3)\lambda_3 \end{aligned}\right\} \qquad (A.5.36)$$

(A.5.36) is identical to (6.70), where the matrix, (H), is defined as :-

$$\begin{bmatrix} 0 & 1 & 0 & 0 & 0 & 0 \\ 0 & 0 & 1 & 0 & 0 & 0 \\ -(130+k_1) & -(146+k_2) & -(17+k_3) & 0 & 0 & 0 \\ q_{11} & 0 & 0 & 0 & 0 & (130+k_1) \\ 0 & q_{22} & 0 & -1 & 0 & (146+k_2) \\ 0 & 0 & q_{33} & 0 & -1 & (17+k_3) \end{bmatrix}$$

(A.5.37)